Investigations into Novel Electrochemical Technology for Boar Taint Detection and Vitamin Analysis

Kelly Louise Westmacott B.Sc. (Hons) AMRSC

A thesis submitted in partial fulfilment of the requirements of the University of the West of England, Bristol for the degree of Doctor of Philosophy

This research programme was carried out in collaboration with the Agricultural Horticultural Development Board Pork and JSR Genetics Ltd

Department of Applied Science, University of the West of England, Bristol

April 2018

Abstract

This thesis presents the evaluation of the novel electrochemical sensor and biosensor technology developed for the direct analysis of the boar taint compounds, androstenone and skatole, in adipose tissue (European Patent 2966441). Gas chromatographic methods and extraction procedures were employed to evaluate the novel sensor technology. The methodologies for the non-destructive sensor technology were evaluated by analysing stored porcine adipose tissue, the samples were subsequently analysed by the destructive gas-chromatographic methodologies for comparison. The results from the two analytical methods exhibited a positive correlation for both compounds of interest in a laboratory environment. Consequently, the sensor and biosensor were integrated into a dual system and evaluated in the laboratory. The dual electrochemical system was optimised for the simultaneous measurement of skatole and androstenone. The prototype device was evaluated in the field; this involved the analysis of carcass subcutaneous adipose tissue at the abattoir processing line, afterwards a sample was taken back to the laboratory for gas-chromatographic analysis. The resulting quantitative data demonstrated a positive correlation of the two analytical methods indicating that this technology is viable for its proposed industrial application.

Other endogenous compounds in boar tissue were also identified prior to sample analysis during a literature review. The reported electrochemical behaviour and concentration ranges of these compounds were used to identify compounds which could result in the novel technology displaying false positive or false negative responses. During this preliminary investigation the identified compounds did not respond at the electrochemical sensor in a similar manner to the analytes of interest under physiological conditions. However, under alkaline conditions an anodic response for thiamine, riboflavin and pyridoxine was observed. As a secondary study to the boar taint analysis a simple voltammetric assay was developed to exploit this behaviour, this was successfully applied to the analysis of a food product and pharmaceutical supplement.

Thesis Contents

Acknowledgements

I feel very fortunate to have had some great lecturers and mentors at UWE over the years, none more so than my director of studies Professor John Hart. Your expertise in electroanalysis and enthusiasm for analytical science has been invaluable. Thank you for all your help.

I would also like to thank my second supervisors Professor Olena Doran and Dr Adrian Crew for their continued guidance and support. Your dedication to research is inspiring and I am looking forward to working with you in the future.

I would like to express my appreciation to the University of the West of England, the Agricultural Horticultural Development Board (AHDB) Pork, and JSR Genetics Ltd for their financial support. I would especially like to thank Caroline Kealey from JSR Genetics Ltd for all her support and guidance.

This journey would not have been possible without the support of my family, thank you for all your encouragement and belief. Thanks to my friends and housemates for all your support and patience over the past four years. Thanks for keeping me fed and sane. I am looking forward to spending some well needed quality time with you all.

Thank you to everyone at UWE, colleagues, technical staff and fellow students, your guidance and friendship is truly appreciated.

Lastly, I would like to say a special thank you to Liz Baldwin, your support and guidance throughout my A-Levels have been pivotal to my academic achievements. Your passion for chemistry has inspired me ever since.

Abbreviations

APCI	Atmospheric pressure chemical ionisation
B_1	Thiamine
B_2	Riboflavin
B_3	Nicotinamide
B_5	Pantothenic acid
B_6	Pyridoxine
B_7	Biotin
B_9	Folic acid
B_{12}	Cobalamin
CA	Chronoamperometry
CDE	Carbon disk electrode
CILE	Carbon ionic liquid electrode
CPE	Carbon paste electrode
CV	Cyclic voltammetry
CV %	Coefficient of variation
D_2	Cholecalciferol
$25(OH)D_3$	25-hydroxycholecalciferol
DAD	Diode array detector
DPV	Differential pulse voltammetry
ECE mechanism	Electron transfer, chemical reaction, electron transfer
Ep	Peak potential
EU	European Union
FID	Flame ionisation detector
GC	Gas chromatography
GCE	Glassy carbon electrode
Gr-PU	Graphite-polyurethane composite electrode
HMDE	Hanging mercury dropping electrode
HSD	Hydroxysteroid dehydrogenase
Ip	Peak current
IU	International Unit
LOQ	Limit of quantification
LSV	Linear sweep voltammetry
NAD+/NADH	Nicotinamide adenine dinucleotide oxidised/reduced form
SCE	Saturated calomel electrode
SD	Standard deviation
SPCE	Screen-printed carbon electrode
SP-Ag/AgCl-E	Screen-printed silver/silver chloride electrode
SWV	Square wave voltammetry
TOFMS	Time-of-flight mass spectrometer
Tris Buffer	Tris[hydroxymethyl]aminomethane
MB	Meldola's Blue
MS	Mass spectrometry
MSMS	Tandem mass spectrometry
NPD	Nitrogen phosphorous detector
P_2	Measurement position for back fat thickness in pig carcasses 6cm from the dorsal midline at the last rib

Chapter One

Introduction and Literature Review

Chapter One Contents

Table of Figures

Chapter Summary

Chapter one introduces the issues surrounding boar taint and the compounds responsible for this unpleasant flavour and aroma sometimes experienced with pork meat. The two principle techniques used for the measurement of boar taint in this thesis, namely electrochemistry and gas chromatography, will be discussed. Details of the fundamental principles that govern these techniques will be described. Finally, the research aims and objectives are addressed.

Chapter One

1.1 The demand for a boar taint detection system

Boar taint is the term given to the unfavourable flavour and aroma sometimes experienced with meat and meat products derived from *Sus scrofa domesticus,* commonly termed the domestic pig. Decades of research indicates that boar taint is due to the excessive accumulation of several naturally occurring compounds in porcine adipose tissue. The endogenous concentration of these compounds has been linked to slaughter weight, level of sexual maturity, and gender (Nicolau-Solano *et al.* 2007). Additional factors such as diet and breed have also been shown to play a role in their relative abundance. Currently there are no EU approved rapid instrumental methods to test for boar taint compounds on the abattoir line (Haugen *et al.* 2012). Boar taint can be prevented by castration but because of animal welfare issues, an increasing number of countries are moving towards an entire male pig production system. The EU legislation on the voluntary ban of pig castration will take effect in 2018, which means that the number of tainted pig carcasses will significantly increase. If not detected, the tainted carcasses can enter the food chain and result in the rejection of pork by consumers, a decrease in repeated purchasing of pork and as the result, economic losses for the pig industry internationally. Therefore, new technology is required which can rapidly detect taint compounds on-line with high specificity and sensitivity without any sample preparation.

1.1.1 Biochemistry of boar taint compounds

The two compounds primarily responsible for boar taint are 3-methylindole (skatole) and 5α-androst-16-en-3-one (androstenone). Both are soluble in fat (Lundström *et al.* 1988) resulting in a greater accumulation in adipose tissue compared to muscle tissue. Skatole is produced in the gut as a breakdown product of the amino acid tryptophan (Vold 1970),

(Walstra and Maarse 1970); the levels of this compound can be reduced with dietary manipulation (Jensen, Cox, and Jensen, 1995). Androstenone is a pheromone produced by the Leydig cells in the testes by entire male pigs in parallel with the biosynthesis of testosterone (Patterson 1968); therefore castration can be used as a preventative measure. Both skatole and androstenone can be transported in the blood stream to the liver where they are metabolised via two separate mechanisms. The metabolites are excreted within the faeces and the remaining skatole and androstenone, which have not been metabolised, are transported to the adipose tissue where they are deposited. Therefore, the concentration of skatole and androstenone in pig adipose tissue depends on two processes: the rate of their bio-synthesis and the rate of their hepatic metabolism. The third compound associated with boar taint is indole, but its input is viewed as minor and therefore indole will not be a focus of this study.

1.1.2 Legislation and current practice

European legislation (EU *Regulation 854/2004)* states that carcases with a pronounced sexual odour are unfit for human consumption, therefore the precise measurement of boar taint is of great importance to the pig industry. In the 1980's surgical castration was phased out in the UK, resulting in the slaughter of pigs at lower live weights to reduce the risk of boar taint. The issue with this approach is twofold. Firstly, it does not completely prevent the development of boar taint as different breeds and different animals within a breed might reach sexual maturity at different weights. Secondly, slaughtering at the lower live weight results in loss of revenue for the farmers. The above issues could be prevented if boar taint could be measured on the slaughter line.

In contrast to the UK, the surgical castration of piglets is still performed in a number of other countries, there are a number of reasons for this. It is known that meat quality characteristics differ between castrated and entire males, with entire males exhibiting less fat deposition and a different fatty acid composition profile (Pauly *et al.* 2012). The

amount and type of fat is very important for the curing process; therefore countries specialising in the production of high quality cured hams, such as Parma ham, are reluctant to change their traditional routine for fear of reduced product quality (Bonneau *et al.* 2017).

Surgical castration, of course, has ethical implications which have recently been raised by the European Union resulting in the implementation of a voluntary ban on the surgical castration of piglets by 2018 for EU countries (European Declaration on the Alternatives to Surgical Castration of Pigs, SANCO, 2011). This will result in a greater demand for a robust analytical system to determine if a carcass is tainted with levels above the acceptable threshold for the country where the product will be sold.

1.1.3 Strategies for the reduction of boar taint compounds in pork

As previously discussed, the most common strategy for reducing boar taint at the present time is surgical castration. A number of alternative approaches have been considered or developed including slaughtering pigs at lower live weight before they reach sexual maturity, dietary manipulation, and sperm sorting. Other potential strategies include immuno-castration (Fàbrega *et al.* 2010) and genetic selection (Grindflek *et al.* 2010). All the above approaches have limitations. Thus, dietary manipulation can reduce boar taint, which is caused by high skatole but not the level of androstenone. Sperm sorting to breed female pigs is at early stages of development, is time consuming and expensive. Identification of genetic markers for boar taint has been rapidly progressing, but has proved to be a complex process because of breed-specific mechanisms of boar taint. Immuno-castration has received increasing attention but faces concerns regarding consumer acceptance in some countries, including the UK. Therefore, there is no immediate solution to boar taint or an effective alternative to surgical castration.

Furthermore, all the avenues described require a rapid and robust method for evaluating their effectiveness in reducing boar taint. Some of these processes, alongside reducing boar taint, may have side effects (e.g. genetic selection) which could lead to an alteration in the chemical composition of the meat, which in turn could have an impact on flavour and texture. Therefore, taste panels will always have their place alongside instrumental analyses to monitor eating quality.

1.1.4 Available boar taint detection and measurement methods

The most common method for the determination of boar taint compounds uses an organoleptic judge to assess the volatile profile of heated adipose tissue samples. Although this is the most popular quality control practice in industry it is fraught with scientific discrepancies and its reliability is poorly documented (Trautmann *et al.* 2014). Human olfactory perception of skatole and androstenone varies between individuals (Griffiths and Patterson 1970)(Beets and Theimer 1970), this has been linked to the genetic variation of human odour receptors (Lunde *et al.* 2012). Studies into the threshold levels at which people perceive boar taint have shown disparity, this is likely to arise from human olfactory genetic variation and differences in meat processing and pig breed (Font-i-Furnols 2012). A review by Walstra and co-workers (1999) identified several published studies reporting the concentrations of androstenone and skatole that were deemed to be associated with an unpleasant aroma or taste from pork. These studies were used to provide general threshold levels for boar taint compounds at which consumers would negatively react to meat from entire male pigs. The thresholds were 0.5 and 1.0 ppm for androstenone (Desmoulin *et al.* 1982)(Mortensen *et al.* 1986) and 0.2 and 0.25 ppm for skatole (Armstrong 1993)(Mortensen *et al.* 1986).

A number of analytical methodologies have been developed for measuring boar taint compounds; however none of these are suitable for rapid online measurement of both androstenone and skatole. An early publication by Andresen (1975) reported the

development of a radioimmunoassay for androstenone determination. Although this method reported good precision with fortified adipose tissue only a single sample could be quantified, additionally a response time of around 30 hours was reported making it unsuitable for rapid online testing. Mortensen and Sørensen (1984) and Squires (1990) both developed colorimetric assays for skatole and androstenone respectively, however issues with specificity and the need for laborious sample preparation have been reported. A later publication by Sørensen *et al.* 2015 reported a surface-enhanced Raman spectroscopy method which can measure both skatole and androstenone however a sample preparation and extraction procedure is still required.

A device utilising conducting polymer technology in a sensor array called the e-NOSE (electronic Neotronics Olfactory Sensing Equipment) was optimised and applied to the monitoring of boar taint (Annor-Frempong *et al.* 1998). This array of twelve conducting polymer sensors used a pattern response to determine the sample components in comparison to a reference pattern obtained with a taint free sample of adipose tissue. Although results were promising, when compared to a taste panel and a GC-MS method, the stability of the conducting polymers was not satisfactory, and the equipment was expensive; making the e-NOSE unsuitable for use on the abattoir processing line.

Many publications for boar taint measurement have featured chromatographic separation techniques. Most laboratories tend to perform the extraction of androstenone and skatole separately, along with their analysis procedures (Haugen *et al.* 2012). de Brabander and Verbeke (1986) successfully developed a high-resolution gas-chromatographic method utilising an electron capture detector to determine androstenone. Whereas, Porter and co-workers (1989) developed a HRGC method with a flame ionisation detector for the measurement of skatole. A high performance liquid chromatography (HPLC) method has however been developed for the simultaneous analysis of both androstenone and skatole (Dehnhard *et al.* 1993). However, all of these

methods are limited to the laboratory, as they lack portability and require laborious sample preparation procedures.

In summary, none of the above mentioned analytical approaches are suitable for on-line measurement in an abattoir.

1.1.5 Advantages of the novel electrochemical sensor and biosensor

The novel electrochemical sensor and biosensor along with the corresponding voltammetric and amperometric methodologies were developed for the detection of boar taint compounds (Hart, Doran, Crew and McGuire, 2017). The data presented in the patent demonstrates the ability of the sensor and the biosensor to quantify skatole and androstenone respectively at the relevant levels required for boar taint identification. The prototype device will simultaneously measure androstenone and skatole using electrochemical techniques. The device can be inserted into adipose-tissue post mortem and achieve responses in under a minute; this could allow for the appropriate sorting of carcasses before they reach the end of the abattoir line. None of the methods described in section 1.1.4 can achieve this goal. The following sections will discuss the principle techniques employed in the dual instrument (voltammetric sensor and amperometric biosensor) and the corresponding reference method (gas chromatography with ionisation detection).

1.2 Electroanalytical chemistry

When electrochemistry is applied in analytical science, it is known as electroanalysis. One of the electrochemical techniques of interest in this thesis utilises current as a function of voltage (voltammetry) whereby reduction-oxidation processes can be studied. The other technique employed is known as chronoamperometry (current vs. time); which is usually more suitable for use with enzyme based biosensors. The practical experimental considerations are introduced and the fundamental principles that govern electroanalytical chemistry are discussed in the following sections.

1.2.1 Practical considerations

1.2.1.1 Electrolyte

To control and measure the electrode potential in an electrochemical cell the electrolyte medium must contain dissolved ions to support current flow (Zoski 2007). Solvent-combinations, for example water and alcohol, are used to aid reactant solubility and ionic species are added to reduce solution resistance (Bard and Faulkner 2001). Buffer and salt solutions are popular electrolytes; phosphate buffers are critical to pH maintenance whereas inorganic salts can provide a more stable charge transfer system. The experimental application often dictates the volume of supporting electrolyte employed. Where larger volumes are available, an electrochemical cell can be used which often holds between 10-50 ml (Sprules *et al.* 1995). However, when sample volume is limited and analyte concentration is low, dilution may not be feasible. Working electrode modifications can be employed to limit the volume of the bulk solution (Pemberton *et al.* 2005) or a microlitre volume coverage can be employed where the electrode has a planar geometry (Nicholas *et al.* 2018).

1.2.1.2 Electrode configuration

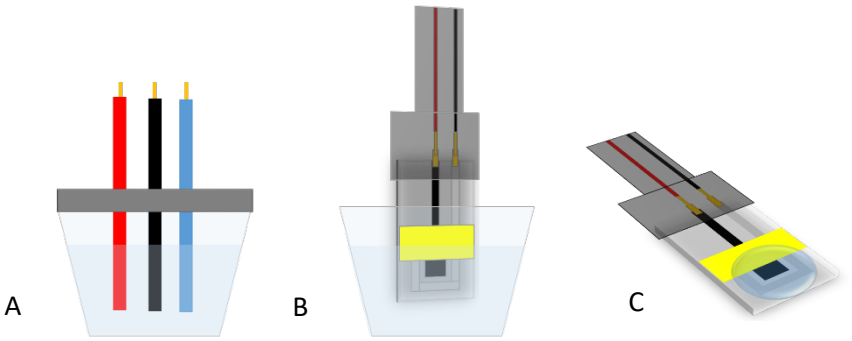

Figure 1.1. Electrode and electrolyte configurations commonly used for electroanalysis. Diagram showing a (A) three electrode cell with millilitre electrolyte volumes; (B) screen printed two electrode cell with millilitre electrolyte volumes; (C) screen printed two electrode strip with a planar microlitre volume electrolyte coverage.

A three-electrode system comprises of a working electrode, an auxiliary electrode, and a reference electrode (Figure 1.1A). A two-electrode system relies on the auxiliary electrode to serve the function of both itself and the reference electrode (Figure 1.1B & 1.1C). The electrochemical behaviour of interest is known to occur at the interface between the working electrode and electrolyte solution. During an electrochemical process, this interface is polarised and this polarisation can be monitored by an additional electrode. This reference electrode, ideally has a large surface area and half-cell reactions that are reversible and rapid (Skoog *et al.* 2007). The circuit is completed by the auxiliary electrode, which allows current to flow from the signal source through the electrolyte to the working electrode. The reference electrode has a reproducible and stable potential for comparison against the working electrode (Wang 2006). If the reference and auxiliary functions are combined in a single electrode (Figure 1.1B & 1.1C) the surface has to be large enough to prevent changes in potential during the experiment (Skoog *et al.* 2007). In this configuration the potential of the combined electrode is assumed to be the set potential applied therefore the output current response should be proportional to the analyte concentration.

1.2.1.3 Potentiostatic control

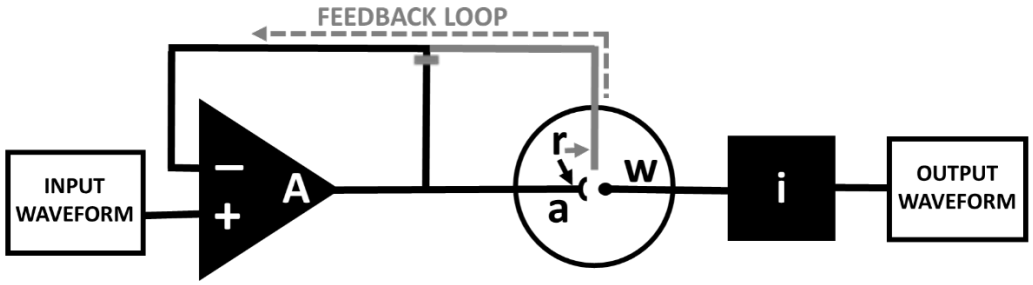

Figure 1.2. Schematic diagram showing potentiostatic control of both a two and three-electrode system: (w) working electrode; (a) auxiliary electrode; (r) reference electrode. Three-electrode operation represented with a feedback loop to the operational amplifier. (A) represents the operational amplifier and (i) represents the current-voltage converter. Reproduced with modification from Hart 1990.

The 'electrolytic cell' is the term used to describe a current induced in an electrical circuit, which subsequently results in reactions occurring at the electrodes (Brett and Brett 1998). The device capable of delivering this external energy is called the potentiostat. With advancements in power storage and wireless interfacing, modern potentiostats are well suited to field-testing. Modern potentiostat devices can be interfaced to either a desktop, laptop or tablet, which controls the device via a software package (eg. Nova or PSTrace). These packages provide methods with editable input parameters and integration functionalities for a wide range of electroanalysis techniques.

In a three electrode set-up the programmable input waveform is applied through the auxiliary electrode to the working electrode, the reference electrode is positioned as closely to the working electrode as possible to be able to monitor the applied potential 'felt' by the working electrode, shown in Figure 1.2. The operational amplifier allows for any compensation in current loss between the input potential and working electrode. Several phenomena can affect the measured cell potential such as the ohmic drop and polarisation effects (Skoog *et al.* 2007). In an electrolytic cell the potential required to drive the ionic current in solution is called the ohmic potential or iR drop (Bard and Faulkner 2001).

Where a two-electrode system is utilised the auxiliary electrode carries the current to complete the circuit and also acts as a reference electrode, therefore the usual feedback system from the operational amplifier is not available (shown in Figure 1.2). In an electrolytic cell where the electrolyte solution has a high conductivity the iR drop can be negligible (Bard and Faulkner 2001), therefore potential feedback and the third electrode can be omitted. It should be mentioned that the schematic in Figure 1.2 illustrates both a two and three-electrode cell under potentiostatic control.

1.2.2 Fundamental principles

1.2.2.1 Nernst equation

Where current is studied as a function of applied potential the electron transfer relates to a redox process. The Nernst equation, Equation 1, describes the relationship between analyte concentration and the electrode potential (E). The reduced form of the analyte will be present at higher concentrations when the standard potential for the redox reaction (E^o) is more positive than the electrode potential. Conversely, when the standard potential for the redox reaction is more negative than the electrode potential the oxidised form will be present at higher concentrations. A faradaic response occurs when the oxidation state of the electroactive species changes. This response, or faradaic current, obeys Faraday's Law and follows the Nernst equation. Faraday's constant states one mole of electrons has a charge of 96,487 C (F). The universal gas constant (R) is equal to 8.314 J K^{-1} mol^{-1} where temperature is measured in Kelvin (T). The number of electrons transferred (n) is related to the concentration of the oxidised electroactive species (C_O) with respect to the concentration of the reduced electroactive species (C_R).

$$E = E^o + \frac{2.3RT}{nF}\log\left(\frac{C_O}{C_R}\right) \qquad \textit{Equation 1}$$

Electrode potential (E); Standard reduction potential (E^o); Universal gas constant (R); Temperature in Kelvin (T); Number of electrons transferred (n); Concentration of the oxidised species (C_O); Concentration of the reduced species (C_R).

The Nernst equation can be re-written using the constants and room temperature, taken as 298 K for *T* (Skoog *et al.* 2007). The resulting simplification displayed in Equation 2 has important applications when determining the redox properties of an analyte with voltammetric techniques where the applied potential is ramped linearly with time; this will be expanded upon in section 1.2.3.1.

$$E = E^o + \frac{0.0592}{n}\log\left(\frac{C_O}{C_R}\right) \qquad \textit{Equation 2}$$

Electrode potential (E); Standard reduction potential (E^o); Number of electrons transferred (n); Concentration of the oxidised species (C_O); Concentration of the reduced species (C_R).

1.2.2.2 Faradaic and charging currents

A faradaic current results at the working electrode when the potential reaches a value where a reduction-oxidation process occurs; however, there is also another current arising as a result of the electrolyte. Non-faradaic current is referred to as charging current, which is also known as capacitance current because it arises from the charging or

discharging of the electrochemical double layer when a potential is applied. This is a result of the so-called double layer arising at the working electrode-solution interface, this is discussed in more detail in the next section.

1.2.2.3 The electrical double layer

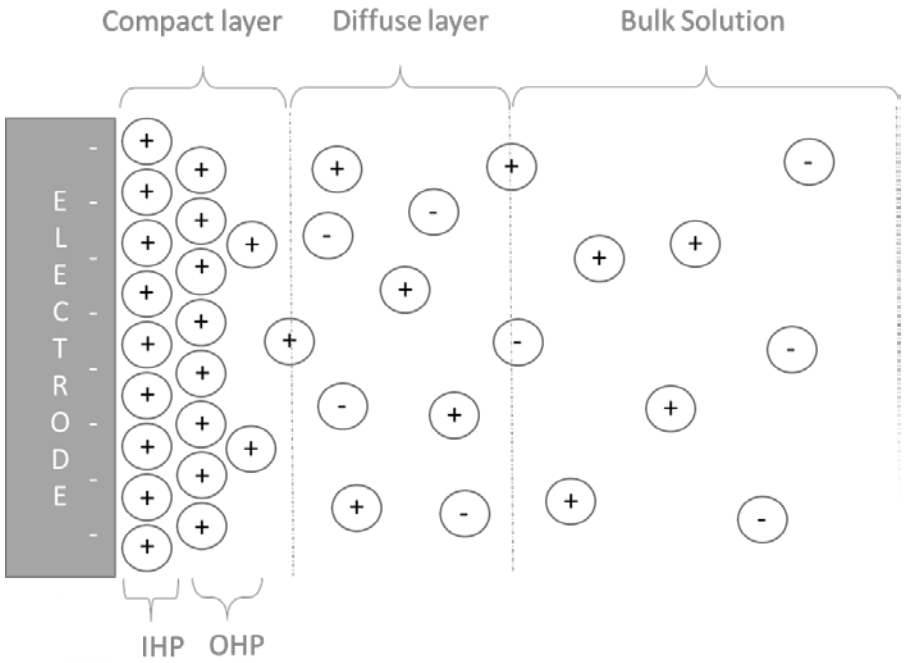

Figure 1.3. Schematic diagram of the electrical double layer theorised to be present at the electrode-electrolyte interface. IHP: inner Helmholtz plane, OHP: outer Helmholtz plane.

A simple schematic of the electrical double layer has been shown in Figure 1.3, the electrode is negatively charged with positively charged ions lining the electrode surface in the solution phase. Since the conception of the Helmholtz double layer there have been many additional contributions to the theory underpinning the arrangement of ions and molecules at the interfacial region between an electrode and the electrolyte solution. Stojek (2010) has coherently summarised these models and their contributions to our current understanding, with more recent models depicting adsorbed water molecules arranged in layers on an electrode surface. When the electrode has a net negative charge

the hydrogen atoms of the water molecules are angled towards the electrode. Conversely, when the electrode is positively charged waters hydrogen atoms are orientated away from the electrode surface. These dipole interactions were a much later addition to our theoretical understanding of the double layer, and are relevant to many practices in experimental electroanalysis today. The electrochemical double layer plays a critical role in electroanalysis. The Helmholtz theory simply suggests that electrolyte ions of charge opposing the electrode line the surface resulting in a neutral interface, which behaves as a capacitor. The initial Helmholtz model describes two distinct layers at this interfacial region; the inner most layer or IHP (inner Helmholtz plane) is formed of specifically adsorbed ions and solvent molecules and the outer layer or OHP (outer Helmholtz plane) is said to pass through the solvated ions that are non-specifically adsorbed. These layers together can be termed the compact layer as they are strongly bound to the surface, the neighbouring layer termed the outer diffuse layer stretches from the OHP to the bulk solution and consists of scattered ions (Wang 2006). The charge at the electrochemical double layer results in the capacitance current described previously, this is distinctly different from the faradaic current as it does not result from redox electron transfer processes at the interfacial region.

1.2.2.4 Mass transport

During an electrochemical reaction, the analyte has to move within the electrolyte solution to interact with the working electrode interface. This analyte transport, known as mass transport, can be described by the following three motions: (a) convection; resulting from an applied movement of either shaking, stirring or heating, (b) diffusion; occurs without the aid of shaking, stirring or heating and is the result of a concentration gradient, and (c) migration; is due to the occurrence of electrostatic forces upon ions. The Nernst-Planck equation, Equation 3, indicates that the flux of a species (*j*) is proportional to the three slopes representing hydrodynamic velocity, concentration, or electrostatic

potential, all with respect to the distance from the surface of the electrode (Bard and Faulkner 2001). Simple experimental practices can be employed to limit the effects of one or two of these terms, which reduces the complexity of the data interpretation.

$$J_j(x) = -D_j \frac{\partial C_j\,(x)}{\partial x} - \frac{z_j F}{RT} D_j C_j \frac{\partial \emptyset(x)}{\partial x} + C_j v(x) \qquad \textit{Equation 3}$$

Flux (*J*) [mol cm^{-2} sec^{-1}]; Species (*j*); Distance (*x*); Diffusion coefficient (*D*) [cm^2 sec^{-1}]; Concentration (*C*) [mol cm-3]; Charge (*z*); Electrostatic potential (Ø); Velocity (*v*) [cm sec^{-1}].

1.2.2.5 Fick's law

The first term in the Nernst-Planck equation relates diffusion to flux and is simply Fick's first law, which is shown in Equation 4. This equation describes the diffusion of a species under the influence of a concentration gradient, taking into account the distance from the electrode in relation to time.

$$J\,(x,t) = -D\,\frac{\partial C(x,t)}{\partial x} \qquad \textit{Equation 4}$$

Flux (*J*) [mol cm^{-2} sec^{-1}]; Distance from the electrode (*x*) [cm]; Time (t) [s]; Diffusion coefficient (*D*) [cm^2 sec^{-1}]; Concentration (*C*) [mol cm^{-3}].

Simplifying the mass transport of an electrochemical experiment can be practically achieved by eliminating forced convection, and preventing migration with the addition of excess salt. An excess of ionic species increases the solution conductivity, which in turn reduces the electric field thereby preventing ion migration (Zoski 2007).

In voltammetric terms it is important to relate Fick's law to the measured current response (*i*). Equation 5 equates the flux (*J*) of an electroactive species to current over the

number of electrons (*n*) per molecule involved in the electrochemical process with respect to Faraday's constant (*F*) and the electrode area [*A*].

$$J = \frac{i}{nFA} \qquad \textit{Equation 5}$$

Flux (*J*) [mol cm^{-2} sec^{-1}]; Current (*i*) [A]; Faradays constant (*F*) [96,485 C mol^{-1}]; Number of electrons (*n*); Electrode area (*A*) [m^2].

Under steady state condition the current is independent of time (i.e. under stirred conditions) therefore rearranging Equation 5, and taking into account Equation 4, leads to Equation 6. Under these conditions the current is directly proportional to the bulk concentration when using a constant stirring rate of the analyte solution (Hart, 1990).

$$i_L = \frac{nFADC}{\delta} \qquad \textit{Equation 6}$$

Limiting current (i_L) [A]; Faradays constant (*F*) [96,485 C mol^{-1}]; Number of electrons (*n*); Electrode area (*A*) [m^2]; Diffusion coefficient (*D*); Concentration (*C*); Nernst diffusion layer thickness (δ).

As described above the diffusional flux is time-dependant, this relationship is described by Fick's second law which is written for a linear diffusion profile in Equation 7. Further mathematical treatment of this law results in the Cottrell equation; Equation 8 (Greef *et al.* 1990). The Cottrell equation is applied in chronoamperometry (section 1.2.3.3) as it relates the current decay over time to the change in the concentration gradient in the vicinity of the electrode surface (Wang 2006).

$$\frac{\partial C(x,t)}{\partial t} = D\frac{\partial^2 C(x,t)}{\partial\, x^2} \qquad \textit{Equation 7}$$

Diffusion coefficient (*D*); Concentration (*C*); Distance (*x*); Time (*t*).

$$i_t = \left(nFAD^{1/2}c\right)/\,\pi t^{1/2} \qquad \textit{Equation 8}$$

Current at a specified time (i_t) [A]; Number of electrons (n); Faradays constant (F) [96,485 C mol^{-1}]; Electrode area (A) [m^2]; Diffusion coefficient (D); Concentration (C); Time (t).

1.2.3 Electroanalytical techniques

1.2.3.1 Potential sweep voltammetry

Cyclic voltammetry (CV) and linear sweep voltammetry (LSV) are potential sweep techniques performed under quiescent conditions. They can be used quantitatively since there is a linear relationship between current and concentration. In addition, they are valuable tools for examining the mechanisms of electrochemical reactions. The important parameters obtained from a voltammogram are the peak potential (E_p) and peak current (i_p); the peak potential value is taken from the potential axis, measured in volts, where the maximum current is observed and this peak current is measured in amperes.

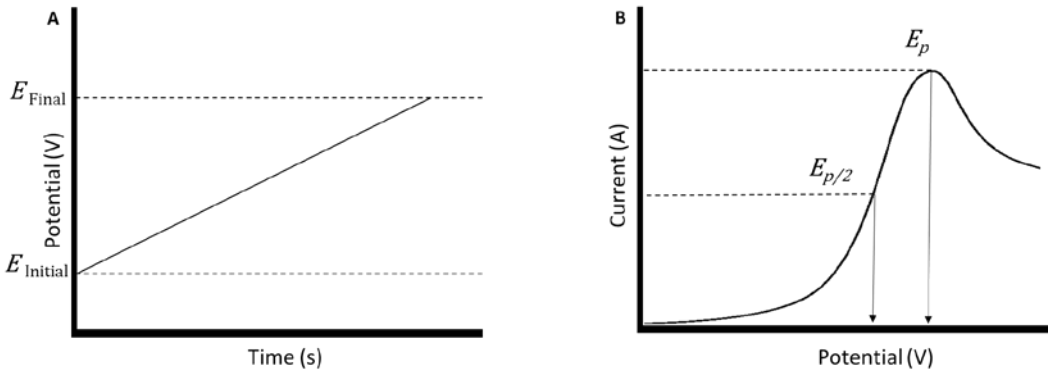

Figure 1.4. Diagrams showing a (A) linear sweep input waveform and a (B) linear sweep output voltammogram.

The input waveform for linear sweep voltammetry shown in Figure 1.4A is an applied potential ramp. The corresponding output profile shown in Figure 1.4B displays an increase in current when the electrode potential is great enough to induce electron transfer, then the current continues to rise until it peaks at a maximum current, after this the current begins to decay as the analyte at the interface is depleted (Fisher 1998). The Ep in a reversible system is independent of sweep rate; the half-wave peak potential ($E_{p/2}$) does not change when the scan rate is altered, making the change in half-wave peak potential ($\Delta E_{p/2}$) a useful and simple diagnostic for reversibility (Bard *et al.* 2012).

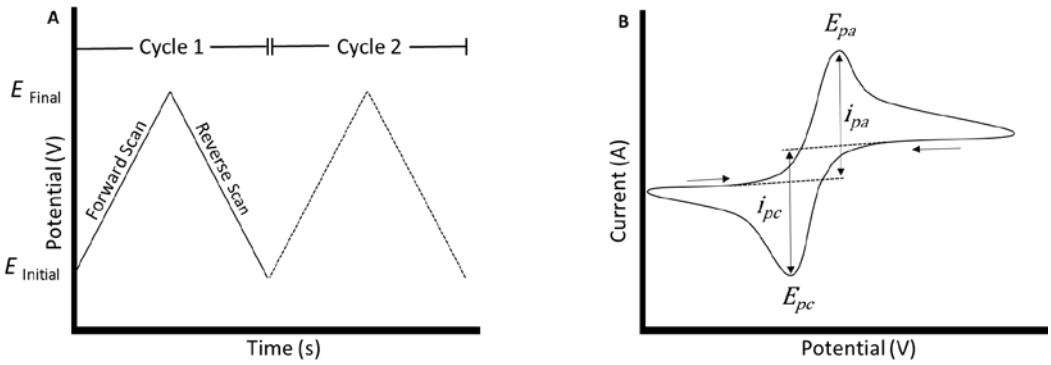

Figure 1.5. Diagrams showing the (A) triangular applied potential waveform used in cyclic voltammetry and (B) the resulting output of current vs. applied potential.

Cyclic voltammetry involves a triangular potential waveform, which can be cycled multiple times in a single run as shown in Figure 1.5A. The resulting response for a reversible reaction is shown in Figure 1.5B. The cathodic and anodic peak potential mid-point can be calculated with Equation 9; the resulting value is called the formal reduction potential, E°, for a reversible couple. The difference between the two peak potentials of a redox couple has relevance to the simplified Nernst equation (Equation 2), which can indicate the numbers of electrons transferred in the electrode reaction; Equation 10.

$$E^{\circ} = \frac{E_{pa} + E_{pc}}{2} \qquad \textit{Equation 9}$$

Formal reduction potential (E°); Anodic peak potential (E_{pa}); Cathodic peak potential (E_{pc}).

$$\Delta E_p = E_{pa} - E_{pc} \approx \frac{0.059}{n} \qquad \textit{Equation 10}$$

Change in peak potential (ΔE_p); Anodic peak potential (E_{pa}); Cathodic peak potential (E_{pc}).

The anodic and cathodic peak potentials should be close for a reversible redox couple; Equation 11 (Kissinger and Heineman 1983). Reversible reactions in cyclic voltammetry are characteristic of electrode kinetics that are fast relative to scan rate (Brett and Brett, 1998).

$$\frac{i_{pa}}{i_{pc}} \approx 1 \qquad \textit{Equation 11}$$

Anodic peak current (i_{pa}); Cathodic peak current (i_{pc}).

The peak current (i_p) of the first forward sweep in both CV and LSV for a reversible couple are described by the Randles-Sevcik equation (Kissinger and Heineman 1983); Equation 12. A scan rate study, measuring peak current at a range of scan rates, can be particularly insightful for the determination of the mode of mass transport when plotted as a function of current (Westmacott *et al.* 2018). As previously mentioned, peak potentials in a reversible system are independent of scan rate whereas in a quasi-reversible system they will shift with scan rate. Where a reaction is completely irreversible no corresponding peak will be visible on the reverse sweep for cyclic voltammetry. However, most redox

couples exhibit electrode kinetics that are limited therefore they are slower relative to scan rate; the peak current for a quasi-reversible couple is defined by Equation 13; both equations are useful for determining the number of electrons in the rate determining step.

$$i_p = (2.69 \times 10^5)\, n^{3/2} A C D^{1/2} v^{1/2} \qquad \textit{Equation 12}$$

$$i_p = (2.99 \times 10^5)\, n\, (\propto n_a)^{1/2} A C D^{1/2} v^{1/2} \qquad \textit{Equation 13}$$

Peak current (i_p); Number of electrons (n); Electrode area (A) [cm^3]; Transfer coefficient ($\propto$); Concentration (C) [mol cm^3]; Diffusion coefficient (D) [cm^2 sec^{-1}]; Scan rate (v) [V/s].

1.2.3.2 Pulsed potential voltammetry

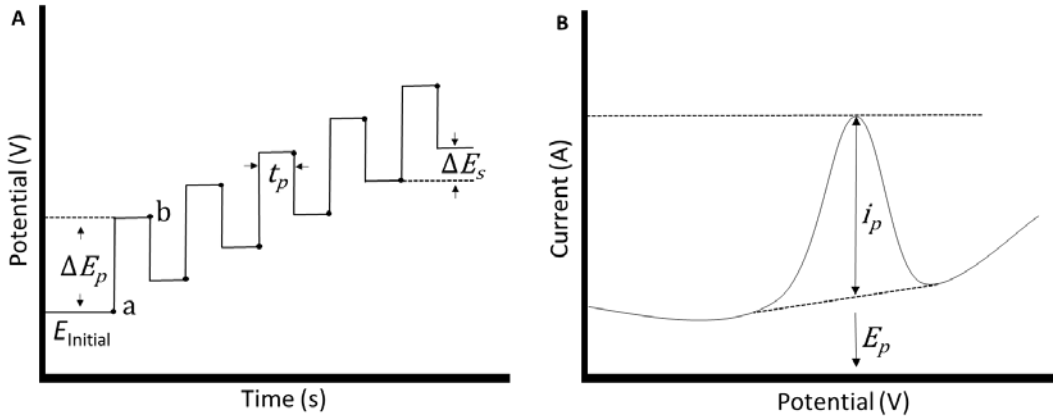

Figure 1.6. Diagrams showing the (A) applied potential waveform used in differential pulse voltammetry and (B) the resulting output of current vs. applied potential. Modifiable input parameters: pulse amplitude (ΔEp), pulse width (tp), step height (ΔEs). Reproduced with modification from Hart (1990).

Pulsed waveforms are well suited to quantification as the current sampling regime allows for better discrimination of the desired faradaic current from the unwanted charging

current. The input waveform for differential pulse voltammetry (DPV) sees potential applied in pulses of a set magnitude on a linearly increasing ramp, the current is measured prior to the pulse (a) and again just before the end of the pulse (b) (Figure 1.6A). The current differences of these measurement values are plotted against the applied potential to give the differential pulse voltammogram (Figure 1.6B).

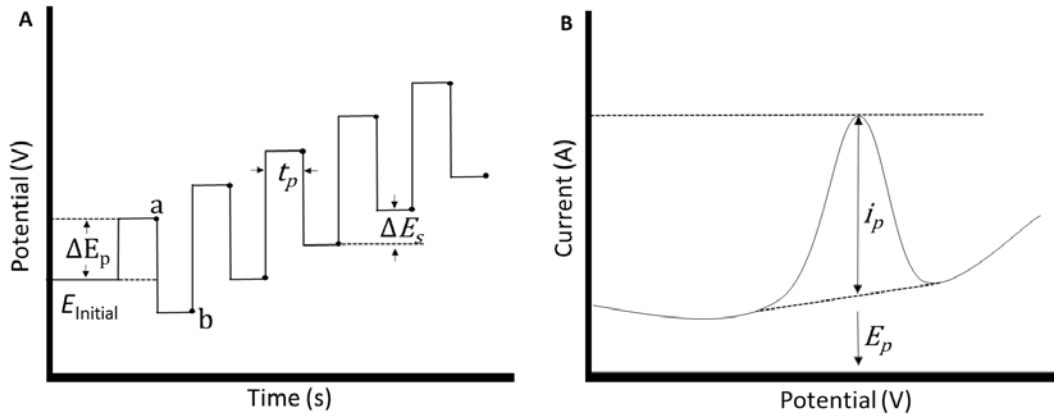

Figure 1.7. Diagrams showing the (A) applied potential waveform used in square wave voltammetry and (B) the resulting output of current vs. applied potential. Modifiable input parameters: pulse amplitude (ΔE_p), pulse width (t_p), step height (ΔE_s). Reproduced with modification from Hart (1990).

The input waveform for square wave voltammetry (SWV) is applied with a forward and reverse pulse procedure, which linearly increases in a staircase form (Figure 1.7A). Current is measured at the end of both the forward (a) and the reverse pulse (b). The current differences of these measurements are plotted against the increasing potential resulting in a square wave voltammogram (Figure 1.7B).

The dual-current-sampling procedure in both pulsed techniques reduces the charging current, which results in improved detection limits when compared to that of linear sweep voltammetry. In summary, the two pulsed potential techniques (SWV and DPV) have different current sampling procedures but provide similar responses, as demonstrated by their output responses.

1.2.3.3 Chronoamperometry

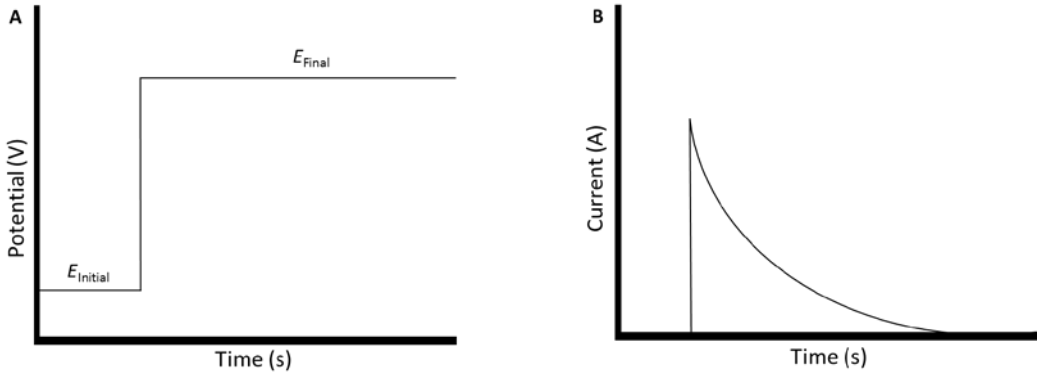

Figure 1.8. Diagram showing the (A) chronoamperometric input waveform and (B) the resulting chronoamperometric output of current vs. time.

The chronoamperometric method steps an applied potential from an initial value to a final value, which is held for a specified duration in which the current response is recorded with passing time. The initial potential step goes from a value where no faradaic response occurs to a value where the electroactive species is depleted, the current response at a specific time point following the final potential change therefore correlates to the initial concentration of electroactive species present. This technique specifically uses a quiescent solution unlike that of hydrodynamic amperometry therefore the only mass transport mechanism is diffusion. The input waveform and output waveform are illustrated in Figure 1.8, the sharp increase in current response followed by a curved steady decay over time can be explained by the Cottrell equation (Equation 8).

1.2.4 Sensors and biosensors for electroanalysis

1.2.4.1 Overview of biosensing

Thévenot and co-workers (2001) have defined a biosensor in the following way, "An electrochemical biosensor is a self-contained integrated device, which is capable of providing specific quantitative or semi-quantitative analytical information using a biological recognition element (biochemical receptor) which is retained in direct spatial contact with an electrochemical transduction element". The successful commercialisation of any novel sensor technology requires substantial monetary investment and in addition to this the final device must be inexpensive to fabricate in a competitive market (Luong *et al.* 2008). Screen-printing has come into its own in this field as it is capable of producing sensors in large batches, in a wide range of geometries, at a relatively low cost. These sensors have the capacity for simple but effective modifications which result in enhanced specificity and sensitivity. The advantages of electroanalysis described in the previous section coupled with the advantages of modern sensor fabrication techniques are the reason that this has become such a lucrative market. Sensors, and more specifically biosensors, are utilised in the defence, clinical, environmental and agri-food sectors and in 2013 the market had an estimated worth of 9.2 billion pounds sterling (Turner 2013). The biosensor which dominates the potentiostatic device market monitors glucose concentrations in blood, and with the prevalence of diabetes rising globally the demand for these diagnostic tools continues to grow (*Global report on diabetes* 2016). Similarly, potentiostat devices have been successfully developed for the measurement of other compounds of clinical importance such as lactate, ethanol, sucrose, uric acid and cholesterol (Dzyadevych *et al*. 2008).

The biomaterials constituting the biological recognition element can be an enzyme, antibody, antigen, DNA or bacteria; when this phase interacts with the analyte an electroactive species is produced which can be monitored directly or indirectly by the

transducer (Skoog *et al.* 2007). Biomaterials operate under the conditions found where they naturally function, once outside of this environment their stability may be compromised (Arnold and Rechnitz 1989). To overcome this possible complication, stabilisers are often employed to improve operational stability and prolong the shelf-life of the active component; which is particularly useful for the commercialisation of disposable biosensors (Gibson 1999). In addition to instability, biological recognition elements can be relatively expensive (Skoog *et al.* 2007) however the advantages such as: specificity, sensitivity, rapid response times, simplicity of operation, and inexpensive instrumentation far outweigh these potential drawbacks (Bahadir and Sezgintürk 2015).

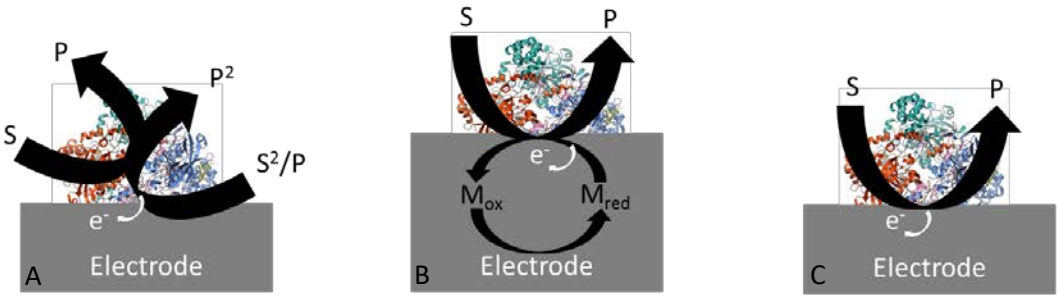

Figure 1.9. Schematic diagram illustrating a (A) first, (B) second, and (C) third generation biosensor.

Electrochemical biosensors may be classified by the route of signal transfer between the biological recognition element and the transducer material constituting the working electrode; first generation (Figure 1.9A) denotes the measurement of secondary substrates (S^2) and products (P) of catalysed reactions; second generation (Figure 1.9B) biosensors utilise a mediator to facilitate electron transfer between the biological recognition element and transducer; whereas the third generation (Figure 1.9C) model refers to the direct electron transfer between these two main components (substrate, S, and product, P) (Wollenberger 2005).

1.2.4.2 Equipment and procedures involved in the fabrication of screen printed sensors and biosensors

The screen printing of inexpensive materials, such as carbon or silver/silver chloride, onto thin polymer substrates is a very simple method of transducer fabrication and sometimes the whole biosensor (Crouch *et al.* 2005). The two-dimensional designs for screen-printed electrodes (SPEs) are initially plotted in a drafting software; this is then translated to a synthetic mesh screen of a fixed thread diameter and spacing. The ink, or paste, is first deposited into the screen stencil, in the shape of the electrode, using a flood blade; the second step involves the use of a squeegee to force the ink onto the plastic substrate below. This simple fabrication technique lends itself well to prototyping, as a variety of SPE geometries can be fabricated using a single screen. Once the optimal SPE configuration is identified, a screen with repeats of this pattern can be made and mass production can begin. A useful website which explains the process of screen-printing can be found on the Gwent Electronic Materials (1997) website; it should be mentioned that this company supplied the screen-printed sensors used in the current project. Other electrode fabrication techniques such as inkjet printing, photolithography, and polymerisation (Zhang *et al.* 2000) are available, however they are not as well suited to mass production as screen-printing. It is common for a combination of these to be utilised for sensor production allowing for the deposition of different chemical and biological components. When immobilising a biological component onto the electrode surface, drop coating using a micropipette to dispense microlitre volumes is a popular deposition technique, this approach is simple and inexpensive with minimal wastage of any expensive biological components.

1.2.4.3 Electrode modifications

Modifications are employed to improve sensitivity, specificity, operational stability and/or shelf-life of the device. By-products, or unwanted electroactive species, are often

generated at a polarised electrode. These species can interfere with the desired reaction process. This interference can be overcome with a membrane modification which prevents the unwanted species reaching the electrode surface (Karube 1989). Another modification which can prevent a response from unwanted species is the inclusion of a redox mediator which lowers the operating potential of sensor or biosensor, this will be explained in more detail in the following section (1.2.4.4).

1.2.4.4 Overpotentials and mediators

The activation overpotential describes the activation energy required to drive a charge transfer reaction (Bard *et al.* 2012). A successful mediator, also known as an electrocatalyst, should substantially reduce overpotential; an applied potential below +0.2 V would be preferential to prevent responses from species which would otherwise oxidise (Gorton and Domínguez 2002). Mediated electron transfer with a Meldola's Blue (7-dimethylamino-1,2-benzophenoxazine) modified graphite electrode was first reported by Gorton and co-workers in 1984. These preliminary studies indicated that this fabrication route held promise for lowering the electrocatalytic oxidation voltage of the coenzyme nicotinamide adenine dinucleotide (NAD) however its stability was not satisfactory (Gorton *et al.* 1984). This redox couple ($NADH/NAD^+$) plays an important role as a substrate or cofactor in many enzymatic reactions of analytical interest (Wilson 1989). Several studies have suggested that a stepwise ECE mechanism occurs when nicotinamide coenzymes are electrochemically oxidised (Moiroux and Elving 1980)(Jaegfeldt 1980). This mechanism (Equation 14) proposes an initial irreversible heterogeneous electron transfer resulting in the cation radical $NAD \cdot H^+$ the second step is a deprotonation resulting in the formation of a neutral radical $NAD \cdot$, the final heterogeneous electron transfer is reversible and results in the formation of NAD^+ (Lobo *et al.* 1997). A decade after Gorton's initial study another research group incorporated the electrocatalyst Meldola's Blue into a carbon electrode, this was achieved during the screen-printing process and the end

product was a disposable MBSPCE (Meldola's Blue screen-printed electrode) (Sprules *et al.* 1994); Figure 1.10 displays a schematic diagram of the electron transfer mechanism for a NADH-MB-SPCE. Hydrodynamic voltammetry of the modified vs. unmodified SPCE in the presence of NADH showed that oxidation only occurred in the presence of the mediator at low applied potentials (-0.4 to +0.3). Importantly, standard addition studies were performed using amperometry, which showed a stable response indicating that Meldola's Blue is stable when present in the screen-printed ink matrix. The application of this mediated electrode to the analysis of lactate was demonstrated in a subsequent study which incorporated a dehydrogenase enzyme, this will be explained in more depth in the following section (Sprules *et al.* 1995).

$$NADH \xrightarrow{-e^-} NAD \cdot H^+ \xrightarrow{-H^+} NAD \cdot \longleftrightarrow NAD^+$$ *Equation 14*

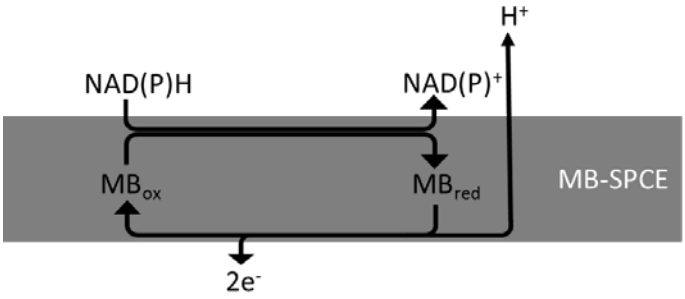

Figure 1.10. Schematic diagram illustrating the electron transfer mechanism of a NADH-MB-SPCE.

For the present research project screen-printed carbon electrodes were modified with the electrocatalyst Meldola's Blue, as this has proved very successful in a wide range of biosensors for a variety of target analytes (Sprules *et al.* 1995, 1996). These devices are used in conjunction with different dehydrogenase enzymes, that convert the cofactor *NAD^+* to *NADH*, and it is the oxidation of the latter that forms the basis of the analytical response for the biosensors used in this thesis. In the context of this thesis the enzyme 3α-hydroxysteroid dehydrogenase (3αHSD) has been incorporated with a Meldola's Blue

modified screen-printed carbon electrode (MB-SPCE) to produce a biosensor for androstenone measurement. This device was employed for boar taint studies in this project, which will be described in detail in later chapters (see chapters two to four).

1.2.4.5 Enzymes for biosensors

Many different enzymes have been identified in nature, each catalysing specific biochemical processes. These macromolecular biological components can be isolated from natural sources or artificially synthesised, these enzymes can be immobilised on the surface of an electrode to form a biosensor. Their purity, specificity and stability are all important qualities in biosensor fabrication (Warner 1989). The enzyme aliquot should be free from contaminating compounds that could possibly lead to an interfering signal. Many compounds in nature share similar structures, termed derivatives. For this reason the enzyme utilised in the biosensor must exhibit high specificity for the analyte of interest. Enzymes are complex proteins which are sensitive to their surrounding environment; they are susceptible to thermal inactivation as well as changes in pH, especially where ionizing groups control enzyme function (Cass and Kenny 1989). For these reasons, it is important to source a high quality enzyme and optimise the operational parameters during biosensor development studies.

Electroanalysis with an enzyme-catalysed reaction involves either monitoring the enzyme product or the substrate consumed (Karube 1989). The electroanalysis technique suitable for these measurements is chronoamperometry, which has been previously described in section 1.2.3.3. Dehydrogenase enzymes exhibit specificity for a particular substrate therefore a wide range of biosensors can be fabricated with a specific analyte in mind (Wilson 1989). Dehydrogenase enzymes, however, require a cofactor, which is normally nicotinamide adenine dinucleotide which exists in the oxidised form, as NAD^+ and the reduced form as *NADH*. As previously explained, this redox-couple plays a critical role in many enzyme-catalysed reactions in nature, and mediator-modified electrodes can be

used to improve the redox efficiency of the cofactor leading to a low operation potential (Elving *et al.* 1976). In the current project, the dehydrogenase enzyme utilised was 3αHSD which catalyses the conversion of the boar taint compound androstenone to androstenol in the presence of reduced *NAD*. This enzyme has been reported for its relevance in clinical sensing for the measurement of androsterone (3α-Hydroxy-5α-androstan-17-one) in human bile and serum (Mundaca *et al.* 2012)(Teodorczyk and Purdyt 1990). This compound is a derivative of our analyte of interest, and is commonly used as an internal standard in the chromatographic analysis of the boar taint compound androstenone (Brennan *et al.* 1986). Androsterone has not been reported to occur naturally in porcine adipose tissue, consequently it is not regarded as a potential interfering compound for the biosensor used in this thesis.

$$Androstenone + NADH \xrightarrow{3\alpha HSD} Androstenol + NAD^+ \qquad \textit{Equation 15}$$

$$NADH + MB^+ \longleftrightarrow NADH \cdot MB^+ \qquad \textit{Equation 16}$$

$$NADH \cdot MB^+ \rightarrow NAD^+ + MBH \qquad \textit{Equation 17}$$

$$MBH \rightarrow MB^+ + 2e^- + H^+ \qquad \textit{Equation 18}$$

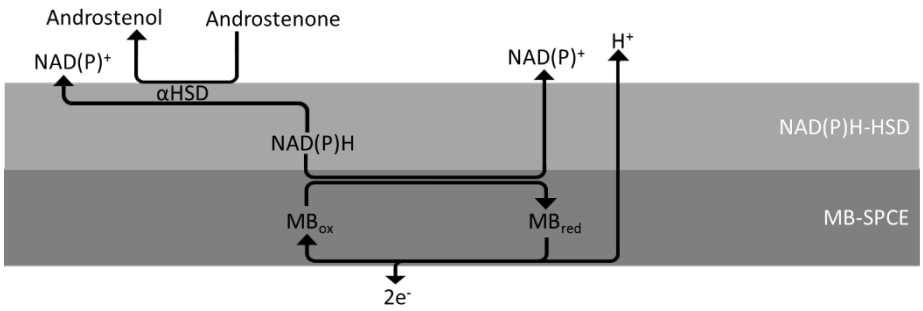

Figure 1.11. Schematic diagram illustrating the electron transfer mechanism of the biosensor (reproduced with modification from European Patent 2966441).

When androstenone is introduced to the biosensor (3αHSD-NADH-MB-SPCE) an enzymatic reaction (Equation 15) occurs to convert *NADH* on the electrode surface to

NAD^+, this results in the decrease in the current obtained as a result of Equation 16-Equation 18. The measured current response at a specific time is subtracted from a control value obtained with a buffered solution, in the absence of androstenone, for that batch of biosensors. The current difference is directly proportional to the concentration of androstenone. The boar taint studies involving this biosensor, schematic displayed in Figure 1.11, will be discussed in chapter's two to four.

1.3 High resolution gas chromatography

Gas chromatography is a popular analytical tool used for both qualitative and quantitative purposes. It is a separation technique that, as the name suggests, uses a specific gas (mobile phase) to transport chemical species through a column of a specific polymeric material (stationary phase). The mechanism of compound separation is complex, involving molecular interactions and thermodynamics. However, for the purpose of a brief introduction to the technique the explanation of separation will be simplified.

The sample is volatilised at the inlet of the column and the analytes are distributed in the mobile phase; this portion is called the eluent. The molecules of each compound in the sample are then distributed between the two phases (gas and mobile). The sample compounds interact with the stationary phase and only move through the column when they are in the mobile phase. The compound molecules that have the least interaction with the stationary phase reach the end of the column first, this is known as eluting from the column, thus entering the detector. If the detector responds to this type of compound an electrical signal will be generated. The size of the response is proportional to the amount of the compound. This signal will be visualised as a peak in the chromatogram output (Figure 1.12). If two compound molecules interact with the stationary phase to a similar degree their response will be visualised as a single peak or overlapping peaks. Therefore, it is important that all of the instrument variables such as stationary phase,

oven temperature, mobile phase and flow rate are suitable for the complete separation of the sample components.

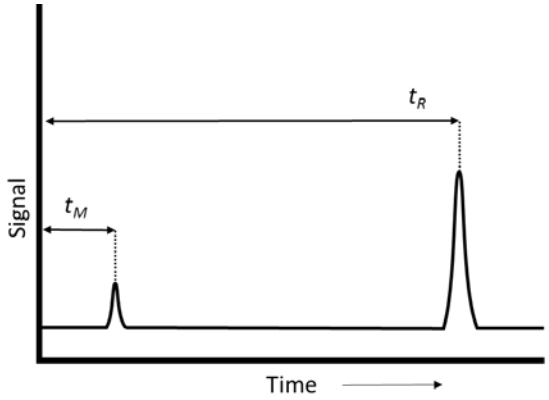

Figure 1.12. Diagram showing the output chromatogram for gas chromatography.

As previously discussed for biosensors, specificity of the analytical method for a target analyte is the ideal scenario; however, few methods can achieve this outcome. The reason being that most biological samples contain a complex mixture of compounds, sometimes these compounds are very closely related in terms of their chemical and physical properties making them difficult to separate or differentiate. Chromatographic methods can be optimised for improved specificity, although they are often only selective for a specific class or group of chemically related compounds.

1.3.1 Chromatographic principles

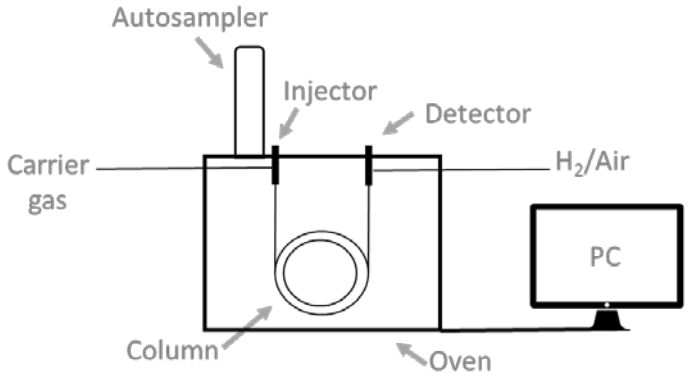

Figure 1.13. Diagram showing the main components of a modern gas chromatograph.

A modern gas chromatographic system is comprised of an injector, detector, oven, column, gas supply, gas flow controller and data recorder. These parts, with the addition of an optional autosampler, are illustrated in Figure 1.13. The integral parts are the injector, gas flow controller, detector and oven. Whereas, the gas supply (carrier gas and detector gas), column and data recording device are usually obtained from a different supplier to the instrument manufacturer (Rood 2007). The data recording device is usually a personal computer (PC), or with older GC systems a chart recorder. Most PC systems can also operate the GC instrumentation, this allows for automation and the use of an autosampler.

A fundamental measurement in gas chromatography is retention time (t_R), this is the duration taken for a compound to elute from the column and is considered to be a qualitative characteristic. The retention time of a compound is simply the sum of the time spent in the mobile phase and the stationary phase. However, as previously mentioned all compounds spend the same amount of time in the mobile phase for a given temperature and carrier gas velocity (Rood 2007). Therefore, the difference in retention time from one compound to another is simply a result of time spent in the stationary

phase. It is possible to measure the time spent in the mobile phase by injecting a non-retained compound. The peak resulting from the non-retained compound will be the first to elute, this is known as the void or dead time (t_M) (Hansen *et al.* 2012).

The solute species separate at different times due to the difference in the strength of the interactions with the stationary phase; these can be theoretically explained by equilibrium constants (Skoog *et al.* 2007). The equilibrium distribution coefficient, also known as the distribution constant, K_C, is equal to the concentration of the analyte in the stationary phase, C_S, over the concentration of the analyte in the mobile phase, C_M, shown in Equation 19. This can also be calculated using the number of moles of the analyte and the volume of both the stationary and mobile phase.

$$K_C = \frac{C_S}{C_M} = \frac{n_S/V_S}{n_M/V_M} \qquad \textit{Equation 19}$$

Distribution constant (K_C); Concentration in stationary phase (C_S); Concentration in mobile phase (C_M); Number of moles in stationary phase (n_S); Number of moles in mobile phase (n_M); Volume of stationary phase (V_S); Volume of mobile phase (V_M).

This partition ratio is ideally constant over a wide concentration window so that the concentration in the stationary phase is proportional to the concentration in the mobile phase; this results in Gaussian peaks (symmetrically shaped) and analyte retention times that are independent of the amount injected (Skoog *et al.* 2007). The distribution constant only describes the theoretical separation of components, and a more practical measurement of separation is the retention time (t_R).

Another useful value is the retention factor, *k*, which is independent of the mobile phase flow rate and column length, this is contrary to the retention time (Hansen *et al.* 2012). The retention factor can be easily determined from the chromatogram using Equation 20.

$$k = \frac{t_R - t_M}{t_M} \qquad \textit{Equation 20}$$

Retention factor (k); Retention time (t_R); Void time (t_M).

It should be mentioned that the instrumental parameters, such as oven temperature and carrier gas flow rate, in order to separate compounds of a similar structure. The resulting chromatogram will then exhibit resolved chromatographic peaks. Chapter three includes a variety of chromatograms that show complete separation of peaks resulting from the target analyte and other compounds present in the sample.

1.3.2 Quantitative analysis

One of the most popular ways of carrying out quantitative analysis in gas chromatography is to use a calibration procedure known as the "internal standard method"; the following section will describe in detail the approach used in this thesis.

Quantitative results were obtained by first identifying the sample analyte peak in the chromatogram by its retention time compared to that of a known standard of the compound of interest (this is the qualitative part of the experiment) and extrapolating the concentration from the compounds respective calibration curve (quantitative). In GC either the peak height or peak area can be used for quantitative purposes, however peak area was used for all GC measurements in this thesis. Peak height has an inverse relationship with peak width, the latter of which broadens when the retention factor increases which results in a decrease in peak height. Therefore, peak height is less reliable

than peak area which is independent of changes in the retention factor (Hansen *et al*. 2012). The calibration curves in this thesis were generated from a set of standard injections of increasing known concentrations. Each concentration was injected in triplicate and an average of the replicate peak areas was calculated and plotted against known concentration, the use of replicates reduces any variation from injection volumes thereby increasing accuracy. All calibration curves were generated from a minimum of four points i.e. using four different known concentrations of the analyte. The use on an internal standard was also employed as an additional measure for improved accuracy for the GC data acquisition in this thesis. An internal standard was included in both the calibration standard solutions and sample solutions, this normalises the data by reducing any variation from detector sensitivity. An internal standard should have a structure very similar to that of the analyte but should be absent from the sample being analysed, the internal standards chosen for this project are described in chapter three section 3.1.2. Calibration curves were generated by plotting the area ratio against concentration. The internal standard concentration is kept the same for every solution prepared, and the peak area of the analyte (standard or sample) is divided by the peak area of the internal standard (area ratio value). The inclusion of an internal standard is particularly important in the operation of a NPD (nitrogen-phosphorous detector) detector, as the sensitivity of this detector tends to drift.

1.3.3 Injector

The gas chromatographic data in this thesis was mostly obtained with an autosampler injection system (Clarus 580, Perkin Elmer), which provides precise sample introduction and eliminates user error. The sample volume must be consistent and should be introduced at a constant flow rate. The sample is introduced at the high temperature inlet with a rapid injection using a calibrated microsyringe, either manually or automatically. The inlet port should be heated to a temperature well above that of the boiling point of

the least volatile sample component (Skoog *et al.* 2007). The needle of the microsyringe pierces the septum housed in the inlet, this consumable part has a relatively short lifetime and regular replacement prevents bleed of volatile compounds onto the column. An inlet splitter is often used with modern capillary columns, which divides the sample between the column and the waste outlet preventing column overloading. Another component located in the inlet section before the column is the liner. This is a deactivated glass tube that allows the sample vapour to be directed onto the column, these can be modified with glass wool which traps any particulate matter and prevents column contamination.

Before samples are introduced to the GC they have to be collected, stored and transported before preparation. Biological samples contain a complex mix of compounds often requiring preparation procedures to extract the analyte and remove as many impurities as possible. There are many different types of extraction procedures such as solid phase extraction, liquid-liquid extraction, or microwave-assisted extraction to name a few. Sample transportation and sample storage requires conditions appropriate for preservation, for biological materials this usually requires refrigeration or freezing. Depending on the sample state, the method of collection and pre-treatment will vary. The primary focus of this project involved the analysis of porcine adipose tissue. Samples collected from the abattoir had to be transported and stored at -18°C until analysis could be performed. The preparation procedure for GC analysis utilised microwave-assisted extraction followed by solvent extraction, centrifugation, and in one method a solvent exchange step (see chapter three). Modern chromatographic systems can be fitted with automated sample preparation systems these utilise techniques such as solid-phase extraction, accelerated solvent extraction, or rapid evaporation. These systems are commercially available however they are often elaborate and expensive (Majors 2013), consequently they were not utilised for this project.

1.3.4 Carrier gas

The carrier gas is the mobile phase of the separation system. It is an inert gas that transports the sample from the injector, through the column, to the detector. The mobile gas phase is usually either high-purity helium, nitrogen or hydrogen. Optimisation of the carrier gas flow rate is required to efficiently separate the sample components. It should be noted that with some detectors, such as the nitrogen-phosphorous detector, the carrier gas must not influence the stability of the detector; in the current project the carrier gas was helium instead of hydrogen as the latter is used in the operation of the detector and would destabilise its response.

1.3.5 Stationary phase

GC columns vary by type (i.e. packed or capillary), dimensions (i.e. inner diameter and length), and stationary phases (i.e. polysiloxanes or polyethylene glycols). Most modern GCs tend to use capillary columns, also known as open-tubular columns, which have small internal diameters and lengths between 6-50 metres (Rotzsche *et al.* 2014). Capillary columns can be categorised into three groups: wall-coated open tubular columns (WCOT); porous-layer open tubular columns (PLOT); and support-coated open tubular columns (SCOT). WCOT columns are by far the most popular today, with use in over 80% of all applications, however PLOT columns are still in use for very volatile compounds whilst SCOT columns are rarely used today and were of most interest in the early days of capillary column development (Rotzsche *et al.* 2014).

Almost all modern commercial capillary columns are made from a fused-silica tubing consisting of high purity silicon dioxide that provides a very inert surface. This is usually coated with polyimide for increased strength and support, this coating results in the usual yellow-brown outer appearance (Rotzsche *et al.* 2014). In the case of WCOT columns the deactivated silica layer is coated with a thin-film of liquid stationary phase. Liquid stationary phases can be produced to achieve different polarities and it is common to use

polar phases for polar analytes and non-polar phases for non-polar analytes (Willett and Kealey 1987). Consequently, two columns were employed in this project to separate the target analytes from the other compounds in the solvent extract of adipose tissue; a low-polarity 5% phenyl 95 % methylpolysiloxane phase was used for androstenone determination and a high-polarity polyethylene glycol phase was used for skatole determination. Therefore, the procedures used in this thesis are considered to be gas-liquid chromatography, the gas is the mobile phase whereas the stationary phase is a high boiling point liquid adsorbed onto a solid coating.

1.3.6 Detectors

This project utilised both a flame ionisation detector (FID) and a nitrogen phosphorous detector (NPD) linked to a gas chromatograph as the reference technique for the analysis of the target analytes androstenone and skatole respectively in porcine adipose tissue samples. The NPD is a specific detector that responses to compounds containing nitrogen and/or phosphorous, whereas the FID is responsive to most compounds however it is less sensitive than the former (Scott, 2005). These detectors both work on the principle of ionisation; compounds eluting from the column are ionised and the magnitude of ionisation response, in the form of an electrical signal, is related to the quantity of the compound of interest (Patterson 1992).

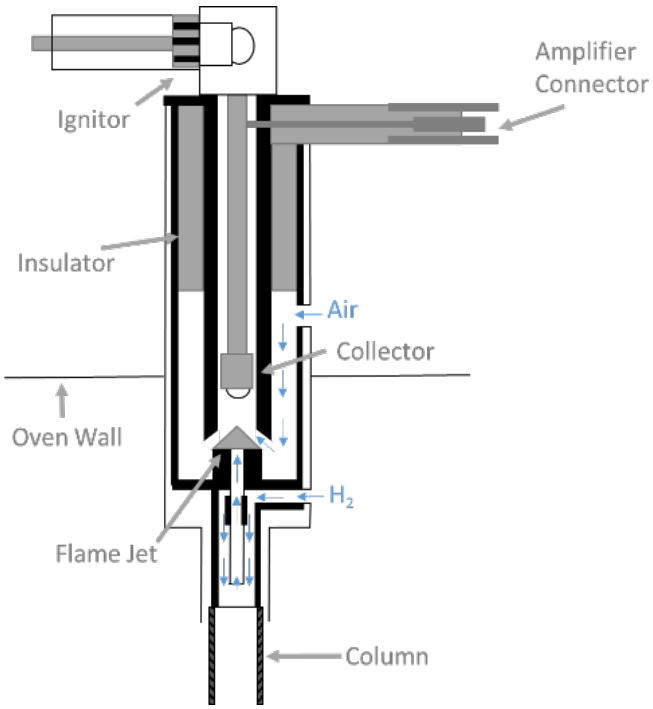

Figure 1.14. Diagram of a flame ionisation detector (FID). Reproduced with modification from the CLARUS 500/580 GC User's Guide (2010).

The FID, illustrated in Figure 1.14, is considered to be a universal detector and is mass sensitive, responding to carbon containing compounds (McMinn and Hill 1992). Ions are generated when the sample enters the detector and burned in the presence of hydrogen and air. These ions are collected and measured by the detector and the resulting signal is directly proportional to the concentration of the compounds present. A negative voltage is applied to the detector which enhances ion collection via a polarised electric field (*CLARUS 500/580 GC User's Guide* 2010).

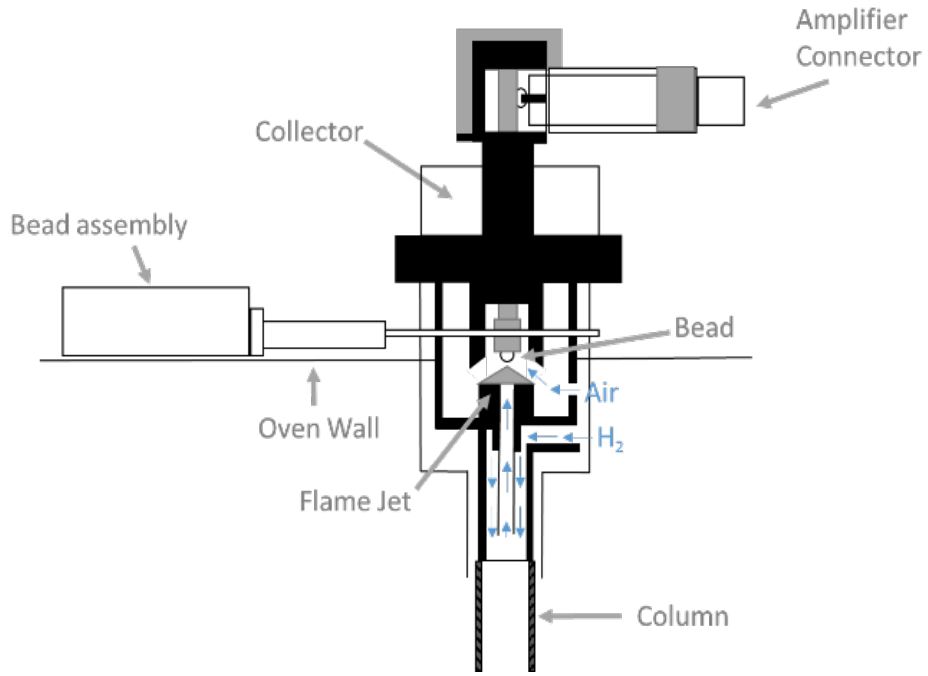

Figure 1.15. Diagram of a nitrogen-phosphorous detector (NPD). Reproduced with modification from the CLARUS 500/580 GC User's Guide (2010).

The NPD, or thermionic detector, employed for the detection of skatole in this project uses a rubidium bead, as illustrated in Figure 1.15. The glass bead containing the alkali metal, in this case rubidium, is moulded onto an electrical heater wire; this controls the source temperature through an adjustable applied current. The bead and wire constitute the thermionic source; this is where a plasma forms in the presence of hydrogen and air, which acts as the combustion zone. The most substantiated theory for the NPD response mechanism is the surface ionisation theory. This model assumes that the sample components are electronegatively decomposed at the source and selectively ionised, the increase in current measured is the result of the negative ions formed from this process (Poole 2015).

1.4 Research aims and objectives

The primary aim of the project was to evaluate, validate and apply the novel electrochemical sensor technology (Hart *et al,* 2017) to the analysis of boar taint compounds in porcine subcutaneous adipose tissue. In addition, studies investigating the electrochemical behaviour of compounds naturally occurring in porcine subcutaneous adipose tissue led to the development of a novel assay for the simultaneous quantification of the water-soluble vitamins thiamine, riboflavin, and pyridoxine.

Objectives:

- Evaluate peer-reviewed literature to identify compounds that naturally occur in porcine subcutaneous adipose tissue, documenting their reported concentrations.
- Evaluate peer-reviewed literature to determine which of these compounds could exhibit electrochemical behaviour that could interfere with the (bio)sensor response.
- Characterise the electrochemical behaviour of any compound identified that could interfere with the electrochemical measurements.
- Characterisation of the electrochemical measurement of skatole and androstenone using voltammetry and amperometry respectively.
- Develop extraction procedures and adapt gas chromatographic methods (the reference method) for the quantification of skatole and androstenone in samples of porcine subcutaneous adipose tissue.
- Validate the novel electrochemical sensor system, for the analysis of subcutaneous adipose tissue samples, against the gas chromatographic reference method.
- Investigate and adapt electrochemical instrumentation and apparatus to allow for dual potentiostatic measurements of skatole and androstenone simultaneously with control from a single portable device.
- Conduct an initial evaluation of the prototype device on the abattoir processing line and validate the responses with the laboratory based reference method.

Chapter Two

Characterisation of an electrochemical sensor and biosensor for the measurement of boar taint compounds

Chapter Two Contents

Table of Figures

Chapter Summary

The second chapter begins with a literature review of the compounds endogenous to pork meat and adipose tissue, this includes the two boar taint analytes, skatole and androstenone, and any other compounds such as amino acids, vitamins, fatty acids and hormones. This review also looks into the redox properties of these compounds as a primary indicator as to whether they may or may not respond at the electrochemical sensor and biosensor used for the measurement of the boar taint compounds. This is followed by a description of the experimental procedures used to quantify the boar taint compounds and determine if the other endogenous compounds identified as possible interferences result in a response at the electrochemical sensor or biosensor. A discussion of the results follows; the quantification of the boar taint compounds in a controlled buffered solution is described and a conclusion is drawn that none of the identified endogenous compounds interfere with the measurement of skatole or androstenone.

Chapter Two

2.1 Introduction and literature review

The voltammetric sensor and amperometric biosensor were developed to measure skatole and androstenone respectively (Hart et al., 2017). These compounds have been attributed to the unfavourable phenomenon known as boar taint in pig meat products. The two electrochemical sensors have been developed with the aim of directly analysing these compounds in porcine adipose tissue. Initial characterisation studies for this sensor system began with an investigation into the endogenous compounds reported in porcine adipose tissue, with an additional search into the redox properties of these naturally occurring compounds. This formed the first phase of the investigation into compounds which could possibly interfere with the voltammetric or amperometric response observed at the sensor and biosensor. The compound groups of interest are vitamins, fatty acids, amino acids, and hormones. The target analytes, skatole and androstenone, and other identified endogenous species, were studied by voltammetry or chronoamperometry using disposable screen-printed carbon sensors; the resulting electrochemical behaviour is discussed in section 2.3.

2.1.1 Endogenous compounds and their redox properties

2.1.1.1 Vitamins

Vitamins are grouped into two classes based on their solubility in either lipid or aqueous media. Vitamins that are more lipophilic can be stored in adipose tissue for long periods of time, whereas water soluble vitamins are easily excreted (Arneson and Brickell 2007). An extensive study of the literature reporting concentrations of both fat and water soluble vitamins in pig tissue are displayed in the Appendix Tables 5-12. There are many variables involved in the measurement of endogenous concentrations, this includes but is not

limited to the feed content, pig breed, age or weight at slaughter, sample preparation method and analytical measurement technique; all of which have been outlined in the tables where available.

2.1.1.1.1 Water soluble vitamins

Vitamin C is the common name for the L-enantiomer of ascorbic acid. This water-soluble compound requires derivatisation to a synthetic compound such as ascorbyl palmitate or ascorbyl stearate before it can be miscible with a lipid phase (Reische *et al.* 2008). Therefore, it is unsurprising that no reports have indicated its detection or measurement in porcine adipose tissue.

L-ascorbic acid is well known to exhibit strong redox properties, which has been exploited by several research groups using carbon based electrodes under similar buffer conditions to those employed in this project (Hu *et al.* 2001, Nassef *et al.* 2008, Revlin and John 2012); Appendix Table 4. The reported concentrations of L-ascorbic acid have been documented in Appendix Table 5 for pig muscle tissue obtained from both loin and ham cuts; this information could be useful for future work where SPCEs could be used to interrogate muscle tissue directly.

Vitamin B is the term used for a group of 8 vitamins: thiamine (B_1), riboflavin (B_2), nicotinamide (B_3), pantothenic acid (B_5), pyridoxine (B_6), biotin (B_7), folic acid (B_7), cobalamin (B_{12}); all of which play important roles in cell metabolism, some of which will be discussed in more detail in chapter five. These B vitamin compounds have little structural resemblance, but they have a physical similarity in that they are all water-soluble. Their concentrations in muscle tissue are well documented and these values have been collated in Appendix Table 6 (Jackson *et al.* 1945, Müller 1993, Hägg and Kumpulainen 1994, Leonhardt and Wenk 1997, Esteve *et al.* 2002, Lombardi-Boccia *et al.* 2005, Böhmer and Roth-Maier 2007, Greenfield *et al.* 2009, USDA 2009). Only a single

literature source has been found to report the concentration of B vitamins in porcine adipose tissue. Greenfield's (2009) research group performed an extensive review into the nutritional composition of pork, in order to update the national food composition database (NUTTAB) compiled by Food Standards Australia New Zealand (FSANZ). This study provides a range of concentrations determined for seven B-vitamins from a variety of pork cuts sourced from several retail outlets; the values have been listed in Appendix Table 7. The B vitamins biotin and cobalamin will not be investigated in the interference studies; biotin was not measurable in adipose tissue, whereas cobalamin was reported at very low concentrations (≤0.01 mg/kg).

The electro-activity of thiamine has been documented at various electrode materials, including some based on carbon (Hart *et al.* 1995, Aboul-Kasim 2000, Oni *et al.* 2002, Sutton and Shabangi 2004); however it should be noted that none of these studies reported a response at a neutral pH (Appendix Table 4).

The electroanalysis of riboflavin has however been achieved at a neutral pH by several research groups using carbon electrodes. However, the oxidation peak potentials were in the negative region, outside of our potential window of interest (Safavi *et al.* 2010, Revlin and John 2012, Nie *et al.* 2013); experimental parameters are outlined in Appendix Table 4.

The electrochemical oxidation of nicotinamide has been documented by Hu and co-workers (2001) at a carbon disk electrode. Other authors who have explored the electrochemistry of niacin have exploited the reduction of this compound at -1.5 V and -1.3 V (Çakir *et al.* 2001, Kotkar and Srivastava 2008); Appendix Table 4.

Only the D (+) form of pantothenic acid is naturally occurring and biologically active (Bird and Thompson 1967). A review of the literature has found that pantothenic acid has not

been measured at carbon electrodes; however the alcohol derivative, pantothenol, is measureable by voltammetry (Wang and Tseng 2001). However, the measurement of this compound has not been reported in porcine adipose tissue.

There are six B_6 vitamers, however, pyridoxine is the only one used as a food fortifier and it is commercially available as its hydrochloride salt (Ball, 2006). Pyridoxine electro-oxidation at carbon based electrode has been reported using pH conditions similar to those of interest in this project (Hu *et al.* 2001, Qu *et al.* 2004, Teixeira *et al.* 2004, Fonseca *et al.* 2011, Zhang 2011); Appendix Table 4. The peak potential values ranged from +0.71 to +1.05 V; this suggests that we may encounter electro-activity at the SPCEs (vs. Ag/AgCl) in our potential window of interest (+0.2 to +1.2 V).

Folic acid, also known as pteroylmonoglutamic acid, has been reported in several studies to be electrochemically active at glassy carbon electrodes (Xiao *et al.* 2008, Kalimuthu and John 2009, Revlin and John 2012); two of these studies were performed with a neutral pH electrolyte and reported an oxidation peak at +0.8 V (Appendix Table 4); this is also within the applied potential window of interest for skatole determination in this project.

2.1.1.1.2 Fat soluble vitamins

Vitamins A, D, E, and K are fat soluble, therefore their measurement in porcine adipose tissue has been reported with regards to the nutritional content of pork far more frequently than that of water-soluble vitamins. Pig producers sometimes supplement animal feed with approved nutritional compounds, including some vitamins (Burild *et al.* 2016), this can enhance the quality of the final product by improving the health of livestock. The antioxidant properties of vitamin E and C have been well documented for their stabilising effects on meat colour and flavour (Warriss 2010). However, the naturally occurring concentrations of both vitamin C and vitamin K in meat are not considered to be of nutritional value (Warriss 2010). Subsequently, like that of vitamin C, values for

vitamin K concentration have only been reported for muscle tissue (Appendix Table 9) and not adipose tissue.

The concentration of vitamin A, retinol, in porcine adipose tissue was shown to increase more than two fold where dietary supplementation was employed (Olivares *et al.* 2009); Appendix Table 10. The retinol concentrations reported in the adipose tissue of shop purchased pork cuts was in the range of 0.17-0.3 mg/kg (Greenfield *et al.* 2009).

There are several forms of vitamin D: vitamin D_3 or cholecalciferol is the most important source of dietary vitamin D along with its metabolite calcifediol or 25-hydroxyvitamin D_3; both of which have been approved for supplementary use in pig feed (Burild *et al.* 2016). Appendix Table 11 displays the reported concentration of these two compounds in porcine adipose tissue; the ranges are D_3 0.057-0.590 µg/100g and 25(OH)D_3 0.186-0.244 µg/100g (Clausen *et al.* 2003, Jakobsen *et al.* 2007).

It is common place for vitamin E, α-tocopherol, and its more stable derivatives to supplement pig diets (Anderson *et al.* 1995). The wealth of studies reporting their concentration in porcine tissue supports this notion (Appendix Table 12). Concentrations of vitamin E in adipose tissue, where the diet was not enriched, ranged from 0.99 to 12.24 mg/kg (Leonhardt *et al.* 1997, Gebert *et al.* 1999).

The electrochemical measurement of these fat-soluble compounds has been achieved in both acetonitrile and methanol, as outlined in Appendix Table 4 (Hart *et al.,* 1984, Wring *et al.,* 1988, Hart *et al*., 1992, Wilson *et al*., 2006). Owing to their lack of solubility in water, measurement in aqueous media has not been reported. Therefore, their measurement will not be investigated in the upcoming interference studies.

2.1.1.2 Fatty acids

Adipose tissue contains a range of hydrophobic compounds including saturated, mono-unsaturated, and poly-unsaturated fatty acids (Sinclair *et al.* 2010). These have not been reported as directly electrochemically active at plain screen-printed carbon electrodes, therefore, their presence was not considered to be a potential interference in the measurement of skatole. In addition, a previous study has shown the fatty acids linoleic acid, oleic acid and palmitic acid do not respond at the androstenone biosensor (Crew, 2018).

2.1.1.3 Amino acids

Many publications reporting amino acid quantification in porcine tissue analysed samples from processed meats which have undergone proteolysis and lipolysis (Toldra´ 1998). The complex biochemical pathways of proteolysis result in high levels of free amino acids, therefore these reports are not comparable to the raw unprocessed tissue concentrations required for this review. The documentation of amino acid concentrations in fresh tissue is limited; Toldrà and co-workers (1992) measured the concentration of nine amino acids in both muscle and adipose tissue whereas Lorenzo and co-workers (2008) only analysed the muscle tissue. A comparison of the concentrations reported in muscle tissue (Appendix Table 13) show lower concentrations for the later study; this could be attributed to the different methods of analysis (HPLC vs. enzyme assay), however a similar distribution pattern was displayed for the concentrations of the different compounds (indicated by the superscript ranking in Appendix Table 13). The adipose tissue levels ranged from 188 mg/kg for alanine down to 6.92 mg/kg for histidine.

Most amino acids and their peptides are not readily oxidisable at common electrode materials (Flanagan, Perrett, and Whelpton, 2005). Jacobs, Peairs, and Venton (2010) note that the three readily electroactive amino acids are tyrosine, tryptophan, and cysteine

and a summary of their electrochemical behaviour at carbon electrodes under neutral pH conditions has been compiled in Appendix Table 14; (Fiorucci and Cavalheiro 2002, Huang *et al.* 2008, Deng *et al.* 2009). These particular amino acids have not been quantified in raw adipose tissue, therefore it is likely that they are either not present as free amino acids or present at negligible concentrations. Therefore, these electroactive amino acid compounds will not be investigated in the interference studies using SPCEs (vs. Ag/AgCl) as they are unlikely to be present at a concentration in adipose tissue that would result in an interference.

The reported amino acids measurable in porcine adipose tissue: alanine, glycine, taurine, glutamine, glutamic acid, proline, arginine, threonine, histidine are only documented in the literature as being electrochemically detectable at modified electrode surfaces, often using amino acid oxidase enzymes (Kacaniklic *et al.* 1994, Sarkar *et al.* 1999, Rosini *et al.* 2008, Revenga-Parra *et al.* 2017). The electrochemical biosensor used in this thesis does not use enzymes that respond to amino acids, therefore it was not considered necessary to further investigate their electrochemical behaviour in this project.

2.1.1.4 Hormones

Hormone compounds can be generally categorised as; single amino acid derived, protein and peptide derived, and steroidal (Kovacs and Ojeda 2011). The steroid hormone group are generally the most lipophilic, therefore their measurement has been most heavily reported in porcine adipose tissue. Appendix Table 15 lists the concentrations of nine steroid hormones measured in porcine tissue (Claus *et al.* 1989, Hartmann *et al.* 1998, Yang *et al.* 2009); the concentrations of which varied depending on whether the measurement was made in muscle or adipose tissue, and also depending on the type of pig. Pig type often relates to gender, ability to breed, and age; the common types are boars, barrows, gilts, and sows. All of these factors, whether based on genetic or

environmental differences, can vary the endogenous levels of chemicals within the animal.

It appears that there are no reports on the electrochemical measurement of steroid hormones at plain SPCEs. Pemberton, Mottram and Hart (2005) note that although some steroids are directly electrochemically oxidisable at traditional electrode materials, such as glassy carbon electrodes, they require high overpotentials and do not exhibit the required specificity for biological samples. Therefore, it is unlikely that steroid hormones would be oxidisable at the relatively low operating potentials applied to the sensor (+0.2 to +1.2 V) and the biosensor (+0.05 V). In addition, a personal communication has confirmed that the biosensor does not respond to several steroid hormones commonly found in porcine adipose tissue at the maximum concentrations reported in the literature (Claus *et al.* 1989); including testosterone (20 ppb), estrone (1.38 ppb) and β-estradiol (0.78 ppb) (Crew, 2018).

2.1.2 Boar taint compounds and their redox properties

2.1.2.1 Skatole

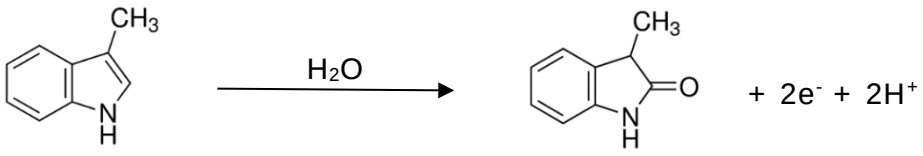

Figure 2.1. Oxidation of 3-methylindole to 3-methyl-2-oxindole (reproduced from European Patent 2966441)

The mechanism in Figure 2.1 (reproduced from European Patent 2966441) shows the proposed reactants and products involved in the electrochemical oxidation of skatole (3-methylindole) which gives rise to a voltammetric response at the SPCE (vs. Ag/AgCl). The

species of interest, commonly known as skatole, is a heterocyclic secondary amine; it is a weak base with a pK_a of 4.6 (Bansal 1999). Skatole is derived from the amino acid tryptophan (Claus *et al.* 1994), it has a fecal odour (Whitmore 1951) which can result in an unpleasant taste or scent when present in pork. Indole, also a derivative of tryptophan (Claus *et al.* 1994), has been suggested to play a minor role in the unpleasant odour of boar taint. It is structuraly similar to skatole but is a stronger base than skatole; with a pK_a of 3.63 (Bansal 1999).

The electrochemical oxidation of indole, and its derivatives, has been of relevance to the clinical sector and food industry for several decades (Goyal, Kumar and Singhal, 1998). A variety of electrode materials have been reported for the determination of indolic-compounds, such as platinum (Pingarron Carrazon, Reviejo Garcia and Polo Diez, 1990), carbon-fibre (Gómez-Gil et al., 2003), mercury (Tucker *et al.* 1989), boron-doped diamond (Belghiti et al., 2016), glassy carbon electrodes and screen printed carbon electrodes (Maesa *et al.* 2013). Many of these would be unsuitable for the proposed measurement in adipose tissue on the abattoir line; for example mercury would be unsuitable due to its toxic nature in a food production environment. Additionally, many of the other electrode materials suffer significant fouling effects, making them unsuitable for rapid analyses owing to the time-consuming cleaning process required between scans. Consequently, the report by Maesa and co-workers (2013) is of most relevance to the patented sensor as they also use screen-printed electrodes to measure skatole, however, they did not achieve a limit of detection suitable for the measurement skatole in real samples. The inventors of the UK patent (application 1212727.0, file date: 31-07-09) were the first to report the application of disposable screen-printed carbon electrodes for the direct voltammetric measurement of skatole in adipose tissue without any sample preparation (Hart *et al*., 2017).

2.1.2.2 Androstenone

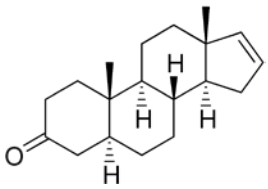

Figure 2.2. Structure of 5α-androst-16-en-3-one

The other analyte of interest in this project is 5α-androst-16-en-3-one, commonly known as androstenone; shown in Figure 2.2. The electrochemical process giving rise to the androstenone response at the patented biosensor has been described in detail in chapter one section 1.2.4.5; a schematic diagram depicting the proposed electron transfer mechanism is shown in chapter one Figure 1.11.

The analyte androstenone is an androgen, it belongs to a group of C19 Δ16 steroid compounds, which after production in the testes can be transported via the blood stream to the liver where it can be metabolised. Remaining androstenone, which has not been metabolised, can be stored in the adipose tissue of pigs (Bonneau and Terqui 1983). Androstenone is the most lipophilic of the C19 Δ16 steroids (Claus 1979). The water solubility of the steroidal compound androstenone has been reported by Amoore and Buttery (1978) to be 0.00023 g/l (at 25°C), indicating that it is more lipophilic than skatole which has a reported solubility of 0.45 g/l (at 20°C) (Windholz and Budavari 1983).

The biosensor (UK patent application 1212727.0, file date: 31-07-09) patented for the determination of androstenone is the first to use 3α-hydroxysteroid dehydrogenase (3α-HSD) as the biological recognition element in a screen printed biosensor (Hart *et al*., 2017). The mapping of this enzyme to chromosome 4q16-4q21 has been successfully

achieved in pigs (von Teichman *et al.* 2001). Another publication in the same year by Dufort and co-workers (2001) confirmed that this enzyme, 3α-HSD, converts androstenone to androstenol in the presence of NADPH. In a later study, Doran and co-workers (2004) demonstrated that the enzyme 3β-HSD is capable of catalysing the same reaction. This study also demonstrated that the level of 3β-HSD protein expression in isolated pig liver microsomes was shown to be positively related to the rate of androstenone metabolism. Therefore, the literature studies demonstrates that both, the rate of androstenone metabolism and the rate of androstenone production play an important role in the regulation of androstenone deposition in the adipose tissue of pigs and consequently the development of boar taint.

The first reported use of 3α-HSD for the electrochemical determination of a steroidal compound was reported by Teodorczyk and Purdyt in 1990; in this study an enzyme modified glassy carbon electrode was used to monitor the NADH produced from the enzymatic oxidation of androsterone. In 2012, Mundaca and co-workers adopted a similar approach to the analysis of androsterone. The composite electrode contained the enzyme 3α-HSD, multi-walled carbon nanotubes, the co-factor NAD+ and an ionic liquid; this biosensor was used in conjunction with amperometry in stirred solution to detect the NADH generated in the enzymatic reaction. The only other reported use of a 3-hydroxysteroid dehydrogenase enzyme for the determination of steroidal compounds, used a mutated strain of the enzyme in conjunction with fluorescence detection (Xiong *et al.* 2009). Therefore, the authors of the patent (European Patent 2966441) are the first to report the use of a screen-printed biosensor incorporating the enzyme 3α-HSD for the measurement of androstenone, via the depletion of NADH, directly in the adipose tissue of pigs post-mortem.

2.2 Experimental

2.2.1 Apparatus and instrumentation

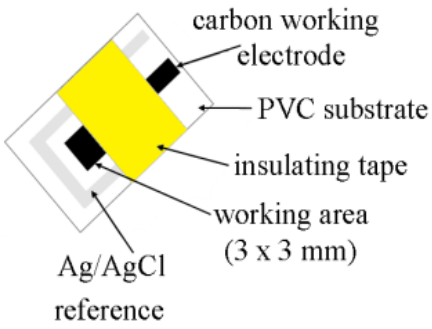

Figure 2.3. Diagram of a screen printed sensor

All voltammetric and chronoamperometric measurements were carried out with a µAutolab III potentiostat interfaced to a PC for data acquisition via the NOVA v1.10 (Metrohm, Netherlands) software package. Figure 2.3 depicts the SPCEs supplied by Gwent Electronic Materials Ltd (Pontypool, UK); the working electrode is fabricated using a carbon ink (C2030519P4) and the reference electrode is fabricated using a Ag/AgCl ink (C61003P7).

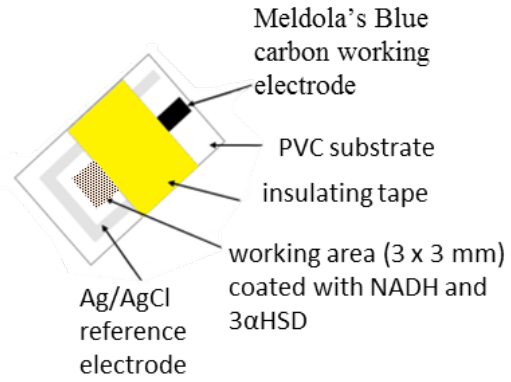

Figure 2.4. Diagram of a screen printed biosensor

Figure 2.4 depicts the screen-printed Meldola's Blue modified carbon electrode (BE2031028D1/247) supplied by Gwent Electronic Materials Ltd (Pontypool, UK) with an additional working electrode modification of drop-coated cofactor (NADH) and enzyme (3α-HSD) (Hart *et al*., 2017).

Measurements of pH were obtained with a Testo 205 probe (Testo Ltd, Alton): this dual device also monitors temperature and has sharp sensor tips suitable for piercing adipose or muscle tissue. The Agriculture and Horticulture Development Board (2010) released a report evaluating a range of pH-temperature probes for pork monitoring, the results concluded that the Testo 205 probe was the most practical in terms of stability, ease of use, and maintenance.

2.2.2 Chemicals and reagents

All reagents were of analytical grade and purchased from Sigma Aldrich (Poole, UK) unless specified otherwise. Monosodium dihydrogen phosphate, disodium monohydrogen phosphate and trisodium phosphate were obtained from BDH Lab Supplies (Poole, UK). Stock solutions of these phosphate buffers were prepared to a concentration of 0.5 M by dissolving the appropriate mass in deionised water; these were then titrated together to achieve the desired pH. Stock solutions of 1.0 M sodium chloride and 0.1 M sodium hydroxide were prepared by dissolving the appropriate mass in deionised water.

A 10 mM skatole stock solution was prepared by dissolving the required mass in methanol (HPLC grade purchased from Fisher Scientific (Loughborough, UK)). Working standards were prepared by diluting the skatole stock solution with phosphate buffer (0.1 M final concentration), sodium chloride (0.1 M final concentration) and methanol (5% final volume); working skatole concentrations specified in each procedure. The pH of the phosphate buffered solution was pH 7 unless specified otherwise.

Stock solutions (50 mM) of thiamine, pantothenic acid, nicotinamide, and pyridoxine were prepared by dissolving the required mass in deionised water. Working standards (5 mM) for cyclic voltammetric studies were prepared by diluting the stock solution with the phosphate buffer and sodium chloride solutions (0.1 M final concentration). Riboflavin and folic acid stock solutions (20 mM) were prepared by dissolving the required mass in 0.1 M sodium hydroxide. Working standards (5 mM) for cyclic voltammetric studies were prepared by diluting the stock solution with the phosphate buffer and sodium chloride solutions (0.1 M final concentration). The working concentrations of each vitamin compound used in the differential pulse voltammetric studies are listed in Table 3.

A 30 µg/ml stock solution of the reduced form of ß-nicotinamide adenine dinucleotide disodium salt (NADH) was prepared with a 0.1 M pH 7.0 phosphate buffer solution. A

solution of 3αHSD, 3α-Hydroxysteroid Dehydrogenase from Pseudomonas testosterone, was prepared by adding 150 µL of 0.1 M phosphate buffer to 50 units of enzyme; this was mixed by slow speed vortex. Then 100 µL of the NADH solution was added to the enzyme vial and mixed by slow speed vortex. The final mass of NADH was 120 µg with 2 units of 3αHSD per biosensor. The solution was deposited using a Barky pipette to dispense 10 µL of the solution onto the MB-SPCEs which were stored in a refrigerated (4°C) desiccator under a vacuum for 24 hours to allow the coating to dry down. All analyses with biosensors were carried out within 48 hours of preparation.

A 1 mg/ml stock solution of androstenone was prepared by dissolving the required mass in methanol. Working standards were prepared by diluting the androstenone stock solution with the phosphate buffer (0.1 M final concentration), sodium chloride (0.1 M final concentration) and methanol (5% final volume); working androstenone concentrations specified in each procedure.

2.2.3 Procedures

2.2.3.1 Cyclic voltammetric behaviour of skatole

All measurements of skatole were performed by lowering a SPCE (vs. Ag/AgCl) into a voltammetric cell containing 10 ml of the working solution (cell configuration shown in chapter one Figure 1.1B). The cyclic voltammetric scan window was 0 V to +1 V, scan rate has been specified in each procedure.

The effect of the presence of sodium chloride on the voltammetric behaviour of skatole (1 mM) was studied at scan rates of 50 and 100 mV/s.

The effect of pH on the cyclic voltammetric behaviour of skatole (1 mM) was observed with a phosphate buffered solution in the range pH 5-9. This study was performed at a 50 mV/s scan rate.

The effect of scan rate on the cyclic voltammetric behaviour of skatole (1 mM) was determined over the scan rate range 20-200 mV/s.

The possibility of re-using screen printed carbon electrodes for the measurement of skatole was investigated; repeat scans were obtained using a single SPCE (vs. Ag/AgCl) in a skatole solution (1 mM) at a scan rate of 50 mV/s.

2.2.3.2 Differential pulse voltammetric calibration of skatole

The parameters for the differential pulse voltammetry procedure were as follows: equilibration time 10 s; starting potential 0 V; end potential +1 V; scan rate 50 mV/s; step potential 0.005 V; step width 0.1 s; modulation amplitude 0.005 V; modulation time 0.05 s. The skatole calibration study was performed over the concentration range 2-100 µM.

2.2.3.3 Interference studies with water soluble vitamins

2.2.3.3.1 Cyclic voltammetry

Initial studies were carried out into the electrochemical behaviour of thiamine, riboflavin, nicotinamide, pantothenic acid, pyridoxine, and folic acid at a scan rate of 50 mV/s.

2.2.3.3.2 Differential pulse voltammetry

The differential pulse voltammetric measurement of skatole (20 µM) was carried out in the presence and the absence of the individual vitamins (concentrations listed in Table 3).

2.2.3.4 Chronoamperometric determination of androstenone

2.2.3.4.1 Androstenone calibration

An androstenone calibration was performed using biosensors (3αHSD-NADH-MB-SPCEs vs. Ag/AgCl) prepared 24 hours prior to use; the biosensor fabrication method is described in section 2.2.2. The standards were prepared in 0.1 M phosphate buffer with 0.1 M sodium chloride, and a 100 µL aliquot was pipetted onto the electrode surface to give full electrode coverage as previously shown in chapter one Figure 1.1C. The androstenone concentration range was 1.835–7.341 µM (0.5-2.0 ppm) with a final methanol volume of 5%. Measurements were performed by applying a potential of 0.05 V at the working electrode 5 s after the solution was pipetted on the electrode surface. The current response was monitored for a duration of 60 s.

2.3 Results and discussions

2.3.1 Voltammetric behaviour of skatole

2.3.1.1 Cyclic voltammetric behaviour and optimisation of buffer conditions

2.3.1.1.1 Effect of sodium chloride

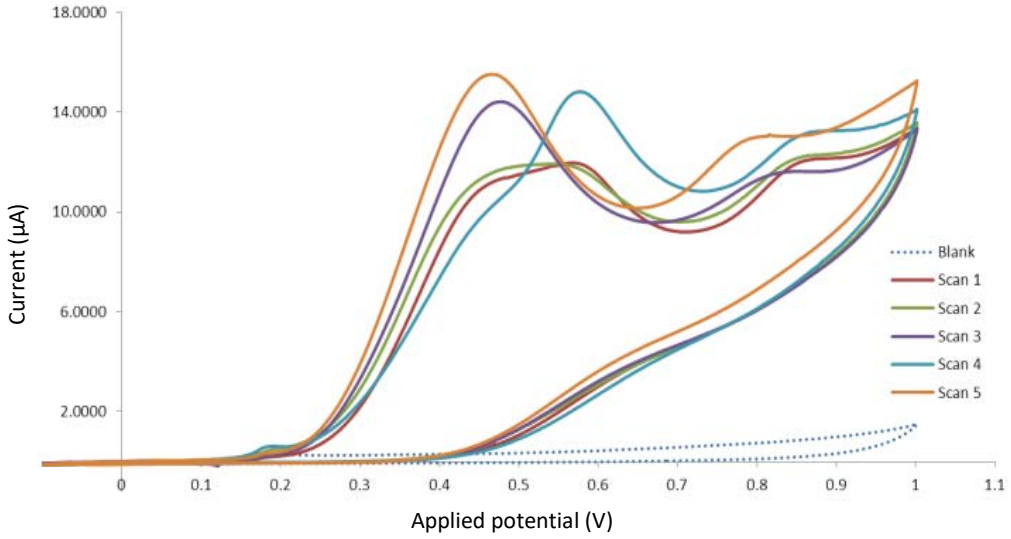

Figure 2.5. Cyclic voltammograms obtai ning using SPCEs (vs. Ag/AgCl) with a solution containing 1 mM skatole in 0.1 M phosphate buffer at pH 7 without sodium chloride. Starting potential: 0 V, switching potential: +1 V. Scan rate: 50 mV/s.

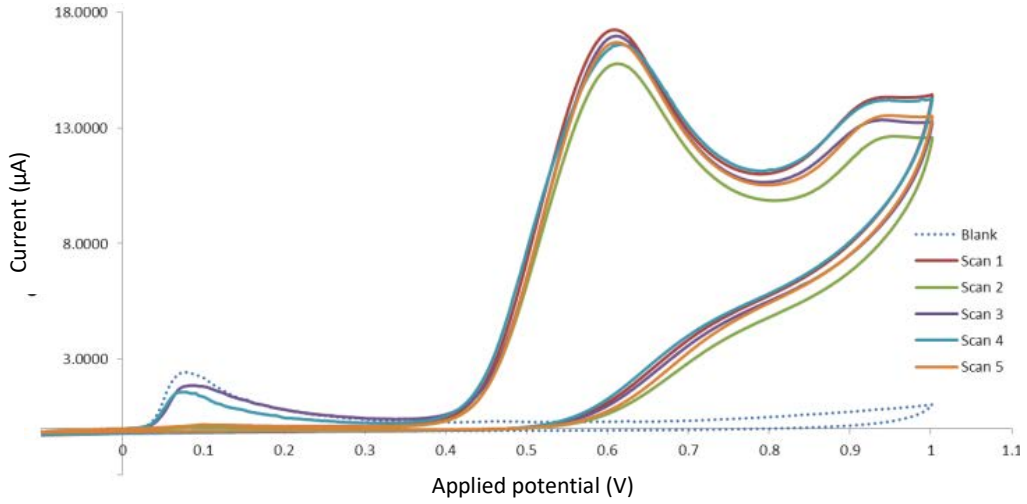

Figure 2.6. Cyclic voltammograms obtaining using SPCEs (vs. Ag/AgCl) with a solution containing 1 mM skatole in 0.1 M phosphate buffer at pH 7 with 0.1 M sodium chloride. Starting potential: 0 V, switching potential: +1 V. Scan rate: 50 mV/s.

Salt naturally occurs in cells, including those found in adipose tissue (Ho *et al.* 1994) therefore any voltammetric studies performed in solution should contain this component to best represent the sample that the sensors will be applied to. Sodium chloride is often used in electroanalysis to improve the conductivity of the electrolyte (Zoski 2007) which allows for a stable half-cell. The cyclic voltammograms in Figure 2.5 and Figure 2.6 demonstrate the stabilisation of the skatole oxidation current response in the presence of sodium chloride (n=5); this study was performed at pH 7 which was the average pH of adipose tissue observed on the abattoir line (Appendix Table 1 – data obtained by K Westmacott). The coefficient of variation values presented in Table 2.1 and Table 2.2 indicate that incorporating sodium chloride into the electrolyte improves response precision. Additionally, these measurements were performed at both 50 and 100 mV/s scan rates; 50 mV/s provided better measurement precision over 100 mV/s. Figure 2.7 demonstrates that the presence of sodium chloride significantly improves precision.

These studies were performed with a single solution using new SPCEs (vs. Ag/AgCl) for each measurement, this data therefore indicates that the electrodes have been printed with excellent precision.

Table 2.1. Effect of sodium chloride concentration and scan rate on the precision of skatole peak current values represented as coefficient of variation calculations (n=5).

Scan rate	0.0 M Sodium chloride	0.1 M Sodium chloride
50 mV/s	Coefficient of variation = 13.4 %	Coefficient of variation = 3.6 %
100 mV/s	Coefficient of variation = 10.3 %	Coefficient of variation = 7.4 %

Table 2.2. Effect of sodium chloride concentration and scan rate on precision of skatole peak potential values represented as coefficient of variation calculations (n=5).

Scan rate	0.0 M Sodium chloride	0.1 M Sodium chloride
50 mV/s	Coefficient of variation = 8.2 %	Coefficient of variation = 0.0 %
100 mV/s	Coefficient of variation = 6.3 %	Coefficient of variation = 3.4 %

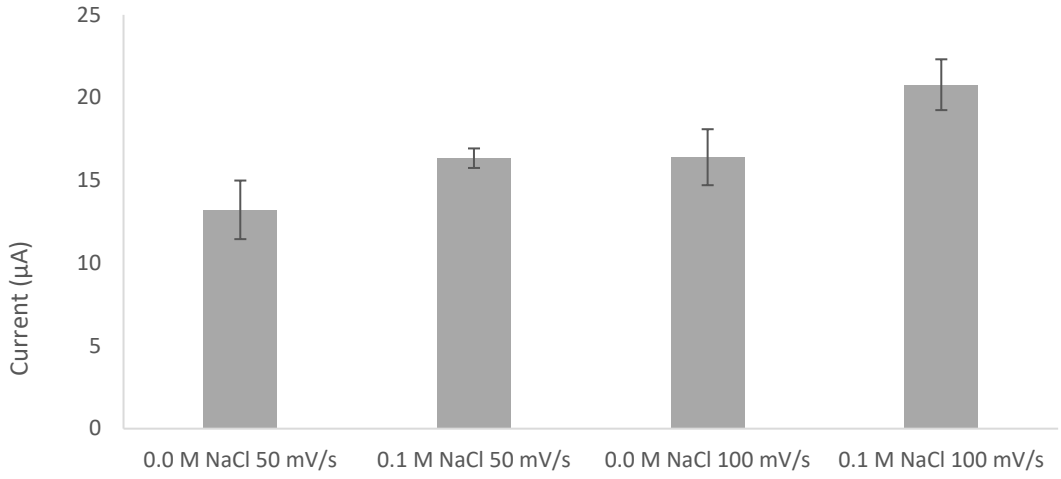

Figure 2.7. Bar chart of skatole peak height (µA) in the presence and absence of sodium chloride at 50 mV/s and 100 mV/s scan rate (n=5).

2.3.1.1.2 Effect of pH

Skatole is electroactive over the pH range 5-9. Figure 2.8A shows that the peak potential decreases with increasing pH with a break point around pH 7; this suggests an apparent pKa value of 7. Figure 2.8B shows that the peak current also decreases with pH and again there is a break point of around 7. It should be mentioned that the pH of adipose tissue is typically pH 7.02 (pH range 6.7-7.54: Appendix Table 2.1), consequently there is little change in the magnitude of the peak current at the expected pH of the samples. At this stage the results indicate that the voltammetric method for the measurement of skatole in adipose tissue is readily feasible.

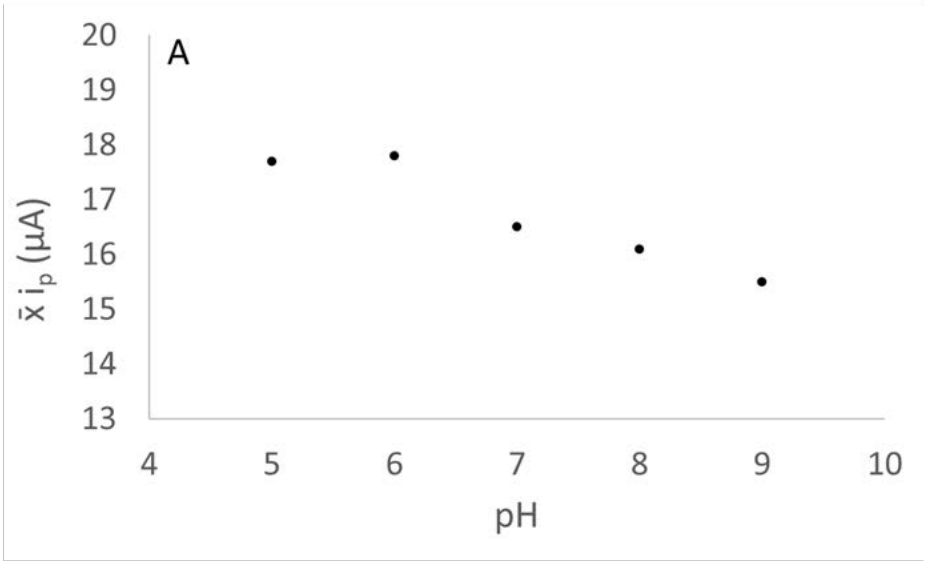

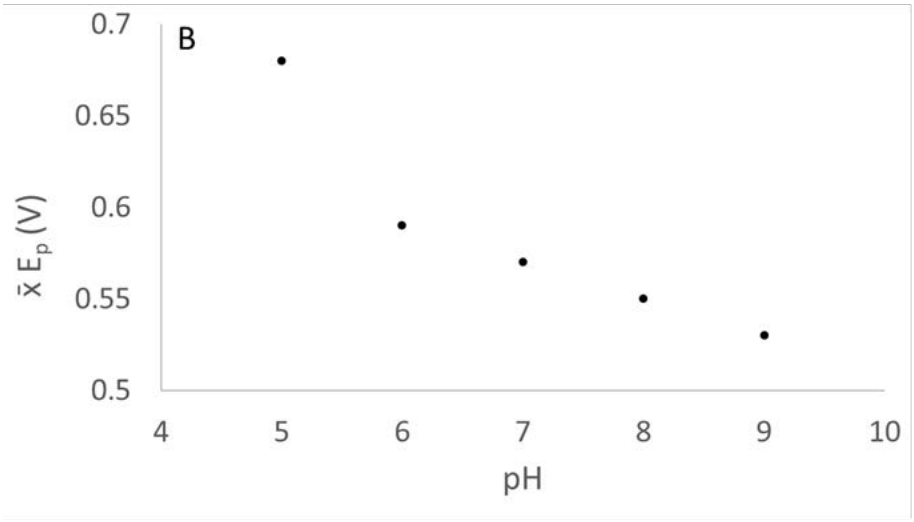

Figure 2.8. (A) Plot of peak current vs. pH and (B) plot of peak potential vs. pH (n=5). Plots were constructed from cyclic voltammograms obtained using SPCEs (vs. Ag/AgCl) with a solution containing 1 mM skatole in 0.1 M phosphate buffer at pH 7 with 0.1 M sodium chloride. Starting potential: 0.0 V, switching potential: +1.0 V. Scan rate: 50 mV/s.

2.3.1.1.3 Effect of scan rate

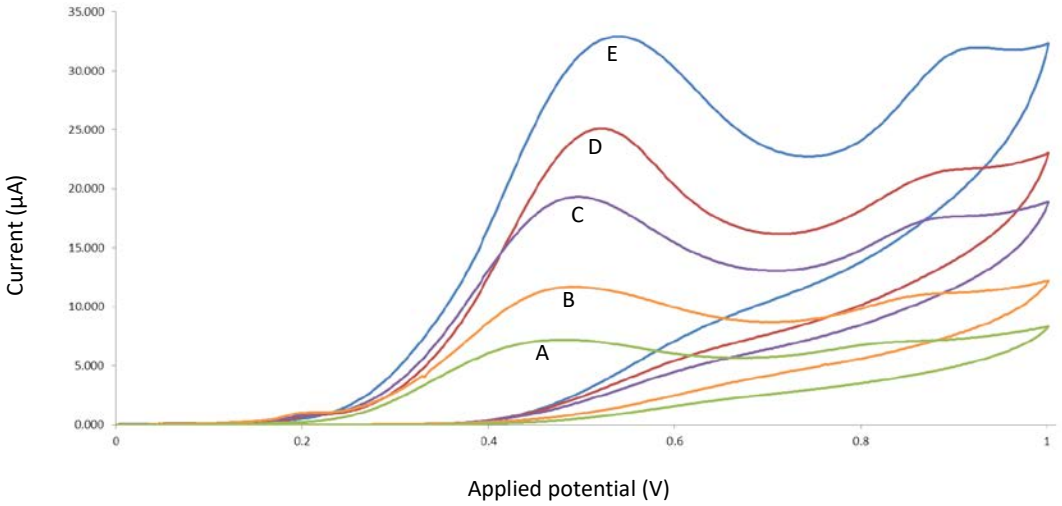

Figure 2.9. Cyclic voltammograms obtained using SPCEs vs (Ag/AgCl) with a solution containing 1 mM skatole in 0.1 M phosphate buffer with 0.1 M sodium chloride at pH 7 using scan rates (mV/s): (A) 20; (B) 50; (C) 100; (D) 150; (E) 200. Starting potential: 0.0 V, switching potential: +1.0 V.

In order to deduce the nature of the electrode reaction occurring at pH 7 the effect of scan rate on the magnitude of the peak current was studied. Figure 2.9 shows the resulting voltammograms obtained with scan rates between 20-200 mV/s. Figure 2.10 shows a deviation in linearity with scan rate which is indicative of reactant adsorption at the electrode surface. All scans were started straight after the electrodes were lowered into the solution, the practical delay between lowering the electrodes and starting a scan is around five seconds. This delay time will not alter the performance of the electrode as the system is held at open circuit until the scan begins and a potential is applied therefore this wait time is standardised.

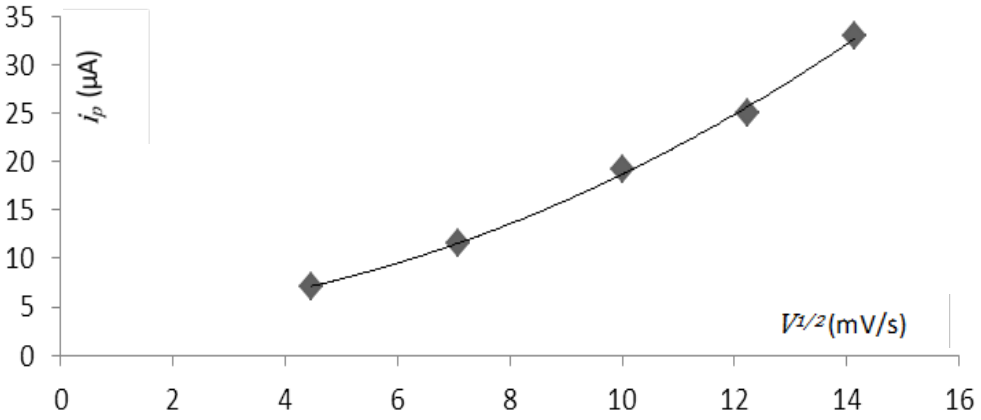

Figure 2.10. Plot of ip vs. v1/2 following direct cyclic voltammetry of 1.0 mM skatole in 0.1 M phosphate buffer with 0.1 M sodium chloride.

2.3.1.1.4 Effect of electrode re-use

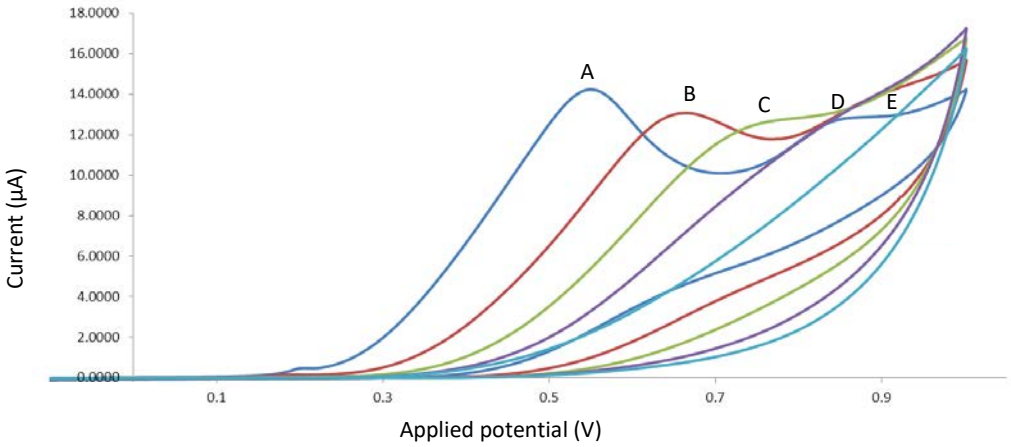

Figure 2.11. Cyclic voltammograms obtained using the same SPCE (vs. Ag/AgCl) with a solution containing 1.0 M skatole in 0.1 M phosphate buffer at pH 7 with 0.1 M sodium chloride. Scans: (A) 1, (B) 2, (C) 3, (D) 4, (E) 5.

To determine if the electrodes could be re-used for subsequent runs a study was performed with a single screen-printed carbon electrode (vs. Ag/AgCl) five times in a solution containing skatole. Figure 2.11 indicates that the product also appears to adsorb

on the electrode surface resulting in electrode fouling. Consequently these electrodes can only be used once for the measurement of skatole. In the interest of preventing carcass contamination, this finding is not a disadvantage.

2.3.1.1.5 Summary of cyclic voltammetric analyses

The cyclic voltammetry experiments show that skatole is oxidised at the SPCE around +0.55 V (vs.Ag/AgCl), therefore an operating scan window +/- 0.5 V of the peak potential was chosen for sufficient observation of the skatole peak. The inclusion of sodium chloride was shown to significantly improve precision, therefore it was included in all future studies. The scan rate study shows reactant adsorption to the electrode surface whereas the electrode re-use study shows product adsorption. Therefore, the each scan is obtained under identical scan conditions and each scan uses a new screen printed strip to avoid electrode fouling. At this point the main operating parameters for the measurement of skatole were considered to be optimised. However, it was decided to use the more sensitive and selective electroanalytical method, known as differential pulse voltammetry (which effectively removes the interfering charging current) in order to measure the endogenous skatole concentrations in adipose tissue; these are expected to be in the low ppm range (boar taint threshold 0.2-0.25 ppm) as mentioned in chapter one section 1.1.4.

2.3.1.2 Differential pulse voltammetry calibration in buffered solution

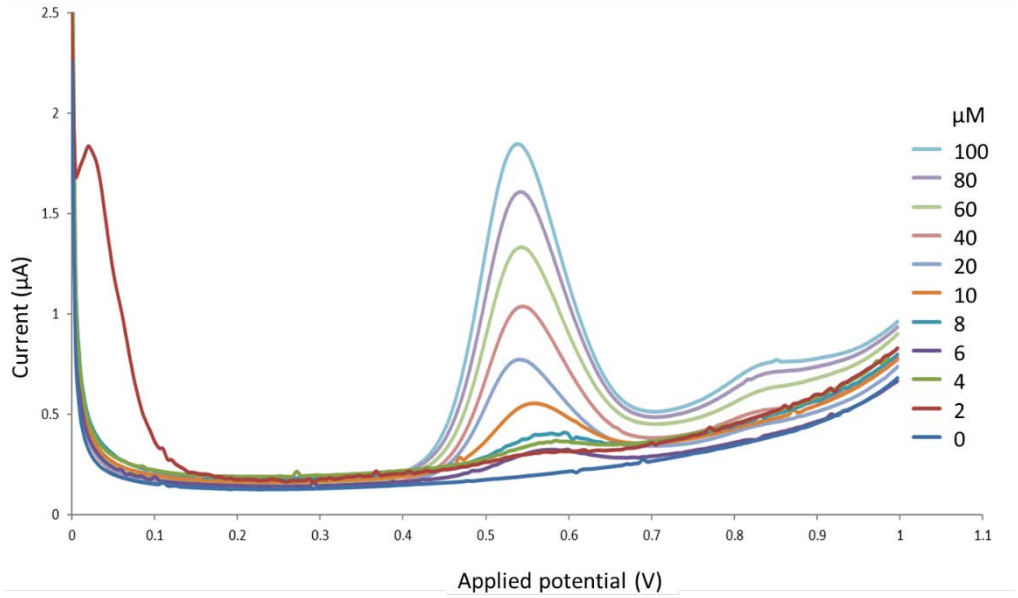

Figure 2.12. Differential pulse voltammograms obtained using SPCEs (vs. Ag/AgCl) with solutions containing µM concentrations of skatole: 0, 2, 4, 6, 8, 10, 20, 40, 60, 80, 100 in 0.1 M phosphate buffer at pH 7 with sodium chloride. Equilibration time 10 s; starting potential 0 V, end potential +1 V, scan rate 50 mV/s, step potential 0.005 V, step width 0.1 s, modulation amplitude 0.005 V, modulation time 0.05 s.

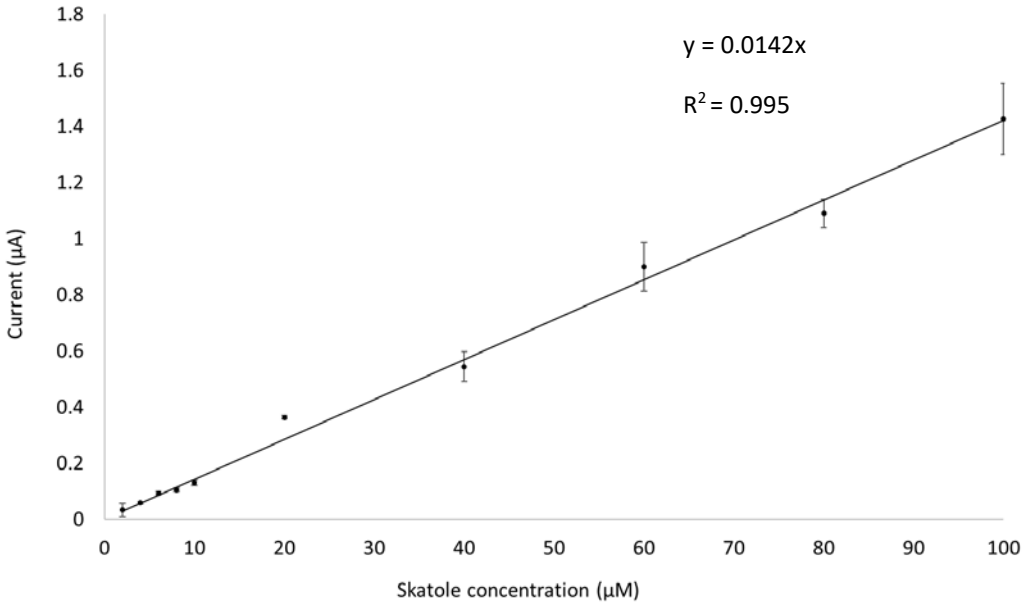

Figure 2.13. Skatole calibration plot prepared from the peak height currents obtained by differential pulse voltammetry (n=3).

Figure 2.12 shows the differential pulse voltammograms of skatole over the concentration range 2-100 µM; well-defined oxidation signals were obtained over the whole range studied. The magnitude of the peak currents were then plotted against the corresponding concentration, as seen in Figure 2.13 a linear response was obtained; the sensitivity was calculated to be 14.2 µA/mM.

The reproducibility of peak current was calculated at a concentration of 10 µM as this is close to the level of interest for boar taint, the resulting coefficient of variation was calculated to be 7.69% (n=3). Further studies on the reproducibility of the voltammetric method is discussed in section 4.3.4.2.1, where samples of adipose tissue were spiked with relevant concentrations of skatole and the sensitivites were similar to that seen in buffered solutions.

2.3.2 Interference studies with water soluble vitamins

2.3.2.1 Cyclic voltammetry

The pH of interest in these interference studies was determined to be pH 7; this value was obtained from the calculated mean value measured from a range of carcasses analysed on the abattoir line (Appendix Table 1). The compounds of interest identified in the literature review (section 2.1), that could potentially result in an interfering response, were analysed by cyclic voltammetry. A vitamin concentration of 5 mM was selected for these studies as it is well above the concentration expected in adipose tissue. For the purpose of ease of interpretation the vitamin cyclic voltammograms have been overlaid with both a buffered control solution and a 1 mM skatole buffered solution; this allows for a comparison of peak potentials where a response has been observed.

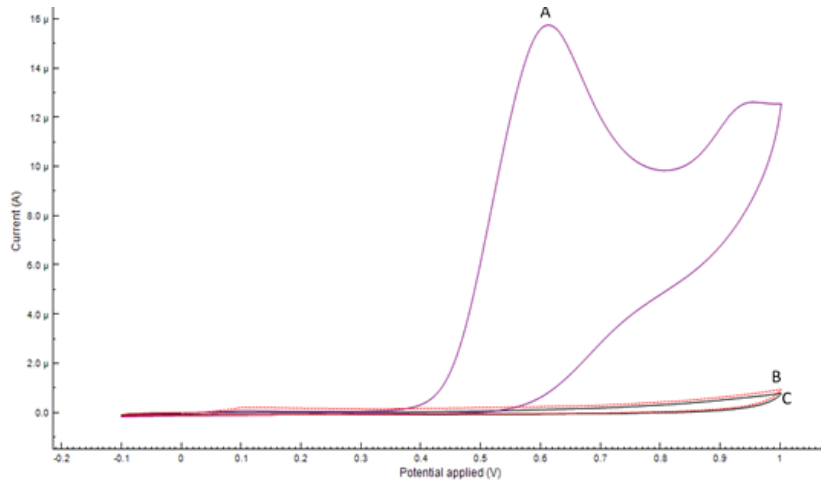

Figure 2.14. Cyclic voltammograms obtained using an SPCE (vs. Ag/AgCl) with a solution containing (A) 1 mM skatole (B) 5 mM thiamine and (C) 0 mM analyte [solid line] solution in 0.1 M phosphate buffer at pH 7 with 0.1 mM sodium chloride. Scan rate: 50 mV/s; start potential: 0.0 V; switching potential: +1.0 V.

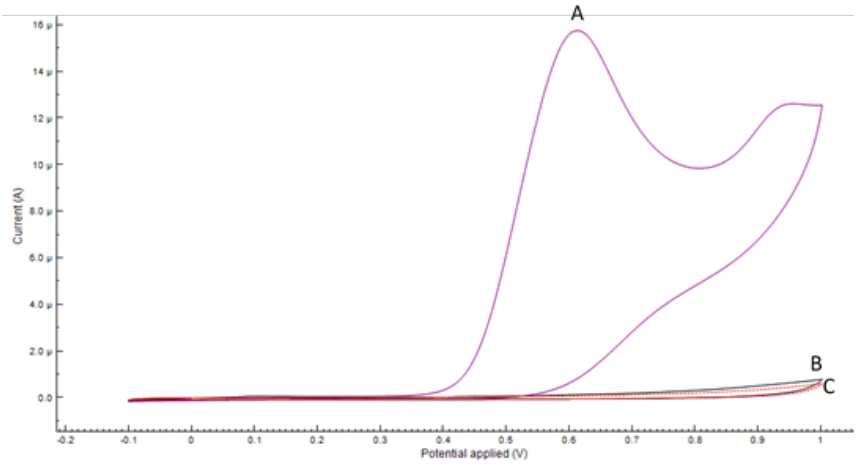

Figure 2.15. Cyclic voltammograms obtained using an SPCE (vs. Ag/AgCl) with a solution containing (A) 1 mM skatole (B) 5 mM riboflavin and (C) 0 mM analyte [solid line] solution in 0.1 M phosphate buffer at pH 7 with 0.1 mM sodium chloride. Scan rate: 50 mV/s; start potential: 0.0 V; switching potential: +1.0 V.

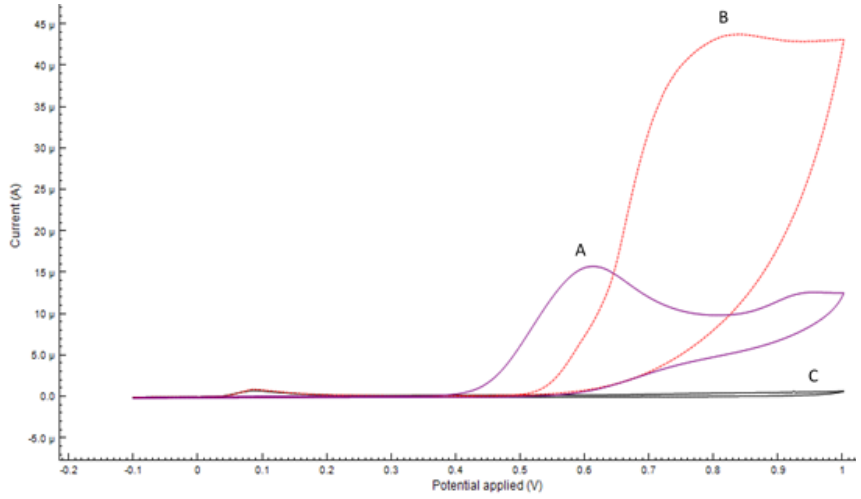

Figure 2.16. Cyclic voltammograms obtained using an SPCE (vs. Ag/AgCl) with a solution containing (A) 1 mM skatole (B) 5 mM pyridoxine and (C) 0 mM analyte [solid line] solution in 0.1 M phosphate buffer at pH 7 with 0.1 mM sodium chloride. Scan rate: 50 mV/s; start potential: 0.0 V; switching potential: +1.0 V.

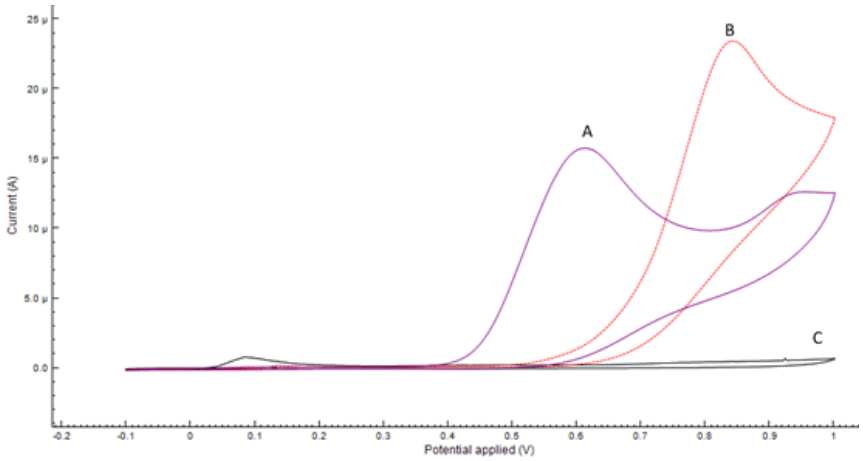

Figure 2.17. Cyclic voltammograms obtained using an SPCE (vs. Ag/AgCl) with a solution containing (A) 1 mM skatole (B) 5 mM folic acid and (C) 0 mM analyte [solid line] solution in 0.1 M phosphate buffer at pH 7 with 0.1 mM sodium chloride. Scan rate: 50 mV/s; start potential: 0.0 V; switching potential: +1.0 V.

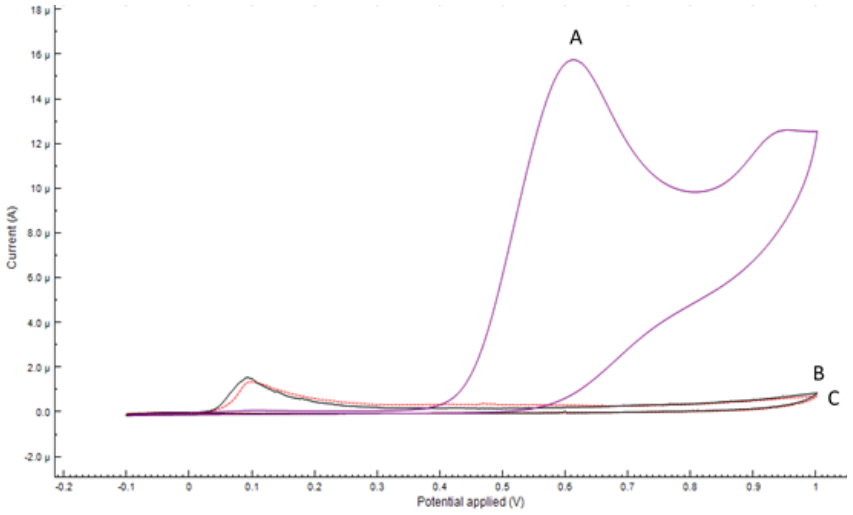

Figure 2.18. Cyclic voltammograms obtained using an SPCE (vs. Ag/AgCl) with a solution containing (A) 1 mM skatole (B) 5 mM nicotinamide and (C) 0 mM analyte [solid line] solution in 0.1 M phosphate buffer at pH 7 with 0.1 mM sodium chloride. Scan rate: 50 mV/s; start potential: 0.0 V; switching potential: +1.0 V.

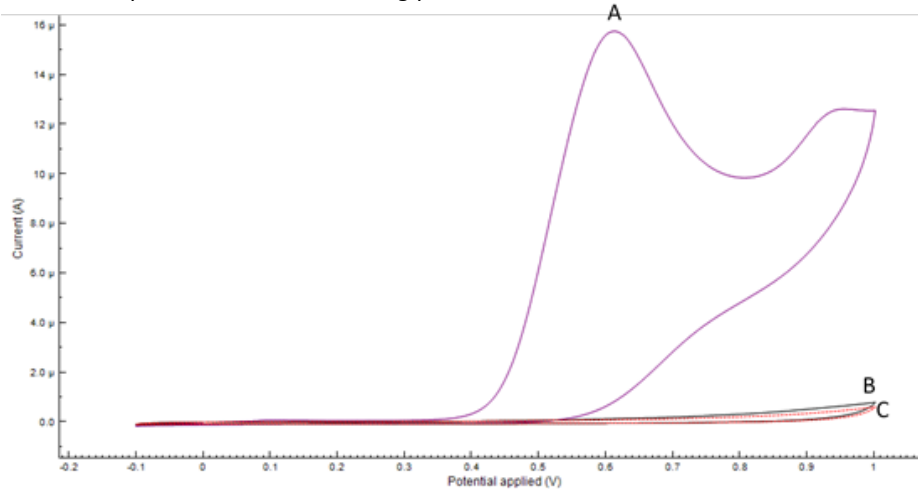

Figure 2.19. Cyclic voltammograms obtained using an SPCE (vs. Ag/AgCl) with a solution containing (A) 1 mM skatole (B) 5 mM pantothenic acid and (C) 0 mM analyte [solid line] solution in 0.1 M phosphate buffer at pH 7 with 0.1 mM sodium chloride. Scan rate: 50 mV/s; start potential: 0.0 V; switching potential: +1.0 V.

The cyclic voltammetric studies into the electrochemical behaviour of thiamine, riboflavin, nicotinamide and pantothenic acid at pH 7 found there to be no current response for these compounds over the potential window of -0.1 to +1.0 V at the SPCE (vs. Ag/AgCl). This can be seen in Figures 2.14, 2.15, 2.18 and 2.19; no peak response was observed at pH 7 (B) in comparison to a buffer solution (C) and a skatole buffered solution (A).

However, the same study of pyridoxine and folic acid at pH 7 revealed a current response over the potential window of -0.1 to +1.0 V at the SPCE (vs. Ag/AgCl). Comparing the peak potential values of pyridoxine and skatole in Figure 2.16 results in a potential separation of 0.2 V. Similarly, the comparison of the peak potentials in Figure 2.17 indicates a good separation for folic acid and skatole; with a difference of 0.25 V. Therefore, the endogenous measurement of skatole is still feasible in the presence of pyridoxine or folic acid; this will be discussed in more detail in section 2.3.2.2.

2.3.2.2 Differential pulse voltammetry

The voltammetric technique differential pulse voltammetry was chosen for the quantification of skatole in adipose tissue using SPCEs (vs. Ag/AgCl), as discussed in section 2.3.1.2. The compounds reported to be present in adipose tissue, and possess redox properties, were further studied close to their minimum and maximum reported concentration ranges with the more sensitive technique differential pulse voltammetry. Table 3 presents the reported concentration ranges of the different compounds found in adipose tissue, these were calculated from those listed in Appendix Table 7 which were originally obtained from various literature sources as discussed in section 2.1.

The differential pulse voltammetry study was performed by first analysing a solution containing a fixed concentration of skatole, prepared in a buffered solution; the peak magnitudes were calculated and recorded. These values were subsequently compared to

the magnitudes measured in the presence of vitamin standards, the standards were pipetted into the original solution at concentrations above the reported minimum and maximum endogenous concentrations; these concentrations are labelled as A1 and A2 in Table 2.3.

Table 2.3. Reported concentration ranges of vitamin compounds in porcine adipose tissue converted to µM values from those shown in Appendix Table 7 reported by Greenfield (2009). The added concentrations used for differential pulse voltammetry studies: (A1) addition 1 and (A2) addition 2 relating to the solutions analysed in Table 2.4.

Vitamin	Reported range (µM)	A1 (µM)	A2 (µM)
Thiamine	5.65-36.65	10.00	50.00
Riboflavin	1.32-4.52	2.00	5.00
Nicotinamide	65.51-335.74	100.00	400.00
Pyridoxine	2.96-18.85	10.00	20.00
Pantothenic acid	13.68-41.05	25.00	50.00
Folic acid	0.23-0.82	0.25	1.00

The ability to measure skatole in the presence of these vitamins has been reported as a percentage difference in peak current, these values were obtained for skatole in the absence and presence of the individual vitamins. All studies were carried out in triplicate, therefore the values reported in Table 2.4 are averages of the skatole peak current values before addition (A0), after addition one (A1) and after addition two (A2). Clearly, there was no significant change in measured skatole concentrations in the presence of the vitamins which demonstrates the applicability of the method for boar taint analysis in the presence of these endogenous compounds. In summary the response for skatole is a simple electro-oxidation at the plain carbon electrode and there is no interference from the vitamins studied as they are oxidised at higher potentials.

Table 2.4. Skatole peak current measurements (n=3) made in the absence of vitamin compounds (A0) and in the presence of a low concentration vitamin (A1) and high concentration vitamin (A2); concentrations added are listed in Table 2.3. All solutions prepared in 0.1 M phosphate buffer with 0.1 M sodium chloride.

	Skatole ip (μA)	*Skatole ip* (μA)		*Skatole ip* (μA)	
Vitamin added	*Before spike (A0)*	*After first spike (A1)*	% Δ A0-A1	*After second spike (A2)*	% Δ A0-A2
Thiamine	0.501	0.482	3.9	0.476	5.0
Riboflavin	0.445	0.414	6.9	0.437	1.8
Nicotinamide	0.463	0.436	6.0	0.437	5.7
Pyridoxine	0.447	0.453	4.4	0.481	3.3
Pantothenic acid	0.460	0.467	1.5	0.442	4.1
Folic acid	0.468	0.499	6.2	0.460	1.7

2.3.3 Chronoamperometric determination of androstenone

Previous research studies leading to the European Patent 2966441 were carried out to optimise the conditions for the fabrication and operation of the biosensor. Consequently, more detailed studies on the performance of the biosensor and its application to boar taint analysis in adipose tissue were performed in this project. The results of these studies are described in the section 2.3.3.1 for buffered solution and sections 3.3.1.2 and 4.3.4.2.2 for application with porcine adipose tissue samples.

2.3.3.1 Calibration in buffered solution

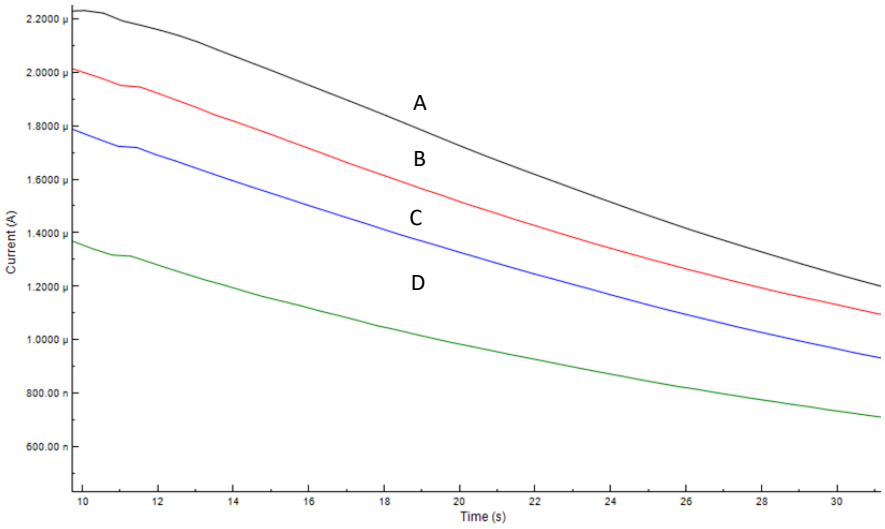

Figure 2.20. Chronoamperograms obtained with biosensors (3αHSD-NADH-MB-SPCE vs. Ag/AgCl) at a range of concentrations (A) 0 µM (B) 1.835 µM (C) 3.671 µM (D) 7.341 µM. Solutions prepared with 0.1 M phosphate buffer containing 0.1 M sodium chloride and 5 % methanol. Applied potential +0.05 V. Solution volume: 100 µl. Biosensors operated at 30°C.

Figure 2.20 shows the chronoamperograms obtained for androstenone over the concentration range 0.5-2.0 ppm (1.8 – 7.3 µM); a buffered solution free of androstenone is also included in the Figure. The current measurements were taken at 10, 20, and 30 seconds after the application of the applied potential (+0.05 V vs. Ag/AgCl). These values

were plotted against concentration in Figure 2.21. It is evident from Figure 2.21 that a linear relationship exists between current and androstenone concentration over the concentration range studied in aqueous buffer solution. This linear current-concentration relationship demonstrates the possibility of measuring this boar taint compound in the fluid of an incision made in adipose tissue.

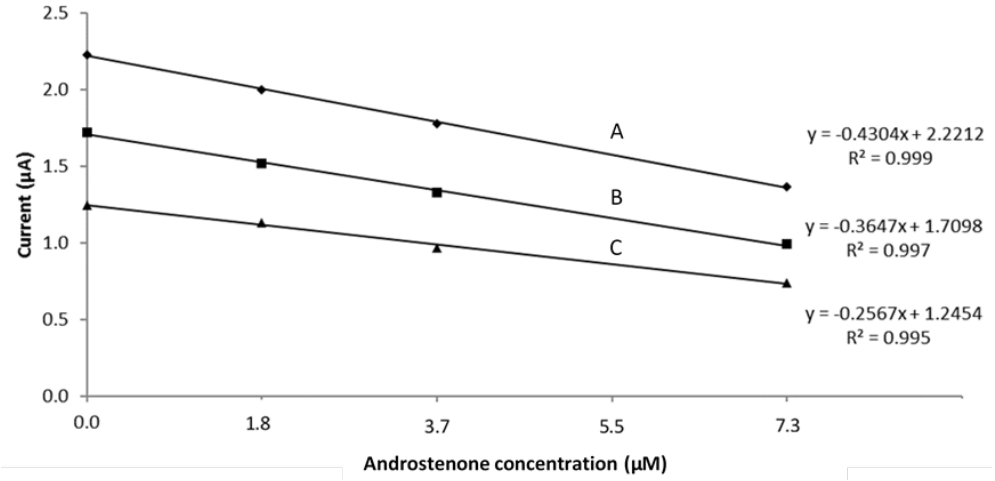

Figure 2.21. Androstenone calibration graph plotting chronoamperometric current measurements at 10s (A) 20s (B) and 30s (C).

2.4 Conclusions

The electrochemical behaviour of skatole at a SPCE (vs. Ag/AgCl) was investigated using cyclic voltammetry. The inclusion of sodium chloride was shown to improve measurement precision and the variation of electrolyte pH showed negligible current difference over the expected pH range in pig adipose tissue (pH 6.7 to pH 7.54). A scan rate study showed that weak reactant adsorption occurs at the SPCE surface. Another adsorption phenomenon was also observed, namely product adsorption; this electrode fouling precluded the multiple use of the SPCE. A calibration study for skatole was performed using the more sensitive technique differential pulse voltammetry. A calibration study for androstenone was performed using chronoamperometry with an electrochemical biosensor.

A selection of endogenous compounds present in adipose tissue have been investigated for their potential interference with the measurement of skatole using plain screen-printed carbon electrodes in conjunction with voltammetric methods. No interfering signals were observed for any of the compounds examined under the relevant conditions investigated.

The performance of the voltammetric method strongly indicated that the approach with a screen-printed carbon electrodes would be suitable for the measurement of skatole in adipose tissue. Similarly, the performance of the chronoamperometric method with a screen-printed androstenone biosensor demonstrated the possibility of measuring this analyte in adipose tissue. The next chapter, chapter 3, will describe the application of the individual sensor and biosensor for the measurement of target analytes, skatole and androstenone, in porcine adipose tissue samples obtained from various sources.

Chapter Three

Preliminary evaluation of a screen-printed sensor and biosensor for the direct analysis of boar taint compounds in adipose tissue

Chapter Three Contents

Table of Figures

Chapter Summary

Chapter three explains the need for an electrochemical sensor and biosensor that can measure boar taint compounds, skatole and androstenone, directly in adipose tissue. The novel sensing system developed for this purpose will be compared to the traditional laboratory based technique, gas chromatography. A review of gas chromatographic methodology for boar taint analysis has been presented, followed by a summary of the adapted methods used for the validation of the sensor technology reported in this thesis.

The experimental procedures are reported for both the electroanalysis and chromatographic analysis of porcine adipose tissue. The application of these methodologies to real samples in a laboratory environment has been presented and the resulting quantitative data of each method has been compared. A positive correlation was observed between the two techniques which demonstrates the viability of the novel sensor technology for the measurement of boar taint compounds on the abattoir processing line.

Chapter Three

3.1 Introduction

In chapter two, the possibility of measuring skatole with a disposable screen-printed carbon electrode in aqueous buffer systems was demonstrated, as well as measuring androstenone with a disposable screen-printed amperometric biosensor. However, as mentioned earlier in the thesis the main purpose of this project was to explore the possibility of developing an analytical approach for the direct measurement of skatole and androstenone in adipose tissue. In this chapter the electrochemical approaches using screen-printed sensors for this purpose will be discussed. In addition the application of this approach to the analysis of a range of adipose tissue samples (obtained from both a pig producer and local retailers) will be described. In order to validate the novel electrochemical technology it was necessary to compare the results from these samples with a conventional analytical technique, for this purpose high-resolution gas-chromatography was considered to be appropriate. No suitable method was available for this purpose, consequently a detailed investigation was carried out to develop new gas chromatographic methods for the analysis of the boar taint compounds in adipose tissue. In this chapter a full description of the development of the gas chromatographic method and its application to a range of samples corresponding to those analysed by the electrochemical approach will be discussed. Finally, the results obtained with the electrochemical techniques will be compared to those obtained with the gas chromatographic techniques.

3.1.1 Rationale for the direct electrochemical analysis of porcine tissue

As previously discussed, there are currently no reported methods for the direct analysis of boar taint compounds in adipose tissue. The novel patented approach, which was

discussed at length in chapter two, will form the basis of the work reported in this thesis.

Having shown that boar taint compounds can be measured by screen printed sensors in aqueous buffer solutions (chapter two) the next step was to develop a suitable approach for the direct analysis of the compounds in adipose tissue. In previous studies Hart and co-workers (2010) demonstrated that a modified screen-printed carbon electrode could be inserted into a whole fruit for the direct measurement of citric-acid. Consequently, it was decided to explore the possibility of a similar approach for the determination of skatole and androstenone in pig adipose tissue.

3.1.2 Gas chromatographic analysis of porcine adipose tissue

The determination of boar taint, using chromatographic techniques, to separate the complex biological matrix that is adipose tissue, has been the subject of many reports. High-resolution gas-chromatography (HRGC) and high-performance liquid-chromatography (HPLC) have been used with a range of detection systems such as mass-spectrometry (Sørensen and Engelsen, 2014)(Meier-Dinkel *et al.*, 2013)(Bekaert *et al.*, 2012), time-of-flight mass spectrometry (Fischer *et al.*, 2014), tandem mass-spectrometry (Buttinger *et al.*, 2014), fluorescence (Verheyden *et al.*, 2007)(Lunde *et al.*, 2012)(Liu *et al.*, 2014)(Trautmann *et al.*, 2014)(Mörlein *et al.*, 2012), and flame ionisation detection (Kaufmann, Ritter and Schubert, 1976). A wide range of approaches have been reported in these publications for the preparation of adipose tissue samples prior to chromatographic separation. The initial step usually involves a form of liquefaction such as ultra-sonication in a solvent, microwaving, or freezing followed by blending. A clean-up step is sometimes included in the preparation procedure such as centrifugation to remove particulate matter, solid-phase-extraction, or size exclusion chromatography. Sometimes, derivatisation procedures are included to improve separation and detection. Evaporating the sample to increase concentration has also been reported. Introduction of the sample to the chromatographic instrumentation also varies, gas chromatography

often uses the analysis of volatiles in headspace or the direct injection of the liquid extract which is subsequently volatilised at the high temperature inlet.

It should be mentioned that, in the current project, the basic gas chromatographic method was supplied by Whittington (2014); this was modified and evaluated for the determination of the target analytes in adipose tissue. The method supplied was similar to those reported in two publications by this research group; which used 5-methylindole as the internal standard for skatole quantification (Nicolau-Solano *et al.*, 2007)(Whittington *et al.*, 2004). The sample preparation method for the liquid-liquid extraction of skatole from liquid adipose tissue was adapted from (Dehnhard *et al.*, 1993). This procedure involves dissolution of liquid fat in hexane, followed by skatole extraction with acetonitrile, the method reported a 98.9% recovery. An additional preparation step was employed for the GC studies in this thesis to ensure that the solvent introduced to the GC was compatible with the nitrogen-phosphorous detector. The exchange of solvent to ethyl acetate provided the opportunity to pre-concentrate the sample extract, this was achieved with rotary evaporation followed by reconstitution in a smaller volume of ethyl acetate. It should be mentioned that this sample preparation procedure has not been previously documented in peer-reviewed literature.

The sample preparation procedure adopted for the extraction of androstenone was modified from a method developed by Verheyden and co-workers (2007). This method involved melting the adipose tissue and centrifuging the liquid fat to remove any water present. The remaining fat was added to a mixed solution of methanol and hexane (9:1) before ultrasonication, vortex mixing, and finally cooled to clarify the supernatant.

All samples were stored at -18°C prior to GC analysis due to the time consuming sample preparation and gas chromatographic analysis methods. A study by Ampuero Kragten and colleagues (2011) reported no degradation of androstenone 2-3 years after sampling after

being stored at -18°C, therefore this storage method was sufficient for the duration of this project.

3.2 Experimental

3.2.1 Electroanalysis

3.2.1.1 Apparatus and instrumentation

The (bio)sensors, potentiostat and pH-temperature probe used in this chapter have been previously described in chapter two section 2.2.1. In some circumstances it was not practical to measure the internal temperature of tissue samples as this would remove interstitial fluid from the incision location which in turn would reduce the available fluid for electroanalysis with the (bio)sensors. In those cases surface temperature was monitored using an infrared thermometer with laser targeting (Maplin Electronics, Rotherham).

3.2.1.2 Chemicals and reagents

The standards skatole and androstenone were prepared at a stock concentration of 1 mg/ml in methanol.

3.2.1.3 Procedures

3.2.1.3.1 Skatole measurement using a voltammetric plain sensor

Figure 3.1 shows a SPCE inserted into a sample of adipose tissue (approximately 10x5cm) temperature controlled at 30°C. The screen-printed electrode was connected to a μautolab potentiostat, interfaced to a computer operated with the NOVA v1.10 (Metrohm, Netherlands) software package to carry out differential pulse voltammetry. The monitor shows a typical differential pulse voltammogram obtained with the adipose tissue sample.

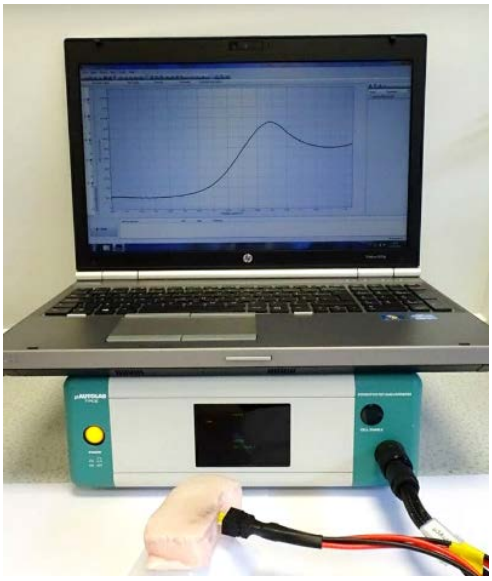

Figure 3.1. Screen printed sensor (shown in chapter two Figure 2.3) inserted into a sample of subcutaneous porcine adipose tissue (warmed to 30°C). The resulting differential pulse voltammogram is displayed.

In order to carry out a representative calibration study, individual adipose tissue sub samples were fortified with different concentrations of skatole prepared in methanol. The fortification additions were calculated using the weight of the section of adipose tissue and the concentration of the skatole solution prepared in methanol: µg/g (skatole/adipose tissue). To ensure that no solution was lost when pipetted into the adipose incision only very small volumes (< 20 µL) of skatole solution were used to fortify the adipose tissue samples. These samples were stored in the fridge for 24 hours to allow skatole to diffuse through the sample. The following day, the samples were brought to 30°C on a temperature controlled heated block and interrogated with the system shown in Figure 3.1. The DPV parameters are described in the previous chapter in section 2.2.3.2.

3.2.1.3.2 Androstenone measurement using an amperometric biosensor

The analysis of androstenone in adipose tissue was performed with the same instrumental set up as shown Figure 3.1, except that the SPCE was replaced with an amperometric

screen printed biosensor and the chronoamperometric waveform was applied. An androstenone calibration was performed using biosensors (3αHSD-NADH-MB-SPCEs vs. Ag/AgCl) prepared 24 hours prior to use; the biosensor fabrication method is described in section 2.2.2. The androstenone solution concentration range analysed was 0.0; 0.1; 0.5; 1.0; 2.0 µg/ml with a final methanol volume of 5%. Measurements were performed by applying a potential of 0.05 V at the working electrode and monitoring the current response for a duration of 60s.The design of the biosensor and the instrumental parameters used in the analysis are described in chapter two; section 2.2.1, section 2.2.2 and section 2.2.3.4.

In order to carry out a calibration study individual adipose tissue sub samples were fortified with different concentrations of androstenone prepared in methanol. The fortification additions were calculated using the weight of the section of adipose tissue and the concentration of the androstenone solution prepared in methanol: µg/g (androstenone/adipose tissue). To ensure that no solution was lost when pipetted into the adipose incision only very small volumes (< 20 µL) of androstenone solution were used to fortify the adipose tissue samples. These samples were stored in the fridge for 24 hours to allow androstenone to diffuse through the sample. The following day, the samples were brought to 37°C on a temperature controlled heated block and interrogated with the system shown in Figure 3.1 (but instead using the technique chronoamperometry).

3.2.2 Gas chromatographic analysis

3.2.2.1 Skatole analysis

3.2.2.1.1 Apparatus and instrumentation

A Clarus 580 Gas Chromatograph with autosampler interfaced to a PC for data acquisition with the TotalChrom Navigator software package was used for the gas chromatographic analyses. The GC has two detectors; a flame ionisation detector (FID) and a nitrogen-

phosphorous detector (NPD). Hydrogen supplied to the instrumentation for was filtered using a Hydrogen Specific Triple Purifier (Bellefonte, Restek) to ensure that no impurities were present in the gas supply for both the mobile phase and detector. Sample injections made to the GC used either a manual SGE syringe 1 µL 23 ga 50 mm needle or a Hamilton autosampler syringe 5 µL 23 ga 70 mm needle (Merck, Darmstadt). The inlet was fitted with a glass inlet focus liner with a 4.0 mm ID single taper with quartz wool (Merck, Darmstadt) to trap non-volatile residues.

A Perkin Elmer Clarus 580 Gas Chromatograph linked to a nitrogen phosphorous detector (also known as a nitrogen specific or thermionic detector) was used for skatole quantification. The capillary column CP-Wax 57 CB [25m x 0.32 mm x 0.2 µm] (Agilent, Santa Clara USA), which has a chemically bonded polyethylene glycol stationary phase, was used for this method. The GC method uses a split injection (4.5:1) and helium (BOC, Guilford) as the carrier gas. To ensure the quality of the gas is as high as possible a Super Clean (helium specific) Trap (Bellefonte, Restek) was fitted between the cylinder and instrumentation. The injector port temperature was 230°C and an oven temperature programme was used; 60°C for 1 min, 20°/min to 200°C held for 5 min, 10°C/min to 220°C held for 5 min. The autosampler programme included a 5 minute equilibrium time between runs to allow for the NPD to stabilise after each run. The detector temperature was set at 250°C with a gas flow of hydrogen 2 ml/min and air 100 ml/min. The NPD sensitivity can be altered by adjusting the voltage at the potentiometer; the baseline reading for the NPD was maintained daily at 0.5 mV. The GC was interfaced to a PC for data acquisition using the Perkin Elmer TotalChrom Navigator software package version 6.3.2. Additional consumables for the instrumentation include: Thermolite septa [max temp 340°C] (Bellefonte, Restek); polar fused silica guard column 0.32 mm (Darmstadt, Merck); fused silica connectors (Darmstadt, Merck); NPD bead assembly (Perkin Elmer, Connecticut USA).

3.2.2.1.2 Chemicals and reagents

3-methylindole (skatole) and 5-methylindole were obtained from Sigma Aldrich (Dorset, UK). Stock solutions of these compounds were prepared by dissolving the required mass in a known volume of solvent. Solvents used were acetonitrile and ethyl acetate where specified. The standard 5-methylindole stock solution was prepared in the relevant solvent to a concentration of 200 µg/ml and added to sample extracts to give a final concentration of 0.5 µg/ml. Standards were stored in a spark-free refrigerator for a maximum of one-week and taken out an hour before use to reach room temperature (20°C) before use. Glassware was cleaned with the following procedure; Decon soak, deionised water rinse, and finally an acetone rinse, before being placed in a drying cabinet.

3.2.2.1.3 Procedures

3.2.2.1.3.1 Solvent extraction method

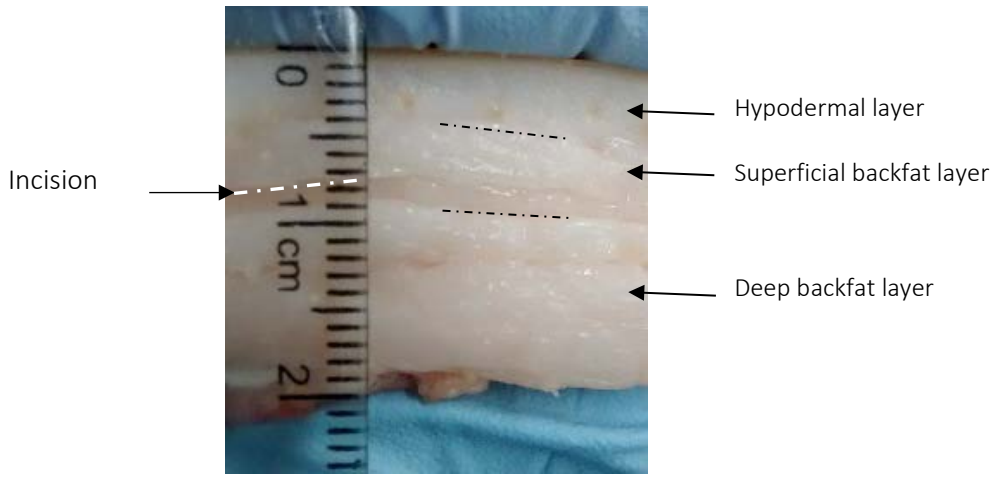

Figure 3.2. Layering of subcutaneous adipose tissue, with an example of an incision in the superficial backfat layer. Incision shown as a white dotted line.

Stored adipose tissue samples (-18°C) were thawed for 24 hours at 4°C, and finally left to reach room temperature (20°C) for one hour. The adipose tissue was then prepared by

removing the skin, hypodermal layer and lower deep back fat layer leaving the superficial back fat layer (Figure 3.2). This layer is then cut into 5 mm^3 pieces, weighed to 10 g in a glass jar and microwaved for 4 minutes at 320 W. Once the liquid adipose had cooled to 50°C 1.5 ml was transferred to an Eppendorf tube; this step was performed in duplicate. The Eppendorf tubes were centrifuged at 10,000 rpm for 5 minutes to clarify the liquid supernatant. Then 1 g of the liquid adipose was transferred to a 50 ml Pyrex centrifuge tube containing 15 ml hexane (this step was again performed in duplicate). The centrifuge tubes were vortexed for 30 seconds and then shaken for 1 minute, this step was repeated two more times and the pressure was released from the tube between each repeat. Then 5 ml acetonitrile was added to each tube and the mixing procedure was repeated again (triplicate vortex and shake). The tubes were centrifuged at 2000 rpm for 15 minutes. The upper hexane layer was then removed and 4 ml of the acetonitrile layer was transferred into a 10 ml round bottom flask containing anti-bumping granules. A rotary evaporator was used to take the sample to dryness. Then 500 µl ethyl acetate was added and the flask, this was vortexed for two minutes followed by one minute of ultrasonication. Then 400 µl of this extract solution was transferred into a sample vial. An internal standard (5-methylindole) was added to give a final concentration of 0.5 µg/ml. The sample vials were mounted on the carousel of the autosampler and 1 µl volumes were injected into the GC using the autosampler.

3.2.2.1.3.2 Calibration method

Initially, acetonitrile was employed in the calibration studies as this was initially proposed as the sample preparation solvent. However, acetonitrile's incompatibility with the NPD was soon realised and this led to a further calibration study using ethyl acetate. Skatole standards were prepared in either acetonitrile or ethyl acetate over the concentration range 0.01-0.5 µg/ml. Each working standard of skatole was prepared with an internal standard (5-methyl indole) at a working concentration of 0.5 µg/ml.

3.2.2.1.3.3 Sample analysis

The reconstituted sample extracts obtained with the procedure in section 3.2.2.1.3.1 were analysed by the gas chromatographic method procedure described in section 3.2.2.1.1. The peak areas of the analyte and internal standard were obtained from the corresponding chromatogram for each sample, these values were compared to slope of the calibration plot to determine the final concentrations in the sample extracts. Using an appropriate calculation, taking into account dilution and concentration steps, the endogenous concentrations of skatole were calculated. To ensure that skatole was not lost in the reconstitution process a recovery study was performed by fortifying liquid adipose tissue extracts (prepared in acetonitrile) that were taken to dryness and reconstituted in ethyl acetate; process described in section 3.2.2.1.3.1. The process was repeated without the fortification step using a portion of the same liquid adipose tissue extract to allow for background skatole concentration subtraction; results discussed in section 3.3.2.3.

3.2.2.2 Androstenone analysis

3.2.2.2.1 Apparatus and instrumentation

A Perkin Elmer Clarus 580 Gas Chromatograph linked (Perkin Elmer, Connecticut USA) to a flame ionisation detector was used for androstenone determination. The capillary column CP-Sil 8 CB [25 m x 25 mm x 0.25 µm] (Agilent, Santa Clara USA), which has a cross-linked and bonded methylpolysiloxane (5% phenyl) stationary phase which is non-polar, was used for this method. The GC method uses a split injection (48:1) and hydrogen (BOC, Guilford) as the carrier gas. The injector port temperature was 285°C and an oven temperature programme was used; 50°C for 8 min, 20°/min to 280°C held for 15 min, 20°C/min to 300°C held for 25 min. The detector temperature was set at 290°C with a gas flow of hydrogen 45ml/min and air 450ml/min. The GC was interfaced to a PC for data acquisition using the Perkin Elmer TotalChrom Navigator software package version 6.3.2.

Additional consumables for the instrumentation include: Thermolite septa [max temp 400°C] (Bellefonte, Restek); non-polar fused silica guard column 0.25 mm (Darmstadt, Merck); fused silica connectors (Darmstadt, Merck).

3.2.2.2.2 Chemicals and reagents

Androstenone and androsterone were obtained from Sigma Aldrich (Dorset, UK). Stock solutions of these compounds were prepared by dissolving the required mass in a known volume of methanol and hexane (9:1). The internal standard (androsterone) stock solution was also prepared in methanol and hexane (9:1) to a concentration of 200 µg/ml and added to sample extracts to give a final concentration of 2 µg/ml. Standard chemical solutions were stored following the procedure described in section 3.2.2.1.2.

3.2.2.2.3 Procedures

3.2.2.2.3.1 Solvent extraction

Stored adipose tissue samples (-18°C) were thawed for 24 hours at 4°C, and finally left to reach room temperature (20°C) for one hour. The adipose tissue was then prepared by removing the skin, hypodermal layer and lower deep back fat layer leaving the superficial back fat layer (Figure 3.2). This layer is then cut into 5 mm^3 pieces, weighed to 10 g in a glass jar and microwaved for 1 minutes at 480 W. Once the liquid adipose had cooled to 50°C 1.5 ml was transferred to an Eppendorf tube; this step was performed in duplicate. The Eppendorf tubes were centrifuged at 10,000 rpm for 5 minutes to clarify the liquid supernatant. Then 0.25 g of the liquid adipose was transferred to a 1.5 ml Eppendorf tube containing 1 ml methanol and hexane at a 9:1 ratio (this step was again performed in duplicate). The Eppendorf tubes were vortexed for 30 seconds and then placed in an ultrasonication bath for 5 minute, this step was repeated two more times and the pressure was released from the tube between each repeat. The tubes were centrifuged at 10,000 rpm for 5 minutes. The tubes were then placed in a cooling block for one hour

to clarify the supernatant. Then 500 µl of this extract supernatant was transferred into a sample vial, the internal standard (androsterone) was added to give a final concentration of 2.0 µg/ml. The sample vials were mounted on the carousel of the autosampler and 1 µl volumes were injected into the GC using the autosampler.

3.2.2.2.3.2 Calibration

Androstenone standards were prepared in methanol over the concentration range 0.1-5.0 µg/ml. Each working standard of androstenone was prepared with an internal standard (androsterone) at a working concentration of 2.0 µg/ml.

3.2.2.2.3.3 Sample analysis

The reconstituted sample extracts obtained with the procedure in section 3.2.2.2.3.1 were analysed by the gas chromatographic method procedure described in section 3.2.2.2.1. The peak areas of the analyte and internal standard were obtained from the corresponding chromatogram for each sample, these values were compared to slope of the calibration plot to determine the final concentrations in the sample extracts. Using an appropriate calculation, taking into account dilution and concentration steps, the endogenous concentrations of androstenone were calculated.

3.3 Results and discussion

3.3.1 Electroanalysis

3.3.1.1 Skatole measurement using differential pulse voltammetry with a plain screen-printed carbon electrode

3.3.1.1.1 Calibration study in adipose tissue

The magnitude of the peak currents in this study were used in the construction of a calibration plot which was used for the subsequent determination of skatole concentration in unknown samples of porcine adipose tissue. Figure 3.3 shows typical differential pulse voltammograms obtained for increasing concentrations of skatole in

fortified adipose tissue samples. As is evident, the magnitude of the currents increase in proportion to the added concentrations and the peak potential is typically + 0.7V +/- 5mV. This behaviour demonstrates that the voltammetric method should be suitable for the measurement of endogenous levels of skatole. Figure 3.4 shows the resulting skatole calibration plot which was found to be linear over the range required for these studies. It should also be mentioned that the differential pulse voltammetric scans were achieved in 20 seconds; the scan rate was 50 mV/s and the scan window was 1 V (0 to +1 V). This is an important aspect of the method as rapid analysis times are required for on-line monitoring in abattoirs.

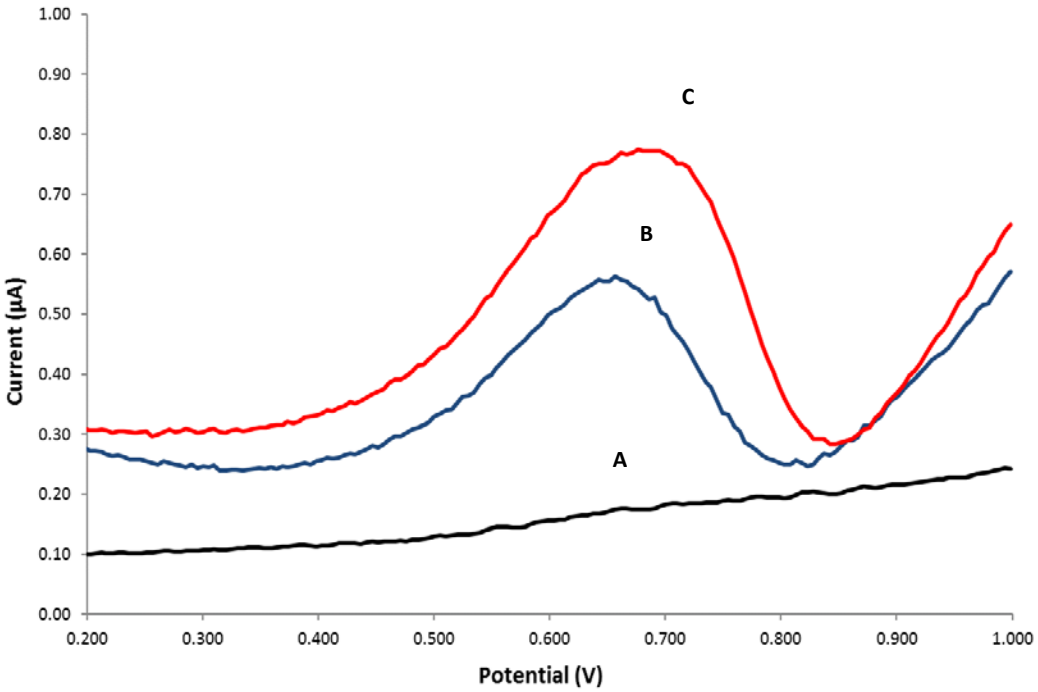

Figure 3.3. Differential pulse voltammograms obtained in adipose tissue fortified with skatole. DPVs obtained with SPCEs (vs. Ag/AgCl) in porcine subcutaneous adipose tissue fortified with (A) 0 µg/g; (B) 5.25 µg/g; (C) 7.85 µg/g skatole.

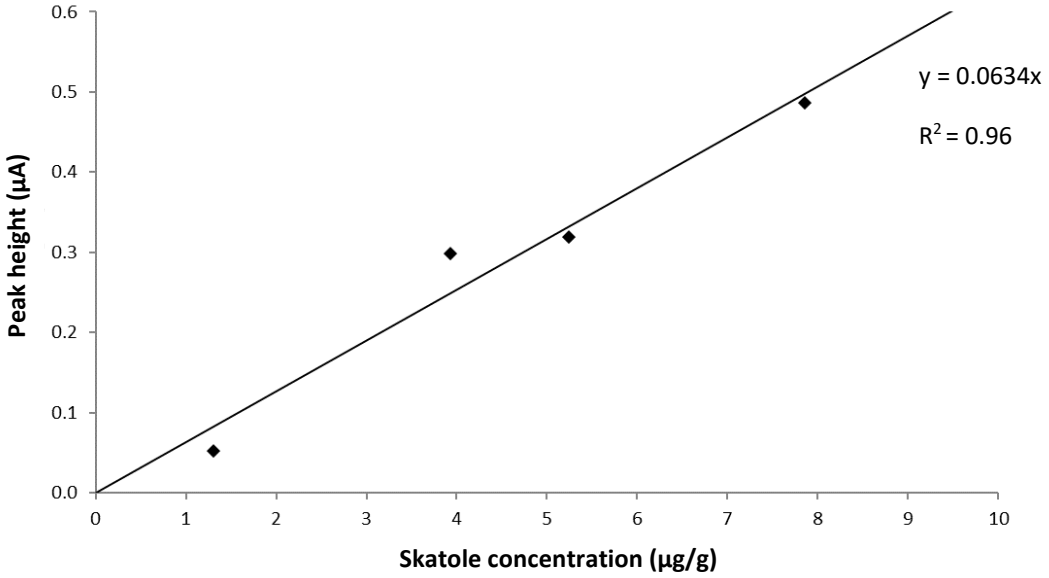

Figure 3.4. Calibration graph plotted from voltammetric peak height current measurements from adipose tissue fortified with 1.23 µg/g 3.95 µg/g; (B) 5.25 µg/g; (C) 7.85 µg/g skatole. Reproduced from patent EP 2966441A1.

3.3.1.1.2 Endogenous concentrations of skatole in adipose tissue samples

Samples of adipose tissue obtained from local retailers and from a pig producer (JSR Genetics Ltd) were interrogated using SPCEs (vs. Ag/AgCl) in conjunction with differential pulse voltammetry; procedure described in section 3.2.1.3.1. The endogenous concentration of skatole was calculated by referring the magnitude of the peak current for the individual samples to the calibration graph constructed from fortified adipose tissue samples; described in section 3.3.1.1.1. Each sample was analysed in duplicate and an average response was calculated. All but one sample showed the presence of skatole. At this point it was clear that the voltammetric approach developed in this study was capable of measuring endogenous skatole directly in adipose tissue. The sample data has been presented in a later section (3.3.2.5), in order to compare the concentrations from those obtained with gas chromatographic method.

3.3.1.2 Androstenone measurement using an amperometric biosensor

3.3.1.2.1 Calibration study in adipose tissue

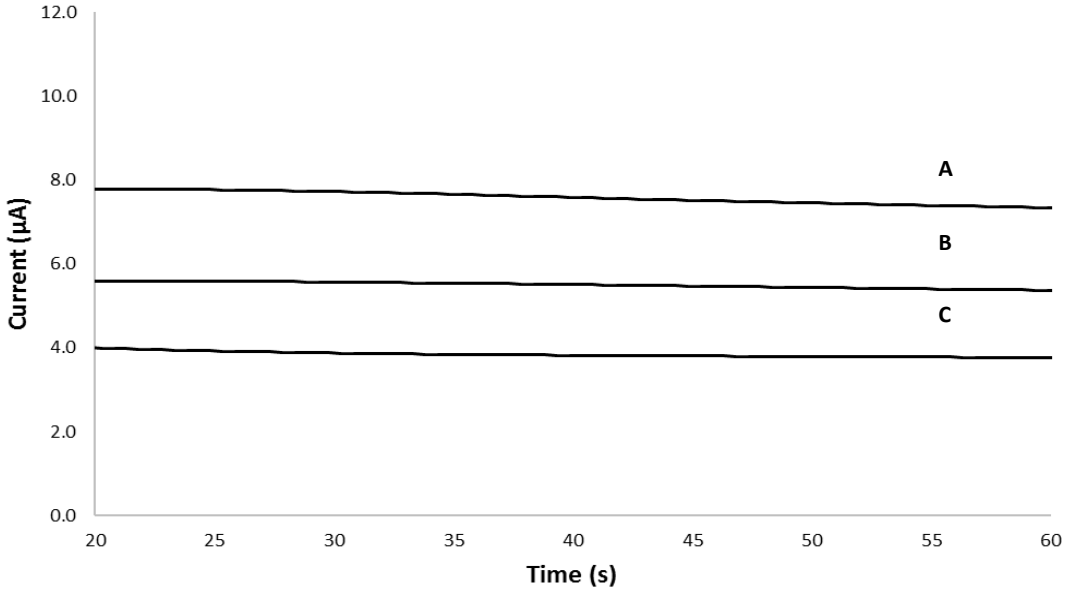

Figure 3.5. Androstenone chronoamperometric responses from fortified adipose tissue samples. Chronoamperograms obtained with biosensors (3αHSD-NADH-MB-SPCE vs. Ag/AgCl) in porcine adipose tissue fortified with (A) 0 µg/g; (B) 1 µg/g; and (C) 2 µg/g. Scans performed simultaneously with differential pulse voltammetry.

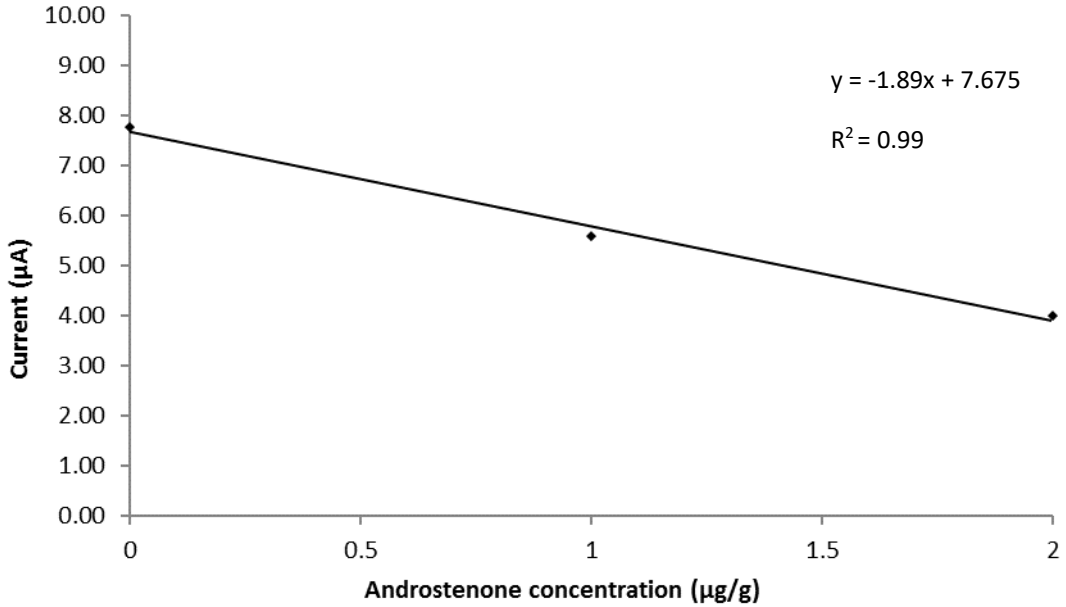

Figure 3.6. Calibration graph for androstenone measured in subcutaneous porcine adipose tissue. Androstenone calibration graph plotted from chronoamperometric currents measurements at 20s obtained from adipose tissue fortified with 0 µg/g, 1 µg/g, and 2 µg/g. Reproduced from patent EP 2 966 441 A1.

The chronoamperograms in Figure 3.5 show that the magnitude of the current decreases in the presence of androstenone and the current difference is proportional to the concentration of the analyte; the sequence of reactions responsible for the analytical response is explained in Figure 1.11 chapter one. The magnitude of the peak currents at 20 seconds were used in the construction of a calibration plot which was used for subsequent determination of androstenone concentration in unknown samples of porcine adipose tissue. Figure 3.6 shows the resulting androstenone calibration plot which was linear over the range required for these studies. As with the differential pulse voltammetric scans, the chronoamperometric scans were performed within a minute and current measurements were taken from the 20 second time point. This demonstrates that both of the electrochemical methods can achieve rapid measurements that would be well suited to the proposed fast-paced abattoir processing line.

3.3.1.2.2 Endogenous concentrations of androstenone in adipose tissue samples

Samples of adipose tissue obtained from local retailers and from a pig producer (JSR Genetics Ltd) were interrogated using biosensors (3αHSD-NADH-MB-SPCEs vs. Ag/AgCl) in conjunction with chronoamperometry; procedure described in section 3.2.1.3.2. The endogenous concentration of androstenone was calculated by referring the current value on the chronoamperogram at 20 seconds for the individual samples to the calibration graph constructed from fortified adipose tissue; described in section 3.3.1.2.1. Each sample was analysed in duplicate and an average response was calculate. At this point it was clear that the chronoamperometric approach developed in this study was capable of measuring endogenous androstenone directly in adipose tissue. The sample data has been presented in a later section (3.3.2.6), in order to compare the concentrations from those obtained with gas chromatographic method.

3.3.2 Gas chromatographic analysis

3.3.2.1 Identification of optimum solvent for GC-NPD studies

Skatole and the internal standard 5-methylindole were prepared in either acetonitrile or ethyl acetate, the two standard preparations were analysed by GC-NPD independently. The resulting gas chromatograms are shown in Figure 3.7 for acetonitrile and Figure 3.8 for ethyl acetate. Clearly, the chromatogram obtained for the latter solvent produced a more stable baseline with better defined peaks. In order to confirm that ethyl acetate was indeed superior to acetonitrile, calibration studies were carried out and the results are discussed in the section 3.3.2.2.

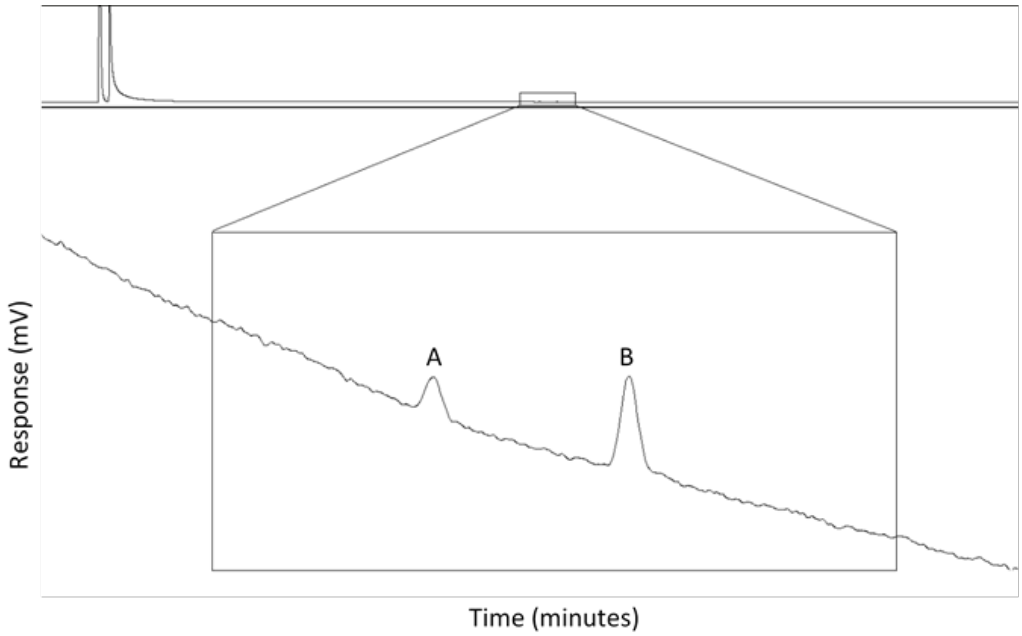

Figure 3.7. Typical gas chromatographic separation of (A) skatole (analyte) and (B) 5-methylindole (internal standard) prepared in acetonitrile.

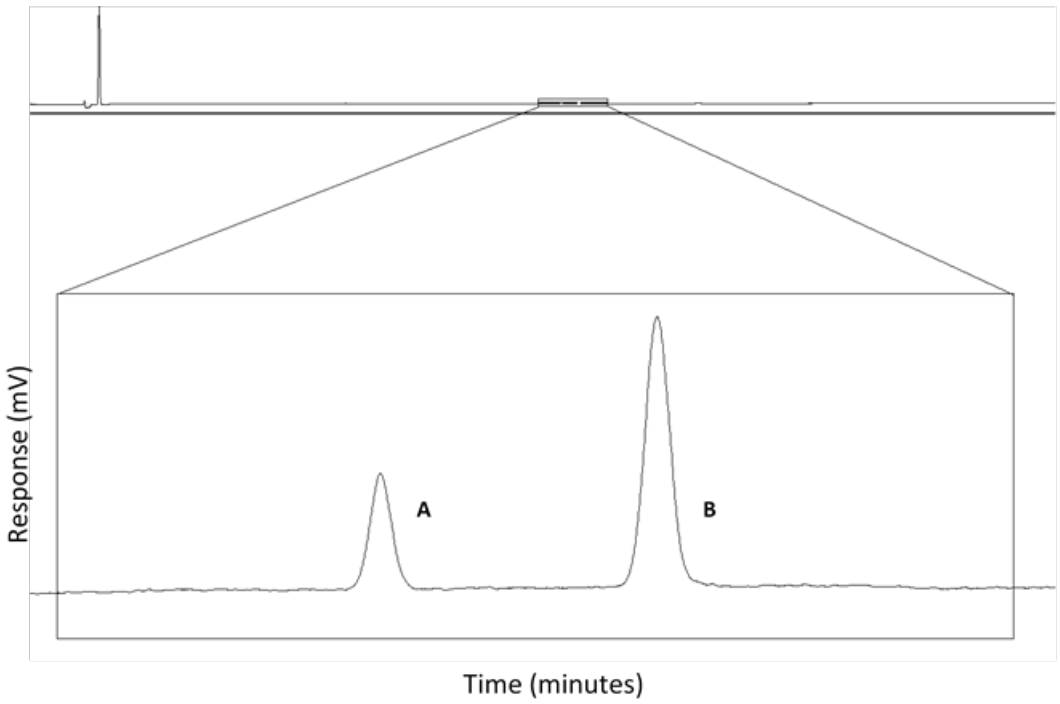

Figure 3.8. Typical gas chromatographic separation of (A) skatole (analyte) and (B) 5-methylindole (internal standard) prepared in ethyl acetate.

3.3.2.2 Skatole calibration studies

Chromatograms were obtained for skatole over the concentration range 0.01-0.5 µg/ml in acetonitrile and ethyl acetate, the peak areas were subsequently plotted against concentration; shown in Figure 3.9 and Figure 3.10 respectively. Standards were run in triplicate and the standard deviation of each data set has been displayed in the error bars of each figure. The error observed for the acetonitrile calibration identified that this solvent was not suitable for use with the detector and therefore could not be used with the final adipose tissue extract. The internal standard method however does allow for normalisation between runs, which significantly reduced the error in the triplicate data sets. The peak ratios were subsequently plotted against concentration, these are shown in Figure 3.11 and Figure 3.12 respectively. As may be seen from these calibration plots, ethyl acetate was shown to be superior as the LOD and precision were better than that obtained with acetonitrile.

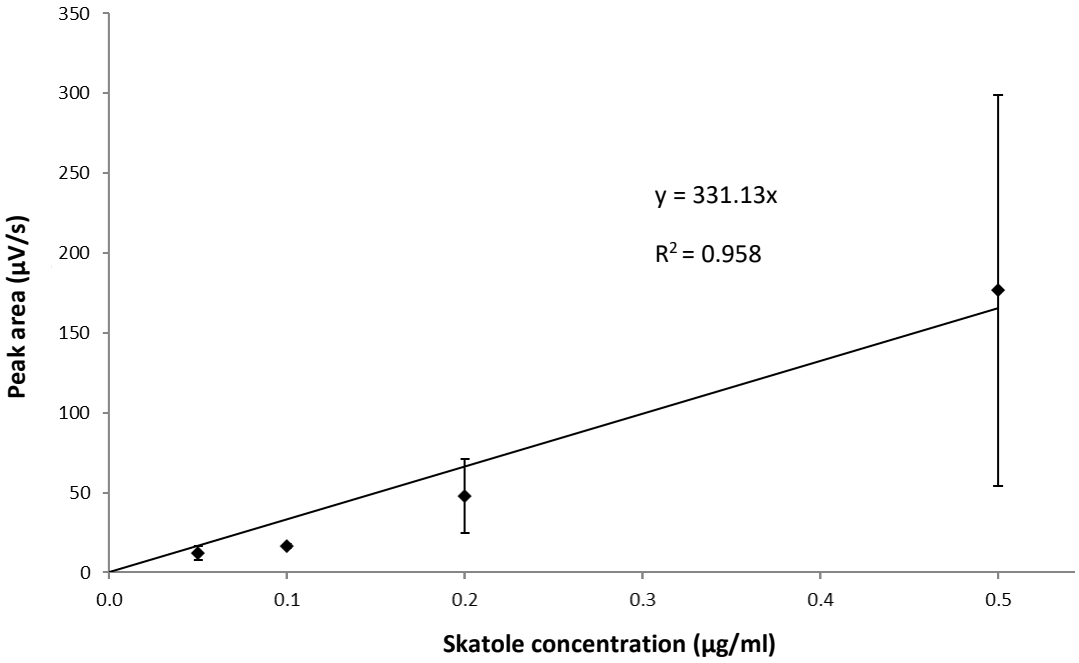

Figure 3.9. Calibration plot of peak area vs. concentration for skatole prepared in acetonitrile (n=3) at 0.05, 0.1, 0.2, and 0.5 µg/ml.

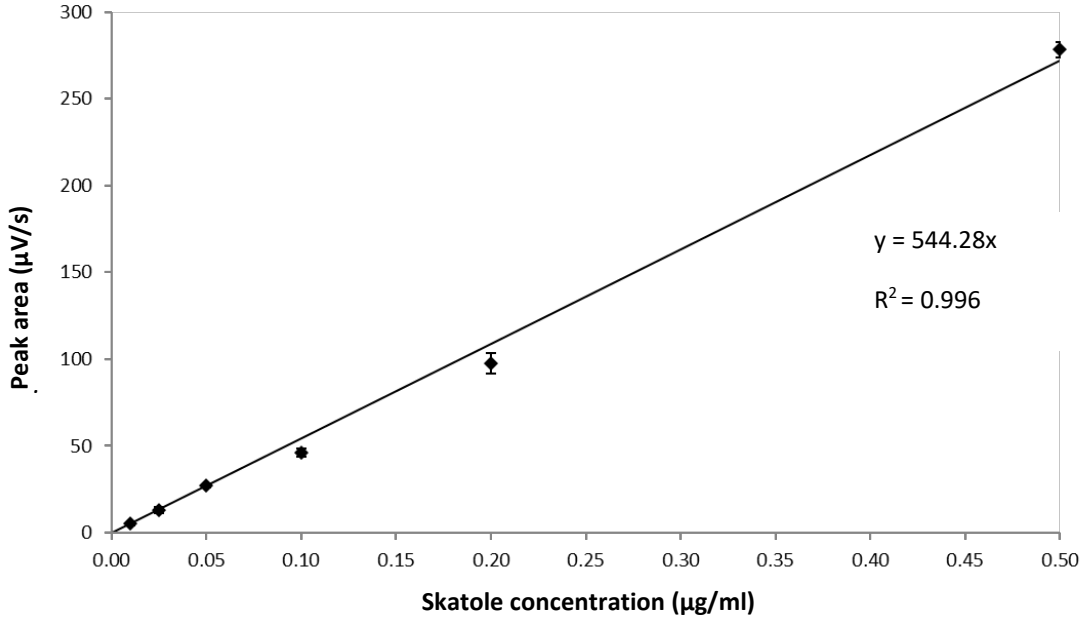

Figure 3.10. Calibration plot of peak area vs. concentration for skatole prepared in ethyl acetate (n=3) at 0.01, 0.025, 0.05, 0.1, 0.2, and 0.5 µg/ml

The lower concentrations investigated were not detectable with the acetonitrile preparation, and the correlation coefficient was calculated to be 0.99 in ethyl acetate compared to 0.95 in acetonitrile. Consequently, an investigation into ethyl acetate was undertaken to determine the suitability of this solvent for the analysis of adipose tissue.

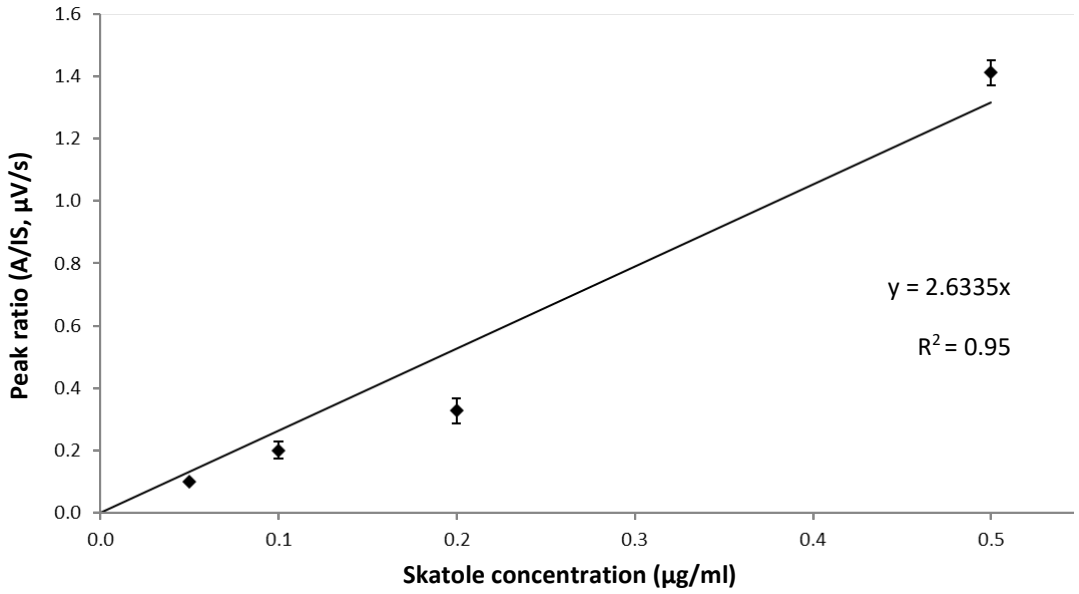

Figure 3.11. Calibration plot of peak ratio (analyte/internal standard) vs. concentration of skatole prepared in acetonitrile (n=3). Internal standard 5-methylindole.

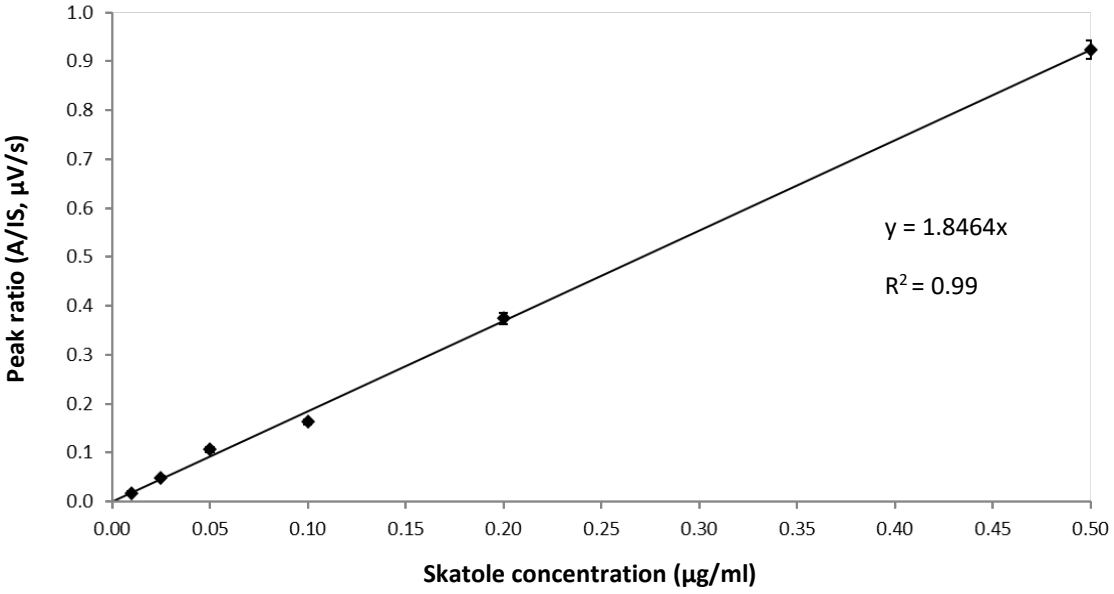

Figure 3.12. Calibration plot of peak ratio (analyte/internal standard) vs. concentration of skatole prepared in ethyl acetate (n=3). Internal standard 5-methylindole.

Figure 3.13 and Figure 3.14, show GC chromatograms for a sample of adipose tissue and a skatole standard preparation respectively; clearly, complete separation of these two compounds has been achieved.

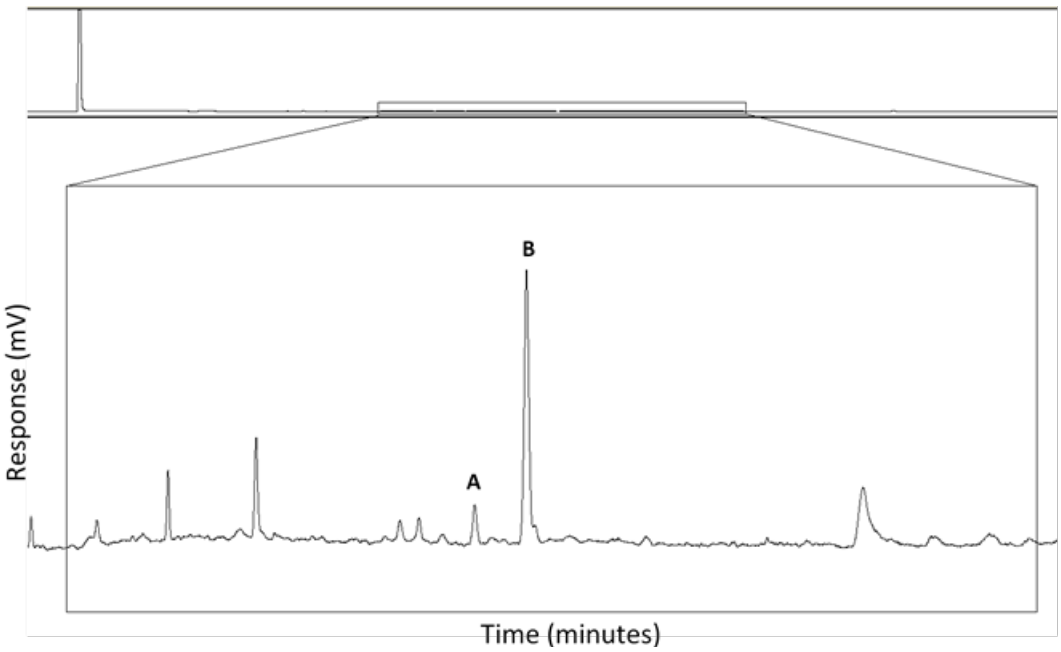

Figure 3.13. Typical gas chromatographic separation of (A) endogenous skatole (analyte) and (B) 0.5 µg/ml 5-methylindole (internal standard) prepared in an ethyl acetate adipose tissue extract. Skatole retention time 10.13 m, peak area: 50.57 µV/s. 5-methylindole retention time 10.47 m, peak area 378.24 µV/s.

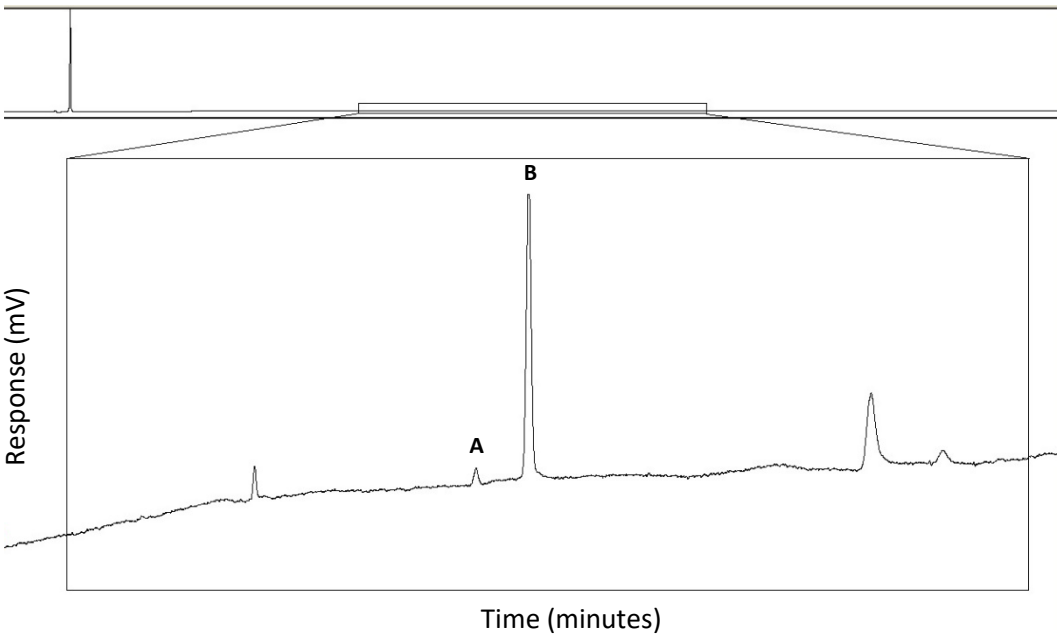

Figure 3.14. Typical gas chromatographic separation of a standard containing (A) 0.025 µg/ml skatole (analyte) and (B) 0.5 µg/ml 5-methylindole (internal standard) prepared in ethyl acetate. Skatole retention time: 10.08 m, Peak area: 13.95 µV/s. 5-methylindole retention time: 10.42 m, Peak area: 268.92 µV/s.

3.3.2.3 Validation of sample preparation with ethyl acetate

In order to extract skatole from adipose tissue a suitable solvent combination must be employed to allow for the subsequent gas chromatographic separation of the analytes from other compounds of a similar affinity for the final solvent phase. The inital method employed for the preparation of adipose tissue used acetonitrile as the final solvent extract. However, the imprecision encountered when using this solvent with the NPD resulted in the investigation of a modified approach. An additional sample preparation step, solvent exchange, allowed for the sample extract to be reconstituted in ethyl acetate; a solvent better suited to use with a NPD. A fortification study was performed to ensure that no significant loss of skatole occurred during this additional sample preparation step. The results presented in Table 3.1 demonstrate that a 96 % recovery was achieved for skatole after reconstitution of the fortified liquid adipose tissue extracts in ethyl acetate (n=4).

Table 3.1. Recovery of skatole from fortified samples reconstituted in ethyl acetate by GC-NPD (n=4).

Skatole added (µg/ml)	Skatole reconstituted (µg/ml)	Peak ratio (A/IS)	Mean peak ratio	Background subtracted peak ratio	Skatole recovered (µg/ml)	Skatole recovered (%)	Average recovery (%)
0.000	0.000	0.13	0.15				
0.000	0.000	0.17					
0.010	0.020	0.20	0.19	0.04	0.02	95.1	95.75
0.010	0.020	0.18					
0.025	0.050	0.24	0.24	0.09	0.05	96.4	
0.025	0.050	0.24					

To ensure that this additional preparation step would provide a more accurate measurement of skatole in adipose tissue samples, a set of six adipose tissue samples were analysed by both the electrochemical method and the GC-NPD method with and without the reconstitution step. The correlation of skatole concentrations shown in Figure 3.15 indicated that the GC-NPD response for endogenous skatole was in better agreement with the electrochemical method when prepared with the additional reconstitution step.

This can be attributed to the improved accuracy of measurements made by the GC-NPD method when the sample extract is reconstituted in ethyl acetate for injection to the GC as opposed to acetonitrile (Figure 3.11 vs. Figure 3.9). Therefore, the modified GC sample preparation method was used in all further studies.

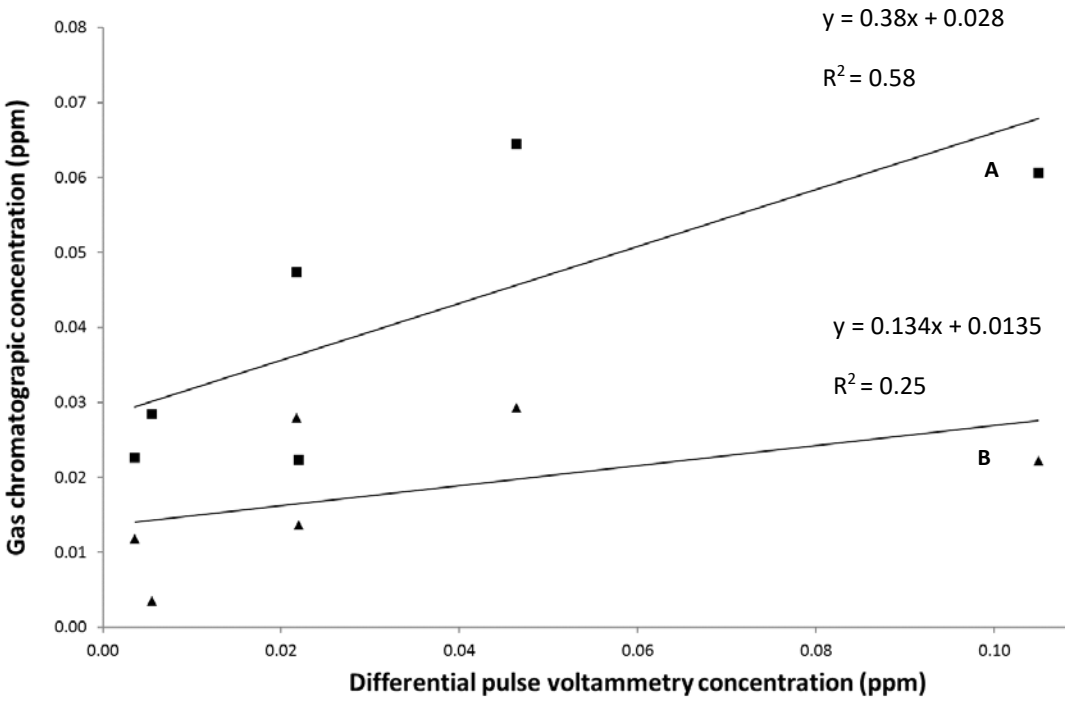

Figure 3.15. Comparison of GC-NPD concentration for skatole in adipose tissue extracts prepared with different solvents: (A) ethyl acetate (B) acetonitrile. Comparison of skatole concentration calculated with GC-NPD method compared to the DPV method (n=6). Responses are averages of duplicate data sets.

3.3.2.4 Androstenone calibration

The chromatogram in Figure 3.16 shows the separation of peak responses for a solution containing standards of both the analyte androstenone and the internal standard androsterone. The chromatogram of an analysed adipose tissue sample extract has been presented in Figure 3.17 for comparative purposes. This chromatogram shows the separation of the peak responses for endogenous androstenone, the internal standard

(androsterone) and the other endogenous compounds present in an analysed adipose tissue sample.

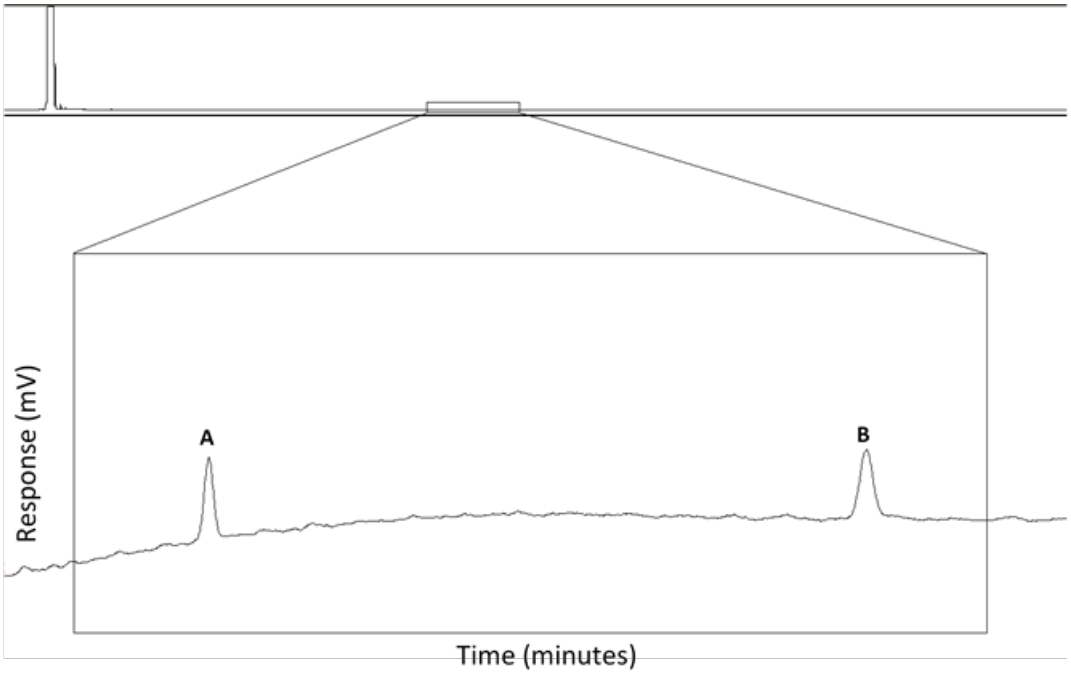

Figure 3.16. Typical gas chromatographic separation of a standard containing (A) 1 µg/ml androstenone (analyte) and internal standard (B) 2 µg/ml androsterone prepared in methanol hexane (9:1) adipose tissue extract. Androstenone retention time 20.6 m, peak area 80.38 µV/s. Androsterone retention time 22.7 m, peak area 97.18 µV/s.

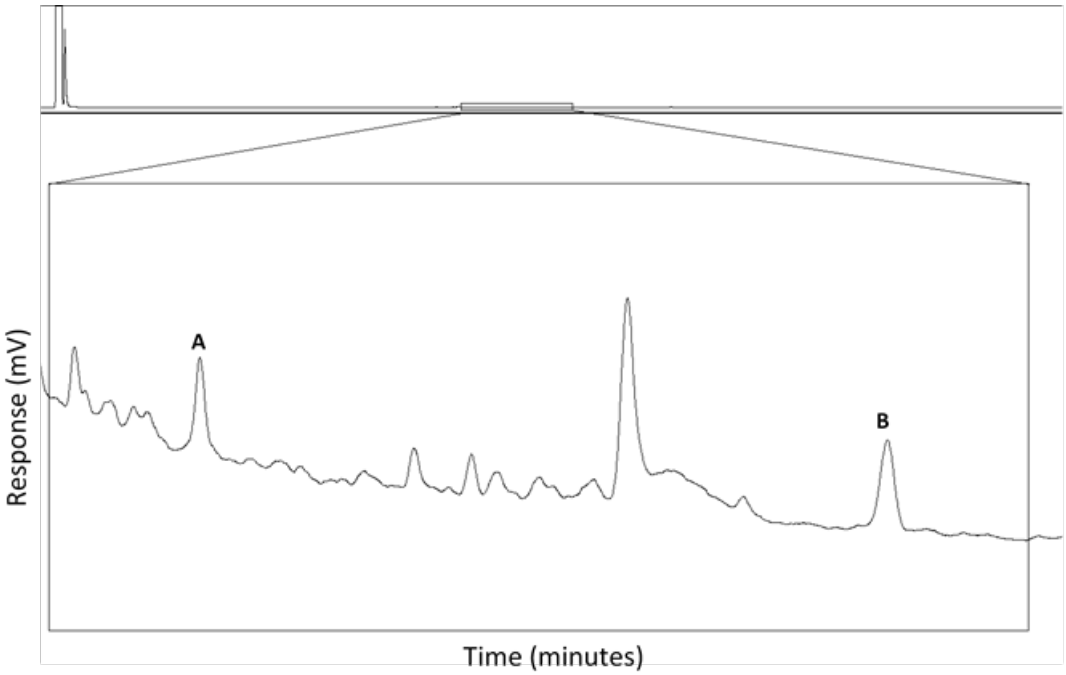

Figure 3.17. Typical gas chromatographic separation of (A) endogenous androstenone (analyte) and (B) added internal standard 2.0 µg/ml androsterone prepared in methanol hexane (9:1) adipose tissue extract. Androstenone retention time 20.1 m, peak area 67.75 µV/s, Androsterone retention time 21.9 m, peak area µV/s.

Chromatograms were obtained for androstenone over the concentration range 0.01-5.00 µg/ml. The peak areas have been plotted against concentration for androstenone in Figure 3.18. The peak area ratios were plotted against concentration, and as shown in Figure 3.19 a linear response was obtained over the concentration range studied. This data demonstrated that the chromatographic method had a sufficient linear range and detection limit to measure androstenone at levels associated with boar taint.

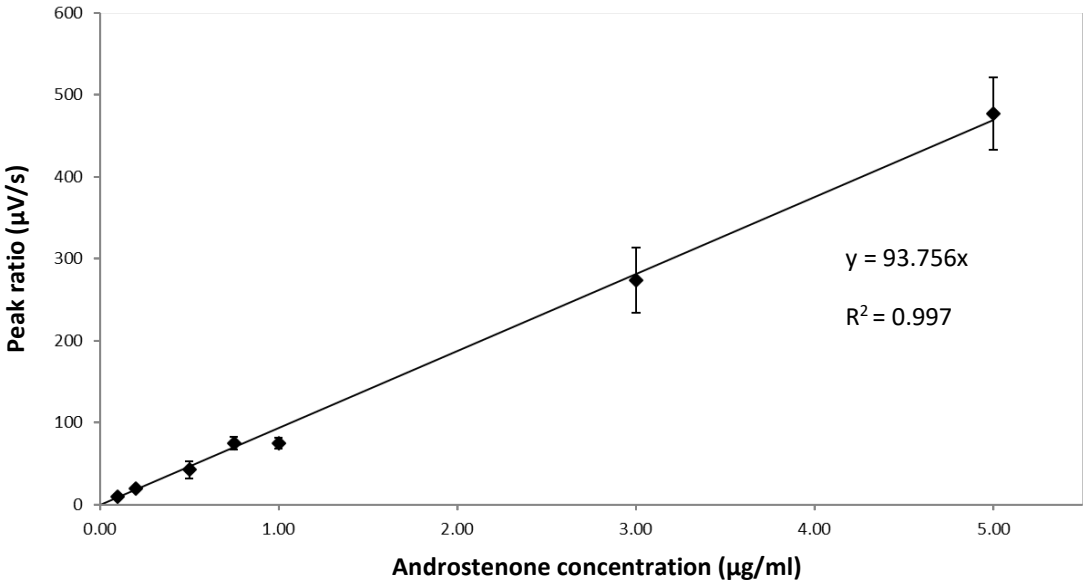

Figure 3.18. Calibration plot of peak area vs. concentration for androstenone prepared in methanol hexane (9:1) (n=3) at 0.1, 0.2, 0.5, 0.75, 1.0, 3.0 and 5.0 µg/ml.

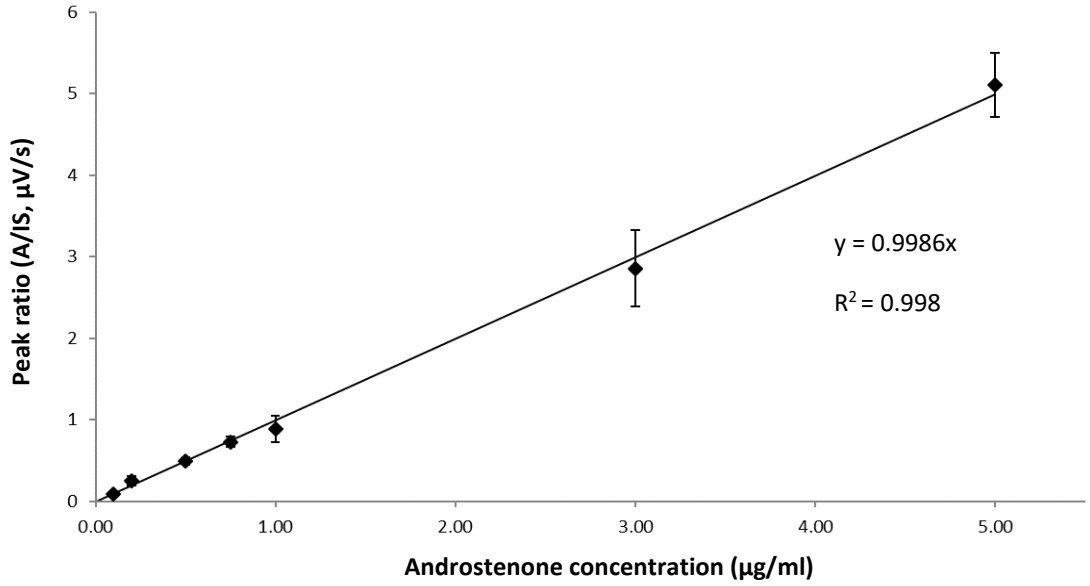

Figure 3.19. Plot of peak ratio (analyte/internal standard) vs. concentration of androstenone (n=3). Internal standard androsterone.

3.3.2.5 Comparison of gas chromatographic response vs. voltammetric sensor

The results obtained in the previous sections (differential pulse voltammetry and gas chromatography with nitrogen-phosphorous detection) were used to construct a correlation plot for skatole. Figure 3.20 shows that a good correlation was obtained, the correlation coefficient was calculated and the value was found to be R^2 0.80. Therefore, the results of this study shows that the sensor is in good agreement with the conventional gas chromatographic method. This demonstrates that the sensor approach shows promise for rapid measurements of skatole on the abattoir processing line, this will be discussed in the next chapter.

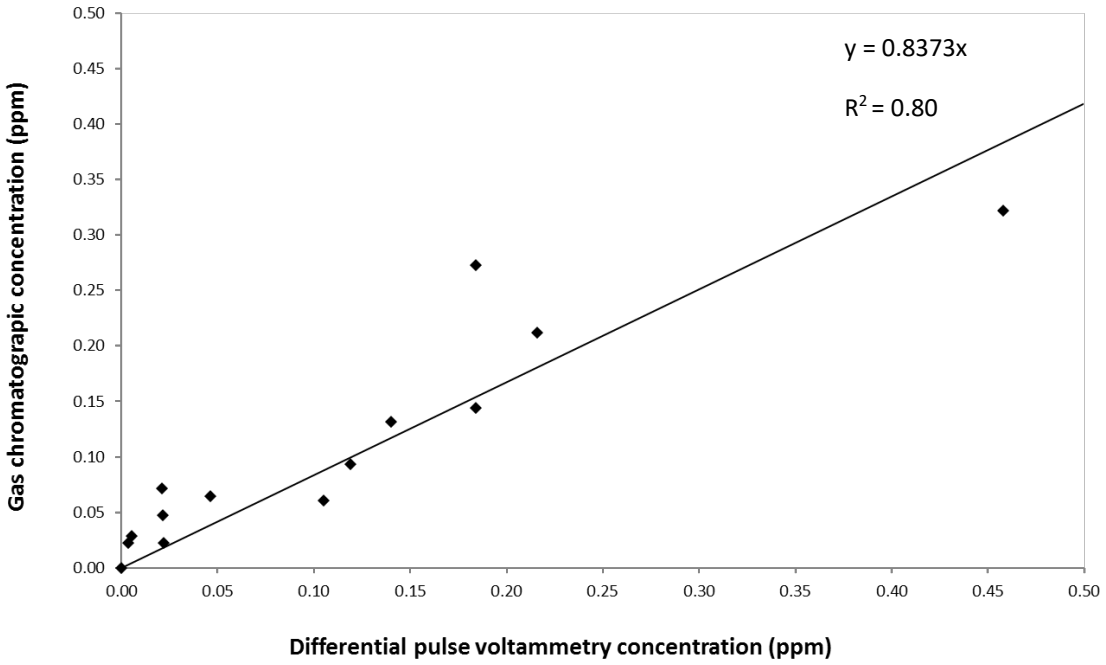

Figure 3.20. Preliminary correlation plot for the concentration of skatole in adipose tissue measured by both the voltammetric sensors and the corresponding GC-NPD method (n=14).

3.3.2.6 Comparison of gas chromatographic response vs. amperometric biosensor

The results obtained in the previous sections (chronoamperometry and gas chromatography with flame ionisation detection) were used to construct a comparison plot for androstenone. Figure 3.21 shows that a good correlation was obtained for concentrations of androstenone in adipose tissue samples from retailers and a pig producer, the correlation coefficient was calculated and the value was found to be R^2 0.93. Therefore, the results of this study shows that the biosensor is in good agreement with the conventional gas chromatographic method. This demonstrates that the biosensor approach shows promise for rapid measurements of androstenone on the abattoir processing line, this will be discussed in the next chapter.

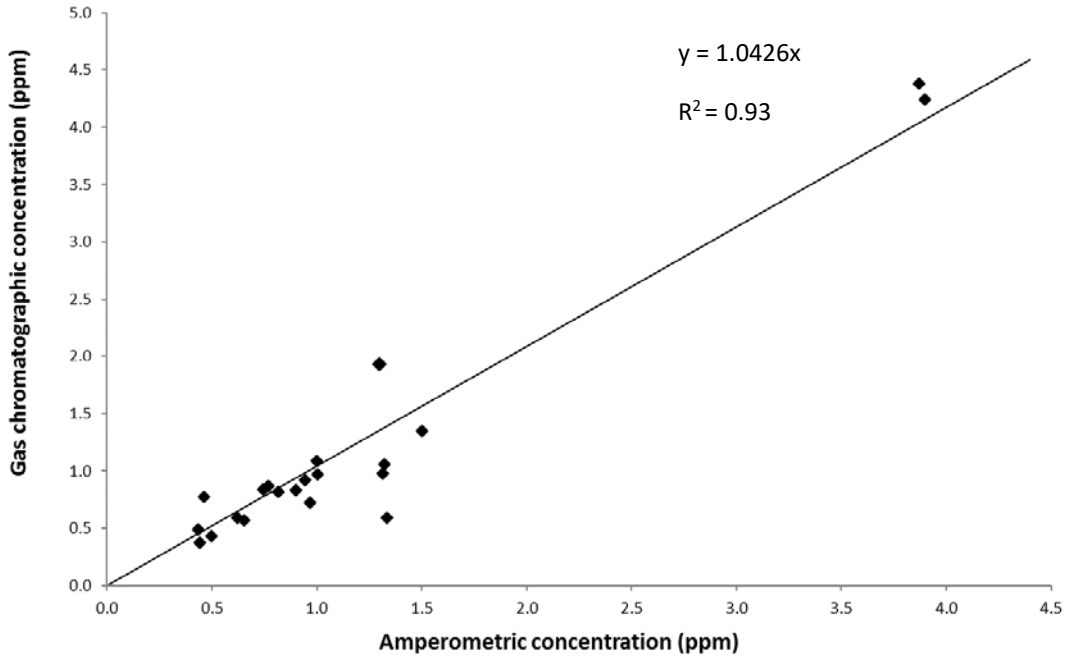

Figure 3.21. Preliminary correlation plot for the concentration of androstenone in adipose tissue measured by both the amperometric biosensors and the corresponding GC-FID method (n=21).

3.4 Conclusion

In this chapter the preliminary studies, using samples from a local retailer and pig producer, have demonstrated the successful application of rapid electroanalytical approaches using a sensor and biosensor for the measurement of boar taint compounds, skatole and androstenone, in adipose tissue. It should be mentioned that these devices were used in the laboratory, on adipose tissue samples, whereby the techniques were used independently. Skatole was measured using differential pulse voltammetry in conjunction with SPCEs (vs. Ag/AgCl). Whereas, androstenone was measured with a biosensor in conjunction with chronoamperometry. The total analysis time for both measurements and the application of the sensor or biosensor to the tissue sample was achieved in under a minute. The biosensor was constructed by depositing an enzyme, namely 3α-hydroxysteroid dehydrogenase, onto the surface of a Meldola's Blue modified screen printed carbon electrode (MB-SPCE). The sensor and biosensor could be simply inserted into the adipose tissue sample for direct measurements. This showed the possibility of developing a dual system for the analysis of both androstenone and skatole simultaneously in adipose tissue. The next chapter will discuss the development of the system and its application for online measurements in an abattoir.

To validate the electrochemical methods reference procedures based on gas chromatography with ionisation detection. Skatole was measured with a nitrogen-phosphorous detector whereas, androstenone was measured with a flame ionisation detector. In both methods an extraction procedure was required, these were adapted from available literature sources. These methods were successful in measuring skatole and androstenone over the concentration range expected in the adipose tissue of pigs. A comparison of the two methods for the same set of samples gave correlation coefficients of 0.8 and 0.93 for skatole and androstenone respectively. This data demonstrated that

the electrochemical techniques should be suitable for the analysis of boar taint compounds on the abattoir processing line; this is discussed in detail in chapter four.

Chapter Four

Investigations into a dual electrochemical system for the analysis of boar taint compounds at the abattoir processing line

Chapter Four Contents

Table of Figures

Chapter Summary

Chapter four investigates the electroanalytical instrumentation configuration suitable for the simultaneous measurement of skatole and androstenone. The pig production industry requires a rapid measurement system to determine if a pork product exhibits boar taint. Therefore, a single device that can measure both compounds simultaneously would suitably achieve this brief.

Simultaneous measurement of the two compounds using the laboratory based potentiostats (mains powered) proved unsuccessful. Consequently, further investigations were performed with portable potentiostats (battery powered) and an electrical isolator to determine a suitable instrument configuration that could be used to successfully measure skatole and androstenone simultaneously in a sample of adipose tissue.

The portable measurement system was taken to an abattoir processing line and used to interrogate the adipose tissue of pig carcasses. The interrogated samples were collected and analysed with the gas chromatographic methodologies for both skatole and androstenone quantification. The endogenous concentrations of the boar taint compounds were compared and a positive correlation was observed between the two measurement techniques.

Chapter Four

4.1 Introduction

In chapter three the direct electroanalysis of adipose tissue for the quantification of boar taint compounds was investigated; the determination and quantification of skatole and androstenone, using an independent sensor and biosensor respectively, was demonstrated. A calibration study was performed by fortifying adipose tissue of a known mass with corresponding concentrations of the target analytes, skatole and androstenone (μg/g) and measuring the change in current with increasing concentration. A linear positive relationship was observed for both compound calibration plots; subsequently measurements of skatole and androstenone were obtained from samples of adipose tissue and referred back to the standard addition calibration to determine their endogenous concentration. The same samples were analysed by gas chromatographic methods and the concentrations were compared; a positive correlation was observed for both compounds.

4.1.1 Development of a dual electrochemical measurement system

The correlation studies in chapter three demonstrated that the voltammetric sensor and amperometric biosensor could be used to quantify skatole and androstenone respectively, however these electrochemical measurements were obtained independently. The pork production industry requires an analytical system that can measure both compounds rapidly and simultaneously in a portable system, allowing processors to make a decision on the presence or absence of boar taint in carcasses to facilitate on-line carcass sorting. In chapter three fast analysis times were demonstrated with both the voltammetric and amperometric scans being achieved in under one minute.

Investigations into a portable system capable of running both a chronoamperometric and differential pulse voltammetric method simultaneously will be discussed in this chapter.

4.1.2 Abattoir measurements of skatole and androstenone

The abattoir processing line is a cold environment, with ambient temperatures maintained below 5°C, this is the temperature recommended by Red Tractor; the largest food standards scheme in the UK (*Meat Processing Scheme v3.1,* 2018). In addition, the heavy dripping carcasses move at speed through the plant. Therefore, any analytical equipment taken into this environment must be able to withstand these conditions. The potentiostat instrumentation must be sealed in a water tight robust housing, have minimal wiring and ideally be small enough to carry around the abattoir. Modern advances in electrochemical instrumentation and equipment have made this a possibility; using Bluetooth technology measurement waveforms can be sent wirelessly to the potentiostat. Additionally, tablets with splash proof coverings can be employed to operate the potentiostatic software which would be a practical solution in this environment. However, the ability to use two potentiostats from a single device via Bluetooth is not yet possible; the software requires new coding to use either Bluetooth or a Wifi connection to achieve this so undoubtedly this will be possible very soon.

4.2 Experimental

4.2.1 Electroanalysis

4.2.1.1 Apparatus and instrumentation

The sensor and biosensors first described in chapter two are used in conjunction with two types of potentiostat in this chapter. The configurations for the connection arrangements are described in the procedures section (4.2.1.3). The sensors and biosensors for dual studies were mounted into a single connector with a back to back layout, this can be seen in Figure 4.1. The µAutolab III potentiostat was interfaced to a laptop for data acquisition

via NOVA v.2.0.2 (Metrohm, Netherlands). The Emstat3 potentiostats (Palmsens BV, Netherlands) were interfaced to a laptop using USB A-B cables (resistance <1 ohm) for data acquisition with the MultiTrace v3.4 and PSTrace software v3.4 depending on whether the two methods of electroanalysis (differential pulse voltammetry or chronoamperometry) were run simultaneously or independently. A USB-ISO (Olimex Ltd., Bulgaria) isolator was fitted between the laptop and potentiostat, using USB A-B cables, where stated.

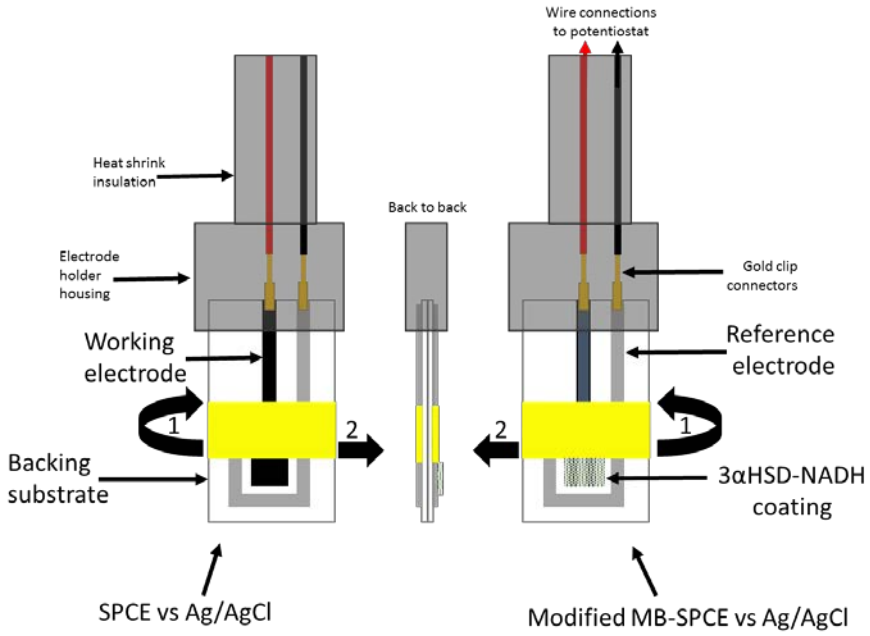

Figure 4.1. Configuration for the dual sensor and biosensor connector. (1) Depicts the planar surfaces of the different screen printed strips, and (2) depicts the sensor strips held back to back in the holder.

4.2.1.2 Chemicals and reagents

All chemicals and reagents have been previously described in chapter two section 2.2.2 and chapter 3 section 3.2.1.2.

4.2.1.3 Procedures

4.2.1.3.1 Simultaneous applied DPV and CA waveforms

Differential pulse voltammograms and chronoamperograms were obtained using SPCEs (vs. Ag/AgCl) in a solution containing 0.01 mM skatole in 0.1 M phosphate buffer pH 7 and 0.1 M sodium chloride. The apparatus set-ups are displayed in Figure 4.2; µAutolab III potentiostats were used in this study.

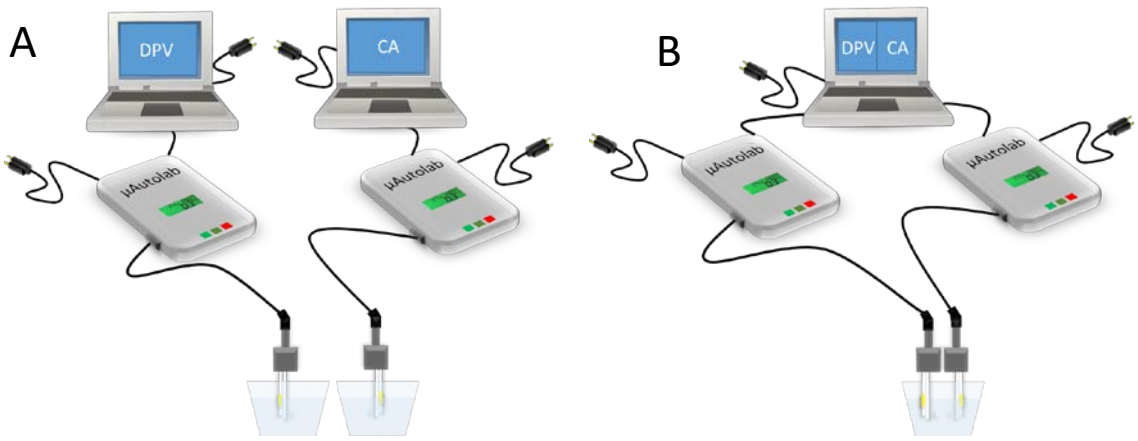

Figure 4.2. Apparatus and instrumentation configuration for the application of independent and simultaneous waveforms with µAutolab potentiostats. (A) µAutolab potentiostats mains powered (MP) operated independently with a laptop (MP) to obtain a differential pulse voltammogram (DPV) and chronoamperogram (CA). (B) µAutolab potentiostats (MP) operated simultaneously with a laptop (MP) to obtain a DPV and CA. SPCEs (vs. Ag/AgCl) side by side with individual holders in the voltammetric cell.

4.2.1.3.2 Investigation to isolate waveforms

4.2.1.3.2.1 µAutolab potentiostats

Differential pulse voltammograms and chronoamperograms were obtained using SPCEs (vs. Ag/AgCl) in a solution containing 0.1 M phosphate buffer pH 7 and 0.1 M sodium chloride. The apparatus set-ups are displayed in Figure 4.3; µAutolab III potentiostats were used in this study and isolators were employed in set-ups B-D.

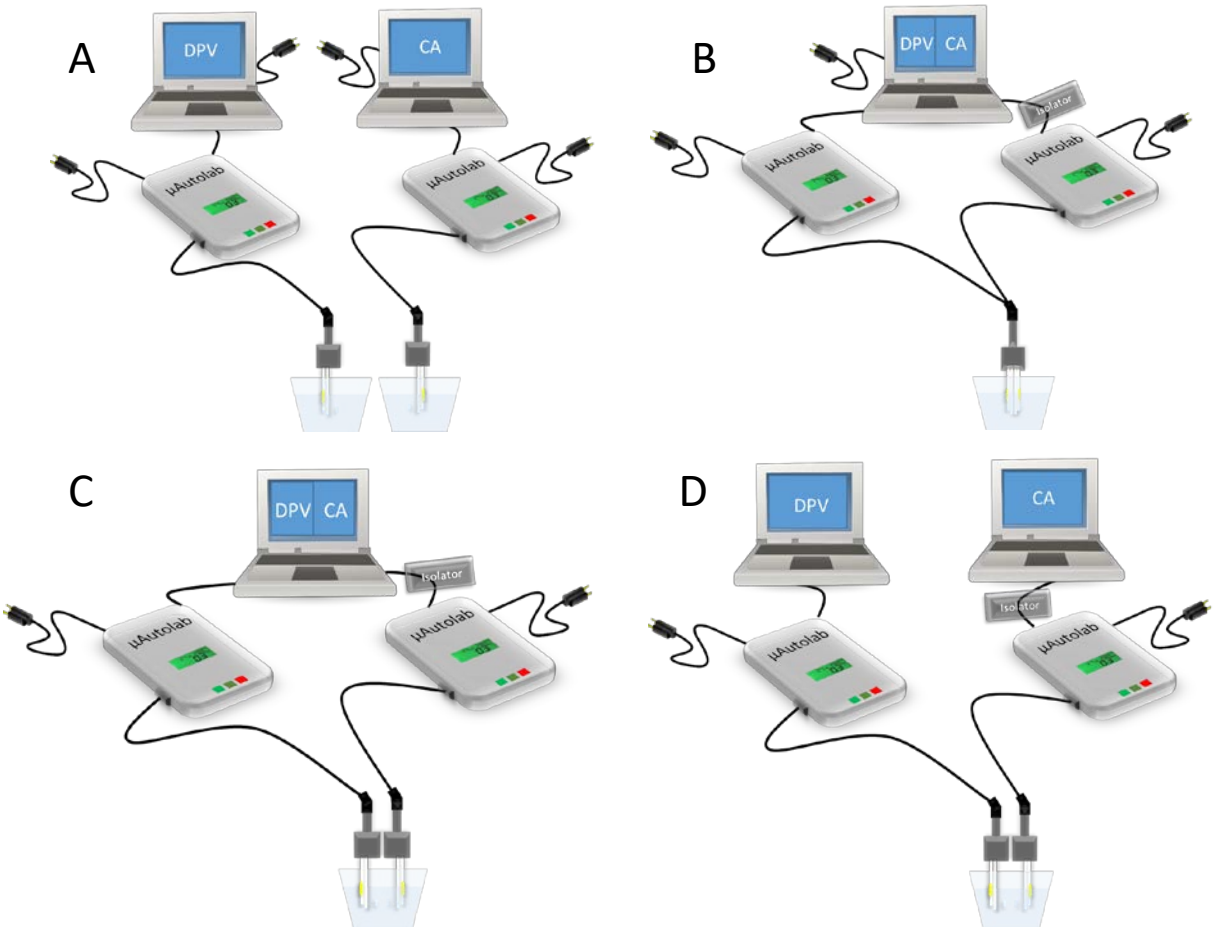

Figure 4.3. Apparatus and instrument configuration for waveform isolation study with µAutolab potentiostats. (A) µAutolab potentiostats mains powered (MP) operated independently with a laptop (MP) to obtain a differential pulse voltammogram (DPV) and chronoamperogram (CA). (B) µAutolab potentiostats (MP) operated simultaneously with a laptop (MP) to obtain a DPV and CA. SPCEs (vs. Ag/AgCl) back to back using one holder in the voltammetric cell. Isolator fitted between the laptop and the CA potentiostat. (C) µAutolab potentiostats (MP) operated simultaneously with a laptop (battery powered) to obtain a DPV and CA. SPCEs (vs. Ag/AgCl) side by side with individual holders in the voltammetric cell. Isolator fitted between the laptop and the CA potentiostat. (D) µAutolab potentiostats (MP) operated independently with a laptops (battery powered) to obtain a DPV and CA. SPCEs (vs. Ag/AgCl) side by side with individual holders in the voltammetric cell. Isolator fitted between the laptop and the CA potentiostat.

4.2.1.3.2.2 Emstat3 potentiostats

Differential pulse voltammograms were obtained using SPCEs (vs. Ag/AgCl) and chronoamperograms were obtained using NADH-MB-SPCEs (vs. Ag/AgCl) in a solution containing 0.1 M phosphate buffer pH 7 and 0.1 M sodium chloride. The apparatus set-ups are displayed in Figure 4.4; Emstat3 potentiostats were used in these studies and isolators were employed in set-ups B, D and E. All laptops and potentiostats were battery powered.

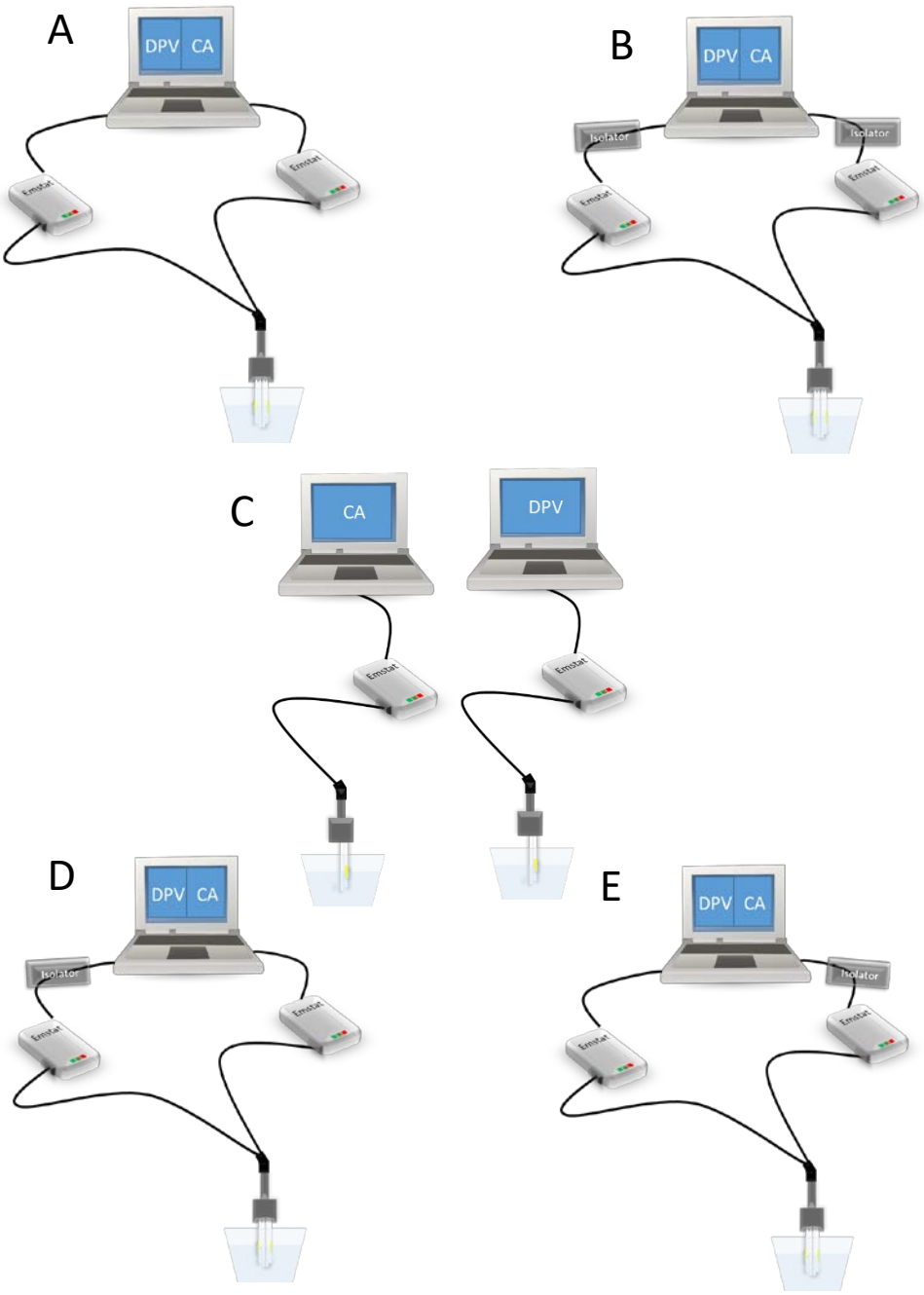

Figure 4.4. Apparatus and instrumentation configuration for waveform isolation study with Emstat3 potentiostats. (A) Emstat3 potentiostats operated simultaneously with a laptop to obtain a differential pulse voltammogram (DPV) and chronoamperogram (CA). (B) Emstat3 potentiostats operated simultaneously with a laptop to obtain a DPV and CA. Isolators fitted between the laptop and both potentiostats. (C) Emstat3 potentiostats operated independently with a laptop to obtain a DPV and CA. (D) Emstat3 potentiostats operated simultaneously with a laptop to obtain a DPV and CA. Isolator fitted between the laptop and the DPV potentiostat. (E) Emstat3 potentiostats operated simultaneously with a laptop to obtain a DPV and CA. Isolator fitted between the laptop and the CA potentiostat. In all set up's except (C) SPCEs (vs. Ag/AgCl) are back to back using one holder in the voltammetric cell.

4.2.1.3.3 Performance comparison of Emstat3 and µAutolab III potentiostats

Calibration studies were performed using the same chemicals and reagents and procedures as those described in chapter two. However, this study was performed in using two different instruments; the µAutolab potentiostat and the Emstat3 potentiostat.

4.2.1.3.4 Dual studies in adipose tissue

4.2.1.3.4.1 Initial endogenous measurement

Differential pulse voltammograms were obtained using SPCEs (vs. Ag/AgCl) and chronoamperograms were obtained using MB-SPCEs (vs. Ag/AgCl) inserted into an adipose tissue sample warmed to 30°C on a heater plate. The apparatus set-ups are displayed in Figure 4.5; Emstat3 potentiostats were used in this study and an isolator was employed in set-up B. All laptops and potentiostats were battery powered.

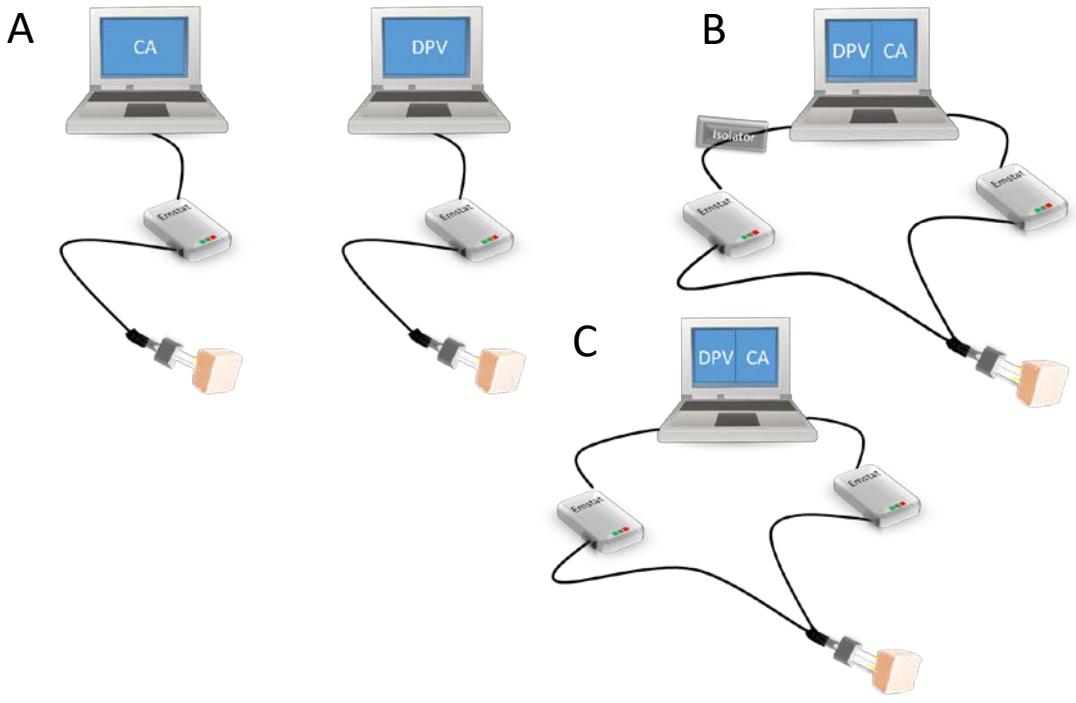

Figure 4.5. Apparatus and instrumentation configuration for the dual electroanalysis of adipose tissue. (A) Emstat3 potentiostats operated independently with a laptop to obtain a differential pulse voltammogram (DPV) and chronoamperogram (CA) from an adipose tissue sample. (B) Emstat3 potentiostats operated simultaneously with a laptop to obtain a DPV and CA. Isolator fitted between the laptop and the DPV potentiostat. (C) Emstat3 potentiostats operated simultaneously with a laptop to obtain a DPV and CA. SPCEs (vs. Ag/AgCl) back to back using one holder inserted into an adipose tissue sample.

4.2.1.3.5 Prototype device implementation on the abattoir processing line

The mobile apparatus set-up, displayed in Figure 4.6, was used in a commercial abattoir to analyse carcasses on the processing line. An incision was made in the subcutaneous adipose tissue of each carcass at the first rib position. The temperature and pH of the adipose tissue was measured before and after each application of the dual electrochemical measurement system; to best represent the temperature and pH at the time of electrochemical measurement an average was calculated from the two values. Differential pulse voltammograms were obtained using SPCEs (vs. Ag/AgCl) and chronoamperograms were obtained using biosensors (3αHSD-NADH-MB-SPCE vs. Ag/AgCl). The measured section of adipose tissue was removed with a scalpel and stored in a grip seal bag in a battery powered cool box. The samples were taken back to the laboratory (refrigerated storage during 24hr transport period) and stored at -18°C until analysis using the gas-chromatographic methods. Figure 4.7 displays photos taken on the abattoir processing line; Figure 4.7A shows the application of the dual electrochemical instrument system, whereas Figure 4.7B shows the use of the Testo 205 probe (Testo Ltd, Alton) for the measurement of adipose tissue pH and temperature.

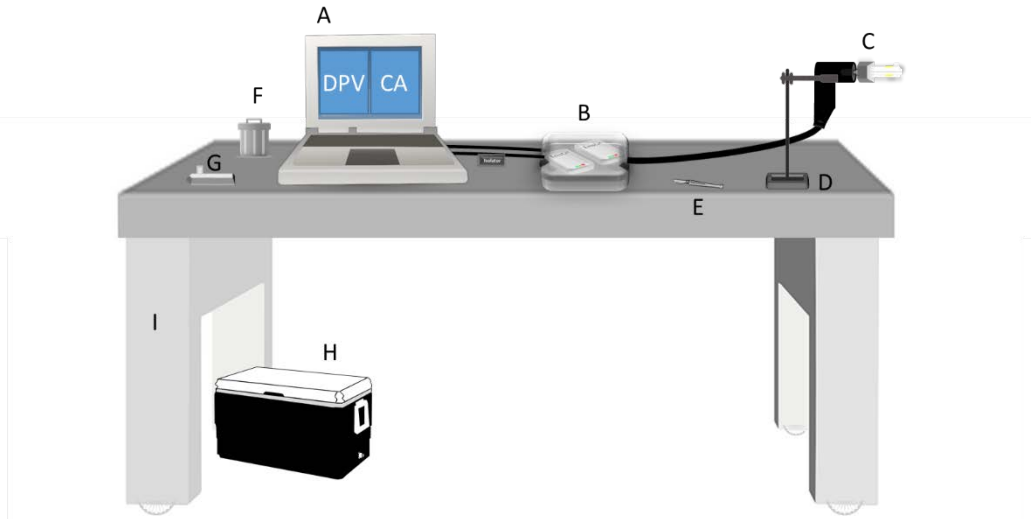

Figure 4.6. Apparatus and instrumentation for abattoir study. (A) Battery powered laptop running differential pulse voltammetry and chronoamperometry via the MultiTrace v3.4 software package interfaced to the; (B) Dual Emstat3 potentiostat prototype device (two Emstat3 potentiostats housed in a water tight case) with an isolator fitted between the laptop and the DPV potentiostat, connected to a; (C) Back to back sensor holder, supported by a; (D) Clamp stand. (E) Scalpel for carcass incisions. (F) Waste bin for used sensors. (G) Temperature and pH meter (H) Cooled storage for sensors, biosensors and adipose tissue samples. (I) Metal trolley.

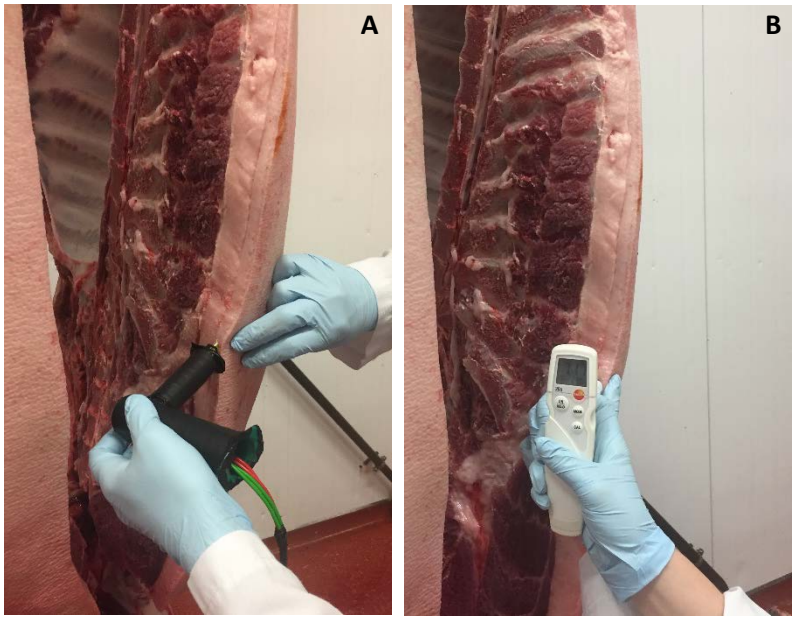

Figure 4.7. Abattoir photos. (A) Prototype device inserted in a carcass for dual electrochemical analysis and (B) a Testo 205 probe inserted into the carcass for temperature and pH measurement.

4.2.2 Chromatographic analysis

4.2.2.1 Apparatus and instrumentation

The apparatus and instrumentation used in this chapter are the same as those previously described in chapter three section 3.2.2.1.1 for skatole and section 3.2.2.2.1 for androstenone.

4.2.2.2 Chemicals and reagents

All chemicals and reagents used in this chapter are the same as those previously described in chapter three section 3.2.2.1.2 for skatole and section 3.2.2.2.2 for androstenone.

4.2.2.3 Procedures

The procedures described for the gas chromatographic sample analysis and calibration are the same as those described in chapter three section 3.2.2.1.3 for skatole and 3.2.2.2.3 for androstenone.

4.3 Results and discussion

4.3.1 Simultaneous applied waveforms

In order to achieve the goal of measuring the two boar taint compounds at a speed appropriate for the abattoir production line we investigated the possibility of measuring skatole and androstenone simultaneously.

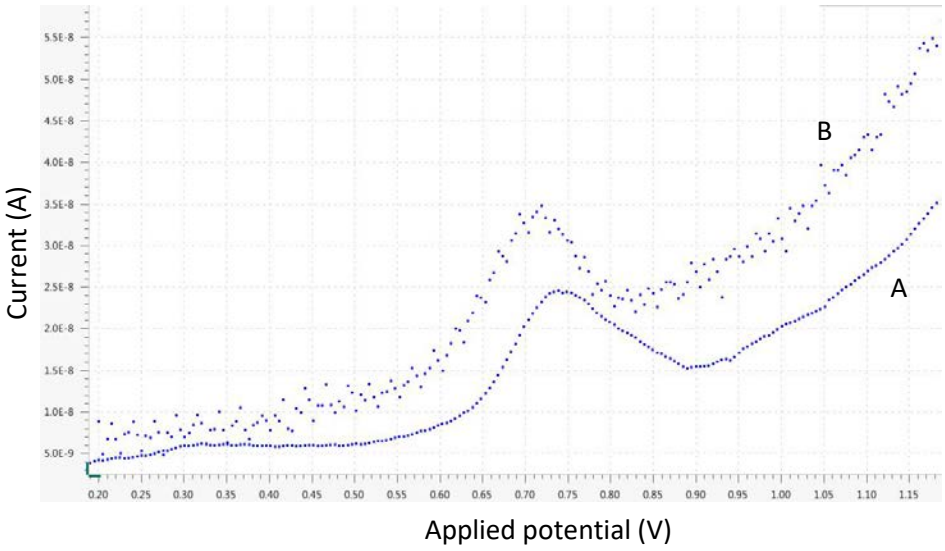

Figure 4.8. Independent (A) and simultaneously (B) obtained differential pulse voltammograms using µAutolab potentiostats. SPCEs (vs. Ag/AgCl) in a solution containing 0.01 mM skatole in 0.1 M phosphate buffer pH 7 with 0.1 M sodium chloride. Instrument and apparatus arrangements displayed in Fig 4.2.

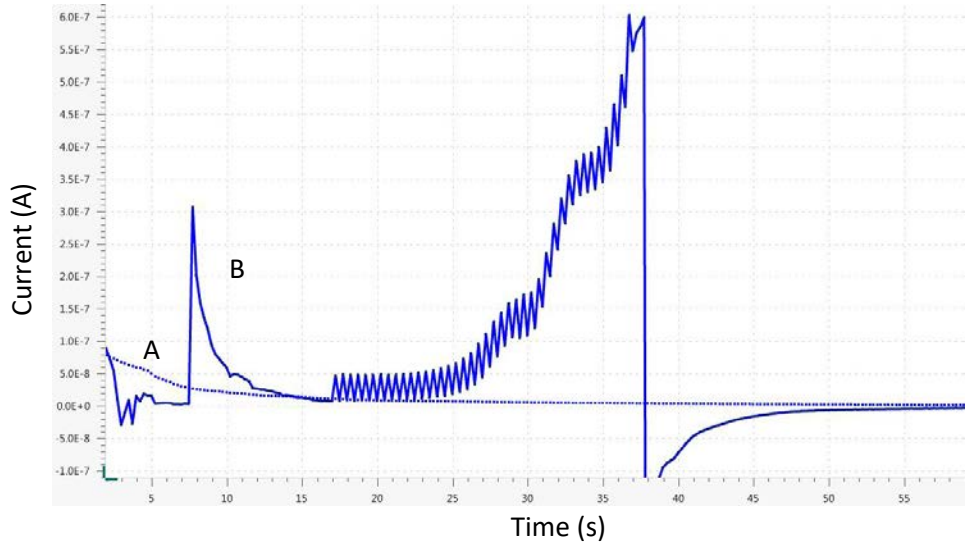

Figure 4.9. Independent (A) and simultaneously (B) obtained chronoamperograms using µAutolab potentiostats. SPCEs (vs. Ag/AgCl) in a solution containing 0.01 mM skatole in 0.1 M phosphate buffer pH 7 with 0.1 M sodium chloride. Instrument and apparatus arrangements displayed in Fig 4.2.

To compare the output waveforms when differential pulse voltammetry and chronoamperometry were ran simultaneously and independently, two instrument configurations were employed (Figure 4.2). Figure 4.8A and Figure 4.9A show the scans performed independently, whereas Figure 4.8B and Figure 4.9B show the simultaneous scans. Both simultaneous responses displayed issues with the output signal; the chronoamperogram (Figure 4.9B) displayed a superimposed differential pulse waveform whereas the differential pulse voltammogram (Figure 4.8B) displayed more noise than the independently operated scans. This can be attributed to the electrical interference resulting from the cross-over of the applied input waveforms. This is confirmed by the shape and duration of the signal cross-over shown in Figure 4.9B which strongly resembles the current output for differential pulse voltammetry (Figure 4.8).

4.3.2 Investigation to isolate waveforms

4.3.2.1 µAutolab potentiostats

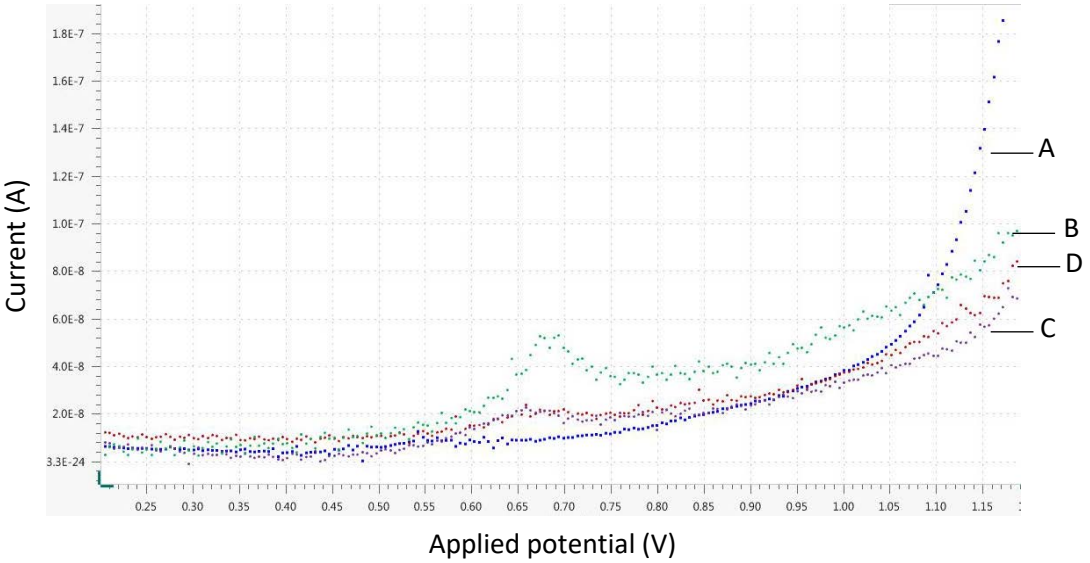

Figure 4.10. Differential pulse voltammograms obtained in an investigation into waveform isolation with µAutolab potentiostats. SPCEs (vs. Ag/AgCl) in a solution containing 0.1 M phosphate buffer pH 7 with 0.1 M sodium chloride. Instrument and apparatus arrangements displayed in Fig 4.3; (A) Independent scan (B) Simultaneous scan with dual control from one laptop with mains power (C) Simultaneous scan with dual control from one laptop without mains power and with the addition of an isolator on the chronoamperometry potentiostat; (D) Simultaneous scan with two laptops (battery power) and an isolator on the chronoamperometry potentiostat.

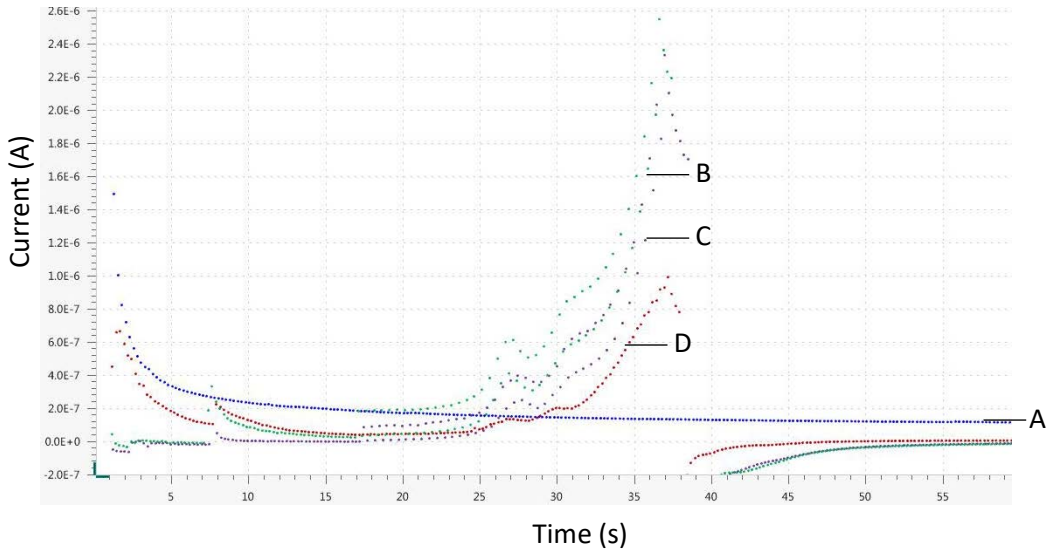

Figure 4.11. Chronoamperograms obtained in an investigation into waveform isolation with µAutolab potentiostats. SPCEs (vs. Ag/AgCl) in a solution containing 0.1 M phosphate buffer pH 7 with 0.1 M sodium chloride. Instrument and apparatus arrangements displayed in Fig 4.3; (A) Independent scan (B) Simultaneous scan with dual control from one laptop with mains power (C) Simultaneous scan with dual control from one laptop without mains power and with the addition of an isolator on the CA potentiostat; (D) Simultaneous scan with two laptops (battery power) and an isolator on the CA potentiostat.

The next step involved a study to try to isolate the applied waveforms and obtain individual output signals, to overcome the unwanted signal cross-over observed in the previous study. The instrument configurations investigated in this study are displayed in Figure 4.3. The resulting differential pulse voltammograms (Figure 4.10) and chronoamperograms (Figure 4.11) show that none of the arrangements employing an isolator with the µAutolab potentiostats prevented signal cross-over. The µAutolab potentiostats are mains powered, it is therefore possible that a circuit was formed between the potentiostats and the electrochemical cell via the mains power. At this point the µAutolab potentiostats did not seem to offer the possibility of dual operation for the measurement of skatole and androstenone using two different applied waveforms in the same electrochemical cell. Consequently, an alternative approach using battery powered potentiostats was investigated. It was decided to investigate applying simultaneous waveforms with Emstat3 potentiostats as these are not mains powered, preventing a possible circuit between the two potentiostats; this study is described in section 4.3.2.2.

4.3.2.2 Emstat3 potentiostats

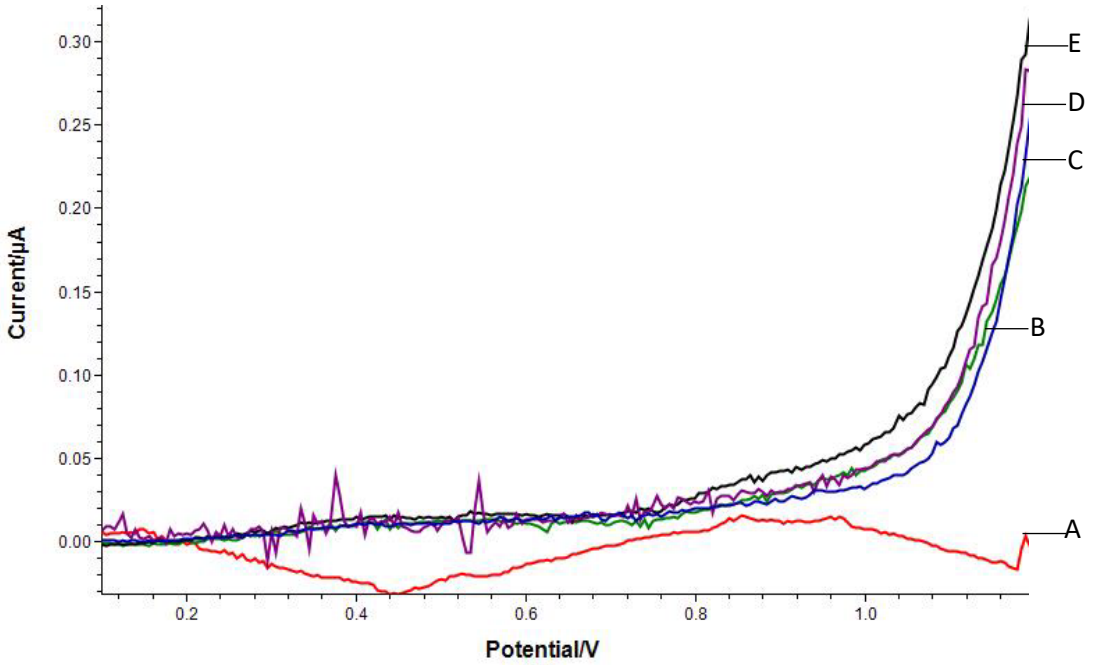

Figure 4.12. Differential pulse voltammograms obtained in an investigation into waveform isolation with Emstat3 potentiostats. SPCE (vs. Ag/AgCl) in a solution containing 0.1 M phosphate buffer pH 7 and 0.1 M sodium chloride. Instrument and apparatus arrangements displayed in Fig 4.4; (A) Simultaneous scan without isolation; (B) Simultaneous scan with isolators on both potentiostats; (C) Independent scan; (D) Simultaneous scan with isolator on the DPV potentiostat; (E) Simultaneous scan with isolator on the CA potentiostat.

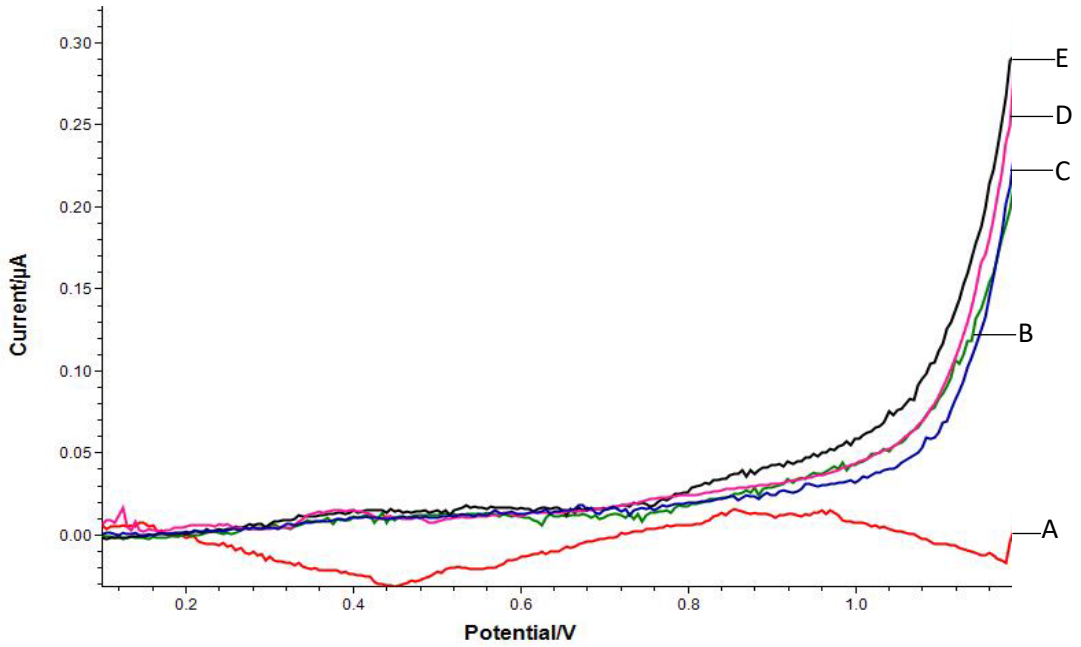

Figure 4.13. Differential pulse voltammograms demonstrating the use of the smooth function to reduce noise. Typical DPVs as described in Figure 4.12. Scan (D) has been smoothed using the inbuilt PSTrace4 v3.4 software function (Palmsens BV).

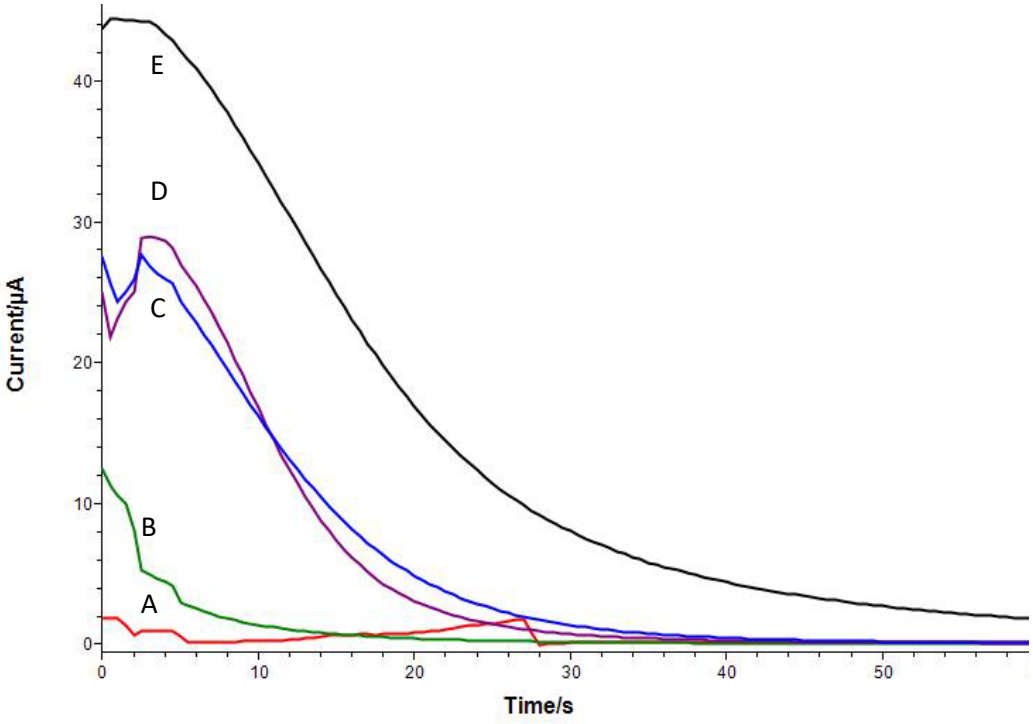

Figure 4.14. Chronoamperograms obtained in an investigation into waveform isolation with Emstat3 potentiostats. NADH-MB-SPCE (vs. Ag/AgCl) in a solution containing 0.1 M phosphate buffer pH 7 and 0.1 M sodium chloride. Instrument and apparatus arrangements displayed in Fig 4.4; (A) Simultaneous scan without isolation; (B) Simultaneous scan with isolators on both potentiostats; (C) Independent scan; (D) Simultaneous scan with isolator on the DPV potentiostat; (E) Simultaneous scan with isolator on the CA potentiostat.

In order to find a dual instrument configuration that allows for the two different waveforms to be applied to a single electrochemical cell without resulting in signal cross-over (i.e. resembles the output signal when operated independently), battery powered potentiostats (Emstat3's) were sourced. In terms of the practical application of this boar taint technology to the analysis of carcass adipose tissue on the abattoir processing line, portable devices would be much better suited. The output waveforms for the different instrument arrangements shown in the experimental section 4.2.1.3.2.2 Figure 4.4 are displayed in Figure 4.13 for differential pulse voltammetry and Figure 4.14 for chronoamperometry. The chronoamperograms indicate that without isolation simultaneous scans result in signal cross-over with the two Emstat3 potentiostats (Figure 4.14A), therefore isolators were used in the following experiments. Figure 4.14C illustrates an interference free chronoamperogram obtained with a single Emstat3

potentiostat. Two isolators appeared to suppress the current response as shown in Figure 4.14B. Incorporating an isolator between the laptop and the potentiostat running the DPV waveform (Figure 4.14D) resulted in a chronoamperogram similar to that obtained on an independent run (Figure 4.14C). Whereas, the current response was amplified when an isolator was incorporated between the laptop and the potentiostat running the chronoamperometry waveform (Figure 4.14E).

Therefore, the most similar output waveform in dual mode to that obtained independently was achieved with the isolator fitted between the laptop and the potentiostat applying the differential pulse voltammetry waveform. The corresponding differential pulse voltammogram for this set-up exhibited more noise than the independently obtained differential pulse voltammogram. Figure 4.13D demonstrates that the additional noise can easily be removed with the inbuilt smooth function provided in the PSTrace/MultiTrace software package for the Emstat3 potentiostats. It should be mentioned that all the experiments performed in this section, employed a holder allowing back to back sensor configuration. Consequently, it should be feasible to insert the sensors into the adipose tissue using this configuration for simultaneous measurement of the two boar taint compounds. This will be discussed in section 4.3.4.

4.3.3 Performance comparison of Emstat3 and µAutolab potentiostats

In order to compare the sensitivities of the µAutolab III potentiostat with the Emstat3 potentiostat, a calibration study was carried out with skatole over a similar concntration range to that reported in chapter two and chapter three. To ensure that the portable potentiostats could operate at a similar sensitivity a calibration study was performed with both the portable and mains powered laboratory instruments. The sensitivites obtained for the two instruments correlate well as demonstrated by the slopes for both sets of calibration data. The Emstat3 could measure concentrations down to 0.15 ppm with ease

whereas the µAutolab III potentiostat gave a peak for only 2 out of 3 scans, this suggests that the limit of detection was better for that the Emstat3 potentiostat.

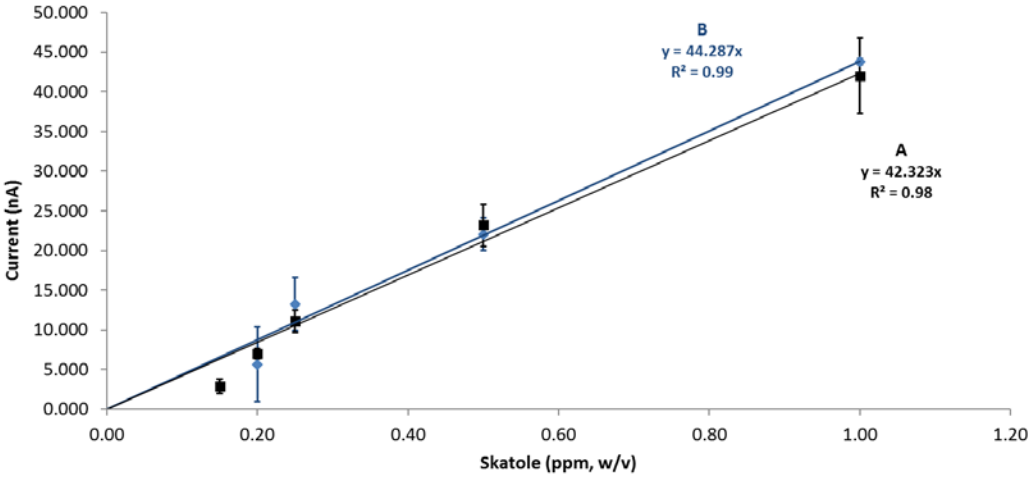

Figure 4.15. Skatole calibration used to compare the performance of the two different potentiostat models A) Emstat3 and B) µAutolab III. Skatole concentrations 0.15 ppm, 0.2 ppm, 0.25 ppm, 0.5 ppm, and 1 ppm prepared in 0.1 M pH 7 phosphate buffer with 0.1 M sodium chloride with 5 % methanol (n=3). Skatole response obtained for 2/3 scans with 0.15 ppm skatole using the µAutolab potentiostat.

4.3.4 Dual studies in adipose tissue

4.3.4.1 Initial studies comparing simultaneous and independent measurements

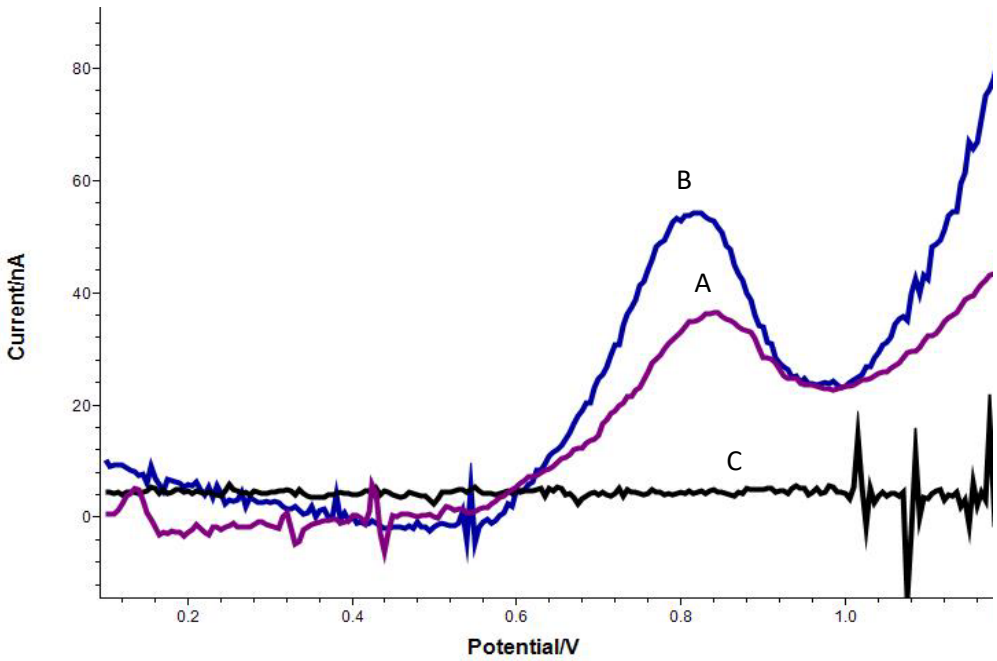

Figure 4.16. Independent and simultaneously obtained differential pulse voltammograms in porcine adipose tissue. SPCEs (vs. Ag/AgCl) inserted into an incision made in an adipose tissue sample. Instrument and apparatus arrangements displayed in Fig 4.5: (A) Independent scan; (B) Dual scan with isolator; (C) Dual scan without an isolator.

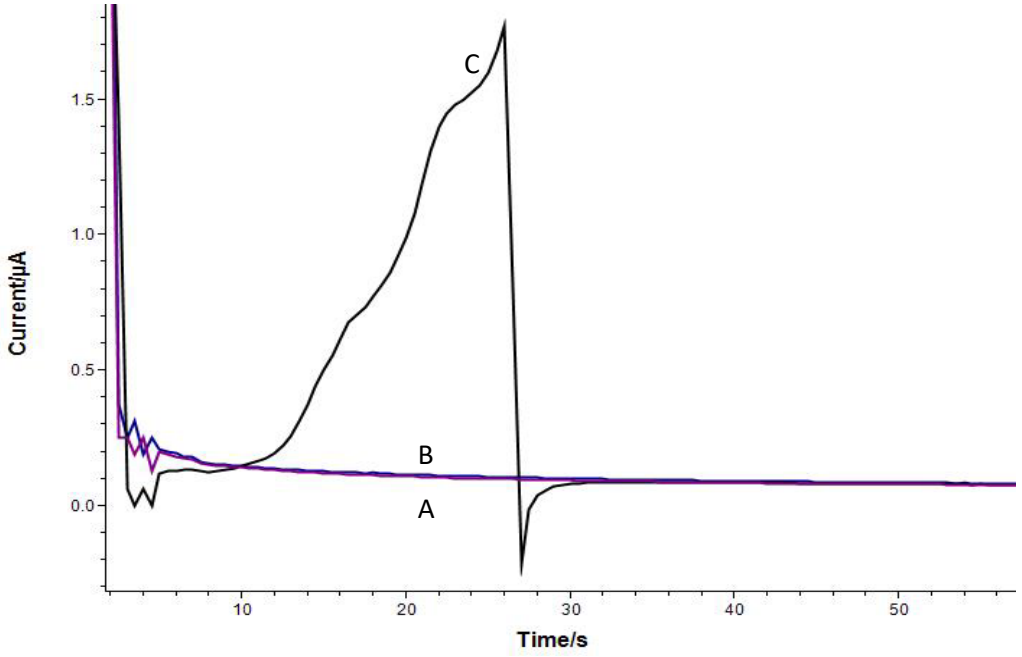

Figure 4.17. Independent and simultaneously obtained chronoamperograms in porcine adipose tissue. MB-SPCEs (vs. Ag/AgCl) inserted into an incision made in an adipose tissue sample. Instrument and apparatus arrangements displayed in Fig 4.5: (A) Independent scan; (B) Dual scan with isolator; (C) Dual scan without an isolator.

The dual studies performed in this section were carried out in adipose tissue, using the sample preparation procedures described in chapter three. The peak potentials measured for skatole in adipose tissue (Figure 4.16) are around +0.2 V higher than those measured in buffered solutions at a similar pH; this peak potential is still well within the potential window scanned. The same incision was used for measurement A and B which both show endogenous skatole peak responses; the first measurement used the dual system with DPV isolator (Figure 4.16B) whereas the second measurement was performed with a single potentiostat (Figure 4.16A). The chronoamperometric response observed in Figure 4.17C showed an interfering DPV signal which prevents the measurement of androstenone current response, whereas the measurements made both independently (Figure 4.17A) and dual with a DPV isolator (Figure 4.17B) show typical chronoamperometric responses.

4.3.4.2 Dual adipose calibration study with skatole and androstenone

4.3.4.2.1 Skatole calibration

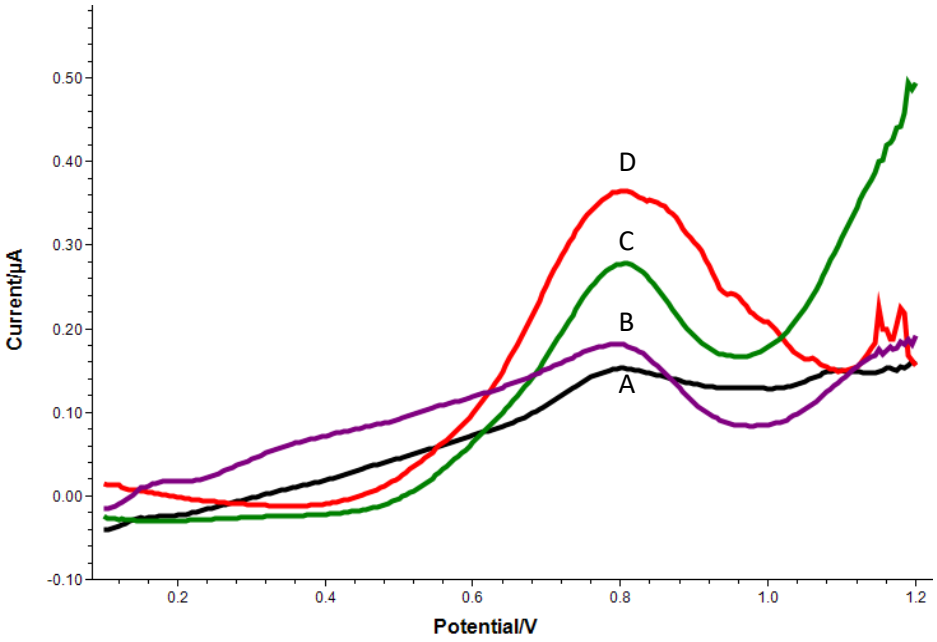

Figure 4.18. Differential pulse voltammograms obtained in adipose tissue for a range of skatole concentrations. SPCEs (vs. Ag/AgCl) in porcine subcutaneous adipose tissue fortified with (A) 0 µg/g; (B) 1 µg/g; (C) 2 µg/g; (D) 4 µg/g skatole. Scans performed simultaneously with chronoamperometry using the optimised dual configuration shown in Fig 4.5B.

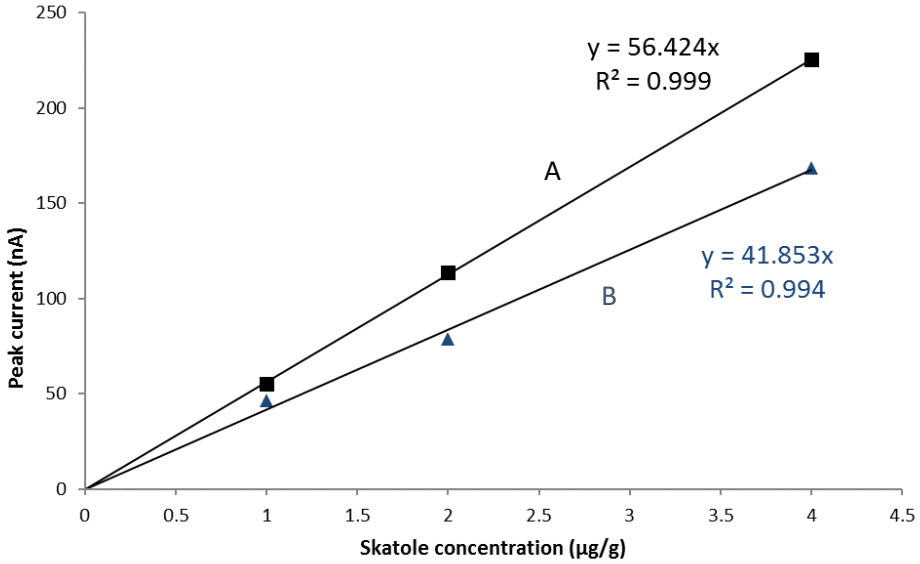

Figure 4.19. Calibration graph for fortified skatole measured in two different subcutaneous porcine adipose tissue samples. Peak height current measurements obtained from subcutaneous porcine adipose tissue fortified with 1 µg/g, 2 µg/g, and 4 µg/g. Peak currents subtracted from endogenous peak current measurement. Study performed in duplicate using subsamples from two different pigs (A & B). Scans performed simultaneously with chronoamperometry.

Adipose tissue sub-samples, from two different pigs, fortified with a range of skatole concentrations were analysed with the dual prototype device. The differential pulse voltammograms from this study are displayed in Figure 4.18; an increase in current response is shown with increasing concentration of skatole over the concentration range 1-4 µg/g. The calibration was performed in duplicate and the peak current data has been plotted against concentration (Figure 4.19). The sensitivity observed for skatole calibration in buffered solution in section 4.3.3 was 44 nA/ppm, which can be converted to 44nA/µg/g; this correlates well with the calibrations presented in Figure 4.19. The successful calibration in adipose tissue, with a sensitivity similar to that in buffered solution, indicates that this method of analysis is suitable for the measurement of skatole in adipose tissue.

4.3.4.2.2 Androstenone calibration

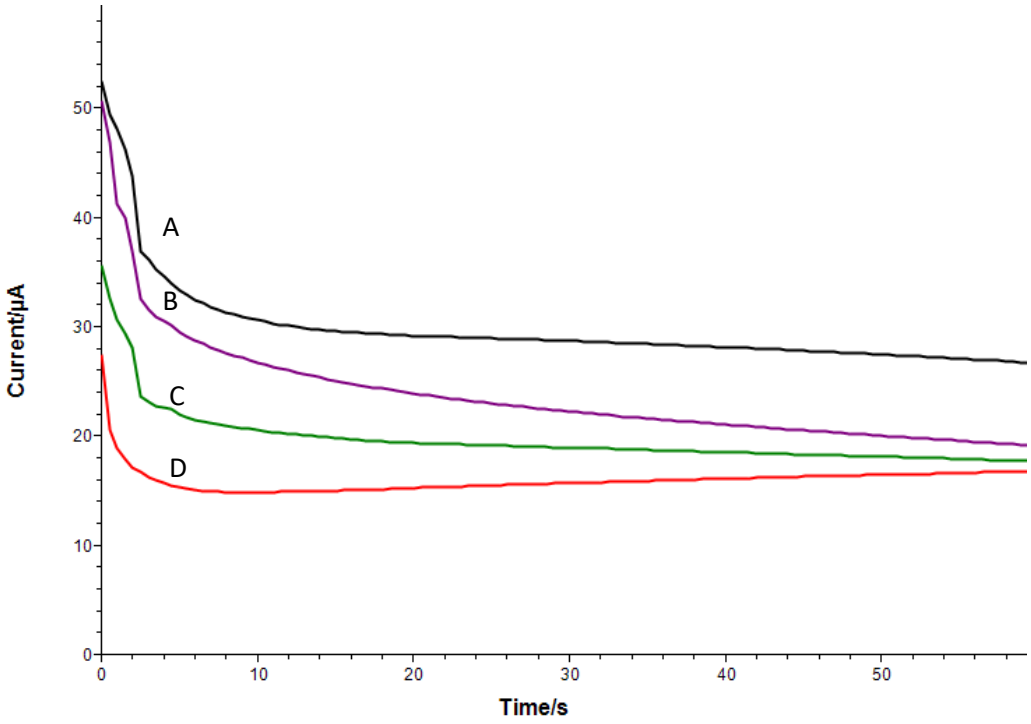

Figure 4.20. Chronoamperograms obtained in adipose tissue for a range of androstenone concentrations. Biosensors (3αHSD-NADH-MB-SPCE vs. Ag/AgCl) in porcine subcutaneous adipose tissue fortified with (A) 0 µg/g; (B) 1 µg/g; (C) 2 µg/g; (D) 4 µg/g androstenone. Scans performed simultaneously with differential pulse voltammetry using the optimised dual configuration shown in Fig 4.5B.

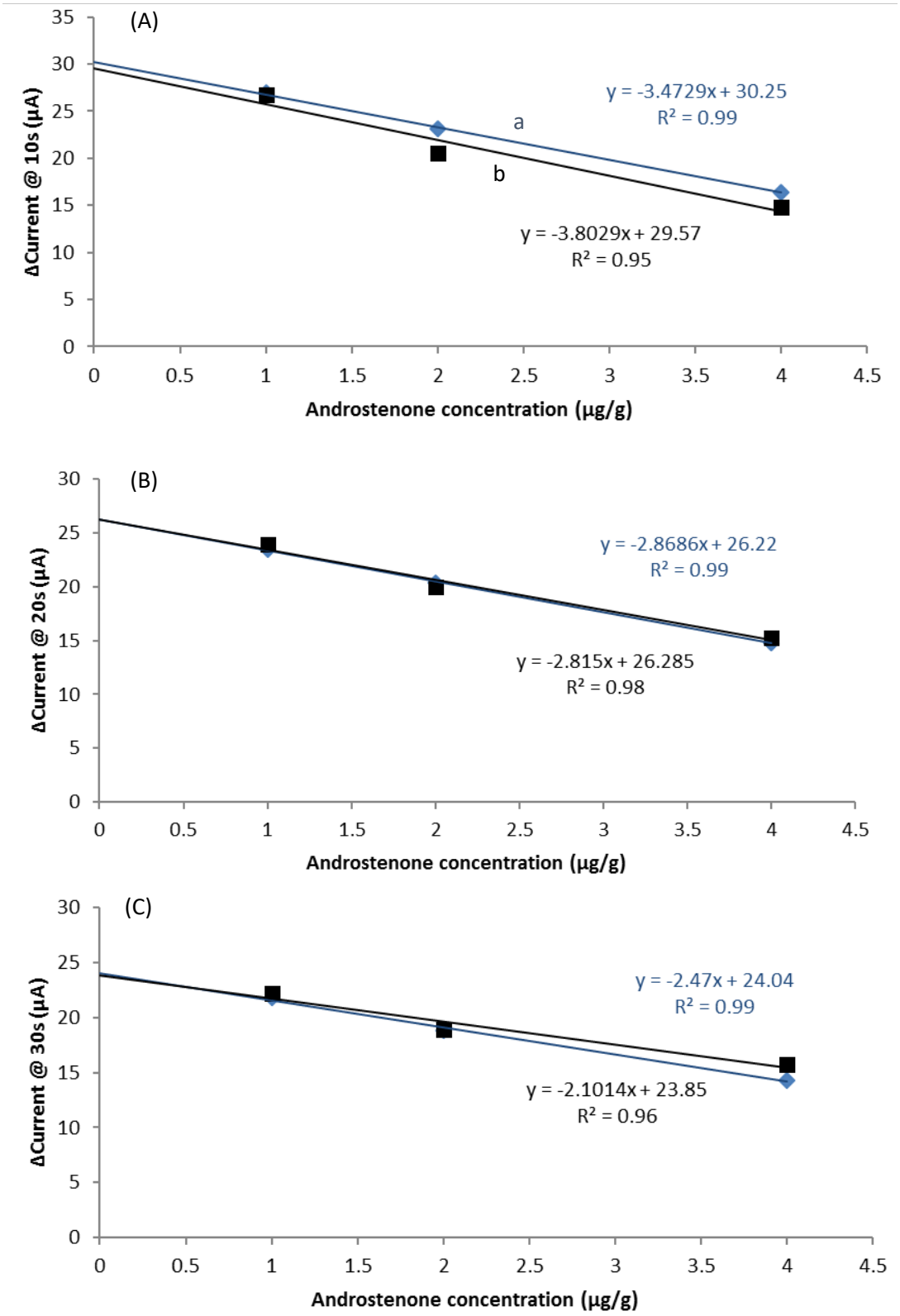

Figure 4.21. Calibration graph for androstenone measured in subcutaneous porcine adipose tissue. Calibration graph plotted from currents measurements at (A) 10s (B) 20s and (C) 30s obtained from adipose tissue fortified with 0 µg/g, 1 µg/g, 2 µg/g, and 4 µg/g androstenone. Study performed in duplicate using subsamples from two different pigs (a & b). Scans performed simultaneously with chronoamperometry.

Fortified adipose tissue sub-samples from two different pigs were analysed with the dual prototype device. Typical chronoamperograms are overlain in Figure 4.20; decreasing current response is displayed with increasing concentration of androstenone over the range of 1-4 µg/g. The current measurements were subtracted from the endogenous response and plotted against androstenone concentration; displayed in Figure 4.21. All of the time points (10 s, 20 s, 30 s) shown in Figure 4.21 could be used to determine concentration for the endogenous levels of androstenone, however the earlier time points provide better sensitivity as demonstrated by the steeper slope for the line of best fit plotted for the calibration data points. The repeatability of the measurements were shown to be within 5 % using a measurement time of 20 seconds.

4.3.5 Abattoir study

Dual measurement of skatole and androstenone in the subcutaneous adipose tissue of pig carcasses on the abattoir processing line resulted in two output responses; typical responses have been displayed in Figure 4.22.

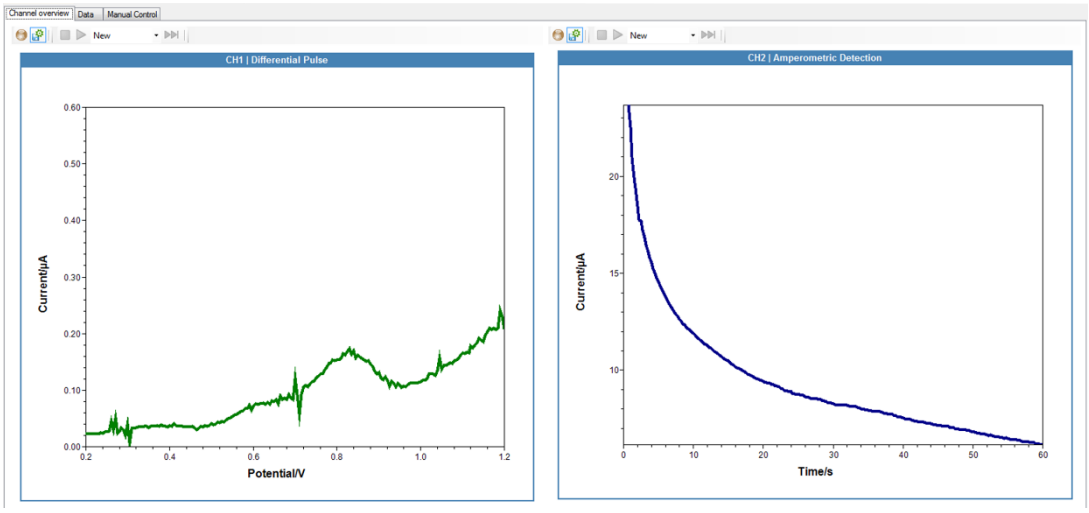

Figure 4.22. Typical simultaneous output responses obtained from the adipose tissue of a pig carcass on the abattoir processing line using the dual instrument system. Differential pulse voltammogram obtained with a SPCE (vs. Ag/AgCl) and a chronoamperogram obtained with a biosensor (3αHSD-NADH-MB-SPCE vs. Ag/AgCl).

4.3.5.1 Skatole determination

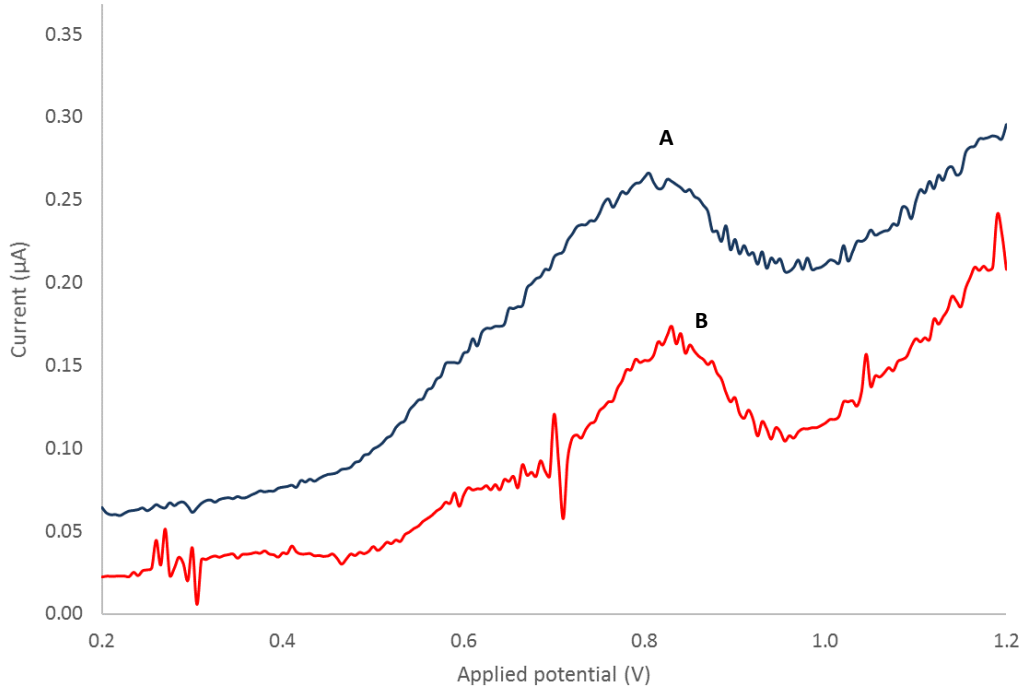

Figure 4.23. Comparison of an endogenous adipose tissue skatole peak and a fortified skatole peak. Differential pulse voltammograms obtained with SPCEs (vs. Ag/AgCl) in (A) a sample of adipose tissue fortified with 0.25 ppm skatole measured in the laboratory, (B) an adipose tissue of a carcass on the abattoir processing line. Scans performed simultaneously with chronoamperometry.

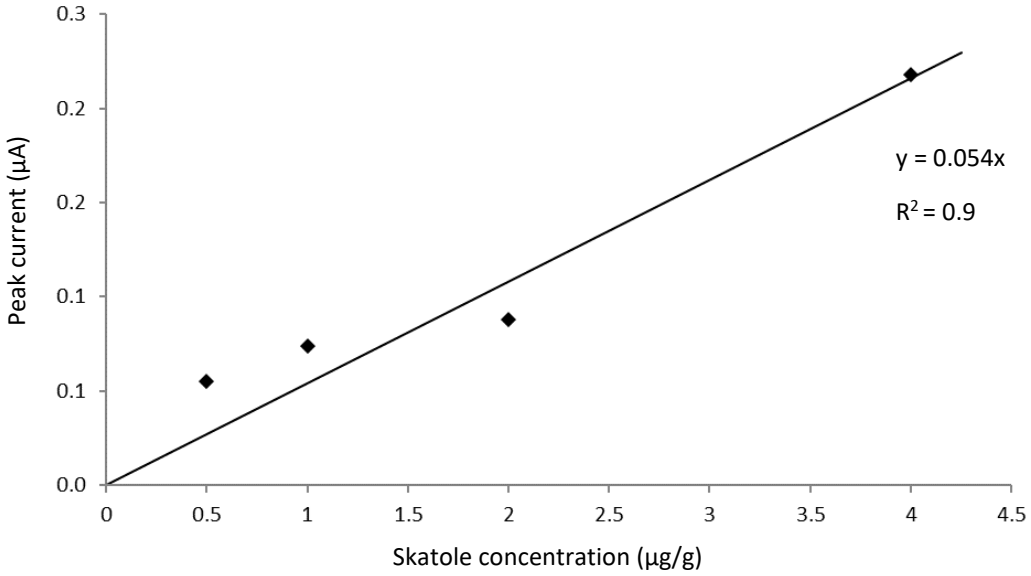

Figure 4.24. Calibration graph for skatole measured in subcutaneous porcine adipose tissue. Peak currents obtained from adipose tissue fortified with 0.5 µg/g, 1.0 µg/g, 2.0 µg/g, and 4.0 µg/g. Peak currents subtracted from endogenous peak current measurement.

Figure 4.23 shows a typical differential voltammogram obtained from a pig carcass online in the abattoir (B) together with a separate sample of adipose tissue fortified with skatole

(A) at 0.25 ppm. This confirms that the analytical peak response, obtained at 0.8V, is due to the presence of skatole. In addition, a large sample of adipose tissue was divided into subsamples and fortified with a range of skatole concentrations. The resulting differential pulse voltammetric peaks were used to construct a calibration plot (Figure 4.24).

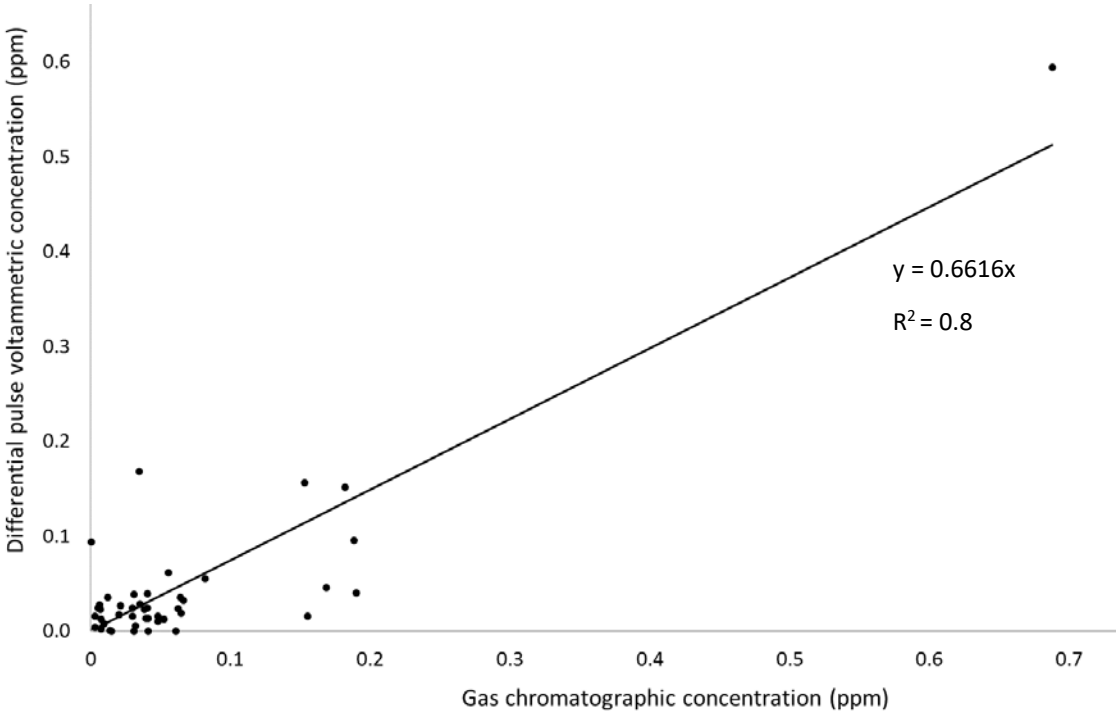

Figure 4.25. Comparison of skatole concentration measured by GC-NPD and differential pulse voltammetry. Comparison between gas chromatographic nitrogen-phosphorous detector analysis and in situ sensor (SPCE vs. Ag/AgCl) measurement of skatole in the subcutaneous adipose tissue of carcasses analysed on the abattoir production line (n = 45).

The concentrations of skatole obtained by differential pulse voltammetry for the carcasses monitored at the abattoir were deduced from the calibration graph previously constructed. The skatole concentration for the same samples were also calculated using the gas-chromatographic method previously described in chapter three. The comparison plot obtained for the two methods is shown in Figure 4.25; the corresponding correlation coefficient was calculated to be 0.8. This data demonstrates the successful application of the dual measurement system to the determination of skatole online in an abattoir. It should be mentioned that the boar taint threshold occurs for skatole at 0.2-0.25 ppm, from Figure 4.25 it was possible to readily detect endogenous concentrations below these

values. As the incidence of boar taint would result in concentrations higher than these values the sensor for skatole would clearly be able to identify the contamination by skatole.

4.3.5.2 Androstenone determination

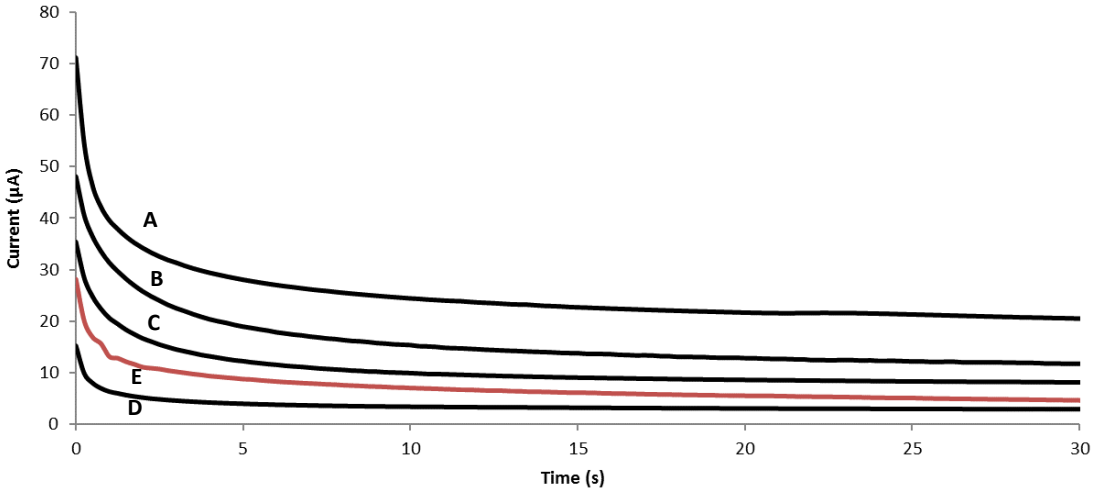

Figure 4.26. Comparison of an endogenous adipose tissue androstenone current response and fortified androstenone current responses. Chronoamperograms obtained with biosensors (3αHSD-NADH-MB-SPCEs vs. Ag/AgCl) in porcine adipose tissue fortified with (A) 0 µg/g; (B) 1 µg/g; (C) 2 µg/g; (D) 4 µg/g and (E) the adipose tissue of a carcass on the abattoir processing line. Scans performed simultaneously with differential pulse voltammetry.

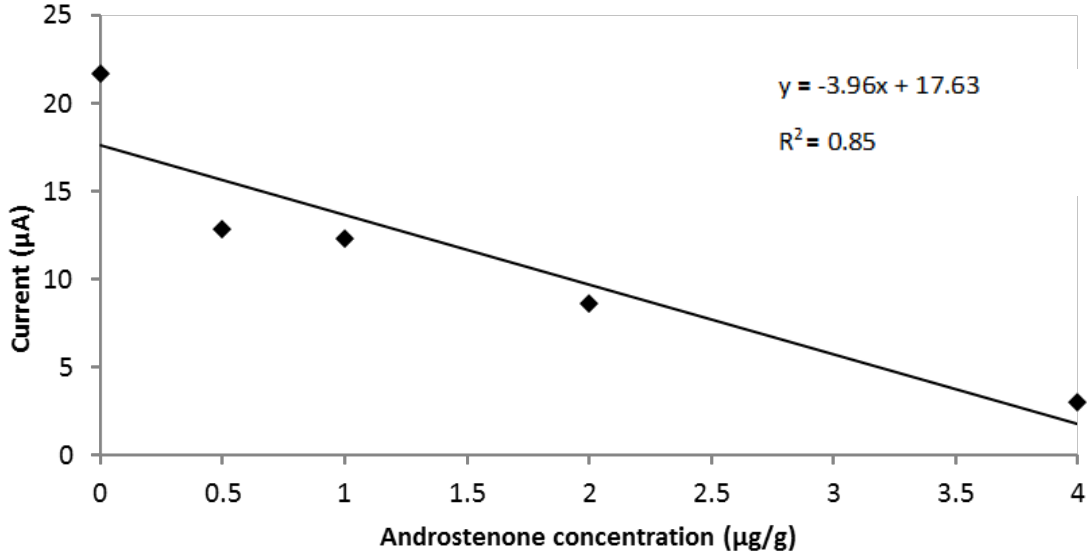

Figure 4.27. Calibration graph for androstenone measured in subcutaneous porcine adipose tissue. Androstenone calibration graph plotted from current measurements at 20 s obtained from adupose tissue fortified with 0 µg/g, 1 µg/g, 2 µg/g, and 4 µg/g

The chronoamperograms in Figure 4.26A-C were obtained from the adipose tissue of an

abattoir carcass sample fortified with a range of androstenone concentrations; the current response was taken at 20 seconds from the application of the applied potential and plotted against concentration in Figure 4.27. Figure 4.26D shows a typical chronoamperogram obtained from the subcutaneous adipose tissue of a carcass measured on the abattoir processing line with the dual instrument system.

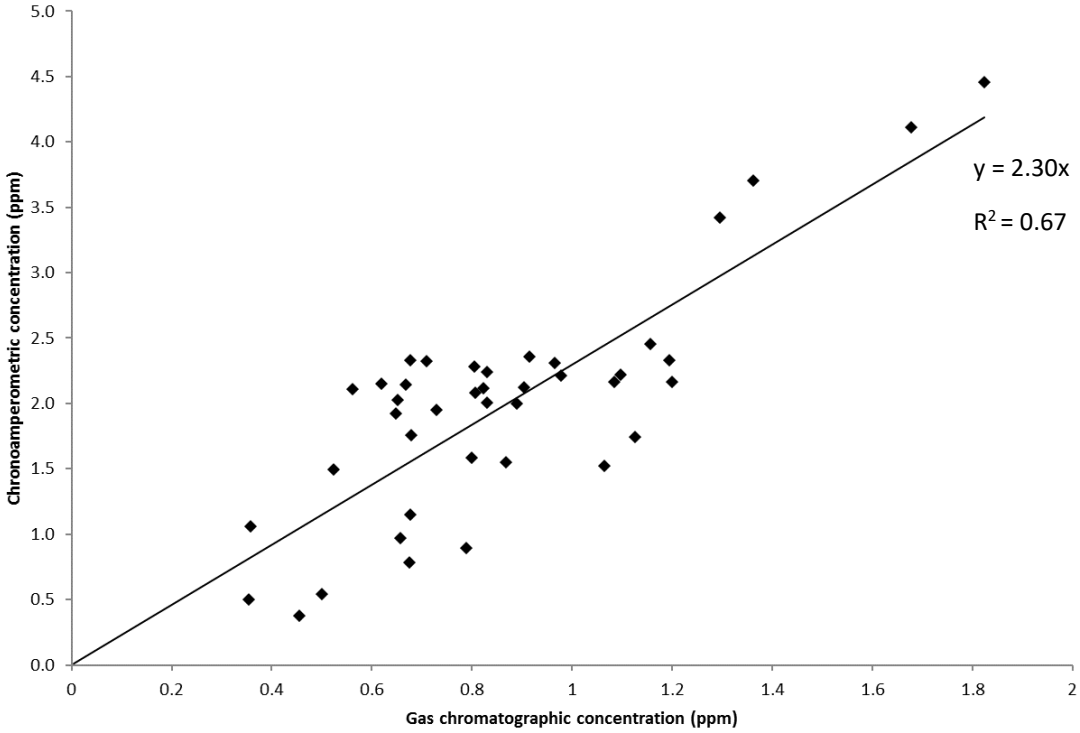

Figure 4.28. Comparison of androstenone concentration measured by GC-FID and chronoamperometry. Comparison between gas chromatographic flame ionisation detector analysis and in situ biosensor (3αHSD-NADH-MB-SPCE vs.Ag/AgCl) measurement of androstenone in the subcutaneous adipose tissue of carcasses analysed on the abattoir production line (n = 40).

The concentrations of androstenone obtained by chronoamperometry for the carcasses monitored at the abattoir were deduced from the calibration graph previously constructed. The androstenone concentration for the same samples were also calculated using the gas-chromatographic method previously described in chapter three. The correlation plot obtained for the two methods is shown in Figure 4.28; the corresponding correlation coefficient was calculated to be 0.67. This data demonstrates the successful application of the dual measurement system to the determination of androstenone online

in an abattoir. It should be mentioned that the boar taint threshold occurs for androstenone at 0.5-1.0 ppm, from Figure 4.28 it was possible to readily detect endogenous concentrations below 0.5 ppm. As the incidence of boar taint would result in concentrations higher than these values the biosensor for androstenone would clearly be able to identify this contaminant.

4.4 Conclusions

The studies in this chapter demonstrate that a portable battery-powered dual instrument system, with sensitivity comparable to the laboratory mains-powered instruments, is capable of measuring androstenone and skatole simultaneously over the concentration range of interest for pig meat considered to exhibit boar taint characteristics. It was demonstrated that the in-house prepared biosensors were capable of giving repeatable responses (within 5 %) in fortified tissue samples from different pigs.

The characterisation studies for the boar taint measurement technology, consisting of a skatole sensor and androstenone biosensor, began with individual measurements using separate potentiostats. The pig production industry requires technology that can measure both skatole and androstenone rapidly in order to keep up with the fast processing line speeds used in many abattoirs today. The preliminary laboratory studies investigating the measurement of the two compounds simultaneously ran into issues involving the cross-over of the electrical input signals from the two applied waveforms (differential pulse voltammetry and chronoamperometry). Subsequent studies determined that an electrical circuit must have been established between the potentiostats and the electrochemical cell via the mains power connections. The investigation of battery powered potentiostats meant that there was no longer a possibility for signal cross-over via the mains power connections, however both potentiostats should ideally be controlled by a single device. A single device would provide a new circuit route for the applied potential to travel

through the electrochemical cell, via the two potentiostats and the laptop. The unwanted electrical signal cross-over was eliminated with the addition of an electrical isolator.

Prior to trialling the dual instrument system on the abattoir processing line a calibration study was performed in the laboratory by fortifying adipose tissue samples with both skatole and androstenone. These fortified samples were interrogating with the sensor and biosensor simultaneously from a single holder fitted to the dual potentiostat system, this system was controlled by a single laptop. The resulting current responses from both the differential pulse voltammograms and the chronoamperograms were plotted against the fortification concentration (μg/g). This in-situ calibration study was repeated and the two data sets were in good correlation with one another, in addition to this the calibration plots also correlate well with the previous calibration studies performed with independent potentiostats.

The dual potentiostat system was taken to an abattoir and trialled on the processing line and the interrogated adipose tissue from pig carcasses was sampled, stored and transported back to the laboratory for analysis via gas chromatographic methodologies. The results from each method, electrochemical vs. gas chromatography, were then compared and a positive correlation was observed between both the novel electrochemical methods and the traditional chromatographic methodologies.

In conclusion, this chapter has described the successful development of a dual electrochemical instrument incorporating a bespoke dual sensor holder for the interrogation of adipose tissue samples online for the determination of boar taint compounds. The data obtained with this dual system compared well with the conventional gas chromatographic methods, and strongly demonstrates that the former has potential for online boar taint detection.

Chapter Five

Measurement of B vitamins in food supplements

Chapter Five Contents

Table of Figures

Chapter Summary

Chapter five describes the development of an electrochemical assay for the measurement of three water-soluble vitamins using screen-printed sensors. During the investigation of electroactive compounds endogenous to adipose tissue (described in chapter two) it was observed that the B-vitamins; thiamine, riboflavin and pyridoxine, gave an anodic voltammetric response when prepared in a phosphate buffer at pH 11. Subsequently, a method for the simultaneous measurement of these compounds, using the rapid technique square wave voltammetry, has been described. This method was successfully applied to the measurement of riboflavin in a food product and the simultaneous measurement of thiamine, riboflavin and pyridoxine in a commercial supplement product.

Chapter Five

5.1 Introduction

Vitamins were first proposed by Funk (1912) when he demonstrated that a deficiency of 'some' substances resulted in disease, he termed these compounds vitamines; in more recent years the word vitamin has replaced the old terminology. Over a century later we understand a great deal more about the importance of these dietary components. They are grouped by their solubility and similarities in chemical structure; water soluble (vitamin B & C) and fat soluble (A, D, E and K). They all play important roles in the human body and the B-group vitamins have a diverse range of functions. Thiamine (vitamin B_1) is a co-enzyme precursor which indirectly contributes to the metabolism of carbohydrates, it has also been shown to play a role in neurological development and the immune system (Manzetti *et al.* 2014). Riboflavin (vitamin B_2) has been linked to wide range of biological processes; some important processes include the oxidation of fatty acids and the transfer of electrons in the generation of ATP (Penberthy 2000). Pyridoxine (vitamin B_6) also has many proposed roles, one of which is the metabolism of amino acids as a component of a co-enzyme (Berdanier 2014). These important micronutrients are present in both processed and unprocessed foods; with some processed foods fortified to improve public health. Fortification has been in practice for over 90 years (World Health Organisation 2006) and supplements are becoming more popular in an ever aging and increasingly health-conscious society. In 2006 a UK regulation on the addition of vitamins and minerals to food was published, this regulation became a law in 2007 therefore it is important that reliable analytical methods are established for the analysis of these compounds in commercial foods and pharmaceutical products.

One of the most commonly used methods for vitamin analysis in industry involves the use of high performance liquid chromatography (Faye Russell 2000). However, this technique

requires high operator skill, can be costly to operate on a routine basis and is time consuming. Simple, low cost, reliable methods for vitamin analysis are required in both the food and pharmaceutical industries and a promising approach is to employ disposable screen-printed carbon electrodes (SPCEs). These can be mass produced in a wide range of geometries at low cost since the working electrode material is carbon; consequently, they can be considered disposable. Most vitamins have been reported to possess electro-activity in media of a specific pH; these reports have involved various electrode materials such as diamond (Chatterjee and Foord 2009), glassy carbon (GCE) (Qu *et al.* 2004), and mercury (Gonzalez-Rodríguez *et al.* 2011). Siddiqui and Pitre (2001) used the latter material for the separate measurement of vitamins B_1 B_2 and B_6, however the authors reported different experimental conditions for each vitamin therefore their simultaneous measurement was not achieved. A recent review of the electroanalysis of vitamins showed that no other publication has described the simultaneous measurement of the three vitamins of interest (Brunetti 2016). Only a few reports have appeared which describe the application of unmodified SPCEs to vitamin analysis, however, these devices have been shown to hold great promise for a wide range of chemical classes (Hughes *et al.* 2016)

The purpose of the present study was to develop a novel voltammetric assay in conjunction with plain SPCEs (vs. Ag/AgCl) for the simultaneous measurement of vitamins thiamine (B_1), riboflavin (B_2), and pyridoxine (B_6) in a pharmaceutical product; these studies will also demonstrate the possibility of using a similar approach for measuring a vitamin in a food product, vitamin B_2 was selected for this purpose. The studies in this chapter determine the optimal pH of the phosphate buffer solution, as well as the initial potential, all three vitamins can be measured in a single anodic scan, using square wave voltammetry, in only 8 seconds.

5.2 Experimental

5.2.1 Apparatus and instrumentation

All voltammetric measurements were carried out with a µAutolab III potentiostat interfaced to a PC for data acquisition via NOVA v1.10 (Metrohm, Netherlands). SPCEs were supplied by Gwent Electronic Materials Ltd (Pontypool, UK); the working electrode is fabricated using a carbon ink (C2030519P4) and the reference electrode is fabricated using a Ag/AgCl ink (C61003P7). All pH measurements were carried out with a Testo 205 (Testo Limited, Hampshire UK) pH meter.

5.2.2 Voltammetry

All voltammetric studies were carried out with a screen-printed strip, comprising the working and reference electrodes mentioned above, placed in a voltammetric cell containing a 10 ml aliquot of 0.1 M phosphate and 0.1 M sodium chloride (PBS). The possibility of using SPCEs more than once was investigated however there was a reduction in sensitivity on subsequent scans; consequently the sensors were disposed of after each analysis.

The initial cyclic voltammetric conditions used to study the effect of pH over the range 7-11 were as follows: (A) for thiamine initial potential -0.1 V; switching potential +1.0 V, final potential -0.1 V; (B) for riboflavin initial potential -1.1 V; switching potential 0.0 V, final potential -1.1 V; (C) for pyridoxine initial potential -0.1 V; switching potential +1.2 V, final potential -0.1 V. The scan rate chosen for all these studies was 100 mV/s. A further cyclic voltammetric study was performed with a phosphate buffer pH 11 using the following scan rates: 20, 50, 100, 150, and 200 mV/s. The data was used to determine the nature of the reactions occurring with our screen-printed carbon electrodes.

After deducing the voltammetric behaviour of each vitamin at the SPCEs (vs. Ag/AgCl) quantitative studies were performed using square wave voltammetry. Calibration studies were carried out at 250 mV/s with a step height of 0.005 V and an amplitude of 0.05 V scanning from an initial potential of -1.0 to a final potential of +1.0. The simultaneous analysis of all three vitamins in a pharmaceutical preparation was performed under the same conditions as those used in the calibration study. To do this a 10 ml extract (details of preparation procedure in section 5.2.4) of the sample containing the three vitamins was first subjected to square wave voltammetry using the conditions stated above with a screen printed strip; this was followed by the addition of standard solutions (0.02 M) of thiamine, riboflavin and pyridoxine after which the second square wave voltammogram was recorded. This process was continued with a further two additions of the individual vitamin solutions. Similarly the analysis of a Marmite® extract was performed at 250 mV/s with a step height of 0.005 V and an amplitude of 0.05 V; the initial potential was -1.0 V and the final potential was 0.0 V. To do this a 10 ml extract of the sample containing riboflavin was first subjected to square wave voltammetry with the conditions stated above using a screen printed strip, this was followed by the addition of a riboflavin standard solution after which the second square wave voltammogram was recorded. This process was continued with a further two additions of the riboflavin standard solution.

5.2.3 Reagents

All chemicals were obtained from Sigma Aldrich (Dorset, UK), unless otherwise stated. Deionised water was obtained from a Purite RO200 – Stillplus HP System (Oxon, UK). Stock solutions of disodium phosphate buffer and trisodium phosphate buffer were made at a concentration of 0.5 M by dissolving the appropriate mass in deionized water, these were then titrated to give the desired pH. Sodium chloride was prepared to a concentration of 1.0 M by dissolving the appropriate mass in deionised water; this was added to the working standard giving a final concentration of 0.1 mM sodium chloride. Primary stock

solutions of thiamine hydrochloride and pyridoxine hydrochloride were prepared by dissolving the required mass in deionised water to give 0.02 M concentration solutions. Sodium hydroxide was prepared to a concentration of 0.1 M by dissolving the appropriate mass in deionised water; a primary stock solution for riboflavin was prepared to a concentration of 0.02 M by dissolving the appropriate mass in 0.1 M sodium hydroxide. Working standards for voltammetric studies were prepared by dilution of the primary stock solution with either phosphate buffer or water to give a final concentration of 0.1 M phosphate buffer.

5.2.4 Sample preparation

The food product Marmite® was prepared by diluting a 2 gram quantity in 5 ml of 0.2 M trisodium phosphate buffer. This was prepared in a 15 ml centrifuge tube and gently warmed to 30°C for 10 minutes to allow the viscous sample to dissolve in the buffer. The sample was then vortexed and finally centrifuged in an MSE Centaur 2 (Fisons, UK) for 10 minutes at 2500 rpm. The final solution was prepared in a voltammetric cell with a 1.25 ml aliquot of the supernatant and 0.1 M phosphate buffer (pH 11) with 0.1 M sodium chloride taking the total volume to 10 ml.

The vitamin B tablet Ultra Vit B Complex™ by Vitabiotics© was prepared by crushing a total of 5 tablets with a pestle and mortar, 0.1 g of the powdered tablets was transferred to a centrifuge tube containing a 5 ml solution of 0.1 M (pH 11) phosphate buffer which was shaken, vortexed, and finally centrifuged in an MSE Centaur 2 for 10 minutes at 2500 rpm. The final solution was prepared in a voltammetric cell with 0.25 ml of the supernatant and 0.1 M phosphate buffer (pH 11) with 0.1 M sodium chloride taking the total volume to 10 ml.

5.3 Results and discussion

5.3.1 Cyclic voltammetric behaviour and optimisation of buffer conditions

In order to determine the optimum conditions for the simultaneous electrochemical measurement of the water soluble vitamins thiamine, riboflavin, and pyridoxine at plain SPCEs, cyclic voltammetric studies were performed over the pH range 7-11 at a fixed scan rate of 100 mV/s.

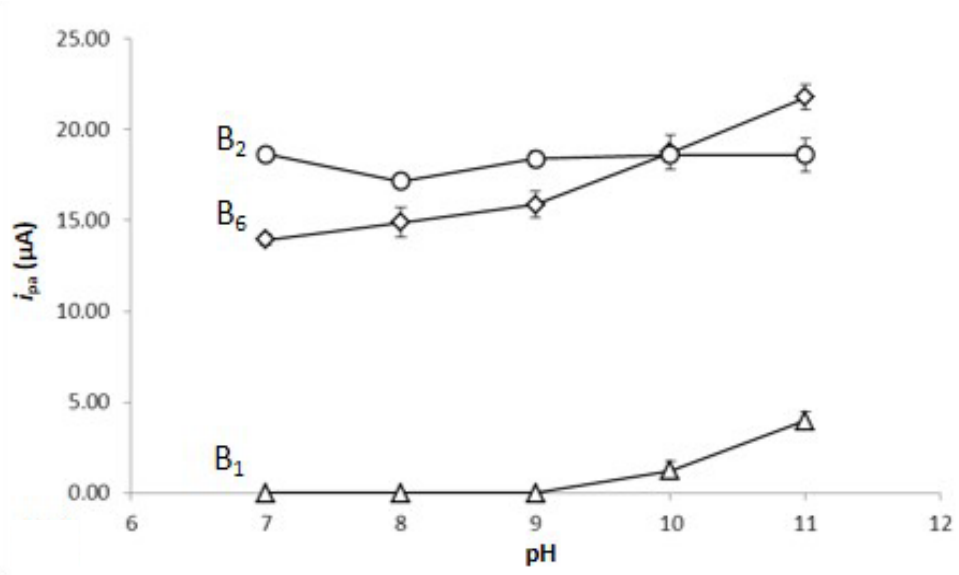

Figure 5.1. Plot summarising the anodic peak currents (i_{pa}) obtained over the pH range 7 – 11 for vitamin B_1, vitamin B_2, and vitamin B_6.

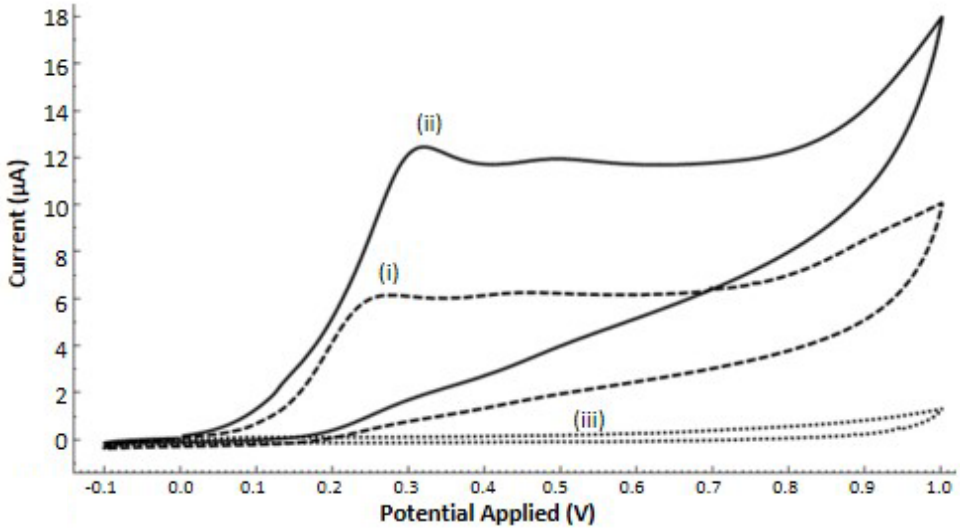

Figure 5.2. Cyclic voltammetric profiles of thiamine in a buffered solution at pH 10 and pH 11. Cyclic voltammograms were obtaining using a SPCE (vs. Ag/AgCl) with a solution containing 0.1 M sodium chloride with 0.1 M phosphate buffer at pH 10 with 1 mM thiamine hydrochloride (i), pH 11 with 1 mM thiamine hydrochloride (ii), and pH 11 with 0 mM thiamine hydrochloride (iii). Initial/final potential 0.0 V, switching potential +1.0 V & -0.1 V, scan rate 100 mV/s.

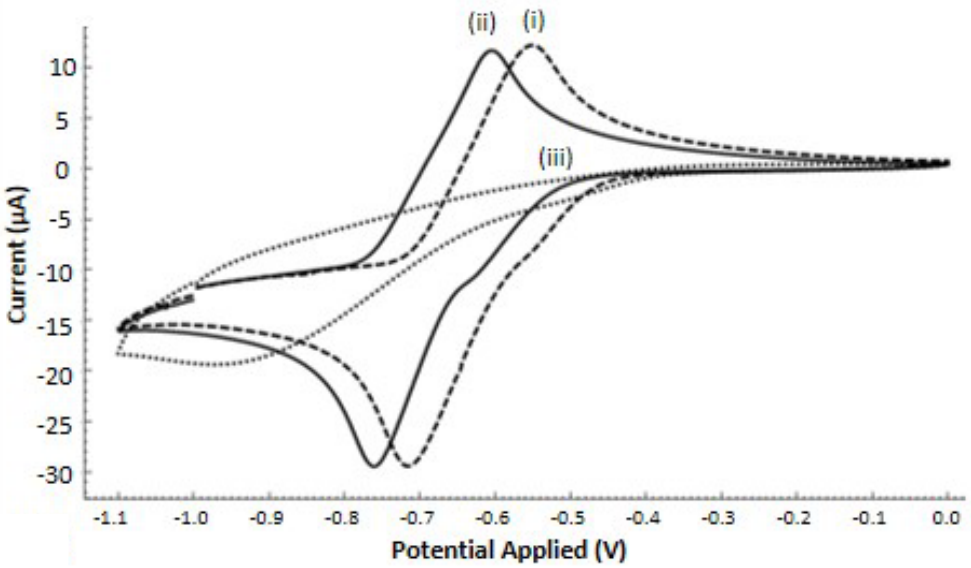

Figure 5.3. Cyclic voltammetric profiles of riboflavin in a buffered solution at pH 10 and pH 11 Cyclic voltammograms were obtaining using a SPCE (vs. Ag/AgCl) with a solution containing 0.1 M sodium chloride with 0.1 M phosphate buffer at pH 10 with 1 mM riboflavin (i), pH 11 with 1 mM riboflavin (ii), and pH 11 with 0 mM riboflavin (iii). Initial/final potential -1.0 V, switching potential 0.0 V & -1.1 V, scan rate 100 mV/s.

.

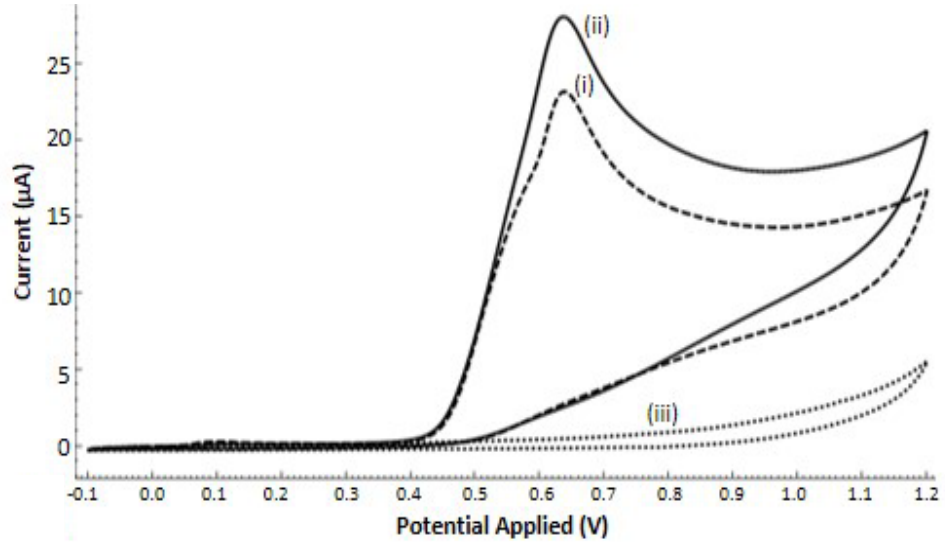

Figure 5.4. Cyclic voltammetric profiles of pyridoxine in a buffered solution at pH 10 and pH 11. Cyclic voltammograms were obtaining using a SPCE (vs. Ag/AgCl) with a solution containing 0.1 M sodium chloride with 0.1 M phosphate buffer at pH 10 with 1 mM pyridoxine hydrochloride (i), pH 11 with 1 mM pyridoxine hydrochloride (ii), and pH 11 with 0 mM pyridoxine hydrochloride (iii). Initial/final potential -0.0 V, switching potential +1.2 V & -0.1 V, scan rate 100 mV/s.

Figure 5.1 summarises the peak responses for the three vitamins of interest over the pH range 7-11. Figure 5.2 clearly shows well defined cyclic voltammetric responses for thiamine in phosphate buffer (0.1 M) at pH 10 and pH 11; no significant oxidation peak was observed below pH 10 (Figure 5.1). Similar behaviour was observed by Hart and co-workers (1995) using a GCE, who suggested that the electrochemically inactive thiamine is converted to an electro-oxidisable thiol derivative at pH values above pH 9. The proposed mechanism is shown in Equation 1, and the proposed free-radical ($RS^{\cdot}$) production and subsequent dimerization are shown in Equations 2 and 3. In order to deduce whether the mechanism obtained with a SPCE was the same as that obtained with the glassy carbon electrode mentioned above, we carried out wave analysis of the voltammogram in Figure 5.2. The *αna* value was calculated using the relationship: $\alpha na = 0.048/Ep\ (V) - Ep_2\ (V)$ (Nicholas *et al.* 2018). The value obtained was 0.52 and as the value of α is usually close to 0.5 this implies that n is 1. Consequently this value is in agreement with that obtained using a GCE.

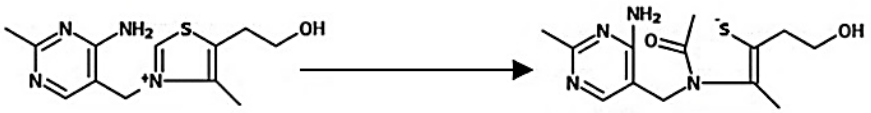

Equation 1

$$RS^- \longrightarrow RS^{\bullet} + e^-$$

Equation 2

$$2RS^{\bullet} \longrightarrow RSSR$$

Equation 3

Riboflavin also exhibited well-defined cyclic voltammetric responses using the same buffers (Figure 5.3). The voltammetric oxidation and reduction peak currents were of similar magnitude over the whole pH range studied (Figure 5.4), suggesting that any of these buffers could be used for the analysis of this vitamin. It should be mentioned that riboflavin is initially in the oxidised form, therefore at the initial potential (-1.0 V) the vitamin is reduced prior to the scan and subsequently re-oxidised during the forward anodic scan. This behaviour is consistent with an electrochemically quasi-reversible redox

couple and has also been reported to occur with other electrode materials and the proposed mechanism is shown in Equation 4 (Qijin *et al.* 2001). The quasi-reversible nature of the redox reaction with a SPCE is evident from the separation of the Epa and Epc values; the expected value would be 59/n (mV) for a truly reversible electrode process (Kissinger and Heineman 1983).

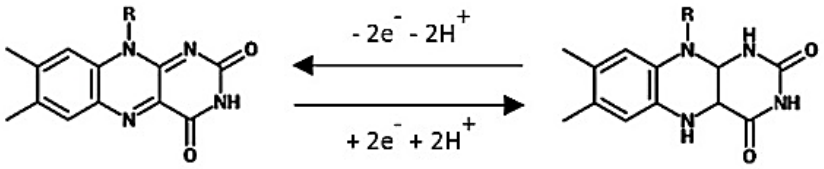

Equation 4

Figure 5.4 shows the cyclic voltammetric behaviour of pyridoxine using pH 10 and pH 11 phosphate buffers; clearly there is an influence of pH on the anodic response of the vitamin. As shown in Figure 5.1 a break point occurs in the plot of peak current vs. pH at a value of pH 9.0. This is consistent with the occurrence of a pKa value at the pyridine moiety of the vitamin (Hart and Hayler 1986). From the data shown in Figure 5.1 we deduced that a pH of 11 was optimum for the voltammetric measurement of all three vitamins.

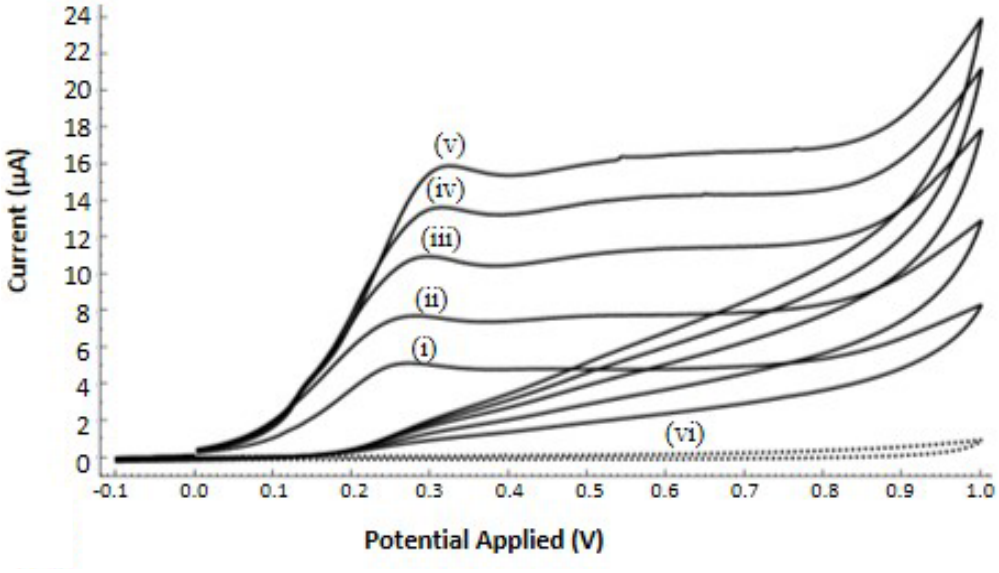

Figure 5.5. Cyclic voltammetric profile of thiamine in a pH 11 buffered solution at different scan rates. Cyclic voltammograms were obtained using SPCEs (vs. Ag/AgCl) with a solution containing 50 mM thiamine hydrochloride prepared in 0.1 M phosphate buffer at pH 11 with 0.1 M sodium chloride. Scan rates: (i) 20, (ii) 50, (iii) 100, (iv) 150, and (v) 200 mV/s. Blank voltammetric scan (vi) was performed at 20 mV/s with the buffered solution. Initial/final potential 0.0 V, switching potential +1.0 V & -0.1 V.

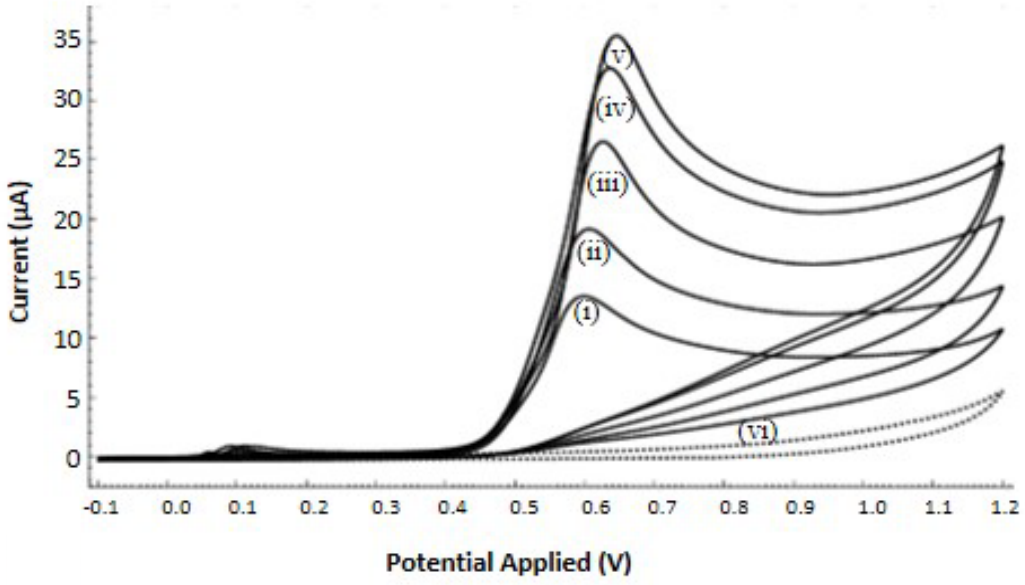

Figure 5.6. Cyclic voltammetric profile of pyridoxine in pH 11 buffered solution at different scan rate. Cyclic voltammograms were obtained using SPCEs (vs. Ag/AgCl) with a solution containing 20 mM pyridoxine hydrochloride prepared in 0.1 M phosphate buffer at pH 11 with 0.1 M sodium chloride. Scan rates: (i) 20, (ii) 50, (iii) 100, (iv) 150, and (v) 200 mV/s. Blank voltammetric scan (vi) was performed at 20 mV/s with the buffered solution. Initial/final potential 0.0 V, switching potential +1.2 V & -0.1 V.

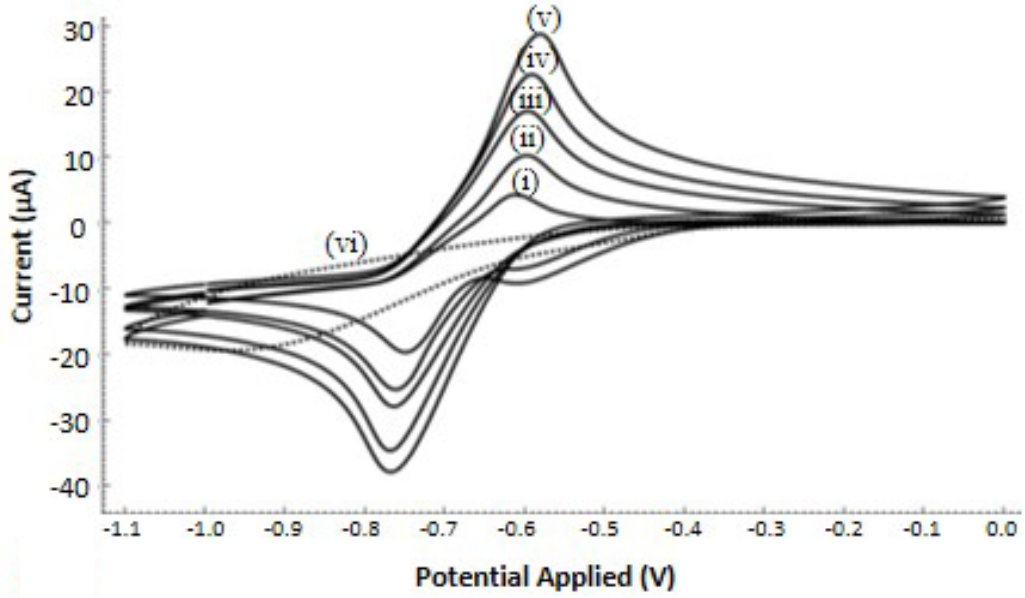

Figure 5.7. Cyclic voltammetric profile of riboflavin in a pH 11 buffered solution at different scan rates. Cyclic voltammograms were obtained using SPCEs (vs. Ag/AgCl) with a solution containing 20 mM riboflavin prepared in 0.1 M phosphate buffer at pH 11 with 0.1 M sodium chloride. Scan rates: (i) 20, (ii) 50, (iii) 100, (iv) 150, and (v) 200 mV/s. Blank voltammetric scan (vi) was performed at 20 mV/s with the buffered solution. Initial/final potential -1.0 V, switching potential 0.0 V & -1.1 V.

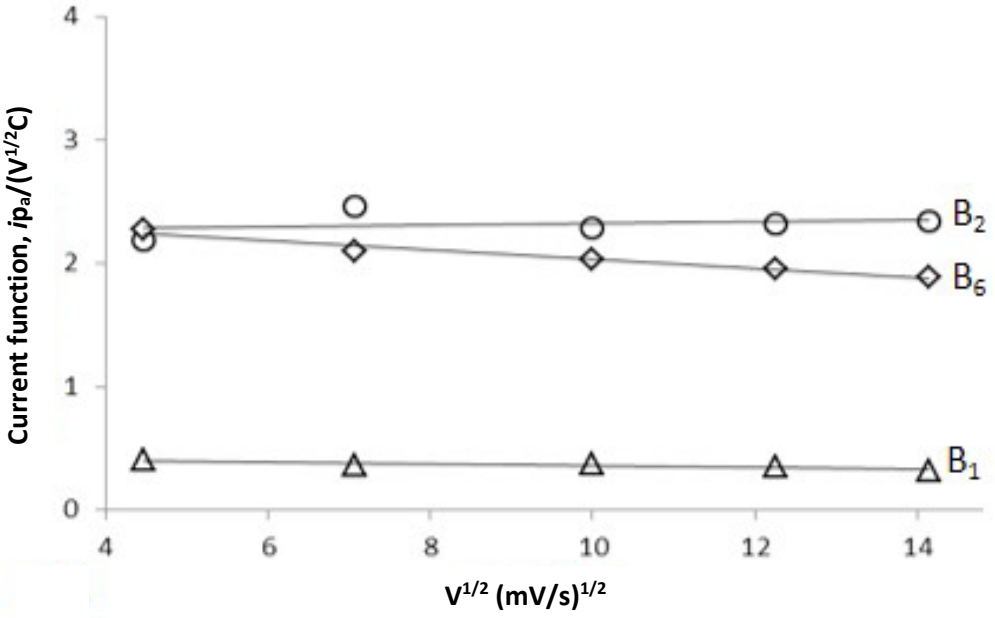

Figure 5.8. Current function versus V½ for the anodic peak of thiamine, riboflavin and pyridoxine.

A scan rate study was performed next in order to further deduce the nature of the electrode reaction for each of the water soluble vitamins at the optimum pH. The cyclic voltammetric behaviour for thiamine (Figure 5.5), riboflavin (Figure 5.7), and pyridoxine (Figure 5.6) were studied over the scan rate range 20-250 mV/s. The current function was plotted against the square root of the scan rate ($V^{½}$) for each vitamin (Figure 5.8). The linear profiles observed in Figure 5.8 indicate the anodic current for both thiamine and riboflavin is controlled by diffusion. However a slight negative slope is observed for pyridoxine which could be a result of adsorption phenomena of the oxidation product at the electrode surface. At the pH used for the analytical determinations (pH 11) the anionic species would be expected to undergo oxidation of the dissociated phenolic group as shown in Equation 5. In a similar manner to that described above for thiamine, we calculated the *αna* value to be 0.52, which implies that the oxidation step involves the transfer of one electron from the anion.

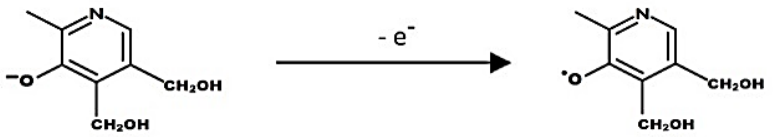

Equation 5

5.3.2 Calibration studies

The cyclic voltammetric studies in section 5.3.1 led to the optimisation of the electrolyte solution for the analysis of thiamine, riboflavin, and pyridoxine. Quantitative studies performed to determine the linear working range of the SPCE's (vs. Ag/AgCl) in the presence of the three analytes were performed in the optimised pH 11 0.1 M phosphate buffered solution with 0.1 M sodium chloride. These studies used the more sensitive voltammetric technique square wave voltammetry, where the anodic peak potentials

(Ep_a) were found to be -0.7 V, +0.2 V, +0.6 V for riboflavin, thiamine, and pyridoxine respectively.

The linear ranges for these vitamins were as follows: thiamine 15-110 µg/ml (R_2 = 0.987); riboflavin 0.1-20.0 µg/ml (R_2 = 0.999); and pyridoxine 2-80 µg/ml (R_2 = 0.999). The sensitivities were thiamine 0.0298 µA µg/ml, riboflavin 4.105 µA µg/ml, and pyridoxine 0.375 µA µg/ml. The precision of the method was calculated as the coefficient of variation (n=4), the calculated values were: thiamine 6.05 % (50 µg/ml); riboflavin 6.26 % (7.5 µg/ml); pyridoxine 5.42 % (32 µg/ml). The limit of detection was calculated from the sensitivity in conjunction with three times the baseline noise for a blank solution at the peak potential of the individual vitamins. The detection limits were: 0.1 µg/ml (riboflavin); 3.5 µg/ml (thiamine); 0.4 µg/ml (pyridoxine).

5.3.3 Analytical application

5.3.3.1 Food analysis

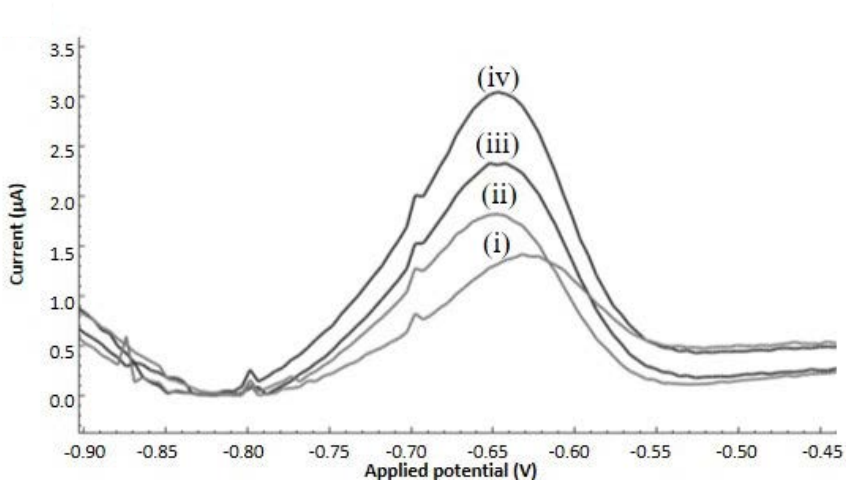

Figure 5.9. Square wave voltammograms of riboflavin standard additions in a Marmite® sample extract. Square wave voltammograms were obtained using SPCEs (vs. Ag/AgCl) with a solution containing Marmite® extract in a pH 11 0.1 M phosphate buffer with 0.1 M sodium chloride with the following standard additions of riboflavin (i) 0.0, (ii) 1.0, (iii) 2.0, (iv) 3.0 µg/ml. Initial potential -1.0 V, final potential 0.0 V, scan rate 250 mV/s.

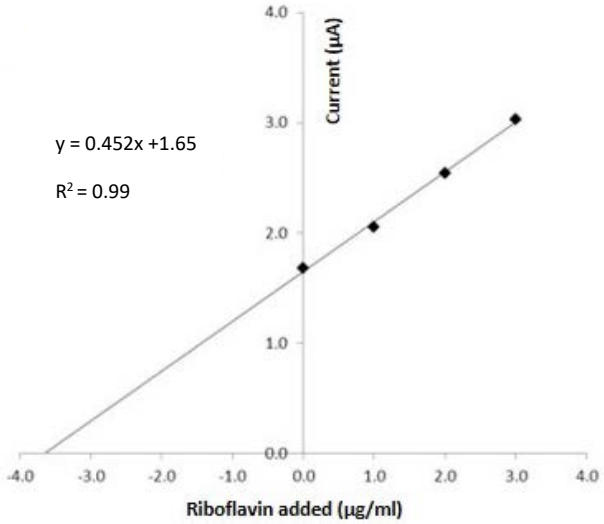

Figure 5.10. Typical riboflavin standard addition plot obtained with a Marmite® sample extract.

The successful measurement of riboflavin in the food spread Marmite® was achieved using the standard addition method. The square wave voltammograms obtained for a typical standard addition study are shown in Figure 5.9. The riboflavin content for each sample was calculated using the method of standard addition (Nicholas *et al.* 2018); a

typical plot is shown in Figure 5.10. The average recovery for riboflavin was calculated to be 95.8 % with the precision (coefficient of variation) calculated to be 3.38 % (Table 5.1) n=5. The recoveries agree well with the declared content provided in the manufacturer's specification and the method could have application for quality control analysis of food products.

Table 5.1 Recovery data for vitamin B_2 in Marmite (n=5).

Vitamin B_2 Sample	Declared (µg/g)	Measured (µg/g)	Recovered (%)
1	70.0	69.3	99.0
2	70.0	69.3	95.9
3	70.0	64.7	92.5
4	70.0	66.3	94.7
5	70.0	64.6	92.3
		Average recovery (%)	95.8
		Standard deviation	3.24
		Coefficient of variation (%)	3.38

5.3.3.2 Pharmaceutical analysis

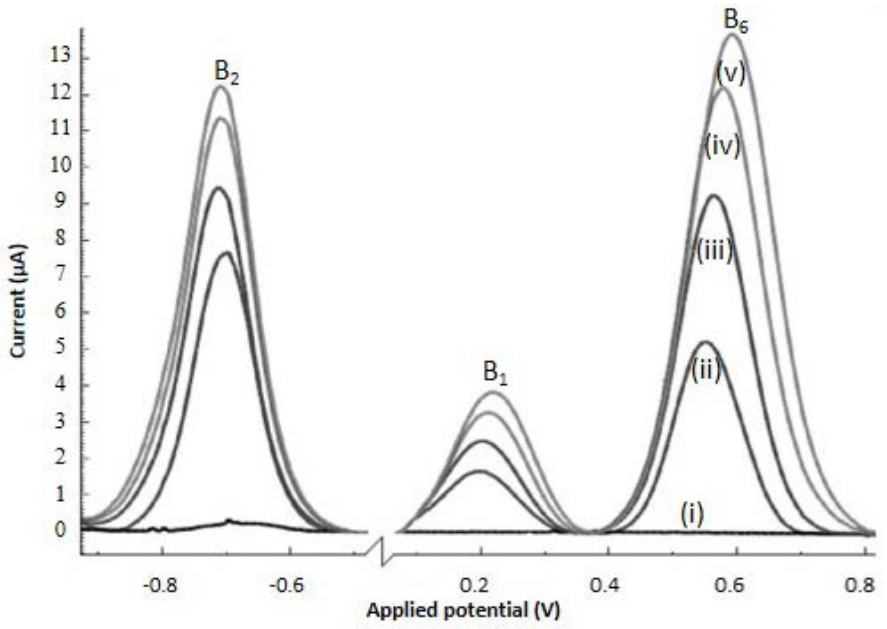

Figure 5.11. Square wave voltammograms of vitamin B_1, B_2, & B_6 standard additions in a supplement extract. Square wave voltammograms were obtained using SPCEs (vs. Ag/AgCl) with a solution containing an extract from a vitamin B tablet (Ultra Vit B Complex™ by Vitabiotics©) in a pH 11 0.1 M phosphate buffer with 0.1 M sodium chloride (i) with the following standard additions of thiamine hydrochloride (ii) 0, (iii) 16, (iv) 32, (v) 48 µg/ml, riboflavin (ii) 0, (iii) 4, (iv) 8, (v) 12 µg/ml, & pyridoxine hydrochloride (ii) 0, (iii) 18, (iv) 34, (v) 50 µg/ml. Initial potential -1.0 V, final potential +1.0 V, scan rate 250 mV/s.

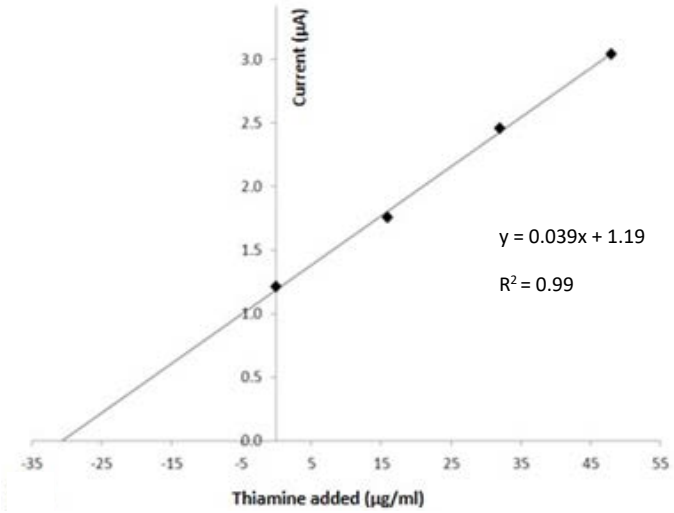

Figure 5.12. Typical thiamine standard addition plot obtained with a Vitabiotics© Ultra Vit B Complex™ sample.

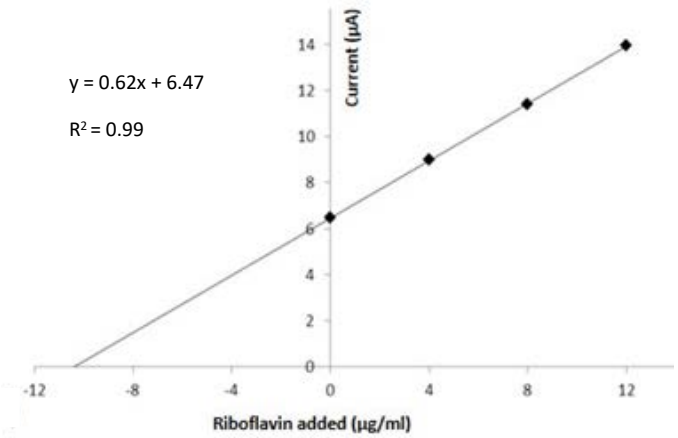

Figure 5.13. Typical riboflavin standard addition plot obtained with a Vitabiotics© Ultra Vit B Complex™ sample.

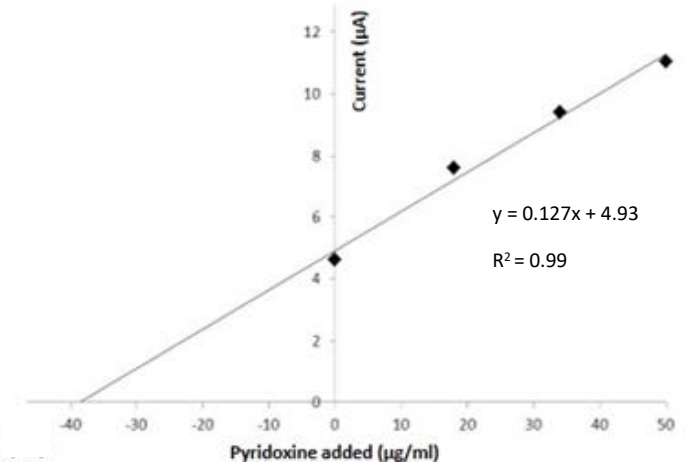

Figure 5.14. Typical pyridoxine standard addition plot obtained with a Vitabiotics© Ultra Vit B Complex™ sample.

The simultaneous measurement of the three water soluble vitamins has been successfully achieved for a commercially available pharmaceutical preparation, (Ultra Vit B Complex™ by Vitabiotics©) using square wave voltammetry in conjunction with unmodified SPCEs. Figure 5.11 shows well defined peaks for all three vitamins in the sample extract with no interference from the other components of the sample matrix. The standard addition plots for thiamine, riboflavin, and pyridoxine are shown in Figure 5.12, Figure 5.13, and Figure 5.14 respectively; the recoveries were calculated to be 110% thiamine; 114% riboflavin; 112 % (pyridoxine) and precision data (coefficient of variation) for the same three vitamins were 7.14 % (thiamine), 6.28 % (riboflavin), 5.66 % (pyridoxine) (Table 5.2). The data shows that the method holds promise for the analysis of pharmaceutical products.

Table 5.2 Recovery data for vitamin B_1, B_2, and B_6 in analysed tablets.

Vitamin B_1 Sample	Declared (mg/tablet)	Measured (mg/tablet)	Recovered (%)
1	5.00	5.78	118
2	5.00	5.55	109
3	5.00	5.94	102
4	5.00	5.19	110
5	5.00	6.12	114
		Average recovery (%)	110
		Standard deviation	7.88
		Coefficient of variation (%)	7.14
Vitamin B_2 Sample	Declared (mg/tablet)	Measured (mg/tablet)	Recovered (%)
1	1.40	1.65	116
2	1.40	1.52	111
3	1.40	1.43	119
4	1.40	1.53	104
5	1.40	1.59	122
		Average recovery (%)	114
		Standard deviation	7.18
		Coefficient of variation (%)	6.28
Vitamin B_6 Sample	Declared (mg/tablet)	Measured (mg/tablet)	Recovered (%)
1	5.00	5.31	106
2	5.00	5.76	115
3	5.00	6.05	121
4	5.00	5.40	108
5	5.00	5.37	107
		Average recovery (%)	112
		Standard deviation	6.32
		Coefficient of variation (%)	5.66

5.4 Conclusions

In this chapter the development of a novel voltammetric assay for the simultaneous measurement of thiamine, riboflavin and pyridoxine using square wave voltammetry in conjunction with unmodified SPCEs has been described. It was possible to perform the analysis in a single voltammetric scan, in only 8 seconds, owing to the judicious choice of the optimum pH 11 phosphate buffer to allow conversion of thiamine to its electroactive thiol form; in addition, the initial negative potential allowed the conversion of the oxidised form of riboflavin to its reduced form which is re-oxidised in the anodic scan. We have also shown that a simple sample pre-treatment step could be used prior to the quantification of these vitamins in both a food (riboflavin alone) and pharmaceutical product (thiamine, riboflavin and pyridoxine). The pre-treatment step simply consisted of mixing the product with trisodium phosphate buffer solution and centrifuging, the supernatant was added to a pH 11 phosphate buffer and sodium chloride solution to form the final solution for interrogation with a SPCE (vs. Ag/AgCl). It should be readily feasible to develop similar methods based on this approach for other important vitamins in a variety of food and pharmaceutical matrices.

Chapter Six

Conclusions and Future Studies

Conclusions and future studies for the electroanalysis of boar taint compounds

The first part of this thesis was concerned with the characterisation of the patented sensor-biosensor system (European Patent 2966441). An initial review of the literature identified a wide range of potential compounds present in porcine adipose tissue. However, of these only the water-soluble vitamins were considered to be possible interferences to the sensor measurements. Voltammetric studies were performed on thiamine, riboflavin, pyridoxine, folic acid, pantothenic acid and nicotinamide under the conditions used for the analysis of skatole. It was shown that there were no responses for any of these vitamins that interfered with the measurement of skatole at the screen printed carbon electrodes (vs. Ag/AgCl).

The characterisation studies were first performed with the skatole sensor and are reported in chapter two. It should be mentioned that these studies were performed in aqueous buffer solutions under a variety of conditions. The results of the voltammetric calibration studies strongly indicated that the approach with a screen-printed carbon electrode (vs. Ag/AgCl) would have the desired sensitivity and selectivity for the measurement of skatole in adipose tissue. Similarly, the results of the chronoamperometric calibration studies with a screen-printed biosensor (vs. Ag/AgCl), prepared by drop-coating a 3α-hydroxysteroid dehydrogenase and NADH solution on the surface of the Meldola's blue screen-printed carbon electrode, demonstrated the feasibility of applying the device to the measurement of this androstenone in adipose tissue.

The next chapter, chapter three, was concerned with demonstrating the application of the sensor and biosensor to the direct measurement of boar taint compounds, skatole and androstenone respectively, in porcine adipose tissue. In the initial application studies samples from a local retailer and pig producer were examined using a simple direct

insertion approach. In parallel, gas chromatographic methods were developed and applied to the quantification of boar taint compounds in the same samples previously analysed by the electrochemical methods. The concentrations calculated for both skatole and androstenone in adipose tissue samples were compared and a positive correlation was observed. This demonstrated the successful application of electroanalytical approaches using a sensor and biosensor for the measurement of boar taint compounds in adipose tissue. It should be mentioned that these devices were used in the laboratory setting, on adipose tissue samples, where the techniques were applied using separate potentiostats for independent measurements.

In contrast in the following chapter, chapter four, it was shown that a convenient approach using a dual potentiostat system could be developed for the simultaneous measurement of skatole and androstenone in adipose tissue. The developed portable system, comprising of a dual potentiostats in conjunction with a dual sensor-biosensor holder, was successfully used for the measurement of the boar taint compounds online in an abattoir. The data obtained with this dual system compared well with the conventional gas chromatographic methods, and strongly demonstrates that the former has potential for online boar taint detection. In conclusion, this investigation has described the successful development of a dual electrochemical instrument, incorporating a bespoke dual sensor holder, for the interrogation of adipose tissue samples online for the determination of boar taint compounds.

In this section some suggestions for future work involving the dual boar taint system are discussed. It should be mentioned that to date there are no systematic studies documenting the distribution of boar taint compounds throughout the whole pig carcass. The main reason for this is the extremely long analysis times that would be required for such a study using traditional chromatographic method. This would provide important

information with regards to the carcass cuts containing the least boar taint, which would be beneficial for the producer and consumer. In addition, it might reveal important information about the metabolism of these compounds. Which could be important for reducing boar taint in live animals. It should also be possible to monitor the boar taint compounds in live pigs using this technology. For example one possibility would be to monitor androstenone levels in saliva, which would be far more convenient that the complicated gas chromatographic methods reported by both Gower (1972) and Dehnhard, Rohrmann and Kauffold (2012). It may also be feasible to measure the boar taint compounds in a very small volumes of blood in a similar way to the measurements of glucose using a glucose biosensor. This simply involves depositing microliter volumes directly onto the surface of the device prior to application of a suitable electrochemical waveform. This could lead to important information on the role of the pig diet on the formation of the boar taint compounds, consequently this could provide information on the most suitable diet to reduce boar taint in pigs.

Ideally producers would like to slaughter at higher weights, like those used in other countries where castration is still performed thereby avoiding the issue of high androstenone levels in boar taint. Studies have shown that a 10 kg increase changed the incidence of androstenone over the acceptable threshold (1 μg/g) from 33% to 55% (D'Souza *et al.*, 2011). Therefore, using the rapid portable sensor system alongside weight trials could allow for carcass weights to be raised without a negative impact on consumers by allowing for the sorting of carcasses. Carcasses with higher incidences of boar taint can be used in processed low value products or can be diluted with untainted meat to lessen the concentration and negative perception of boar taint.

This dual sensor-biosensor technology could be used with a wireless system, which would be better suited to an abattoir environment. Where the results are made available to

operators more rapidly to remove contaminated carcasses; this is an important aspect for operations in large abattoirs where the system could be automated. In 2018 the voluntary ban on pig castration will come into operation, therefore it is envisaged that the implementation of this technology will play an important role in the future production of boar taint free pig meat.

Conclusions and future studies for the electroanalysis of vitamins

An investigation into the development of a novel electrochemical assay for the measurement of water-soluble vitamins in food and pharmaceutical products has been successfully developed and is described in chapter five (Westmacott *et al.*, 2018). The optimum conditions for the determination of vitamin B_1 (thiamine), B_2 (riboflavin) and B_6 (pyridoxine) in phosphate buffer were established using cyclic voltammetry in conjunction with screen printed carbon electrodes (SPCEs). The optimum current response for all three vitamins was achieved in 0.1 M phosphate buffer pH 11 using an initial potential of -1.0 V. Using square wave voltammetry, the linear ranges for thiamine, riboflavin, and pyridoxine were found to be: 15-110 µg/ml, 0.1-20 µg/ml, and 2-80 µg/ml respectively. The application of the method to a commercial food product yielded a recovery of 95.78 % for riboflavin, with a coefficient of variation (CV) was 3.38% (n=5). The method was also applied to a multi-vitamin supplement for the simultaneous determination of thiamine, riboflavin and pyridoxine. In both cases only simple dilution with buffer followed by centrifugation was required prior to analysis. The resulting square wave voltammetric signals were completely resolved with Ep values of -0.7 V, +0.2 V, and +0.6 V respectively. The recoveries determined for the vitamin B complex in a commercial supplement product were found to be 110 %, 114 %, and 112 % respectively (CV= 7.14%, 6.28 %. 5.66 % respectively, n=5).

In this section some suggestions for future work are discussed. As mentioned in earlier chapters several important markers of boar taint could be analysed by direct insertion of the (bio)sensor into porcine subcutaneous adipose tissue. Consequently, it should be feasible to apply a similar approach to the measurement of a range of vitamins directly in food samples. For example it has been shown that citric acid could be measured by direct insertion of a SPCE into the flesh of a lime (Honeychurch, Gilbert and Hart, 2010). As mentioned above B_1 B_2 and B_6 could be determined simultaneously following a simple sample preparation step, therefore it should be feasible to carry out the analysis of pumpkin fruit, which contains the same three vitamins (Assous, Saad and Dyab, 2014), by direct insertion of the screen printed sensors. It is known that vitamin C is electrochemically active under a wide range of conditions, so it should be possible to simply insert the screen-printed sensor into various citrus fruits, including oranges and lemons. In addition tomatoes are known to contain both ascorbic acid and vitamin A (retinol), both are oxidisable at carbon electrodes (see Table 4: Wring, Hart and Knight, 1988; Pemberton, Mottram and Hart, 2005; Revlin and John, 2012, Hu *et al.*, 2001) therefore, it should be feasible to carry out analysis of these vitamins by direct insertion into the fresh flesh of the fruit using SPCEs (Klein and Perry, 1982). It should also be feasible to apply a similar procedure to the direct measurement of vitamins in a range of vegetables.

In chapter two, a review of the literature revealed that various vitamins, both water soluble and fat soluble, were present in the muscle tissues of pigs. Therefore, a similar direct measurement approach could be employed for the determination of a range of water soluble vitamins, including vitamin C (Eichenberger *et al.*, 2004; Gebert *et al.*, 2006; Lechowski, 2006) and eight B vitamins (Jackson *et al.*, 1945; Müller, 1993; Hägg and Kumpulainen, 1994; Leonhardt and Wenk, 1997; Esteve *et al.*, 2002; Lombardi-Boccia,

Lanzi and Aguzzi, 2005; Böhmer and Roth-Maier, 2007; Greenfield *et al.*, 2009; USDA, 2009); Appendix Tables 5 and 6.

These methods could be exploited in the food industry as simple quality control tools as well as for application in nutritional research.

References

Aboul-Kasim, E., 2000. Anodic adsorptive voltammetric determination of the vitamin B1 (thiamine). Journal of Pharmaceutical and Biomedical Analysis, 22 (6), 1047–1054.

Agriculture and Horticulture Development Board (AHDB), 2010. Use of pH meters at pork processing plants. Warwickshire.

Amoore, J.E., and Buttery, R.G., 1978. Partition coefficients and comparative olfactometry. Chemical Senses and Flavour, 3 (1), 57–71.

Ampuero Kragten, S., Verkuylen, B., Dahlmans, H., Hortos, M., Garcia-Regueiro, J. a, Dahl, E., Andresen, O., Feitsma, H., Mathur, P.K., and Harlizius, B., 2011. Inter-laboratory comparison of methods to measure androstenone in pork fat. Animal : an international journal of animal bioscience, 5 (10), 1634–42.

Anderson, L.E., Myer, R.O., Brendemuhl, J.H., and McDowell, L.R., 1995. Bioavailability of various vitamin E compounds for finishing swine. Journal of animal science, 73 (2), 490–495.

Andresen, O., 1975. 5alpha-androstenone in peripheral plasma of pigs, diurnal variation in boars, effects of intravenous HCG administration and castration. Acta Endocrinologica, 78 (2), 385–91.

Annor-Frempong, I.E., Nute, G.R., Whittington, F.W., and Wood, J.D., 1997. The problem of taint in pork—II. The influence of skatole, androstenone and indole, Presented individually and in combination in a model lipid base, on odour perception. Meat Science, 47 (1–2), 49–61.

Annor-Frempong, I.E., Nute, G.R., Wood, J.D., Whittington, F.W., and West, A., 1998. The measurement of the responses to different odour intensities of 'boar taint' using a sensory panel and an electronic nose. Meat Science, 50 (2), 139-151.

Armstrong, H., 1993. Test to track boar taint. Pigs, 9, 14–16.

Arneson, W.L., and Brickell, J.M., 2007. Clinical Chemistry: A Laboratory Perspective. USA: F.A. Davis Company.

Arnold, M. and Rechnitz, G., 1989. Biosensors based on plant and animal tissue. In: Turner, A.P.F., Karube, I., and Wilson, G.S., (Eds). Biosensors Fundamentals and Applications. New York: Oxford University Press, 45.

Assous, M.T.M., Saad, E.M.S., and Dyab, A.S., 2014. Enhancement of quality attributes of canned pumpkin and pineapple. Annals of Agricultural Sciences, 59 (1), 9–15.

Bahadir, E.B., and Sezgintürk, M.K., 2015. Applications of commercial biosensors in clinical, food, environmental, and biothreat/biowarfare analyses. Analytical Biochemistry, 478, 107–120.

Bansal, R.K., 1999. Heterocyclic Chemistry. 3rd Ed. New Dehli: New Age International Publishers.

Bard, A.J. and Faulkner, L.R., 2001. Electrochemical Methods: Fundamentals and Applications, 2nd Ed. USA: John Wiley and Sons.

Bard, A.J., Inzelt, G., and Scholz, F., 2012. Electrochemical Dictionary. 2nd Ed. Germany: Springer.

Beets, M.G.J., and Theimer, E.T., 1970. Odour Similarity Between Structurally Unrelated Odorants. In: Ciba Foundation Symposium - Internal Secretions of the Pancreas (Colloquia on Endocrinology). John Wiley & Sons, 313–323.

Bilodeau, L., Dufresne, G., Deeks, J., Clément, G., Bertrand, J., Turcotte, S., Robichaud, A., Beraldin, F., and Fouquet, A., 2011. Determination of vitamin D3 and 25-hydroxyvitamin

D3 in foodstuffs by HPLC UV-DAD and LC–MS/MS. Journal of Food Composition and Analysis, 24 (3), 441–448.

Bird, O., and Thompson, K., 1967. Pantothenic acid. In: Gyorgy P., and Pearson, W., (Eds). The Vitamins: chemistry, physiology, pathology, methods. New York: Academic Press Inc, 209–237.

Böhmer, B.M., and Roth-Maier, D.A., 2007. Effects of high-level dietary B-vitamins on performance, body composition and tissue vitamin contents of growing/finishing pigs. Journal of animal physiology and animal nutrition, 91 (1–2), 6–10.

Bonneau, M. and Terqui, M., 1983. A note on the metabolism of 5 alpha-androst-16-en-3-one in the young boar in vivo. Reprod Nutr Dev, 23 (5), 899-905.

Bonneau, M., Čandek-Potokar, M., Škrlep, M., Font-i-Furnols, M., Aluwé, M., and Fontanesi, L., 2017. Potential sensitivity of pork production situations aiming at high-quality products to the use of entire male pigs as an alternative to surgical castrates. Animal, 12 (6), 1–9.

Brennan, J.J., Shand, P.J., Fenton, M., Nicholls, L.L., and Aherne, F.X., 1986. Androstenone, Androstenol and Odor Intensity in Backfat of 100- and 130-Kg Boars and Gilts. Canadian Journal of Animal Science, 66 (3), 615–624.

Brett, C.M.A., and Brett, A.M.O., 1998. Electroanalysis. USA: Oxford University Press.

Brunetti, B., 2016. Recent Advances in Electroanalysis of Vitamins. Electroanalysis, 28 (9), 1930–1942.

Burild, A., Lauridsen, C., Faqir, N., Sommer, H.M., and Jakobsen, J., 2016. Vitamin D3 and 25-hydroxyvitamin D3 in pork and their relationship to vitamin D status in pigs. Journal of Nutritional Science, 5, e3.

Çakir, S., Bulut, I., Biçer, E., Coşkun, E., and Çakir, O., 2001. Electrochemical study of the interaction of nicotinamide with tryptophan in the presence and absence of nickel(II). Journal of Electroanalytical Chemistry, 511 (1–2), 94–100.

Cass, A., and Kenny, E., 1989. Protein engineering and its potential application to biosensors. In: Turner, A.P.F., Karube, I., and Wilson, G.S, (Eds). Biosensors Fundamentals and Applications. New York: Oxford University Press, 129.

Chatterjee, A., and Foord, J.S., 2009. Biological applications of diamond electrodes; electrochemical studies of riboflavin. Diamond and Related Materials, 18 (5–8), 899–903.

CLARUS 500/580 GC User's Guide, 2010. Connecticut.

Claus, R., 1979. Pheromone bei Säugetieren unter besonderer Berücksichtigung des Ebergeruchstoffes und seiner Beziehung zu anderen Hodensteroïden anderen Hodensteroiden. Z Tierphysiol Tierernähr Futtermittelkd, 10 (1), 3–136.

Claus, R., Munch, U., Nagel, S., and Schopper, D., 1989. Concentrations of 17 β-estradiol, estrone, and testosterone in tissues of slaughterweight boars compared to barrows and gilts. Journal of Food Safety and Food Quality [Germany], 40 (6), 123–126.

Claus, R., Weiler, U., and Herzog, A., 1994. Physiological aspects of androstenone and skatole formation in the boar—A review with experimental data. Meat Science, 38 (2), 289–305.

Clausen, I., Jakobsen, J., Leth, T., and Ovesen, L., 2003. Vitamin D-3 and 25-hydroxyvitamin D-3 in raw and cooked pork cuts. Journal of Food Composition and Analysis, 16 (5), 575–585.

Crew, A., 2018. Personal communication. UWE Bristol.

Crouch, E., Cowell, D.C., Hoskins, S., Pittson, R.W., and Hart, J.P., 2005. A novel, disposable, screen-printed amperometric biosensor for glucose in serum fabricated using a water-based carbon ink. Biosens Bioelectron, 21 (5), 712–718.

De Brabander, H.F., and Verbeke, R., 1986. Quantitative determination of androstenone in pig adipose tissue. Journal of Chromatography A, 363 (2), 293–302.

Dehnhard, M., Claus, R., Hillenbrand, M., and Herzog, A., 1993. High-performance liquid chromatographic method for the determination of 3-methylindole (skatole) and indole in adipose tissue of pigs. Journal of Chromatography B: Biomedical Sciences and Applications, 616 (2), 205–209.

Dehnhard, M., Rohrmann, H., and Kauffold, J., 2012. Measurement of 16-Androstenes (5α-Androst-16-en-3-One, 5α-Androst-16-en-3α-ol, 5α-Androst-16-en-3β-ol) in Saliva of German Landrace and Göttingen Minipig Boars. In: East, M. L. and Dehnhard, M. (eds) Chemical Signals in Vertebrates 12. New York: Springer, 381–390.

Deng, C., Chen, J., Chen, X., Wang, M., Nie, Z., and Yao, S., 2009. Electrochemical detection of l-cysteine using a boron-doped carbon nanotube-modified electrode. Electrochimica Acta, 54 (12), 3298–3302.

Desmoulin, B., Bonneau, M., Frouin, A., and Bidard, J., 1982. Consumer testing of pork and processed meat from boars: The influence of fat androstenone level. Livestock Production Science, 9 (6), 707–715.

Doran, E., Whittington, F.M., Wood, J.D., and McGivan, J.D., 2004. Characterisation of androstenone metabolism in pig liver microsomes. Chemico-Biological Interactions, 147 (2), 141–149.

D'Souza, D.N., Dunshea, F., Hewitt, R.J.E., Luxford, B.G, Meaney, D., Schwenke, F., Smits, R.J., and Van Barneveld, R.J., 2011. High Boar Taint Risk in Entire Male Carcases.

Manipulating Pig Production XIII - Proceedings of the Thirteenth Biennial Conference of the Australasian Pig Science Association (APSA). 259.

Dufort, I., Soucy, P., Lacoste, L., and Luu-The, V., 2001. Comparative biosynthetic pathway of androstenol and androgens. Journal of Steroid Biochemistry and Molecular Biology, 77 (4–5), 223–227.

Dzyadevych, S.V., Arkhypova, V.N., Soldatkin, A.P., El'skaya, A.V., Martelet, C., and Jaffrezic-Renault, N., 2008. Amperometric enzyme biosensors: Past, present and future. IRBM, 29 (2–3), 171–180.

Eichenberger, B., Pfirter, H.P., Wenk, C., Gebert, S., 2004. Influence of dietary vitamin E and C supplementation on vitamin E and C content and thiobarbituric acid reactive substances (TBARS) in different tissues of growing pigs. Arch Anim Nutr, 58 (3), pp. 195–208.

Elder, S.J., Haytowitz, D.B., Howe, J., Peterson, J.W., and Booth, S.L., 2006. Vitamin K contents of meat, dairy, and fast food in the US diet. Journal of Agricultural and Food Chemistry, 54 (2), 463–467.

Elving, P.J., Schmakel, C.O., and Santhanam, K.S. V, 1976. Nicotinamide-nad sequence: Redox processes and related behavior: Behavior and properties of intermediate and final products. C R C Critical Reviews in Analytical Chemistry, 6 (1), 1–67.

Esteve, M.J., Farrē, R., Frigola, A., and Pilamunga, C., 2002. Contents of vitamins B1, B2, B6, and B12 in pork and meat products. Meat Science, 62 (1), 73–78.

European Commission Implementing Decision adopting a work programme for the financing of the activities of the Union on alternatives to surgical castration of pigs C243/5, 2011. Official Journal of the European Union.

Fàbrega, E., Velarde, A., Cros, J., Gispert, M., Suárez, P., Tibau, J., and Soler, J., 2010. Effect of vaccination against gonadotrophin-releasing hormone, using Improvac, on growth performance, body composition, behaviour and acute phase proteins. Livestock Science, 132 (1–3), 53–59.

Faye Russell, L., 2000. Quantitative Determination of Water-Soluble Vitamins. In: L.M.N. Nollet, ed. Food Analysis by HPLC. New York USA: Marcel Dekker Inc, 403.

Fiorucci, A.R. and Cavalheiro, E.T.G., 2002. The use of carbon paste electrode in the direct voltammetric determination of tryptophan in pharmaceutical formulations. Journal of pharmaceutical and biomedical analysis, 28 (5), 909–915.

Fisher, A.C., 1998. Electrode Dynamics. New York USA: Oxford University Press.

Flanagan, R.J., Perrett, D., and Whelpton, R., 2005. Electrochemical detection in HPLC analysis of drugs and poisons. Cambridge: The Royal Society of Chemistry.

Fonseca, C.A., Vaz, G.C.S., Azevedo, J.P.A., and Semaan, F.S., 2011. Exploiting ion-pair formation for the enhancement of electroanalytical determination of pyridoxine (B6) onto polyurethane-graphite electrodes. Microchemical Journal, 99 (2), 186–192.

Font-i-Furnols, M., 2012. Consumer studies on sensory acceptability of boar taint: A review. Meat Science, 92 (4), 319–329.

Funk, C., 1912. The etiology of the deficiency diseases. Beriberi, polyneuritis in birds, epidemic dropsy, scurvy, experimental scurvy in animals, infantile scurvy, ship beriberi, pellagra. Journal of State Medicine, 20, 341.

Gebert, S., Bee, G., Pfirter, H.P., and Wenk, C., 1999. Phytase and vitamin E in the feed of growing pigs: 2. Influence on carcass characteristics, meat and fat quality. Journal of Animal Physiology and Animal Nutrition-Zeitschrift Fur Tierphysiologie Tierernahrung Und Futtermittelkunde, 81 (1), 20–30.

Gebert, S., Eichenberger, B., Pfirter, H.P., and Wenk, C., 2006. Influence of different dietary vitamin C levels on vitamin E and C content and oxidative stability in various tissues and stored m. longissimus dorsi of growing pigs. Meat Science, 73 (2), 362–367.

Gibson, T.D., 1999. Biosensors: The Stability Problem. ANALUSIS, 27, 630–638.

Global report on diabetes - World Health Organisation, 2016. Switzerland: WHO Press.

Gonzalez-Rodríguez, J., Sevilla, J., Pineda, T., and Blázquez, M., 2011. A comparative study of the electrochemical properties of vitamin B-6 related compounds at physiological pH. Russian Journal of Electrochemistry, 47 (7), 835–845.

Gorton, L., and Domínguez, E., 2002. Electrocatalytic oxidation of NAD(P)H at mediator-modified electrodes. Reviews in Molecular Biotechnology, 82 (4), 371–392.

Gorton, L., Torstensson, A., Jaegfeldt, H., and Johansson, G., 1984. Electrocatalytic oxidation of reduced nicotinamide coenzymes by graphite electrodes modified with an adsorbed phenoxazinium salt, meldola blue. Journal of Electroanalytical Chemistry and Interfacial Electrochemistry, 161 (1), 103–120.

Gower, D.B., (1972). 6-Unsaturated c19 steroids a review. Journal of Steroid Biochemistry, 3 (1), 45–64.

Greef, R., Peat, R., Peter, L.M., Pletcher, D., and Robinson, J., 1990. Instrumental Methods in Electrochemistry. Ellis Horwood Ltd.

Greenfield, H., Arcot, J., Barnes, J.A., Cunningham, J., Adorno, P., Stobaus, T., Tume, R.K., Beilken, S.L., and Muller, W.J., 2009. Nutrient composition of Australian retail pork cuts 2005/2006. Food Chemistry, 117 (4), 721–730.

Griffiths, N.M. and Patterson, R.L.S., 1970. Human olfactory responses to 5α-androst-16-EN-3-one— principal component of boar taint. Journal of the Science of Food and Agriculture, 21 (1), 4–6.

Grindflek, E., Berget, I., Moe, M., Oeth, P., and Lien, S., 2010. Transcript profiling of candidate genes in testis of pigs exhibiting large differences in androstenone levels. BMC genetics, 11 (4), 1-11.

Guidera, J., Kerry, J.P., Buckley, D.J., Lynch, P.B., and Morrissey, P.A., 1997. The effect of dietary vitamin E supplementation on the quality of fresh and frozen lamb meat. Meat Science, 45 (1), 33–43.

Gwent Electronic Materials (1997) Screen printing for the industrial user. Available from: http://www.gwent.org/gem_screen_printing.html#principle [Accessed 21 September 2017].

Hägg, M. and Kumpulainen, J., 1994. Thiamine and Riboflavin contents in Finnish Pig, Heifer, and Cow Livers and in Pork Loin. Journal of Food Composition and Analysis, 7, 301–306.

Hansen, S., Pedersen-Bjergaard, S., and Rasmussen, K., 2012. Introduction to Pharmaceutical Chemical Analysis. West Sussex: John Wiley & Sons, Ltd.

Hart, J., Crew, A., McGuire, N., and Doran, O., 2016. Sensor and method for detecting androstenone or skatole in boar taint. European Patent 2966441. Priority date 2014. UK patent application 1212727.0, File date: 31-07-09.

Hart, J.P. and Hayler, P.J., 1986. Preliminary studies towards an assay for circulating vitamin b6 levels in plasma using high performance liquid chromatography with electrochemical detection. Anal. Proc., 23, 439–441.

Hart, J.P., 1990. Electroanalysis of biologically important compounds. Chichester: E. Horwood.

Hart, J.P., Norman, M.D., and Lacey, C.J., 1992. Voltammetric behaviour of vitamins D2 and D3 at a glassy carbon electrode and their determination in pharmaceutical products by using liquid chromatography with amperometric detection. Analyst, 117 (9), 1441–1445.

Hart, J.P., Norman, M.D., and Tsang, S., 1995. Voltammetric Behavior of Vitamin-B1 (Thiamine) At a Glassy-Carbon Electrode and Its Determination in Multivitamin Tablets using Anion-Exchange Liquid-Chromatography with Amperometric Detection under Basic Conditions. Analyst, 120 (4), 1059–1064.

Hart, J.P., Shearer, M.J., McCarthy, P.T., and Rahim, S., 1984. Voltammetric behaviour of phylloquinone (vitamin K 1) at a glassy-carbon electrode and determination of the vitamin in plasma using high-performance liquid chromatography with electrochemical detection. Analyst, 109 (4), 477–481.

Hartmann, S., Lacorn, M., and Steinhart, H., 1998. Natural occurrence of steroid hormones in food. Food Chemistry, 62 (1), 7–20.

Haugen, J.-E., Brunius, C., and Zamaratskaia, G., 2012. Review of analytical methods to measure boar taint compounds in porcine adipose tissue: the need for harmonised methods. Meat Science, 90 (1), 9–19.

Ho, C.-T., Oh, Y.-C., and Bae-Lee, M., 1994. The flavour of pork. In: Flavor of Meat and Meat Products. 38–51.

Höller, U., Quintana, A.P., Gössl, R., Olszewski, K., Riss, G., Schattner, A., and Nunes, C.S., 2010. Rapid determination of 25-hydroxy vitamin D3 in swine tissue using an isotope dilution HPLC-MS assay. Journal of Chromatography B, 878 (13–14), 963–968.

Honeychurch, K. C., Gilbert, L., and Hart, J. P., 2010. Electrocatalytic behaviour of citric acid at a cobalt phthalocyanine-modified screen-printed carbon electrode and its application in pharmaceutical and food analysis. Analytical and Bioanalytical Chemistry, 396 (8), 3103–11.

Hu, Q., Zhou, T., Zhang, L., Li, H., and Fang, Y., 2001. Separation and determination of three water-soluble vitamins in pharmaceutical preparations and food by micellar electrokinetic chromatography with amperometric electrochemical detection. Analytica Chimica Acta, 437 (1), 123–129.

Huang, K.J., Luo, D.F., Xie, W.Z., and Yu, Y.S., 2008. Sensitive voltammetric determination of tyrosine using multi-walled carbon nanotubes/4-aminobenzeresulfonic acid film-coated glassy carbon electrode. Colloids and Surfaces B: Biointerfaces, 61 (2), 176–181.

Hughes, G., Westmacott, K., Honeychurch, K.C., Crew, A., Pemberton, R.M., and Hart, J.P., 2016. Recent advances in the fabrication and application of screen-printed electrochemical (bio)sensors based on carbon materials for biomedical, agri-food and environmental analyses. Biosensors, 6 (4), 1-39.

Jackson, S., Crook, A., Malone, V., and Drake, T., 1945. The retention of thiamine, riboflavin and niacin in cooking pork and in processing bacon. The Journal of Nutrition, 29, 391–403.

Jacobs, C.B., Peairs, M.J., and Venton, B.J., 2010. Review: Carbon nanotube based electrochemical sensors for biomolecules. Analytica Chimica Acta, 662 (2), 105–127.

Jaegfeldt, H., 1980. Adsorption and electrochemical oxidation behaviour of NADH at a clean platinum electrode. Journal of Electroanalytical Chemistry and Interfacial Electrochemistry, 110 (1–3), 295–302.

Jakobsen, J., Maribo, H., Bysted, A., Sommer, H.M., and Hels, O., 2007. 25-hydroxyvitamin D3 affects vitamin D status similar to vitamin D3 in pigs--but the meat produced has a lower content of vitamin D. The British Journal of Nutrition, 98 (5), 908–913.

Jensen, M.T., Cox, R.P., and Jensen, B.B., 1995. Microbial production of skatole in the hind gut of pigs given different diets and its relation to skatole deposition in backfat. Animal Science, 61 (2), 293–304.

Kacaniklic, V., Johansson, K., Marko-Varga, G., Gorton, L., Jonsson Pettersson, G., and Csoregi, E., 1994. Amperometric biosensors for detection of L and D amino acids based on coimmobilized peroxidase and L and D amino acid oxidases in carbon paste electrodes. Electroanalysis, 6, 381–390.

Kalimuthu, P. and John, S.A., 2009. Selective electrochemical sensor for folic acid at physiological pH using ultrathin electropolymerized film of functionalized thiadiazole modified glassy carbon electrode. Biosensors and Bioelectronics, 24 (12), 3575–3580.

Kamao, M., Suhara, Y., Tsugawa, N., Uwano, M., Yamaguchi, N., Uenishi, K., Ishida, H., Sasaki, S., and Okano, T., 2007. Vitamin K content of foods and dietary vitamin K intake in Japanese young women. Journal of Nutritional Science and Vitaminology, 53 (6), 464–470.

Karube, I., 1989. Micro-organism based sensors biosensors. In: A.P.F. Turner, I. Karube, and G.S. Wilson, (Eds). Biosensors Fundamentals and Applications. New York: Oxford University Press, 23.

Kenkel, J. (2014) Analytical Chemistry for Technicians. 4th ed. Florida: CRC Press.

Kissinger, P.T. and Heineman, W.R., 1983. Cyclic voltammetry. Journal of Chemical Education, 60 (9), 702.

Klein, B.P. and Perry, A.K., (1982). Ascorbic Acid and Vitamin A Activity in Selected Vegetables from Different Geographical Areas of the United States. Journal of Food Science, 47 (3), 941–945.

Koivu-Tikkanen, T.J., Ollilainen, V., and Piironen, V.I., 2000. Determination of phylloquinone and menaquinones in animal products with fluorescence detection after postcolumn reduction with metallic zinc. Journal of Agricultural and Food Chemistry, 48 (12), 6325–6331.

Kotkar, R.M. and Srivastava, A.K., 2008. Electrochemical behavior of nicotinamide using carbon paste electrode modified with macrocyclic compounds. Journal of Inclusion Phenomena and Macrocyclic Chemistry, 60 (3–4), 271–279.

Kovacs, W. and Ojeda, S., 2011. Textbook of Endocrine Physiology. 6th ed. New York: Oxford University Press.

Lechowski, J., 2006. Synthesis of ascorbic acid in the tissues and organs of Polish Landrace fatteners. Animal Science Papers and Reports, 24 (3), 151–156.

Leonhardt, M. and Wenk, C., 1997. Animal species and muscle related differences in thiamine and riboflavin contents of Swiss meat. Food Chemistry, 59 (3), 449–452.

Leonhardt, M., Gebert, S., and Wenk, C., 1997. Vitamin E content of different animal products: influence of animal nutrition. Zeitschrift für Ernährungswissenschaft, 36 (1), 23–7.

Lobo, M.J., Miranda, A.J., and Tuñón, P., 1997. Amperometric Biosensors Based on NAD(P)-Dependent Dehydrogenase Enzymes. Electroanalysis, 9 (3), 191-202.

Lombardi-Boccia, G., Lanzi, S., and Aguzzi, A., 2005. Aspects of meat quality: Trace elements and B vitamins in raw and cooked meats. Journal of Food Composition and Analysis, 18 (1), 39–46.

Lorenzo, J.M., Fontan, M.C.G., Franco, I., and Carballo, J., 2008. Proteolytic and lipolytic modifications during the manufacture of dry-cured lacon, a Spanish traditional meat product: Effect of some additives. Food Chemistry, 110 (1), 137–149.

Lunde, K., Egelandsdal, B., Skuterud, E., Mainland, J.D., Lea, T., Hersleth, M., and Matsunami, H., 2012. Genetic variation of an odorant receptor OR7D4 and sensory perception of cooked meat containing androstenone. PLoS ONE, 7 (5), 3–9.

Lundström, K., Malmfors, B., Malmfors, G., Stern, S., Petersson, H., Mortensen, A.B., and Sørensen, S.E., 1988. Skatole, androstenone and taint in boars fed two different diets. Livestock Production Science, 18 (1), 55–67.

Luong, J.H.T., Male, K.B., and Glennon, J.D., 2008. Biosensor technology: Technology push versus market pull. Biotechnology Advances. 26 (5), 492-500.

Maesa, J.-M., Muñoz-Pascual, F.-X., and Baldrich, E., 2013. Voltammetric discrimination of skatole and indole at disposable screen printed electrodes. Analyst, 138 (5), 1346.

Majors, R., 2013. Sample preparation fundamentals for chromatography. Canada: Agilent Technologies.

Manzetti, S., Zhang, J., and Van Der Spoel, D., 2014. Thiamin function, metabolism, uptake, and transport. Biochemistry, 53 (5), 821–835.

Mattila, P.H., Piironen, V.I., Uusi-Rauva, E.J., and Koivistoinen, P.E., 1995. Contents of cholecalciferol, ergocalciferol, and their 25-hydroxylated metabolites in milk products and raw meat and liver as determined by HPLC. Journal of Agricultural and Food Chemistry, 43 (9), 2394–2399.

McMinn, D.G. and Hill, H.H., 1992. The Flame Ionization Detector. In: D. McMinn and H.H. Hill, eds. Detectors for Capillary Chromatography. USA: John Wiley & Sons, Ltd, 7–20.

Meat Processing Scheme v3.1. Red Tractor. 2018.

Moiroux, J. and Elving, P.J., 1980. Mechanistic Aspects of the Electrochemical Oxidation of Dihydronicotinamide Adenine Dinucleotide (NADH). Journal of the American Chemical Society, 102 (21), 6533–6538.

Mortensen, A.B. and Sørensen, S.E., 1984. Relationship between boar taint and skatole determined with a new analysis method. In: Proceedings of the 30th European Meeting of Meat Research Workers. Bristol UK, 394–396.

Mortensen, A.B., Bejerholm, C., and Pedersen, J.K., 1986. Consumer test of meat from entire males, in relation to skatole in backfat. In: Proc 32nd European Meeting of Meat Research Workers. 23–26.

Müller, H., 1993. The determination of the folic acid content of foods of animal origin using high performance liquid chromatography. European Journal of Nutrition, 6, 518–521.

Mundaca, R.A., Moreno-Guzmán, M., Eguílaz, M., Yáñez-Sedeño, P., and Pingarrón, J.M., 2012. Enzyme biosensor for androsterone based on 3α-hydroxysteroid dehydrogenase immobilized onto a carbon nanotubes/ionic liquid/NAD+ composite electrode. Talanta, 99, 697–702.

Nassef, H.M., Civit, L., Fragoso, A., and O'Sullivan, C.K., 2008. Amperometric determination of ascorbic acid in real samples using a disposable screen-printed electrode modified with electrografted o-aminophenol film. The Analyst, 133, 1736–1741.

Nicholas, P., Pittson, R., and Hart, J.P., 2018. Development of a simple, low cost chronoamperometric assay for fructose based on a commercial graphite-nanoparticle modified screen-printed carbon electrode. Food Chemistry, 241, 122–126.

Nicolau-Solano, S., Wittington, F., Wood, J., and Doran, O., 2007. Relationship between carcass weight, adipose tissue androstenone level and expression of the hepatic 3bhydroxysteroid dehydrogenase in entire commercial pigs. Animal, 1 (7), 1053–1059.

Nie, T., Xu, J.K., Lu, L.M., Zhang, K.X., Bai, L., and Wen, Y.P., 2013. Electroactive species-doped poly(3,4-ethylenedioxythiophene) films: Enhanced sensitivity for electrochemical simultaneous determination of vitamins B2, B6 and C. Biosensors and Bioelectronics, 50, 244–250.

Olivares, A., Rey, A.I., Daza, A., and Lopez-Bote, C.J., 2009. High dietary vitamin A interferes with tissue α-tocopherol concentrations in fattening pigs: a study that examines administration and withdrawal times. Animal, 3 (9), 1264–1270.

Oni, J., Westbroek, P., and Nyokong, T., 2002. Voltammetric Detection of Vitamin B 1 at Carbon Paste Electrodes and Its Determination in Tablets. Electroanalysis, 14 (17), 1165–1168.

Onibi, G.E., Scaife, J.R., Murray, I., and Fowler, V.R., 2000. Supplementary α-tocopherol acetate in full-fat rapeseed-based diets for pigs: effect on performance, plasma enzymes and meat drip loss. Journal of the Science of Food and Agriculture, 80 (11), 1617–1624.

Patterson, P., 1992. The Nitrogen-Phosphorous Detector. In: H.H. Hill and D.G. McMinn, eds. Detectors for Capillary Chromatography. USA: John Wiley & Sons, Ltd, 139–166.

Patterson, R.L.S., 1968. 5α-androst-16-ene-3-one:—Compound responsible for taint in boar fat. Journal of the Science of Food and Agriculture, 19 (1), 31–38.

Pauly, C., Luginbühl, W., Ampuero, S., and Bee, G., 2012. Expected effects on carcass and pork quality when surgical castration is omitted — Results of a meta-analysis study. Meat Science, 92 (4), 858–862.

Pemberton, R.M., Mottram, T.T., and Hart, J.P., 2005. Development of a screen-printed carbon electrochemical immunosensor for picomolar concentrations of estradiol in human serum extracts. Journal of Biochemical and Biophysical Methods, 63 (3), 201–212.

Penberthy, W.T., 2000. Niacin, Riboflavin, and Thiamine. In: Biochemical, Physiological, and Molecular Aspects of Human Nutrition. Missouri: Elsevier Saunders, 548.

Pfalzgraf, A., Frigg, M., and Steinhart, H., 1995. Alpha-Tocopherol Contents and Lipid Oxidation in Pork Muscle and Adipose Tissue during Storage. Journal of Agricultural and Food Chemistry, 43 (5), 1339–1342.

Poole, C.F., 2015. Ionization-based detectors for gas chromatography. Journal of Chromatography A, 1421, 137–153.

Porter, M.G., Hawe, S.M., and Walker, N., 1989. Method for the determination of indole and skatole in pig fat. Journal of the Science of Food and Agriculture, 49 (2), 203–209.

Qijin, W., Nianjun, Y., Haili, Z., Xinpin, Z., and Bin, X., 2001. Voltammetric behavior of vitamin B 2 on the gold electrode modified with a self-assembled monolayer of L - cysteine and its application for the determination of vitamin B 2 using linear sweep stripping voltammetry. Talanta, 55, 457–467.

Qu, W., Wu, K., and Hu, S., 2004. Voltammetric determination of pyridoxine (Vitamin B 6) by use of a chemically-modified glassy carbon electrode. Journal of Pharmaceutical and Biomedical Analysis, 36 (3), 631–635.

Regulation (EC) No 854/2004 of the European Parliament and of the Council: laying down specific rules for the organisation of official controls on products of animal origin intended for human consumption, 2004. Official Journal of the European Union.

Reische, D.W., Lillard, and Eitenmiller, R.R., 2008. Antioxidants. In: D.B. Min, ed. Food Lipids: Chemistry, Nutrition, and Biotechnology. Florida: CRC Press, 409–433.

Revenga-Parra, M., Martínez-Periñán, E., Moreno, B., Pariente, F., and Lorenzo, E., 2017. Rapid taurine and lactate biomarkers determination with disposable electrochemical detectors. Electrochimica Acta, 240, 506–513.

Revlin, S. and John, S.A., 2012. Simultaneous determination of vitamins B2, B9 and C using a heterocyclic conducting polymer modified electrode. Electrochimica Acta, 75, 35–41.

Rood, D., 2007. The Troubleshooting and Maintenance Guide for Gas Chromatographer. Fourth Ed. Germany: Wiley-VCH.

Rosini, E., Molla, G., Rossetti, C., Pilone, M.S., Pollegioni, L., and Sacchi, S., 2008. A biosensor for all d -amino acids using evolved d- amino acid oxidase, 135, 377–384.

Rotzsche, H., Dettmer-Wilde, K., and Engewald, W., 2014. Columns and Stationary Phases. In: K. Dettmer-Wilde and W. Engewald, eds. Practical Gas Chromatography: A Comprehensive Reference. New York: Springer, 59–117.

Safavi, A., Maleki, N., Ershadifar, H., and Tajabadi, F., 2010. Development of a sensitive and selective Riboflavin sensor based on carbon ionic liquid electrode. Analytica Chimica Acta, 674 (2), 176–181.

Sarkar, P., Tothill, I.E., Setford, S.J., and Turner, A.P.F., 1999. Screen-printed amperometric biosensors for the rapid measurement of L- and D-amino acids. The Analyst, 124 (6), 865–870.

Schurgers, L.J., and Vermeer, C., 2000. Determination of phylloquinone and menaquinones in food. Pathophysiology of Haemostasis and Thrombosis, 30 (6), 298–307.

Siddiqui, I., and Pitre, K.S., 2001. Voltammetric determination of vitamins in a pharmaceutical formulation. Journal of Pharmaceutical and Biomedical Analysis, 26 (5–6), 1009–1015.

Sinclair, A.J., Barone, S., Stobaus, T., Tume, R., Beilken, S., Müller, W., Cunningham, J., Barnes, J.A., and Greenfield, H., 2010. Lipid composition of Australian pork cuts 2005/2006. Food Chemistry, 121 (3), 672–681.

Skoog, D.A., Holler, F.J., and Crouch, S.R., 2007. Principles of Instrumental Analysis. USA: Thomson Higher Education.

Sørensen, K.M., Westley, C., Goodacre, R., and Engelsen, S.B., 2015. Simultaneous quantification of the boar-taint compounds skatole and androstenone by surface-enhanced Raman scattering (SERS) and multivariate data analysis. Analytical and Bioanalytical Chemistry, 407 (25), 7787–7795.

Sprules, S.D., Hart, J.P., Wring, S.A., and Pittson, R., 1994. Development of a disposable amperometric sensor for reduced nicotinamide adenine dinucleotide based on a chemically modified screen-printed carbon electrode. The Analyst, 119 (2), 253.

Sprules, S.D., Hart, J.P., Wring, S.A., and Pittson, R., 1995. A reagentless, disposable biosensor for lactic acid based on a screen-printed carbon electrode containing Meldola's Blue and coated with lactate dehydrogenase, NAD+ and cellulose acetate. Analytica Chimica Acta, 304 (1), 17–24.

Sprules, S.D., Hartley, I.C., Wedge, R., Hart, J.P., and Pittson, R., 1996. A disposable reagentless screen-printed amperometric biosensor for the measurement of alcohol in beverages. Analytica Chimica Acta, 329 (3), 215-221.

Squires, E.J., 1990. Studies on the suitability of a colorimetric test for androst-16-ene steroids in the submaxillary gland and fat of pigs as a simple chemical test for boar taint. Canadian Journal of Animal Science, 70, 1029–1040.

Stojek, Z., 2010. The electrical double layer and its structure. In: Scholz, F., Electroanalytical Methods: Guide to Experiments and Applications Berlin: Springer.

Sutton, J. and Shabangi, M., 2004. Activation of the electrochemical properties of thiamin and its phosphate esters in acidic solutions. Journal of Electroanalytical Chemistry, 571 (2), 283–287.

Teixeira, M.F.S., Marino, G., Dockal, E.R., and Cavalheiro, É.T.G., 2004. Voltammetric determination of pyridoxine (Vitamin B6) at a carbon paste electrode modified with vanadyl(IV)-Salen complex. Analytica Chimica Acta, 508 (1), 79–85.

Teodorczyk, M. and Purdyt, W.C., 1990. An amperometric enzyme electrode for the determination of 3alpha-hydroxysteroids. Talanta, 37 (8), 795–800.

Thévenot, D.R., Toth, K., Durst, R.A., and Wilson, G.S., 2001. Electrochemical biosensors: Recommended definitions and classification. Biosensors and Bioelectronics, 16 (1–2), 121–131.

Toldrà, F., Aristoy, M., Part, C., Cerveró, C., Rico, E., Motilva, M., and Flores, A., 1992. Muscle and Adipose Tissue Aminopeptidase Activities in Raw and Dry-Cured Ham. Journal of Food Science, 57 (4), 816–818.

Toldra´, F., 1998. Proteolysis and lipolysis in flavour development of dry-cured meat products. Meat Science, 49 (98), S101–S110.

Trautmann, J., Gertheiss, J., Wicke, M., and Mörlein, D., 2014. How olfactory acuity affects the sensory assessment of boar fat: A proposal for quantification. Meat Science, 98 (2), 255-62.

Tucker, D.J., Bond, A.M., Qing, Z., and Rivett, D.E., 1989. A study of the electrochemistry of tryptophan, peptides containing tryptophan, and related compounds (indoles) at mercury electrodes. Journal of Electroanalytical Chemistry, 261 (1), 127–146.

Turner, A.P.F., 2013. Chemical Society Reviews Biosensors: sense and sensibility. Chem. Soc. Rev. Chem. Soc. Rev, 42 (8), 3175–3648.

USDA, 2009. Nutrient Data Set for Fresh Pork. Release 2.0.

Vold, E., 1970. Fleishproduktionseigenschaften bei Ebern und Kastraten. IV. Organoleptische und gaschromatografische Untersuchungen wasserdampfflüchtiger Stoffe des Rückenspeckes von Ebern. Meldinger fra Norges Landbrukshøgskole, 49, 1–25.

Von Teichman, A., Joerg, H., Werner, P., Brenig, B., and Stranzinger, G., 2001. cDNA cloning and physical mapping of porcine 3β-hydroxysteroid dehydrogenase/Δ5-Δ4 isomerase. Animal Genetics, 32 (5), 298–302.

Walstra, P., Claudi-Magnussen, C., Chevillon, P., Von Seth, G., Diestre, A., Matthews, K.R., Homer, D.B., and Bonneau, M., 1999. An international study on the importance of androstenone and skatole for boar taint: Levels of androstenone and skatole by country and season. Livestock Production Science, 62 (1), 15–28.

Walstra, P; Maarse, G., 1970. Onderzoek gestachlengen van mannelijke mestvarkens. IVO-rapport C-147, Rapport 2. Zeist, The Netherlands.

Wang, J., 2006. Analytical Electrochemistry. Third Ed. USA: Wiley-VCH.

Wang, L. and Tseng, S., 2001. Direct determination of d -panthenol and salt of pantothenic acid in cosmetic and pharmaceutical preparations by differential pulse voltammetry. Analytica Chimica Acta, 432, 39–48.

Warner, P.J., 1989. Genetic Engineering. In: Turner, A.P.F., Karube, I., and Wilson, G.S., (Eds) Biosensors Fundamentals and Applications. New York: Oxford University Press.

Warriss, P.D., 2010. Meat Science an introductory text. 2nd ed. UK: CABI.

Westmacott, K.L., Crew, A., Doran, O., and Hart, J.P., 2018. A novel electroanalytical approach to the measurement of B vitamins in food supplements based on screen-printed carbon sensors. Talanta, 181, 13–18.

Whitmore, F.C., 1951. Organic Chemistry Volume 2. 2nd Ed. New York: Dover Publications.

Whittington, F.M., Nute, G.R., Hughes, S.I., McGivan, J.D., Lean, I.J., Wood, J.D., and Doran, E., 2004. Relationships between skatole and androstenone accumulation, and cytochrome P4502E1 expression in Meishan x Large White pigs. Meat Science, 67 (4), 569–576.

Willett, J. and Kealey, I., 1987. Gas Chromatography: Analytical Chemistry by open learning. Great Britain: John Wiley & Sons.

Wilson, G.J., Lin, C.Y., and Webster, R.D., 2006. Significant Differences in the Electrochemical Behaviour of the α-, β-, γ-, and δ-Tocopherols (Vitamin E). The Journal of Physical Chemistry B, 110 (23), 11540–11548.

Wilson, G.S., 1989. Fundamentals of amperometric sensors. In: A.P.F. Turner, I. Karube, and G.S. Wilson, (Eds). Biosensors Fundamentals and Applications. New York: Oxford University Press, 169.

Windholz, M. and Budavari, S., 1983. The Merck index : an encyclopedia of chemicals, drugs, and biologicals. 10th ed. USA: Merck & Co.

Wollenberger, U., 2005. Chapter 2 Third generation biosensors-integrating recognition and transduction in electrochemical sensors. Comprehensive Analytical Chemistry, 44, 65-130

World Health Organisation, 2006. Guidelines on food fortification with micronutrients [online]. Switzerland.

Wring, S.A., Hart, J.P., and Knight, D.W., 1988. Voltammetric behaviour of all-trans-retinol (vitamin A 1) at a glassy carbon electrode and its determination in human serum using high-performance liquid chromatography with electrochemical detection. Analyst, 113 (12), 1785–1789.

Xiao, F., Ruan, C., Liu, L., Yan, R., Zhao, F., and Zeng, B., 2008. Single-walled carbon nanotube-ionic liquid paste electrode for the sensitive voltammetric determination of folic acid. Sensors and Actuators B: Chemical, 134 (2), 895–901.

Xiong, G., Luo, Y., Jin, S., and Maser, E., 2009. Cis- and trans-regulatory elements of 3α-hydroxysteroid dehydrogenase/carbonyl reductase as biosensor system for steroid determination in the environment. Chemico-Biological Interactions, 178 (1–3), 215–220.

Yang, Y., Shao, B., Zhang, J., Wu, Y., and Duan, H., 2009. Determination of the residues of 50 anabolic hormones in muscle, milk and liver by very-high-pressure liquid chromatography-electrospray ionization tandem mass spectrometry. Journal of Chromatography B: Analytical Technologies in the Biomedical and Life Sciences, 877 (5–6), 489–496.

Zhang, S., Wright, G., and Yang, Y., 2000. Materials and techniques for electrochemical biosensor design and construction. Biosensors and Bioelectronics, 15 (5-6), 273-282.

Zhang, Y., 2011. Voltammetric Determination of Vitamin B6 at Glassy Carbon Electrode Modified with Gold Nanoparticles and Multi-Walled Carbon Nanotubes. American Journal of Analytical Chemistry, 2 (2), 194–199.

Zoski, C.G., 2007. Handbook of electrochemistry. Handbook of Electrochemistry. Berdanier, C.D., 2014. Nutritional Biochemistry. In: Berdanier, C.D., Dwyer, J.T., and Heber, D., (Eds). Handbook of Nutrition and Food. Florida: CRC Press, 237.

Appendices

The data in the Tables 1-3 were obtained on the abattoir line by K Westmacott.

Table 1 - Values of pH, temperature and back fat thickness from P_2 location of back fat 15 mins after kill.			
Reading	pH	^0C	P_2 (mm)
1	7.09	33.8	9.0
2	6.80	35.0	6.0
3	6.71	31.7	8.0
4	7.28	37.4	13.0
5	6.94	38.6	11.0
6	7.54	36.9	7.0
7	7.22	37.2	7.0
8	6.94	37.9	7.0
9	6.86	35.6	8.0
10	6.90	36.8	10.0
Average	7.03	36.1	8.6

Table 2 - Values of pH, temperature and back fat thickness from P_2 location of back fat 24 hrs after kill in blast chiller.			
Reading	pH	^0C	P_2 (mm)
1	5.74	4.1	11
2	5.76	3.9	12
3	5.97	3.9	8
4	6.71	3.9	12
5	6.94	3.9	11
6	7.00	3.8	12
7	5.64	3.8	11
8	6.96	4.2	8
9	5.80	3.7	9
10	5.85	3.8	12
Average	6.24	3.90	10.60

Table 3 - Values of pH, temperature and back fat thickness from P_2 location of back fat 24 hrs after kill in the chiller.			
Reading	pH	^0C	P_2 (mm)
1	7.05	7.9	18
2	6.97	7	12
3	6.23	7.1	11
4	6.85	9.4	12
5	7.19	6.3	12
6	7.08	6.1	8
7	6.70	8	9
8	6.70	8.2	12
9	6.69	7.8	11
10	6.85	7.2	9
Average	6.83	7.50	11.40

Table 4. Data from published sources reporting the electrochemical behaviour of vitamins

Vitamin	Ep	pH	Electrolyte	Electrodes*	Reference
A Retinol	+ 0.75 - 0.80	2.75 - 7.00 (Effective pH 4.72 - 8.60)	95% Methanolic acetate Buffer	GCE W SCE R Pt A	Wring 1988
B_1 Thiamine	-0.62 V	3.5 - 6.5 > 6.5 no oxidation	NaOH KCl HCl mixtures	Pt W Ag/AgCl R Pt A	Sutton 2004
	-0.31 V	6.2	Phosphate Buffer	HMDE W Ag/AgCl R Pt A	Aboul 2000
	+0.33 V	9.0-13.0	NaOH	GCE W Ag/AgCl R Pt A	Hart 1995
	+0.4 V & +0.6 V	10.0 4 & 7 no oxidation	Tris Buffer with HCl	CPE W Ag/AgCl R Pt A	Oni 2002
B_2 Riboflavin	- 0.19 V	2.0 - 8.0	Britton Robinson Buffer	CILE W Ag/AgCl R Pt A	Safavi 2010
	No oxidation	7.0	Phosphate Buffer	GCE W SCE R Pt A	Nie 2013
	- 0.48 V	7.2	Phosphate Buffer	GCE W Ag/AgCl R Pt A	Revlin 2012
B_6 Pyridoxine	+ 0.85 V	7.0 (ox 2.0 - 12.0)	Acetate Buffer	Gr-PU W Ag/AgCl R Pt A	Fonseca 2011
	+ 1.05 V	7.0	KCl	CPE W SCE R Pt A	Teixeira 2004
	+ 0.85 V	6.0	Phosphate Buffer	GCE W SCE R Pt A	Qu 2004
	+ 0.71 V	7.0	Phosphate Buffer	GCE W SCE R Pt A	Zhang 2011
	+0.99 V	8.8	Phosphate-Borate Buffer	CDE W Ag/AgCl R Pt A	Hu 2001
B_3 Nicotinamide	+0.16 V	8.8	Phosphate-Borate Buffer	CDE W Ag/AgCl R Pt A	Hu 2001
B_9 Folic Acid	+ 0.79 V	7.2	Phosphate Buffer	GCE W Ag/AgCl R Pt A	Revlin 2012
	+ 0.20 V	5.5	Phosphate Buffer	GCE W SCE R Pt A	Xiao 2008
	+ 0.82 V	7.2	Phosphate Buffer	GCE W Ag/AgCl R Pt A	Kalimuthu 2009
C Ascorbic Acid	+ 0.21 V	7.2	Phosphate Buffer	GCE W Ag/AgCl R Pt A	Revlin 2012
	+ 0.42 V	8.8	Phosphate-Borate Buffer	CDE W Ag/AgCl R Pt A	Hu 2001
	+ 0.3 V	7.2	Phosphate Buffer	SPCE W Ag/AgCl R Pt A	Nassef 2008
D_3 Cholecalciferol	+ 1.1 V	6.0 – 9.0	Methanolic (90%) Acetate Buffer (0.05 mol dm^{-3})	GCE W Ag/AgCl R Pt A	Hart 1992
E Tocopherol	+0.5–0.6 V	7.0	CH_3CN	Pt W Ag R Pt A	Wilson 2006
K Phylloquinone	- 0.1 V	3.0	0.05M sodium acetate-acetic acid buffer	GCE W Ag/AgCl R Pt A	Hart 1984

*Electrode material described for: W- working electrode, R- reference electrode, A- auxiliary electrode

Table 5. Reported concentrations of vitamin C in porcine muscle tissue

Analysis Method	Extraction Method	Concentration in Feed and Tissue Sample	Weight at start and end of program	Breed	Sex type	Reference
HPLC	Homogenised	Low concentration: 2.70 mg/kg (loin) 2.90 mg/kg (ham) High concentration: 2.90 mg/kg [feed: 141 mg/kg]	Start: 25 kg End: 106 kg	Large White	Barrows	Eichenberger (2004)
HPLC	Homogenised	Low concentration: 45.0 mg/kg [feed: not known] High concentration: 48.5 mg/kg [feed: 684 mg/kg]	Start: 24 kg End: 106 kg	Large White	Barrows	Gebert (2006)
In text reference	In text reference	Loin: 36.27 mg/kg Ham: 29.30 mg/kg	End: 90 kg	Polish Landrace	Boars & Gilts	Lechowski (2006)

Table 6. Reported concentrations of B-vitamins (mg/kg) in porcine muscle tissue

Thiamine B_1	Riboflavin B_2	Pyridoxine B_6	Cobalamin B_{12}	Nicotinamide B_3	Pantothenic acid B_5	Folic acid B_9	Biotin B_7	Reference
7.2	2.3	5.2	0.0055	-	-	-	-	Esteve 2002
11.0	1.4	-	-	-	-	-	-	Hägg 1994
8.0	1.3	-	-	50.3	-	-	-	Lombardi-Boccia 2005
1.89	0.83	1.73	0.0092	29.83	3.84	-	-	USDA
-	-	-	-	-	-	0.01-0.04	-	Müller 1993
-	0.9	5.1	-	-	4.0	-	0.017	Böhmer 2007
1.2-12.3	1.3-4.7	-	-	-	-	-	-	Leonhardt 1997
7.00-7.73	1.22	-	-	34.5-37.83	-	-	-	Jackson 1945
7.60	1.43	3.40	0.0020	68.30	7.90	0.42	-	Greenfield 2009

Table 7. Reported concentrations of B-vitamins (mg/kg) in porcine adipose tissue (Greenfield 2009)

Thiamine B_1	Riboflavin B_2	Pyridoxine B_6	Cobalamin B_{12}	Nicotinamide B_3	Pantothenic acid B_5	Folic acid B_9	Cut Location
1.70	1.07	0.60	0.0106	16.0	3.4	0.14	Loin Chop
2.10	<0.5	1.50	0.0088	37.0	5.0	0.36	Loin Steak
11.0	0.7	3.00	0.0087	41.0	9.0	0.14	Rump Steak
1.90	1.0	0.50	0.0111	8.0	3.0	0.36	Loin Roast
3.30	1.7	1.80	-	41.0	ND	0.10	Round Roast
3.30	0.8	2.20	0.0096	38.0	4.0	0.13	Scotch Roast

Table 8. Summary of B-vitamins concentration ranges calculated from values reported in Table 5 and Table 6

B- Vitamin	Muscle Tissue Concentration		Adipose Tissue Concentration	
	mg/kg	mM	mg/Kg	mM
Thiamine	1.20-12.30	0.00399-0.04089	1.70-11.00	0.00565-0.03665
Riboflavin	0.83-2.30	0.00221-0.00611	<0.50-1.70	0.00132-0.00452
Pyridoxine	1.73-5.20	0.01023-0.02529	0.50-3.00	0.00296-0.01885
Cobalamin	0.0020-0.0092	0.00148-0.00679 µM	0.0087-0.0111	0.00064-0.00082 µM
Nicotinamide	29.83-68.30	0.24427-0.55929	8.00-41.00	0.06551-0.33574
Pantothenic acid	3.84-7.90	0.01751-0.03604	3.00-9.00	0.01368-0.04105
Folic acid	0.01-0.42	0.02266-0.95152 µM	0.10-0.36	0.22655-0.81559 µM
Biotin	0.017	0.06958 µM	-	-

Table 9. Reported concentrations of vitamin K in porcine muscle tissue

Analysis Method	Extraction Method	Concentration in Tissue (µg/100 g)	Age/Weight at Slaughter	Reference
HPLC - Fluorescence detector	Solvent (2-propanol:hexane 3:2 v/v) and Solid Phase Extraction.	Menaquinone-4 in pork loin : 0.2-2.0 µg/ 100g [$\bar{x}$ = 0.9] Menaquinone-4 in bacon : 2.9-7.8 µg/ 100g [$\bar{x}$ = 5.6] Menaquinone-4 in ham : 1.9-9.9 µg/ 100g [$\bar{x}$ = 5.1]	Retail purchase USA	Elder et al. (2006)
HPLC - MS	Solvent extraction (2-propanol:hexane)	Menaquinone-4 in pork chop: 3.1 ± 0.46 µg/ 100g	Retail purchase Helsinki 1998	Koivu-Tikkanen et al. (2000)
HPLC - Fluorescence detector	Solvent extraction (Acetone, diethyl ether, hexane)	Menaquinone-4 in pork thigh: 6.0 ± 2.0 µg/ 100g	Retail purchase Kobe, Japan 2004/5	Kamao et al. (2007)
HPLC - Fluorescence detector	Solvent extraction (hexane)	Menaquinone-4 in pork steak: 1.7-2.4 µg/ 100g Phylloquinone in pork steak: 0.1-0.3 µg/ 100g	Retail purchase Netherlands	Schurgers and Vermeer (2000)

Table 10. Reported concentrations of vitamin A (retinol) in porcine adipose tissue

Analysis Method	Extraction Method	Concentration in Feed and Tissue Sample	Weight at start and end of program	Breed	Sex type	Reference
HPLC DAD	Saponification: KOH, KCL, pyrogallol Extraction: hexane, conc. ethanol.	Low concentration: 0.47 mg/kg [feed: 0.39 mg/kg] High concentration: 1.23 mg/kg [feed: 3.90 mg/kg]	Start: 56.8 ± 1.2 kg End: 126.3 ± 2.5 kg	Landrace x Large White	Barrows	Olivares *et al.* (2009)
HPLC	In text reference	Loin Chop Cut: <0.18 mg/kg Loin Steak Cut: 0.3 mg/kg Rump Steak Cut: 0.26 mg/kg Loin Roast Cut: 0.28 mg/kg Round (mini) Roast Cut: 0.24 mg/kg Scotch Roast Cut: 0.17 mg/kg	-	Shop purchased	-	Greenfield *et al.* (2009)

Table 11. Reported concentration of vitamin D in porcine muscle and adipose tissue

Analysis Method	Extraction Method	Concentration in Feed and Tissue Sample		Age/Weight at Slaughter	Breed	Reference
HPLC UV	Saponification: KOH Extraction: Diethyl ether: Petroleum ether	[20-30 µg Vitamin D per kg feed]		5-6 Months 74.1 – 75.6 kg	-	Clausen (2003)
		Neck Intermuscular fat:	D_3 : 0.59 µg/100 g 25(OH)D_3 : 0.23 µg/100 g			
		Neck lean meat:	D_3 : 0.08 µg/100 g 25(OH)D_3 : 0.11 µg/100 g			
HPLC UV-DAD APCI MS/MS	Saponification: KOH, pyrogallol, EtOH Extraction: 80:20 Petroleum ether: Diethyl ether Purification: x2 via HPLC	Centre chop (boneless, raw whole):	D_3 : 0.17 µg/100 g 25(OH)D_3 : 0.08 µg/100 g	~93 kg*	-	Bilodeau (2011)
		Pork back ribs (raw whole):	D_3 : 0.39 µg/100 g 25(OH)D_3 : 0.13 µg/100 g			
		Pork shoulder blade roast: (boneless, raw whole)	D_3 : 0.37 µg/100 g 25(OH)D_3 : 0.12 µg/100 g			
HPLC UV	Saponification: Alkali Extraction: 1:1 Petroleum ether: Diethyl ether Purification: x2 via HPLC	[Fat: 6.6 %] Pork Fillet:	D_3 : 0.11 µg/100 g 25(OH)D_3 : <0.06 µg/100 g	~73.3 kg* Sep 1993 ~76.8 kg* May 1994	-	Mattila (1995)
		[Fat: 14.0 %] Pork shoulder: (Boston Butt)	D_3 : 0.34 µg/100 g 25(OH)D_3 : 0.07 µg/100 g			
HPLC MS	Gound: with SDS, MeOH Centrifugation Solid Phase Extraction	[50 µg Vitamin D_3 and 25(OH)D_3 per kg feed]		~ 5 Months	Large White X Landrace	Höller (2010)
		Subcutaneous Fat:	25(OH)D_3 : <LOQ (20ng/g)			
HPLC DAD	Saponification: Ethanolic KOH Extraction: 1:1 Petroleum ether: Diethyl ether SPE and HPLC purification	Loin subcutaneous fat:		~ 5½ Months	-	Jakobsen (2007)
		Diet A- Vitamin D: D_3 only:	D_3 : 0.747 µg/100 g 25(OH)D_3 : 0.187 µg/100 g			
		Diet B – Vitamin D: D_3 and 25(OH)D_3:	D_3 : 0.351 µg/100 g 25(OH)D_3 : 0.244 µg/100 g			
		Diet C – Vitamin D: 25(OH)D_3 only:	D_3 : 0.057 µg/100 g 25(OH)D_3 : 0.186 µg/100 g			

Table 12. Reported concentration of vitamin E in porcine adipose tissue

Analysis Method	Extraction Method	Concentration in Feed and Tissue Sample		Age/Weight at start/end of program	Breed	Sex type	Reference
HPLC Fluorescence detector	Saponification, single-step extraction	Low Feed: High Feed:	12 mg/kg [feed: 40 mg/kg] 20 mg/kg [feed: 200 mg/kg]	Start: 30 kg End: 95 kg	Hybrid	Barrows and Sows	Pfalzgraf *et al.* (1995)
HPLC	In text reference	No diet alteration Upper subcutaneous fat: Lower subcutaneous fat: 200 mg/kg supplementation Upper subcutaneous fat: Lower subcutaneous fat:	 2.56 mg/kg 3.61 mg/kg 18.08 mg/kg 25.68 mg/kg	Age: 24 days Age: 150 days	Landrace x Large White	Mixed Sex	Sisk *et al.* (1993)
HPLC Fluorescence detector	Saponification, extraction n-hexane/ toluene	Low feed: High feed:	0.99 mg/kg [feed: 15 mg/kg] 2.92 mg/kg [feed: 258 mg/kg]	Start: 25 kg End: 105 kg	-	Barrows	Leonhardt *et al.* (1997)
HPLC Fluorescence detector	Saponification, extraction n-hexane/ toluene	Back fat outer layer Low feed: High feed:	 12.24 mg/kg [feed: 15 mg/kg] 34.91 mg/kg [feed: 258 mg/kg]	Start: 26 kg End: 105 kg	Large White	Barrows	Gebert *et al.* (1999)
HPLC DAD	Saponification: KOH, KCL, pyrogallol Extraction: hexane, conc. ethanol.	Saturated fat source: Polyunsaturated fat source:	6.77 mg/kg [feed: 105.9 mg/kg] 7.74 mg/kg [feed: 111.4 mg/kg]	Start: 56.4 ± 1.5 kg End: 115 ± 2.2 kg	Landrace X Large White	Barrows	Olivares *et al.* (2009)

Table 12. Reported concentration of vitamin E in porcine adipose tissue (continued)

Analysis Method	Extraction Method	Concentration in Feed and Tissue Sample		Age/Weight at start/end of program	Breed	Sex type	Reference
HPLC Fluorescence detector	In text reference	No vitamin E supp: DL-α- tocopheryl acetate: D-α- tocopheryl acetate: DL-α- tocopherol: D-α- tocopherol:	1.4 mg/kg [feed: 5-10 IU/kg] 4.3 mg/kg [feed: 56-94 IU/kg] 4.8 mg/kg [feed: 72-113 IU/kg] 3.2 mg/kg [feed: 13-94 IU/kg] 1.6 mg/kg [feed: 15-83 IU/kg]	Diet fed for 28 days Prior feed was standard 22 IU/kg of DL-α-tocopheryl acetate	Cross-breed	Barrows and Gilts	Anderson *et al.* (1995)
HPLC Fluorescence detector	Saponification, extraction n-hexane/ toluene	No vitamin E supp: Vitamin E supp: Vitamin E&C supp:	7.43 ± 1.13 mg/kg [feed: 31 mg/kg] 23.05 ± 1.50 mg/kg [feed: 195 mg/kg] 27.34 ± 2.05 [feed: 169 mg/kg]	Start: 25 kg End: 106 kg	Large White	Barrows	Eichenberger *et al.* (2004)
HPLC Fluorescence detector	In text reference	Control: High feed: Very high feed:	8.4 ± 0.18 mg/kg [feed: unknown] 12.8 ± 1.07 mg/kg [feed: 200 mg/kg] 13.4 ± 0.88 mg/kg [feed: 500 mg/kg]	Start: 50 kg End: 90 kg	Landrace x Large White	Boars and Gilts	Onibi *et al.* (2000)
HPLC	In text reference	Loin chop cut: Loin steak cut: Rump steak cut: Loin roast cut: Round (mini) roast cut: Scotch roast cut:	3.4 mg/kg Not detected 6.0 mg/kg 5.3 mg/kg Not detected 4.3 mg/kg	Shop purchased	<	<	Greenfield *et al.* (2009)

Table 13. Reported concentration of amino acids in porcine tissue

Amino Acid	Tissue Sampled		
	Adipose (mg/kg)	Muscle (mg/kg)	Muscle (mg/kg)
Alanine	118.05	1979.00[3]	[3]368.00
Glycine	81.80	1179.00[4]	[6]238.00
Taurine	47.67	4087.00[1]	[2]382.00
Glutamine	43.13	3819.00[2]	[1]444.00
Glutamic Acid	39.31	632.00[9]	[9]152.00
Proline	38.97	932.00[5]	[4/5]258.00
Arginine	21.98	708.00[7]	[4/5]258.00
Threonine	16.91	675.00[8]	[7]175.00
Histidine	06.92	829.00[6]	[8]160.00
Reference	Toldrá *et al*. (1992)	Toldrá *et al*. (1992)	Lorenzo *et al*. (2008)

Table 14. Data from published sources reporting the electrochemical behaviour of amino acids

Amino Acid	Ep	pH	Electrolyte	Electrode*	Reference
Cysteine	+ 0.6 V	7.4	Phosphate Buffer	GCE W SCE R Pt A	Deng (2009)
Tryptophan	+ 0.7 V	7.4	Phosphate Buffer	CPE W Ag/AgCl R Pt A	Fiorucci (2002)
Tyrosine	+ 0.7 V	7.0	Phosphate Buffer	GCE W SCE R Pt A	Huang (2008)

*Electrode material described for: W- working electrode, R- reference electrode, A- auxiliary electrode

Table 15. Reported concentrations (µg/kg) of steroid hormone in porcine tissue

Type	Testosterone	17 β-Estradiol	Estrone	Progesterone	Pregnenolone	DHEA	Androstenedione	Cortisol	Cortisone	Reference
Chop Gilt	<0.02	<0.03	<0.02	1.10-1.76	0.27-0.37	0.01-0.14	0.11-0.19	-	-	Hartmann et al. (1998)
Chop Barrow	<0.02	<0.03	<0.02	0.35-0.76	0.10-0.33	<0.02	0.12-0.17	-	-	
Retail Pork	0.06-1.42	-	-	0.22-0.61	-	-	-	5.89-24.80	0.1-0.22	Yang et al. (2009)
Muscle Boar	0.18-8.40	0.16-2.45	0.02-0.33	-	-	-	-	-		
Backfat Boar	1.26-20.34	0.12-0.78	0.09-1.38	-	-	-	-	-		
Muscle Barrow	0.00-0.16	0.00-0.07	0.01-0.16	-	-	-	-	-		Claus *et al.* (1989)
Backfat Barrow	0.00-0.22	0.00-0.06	0.00-0.10	-	-	-	-	-		
Muscle Gilt	0.00-0.23	0.00-0.20	0.00-0.16	-	-	-	-	-		
Backfat Gilt	0.00-0.32	0.00-0.12	0.00-0.20	-	-	-	-	-		

Table 16. Skatole concentrations, measured in adipose tissue samples, values for the preliminary comparison of the voltammetric sensor method and the corresponding GC-NPD method (n=14). All concentrations are mean values calculated from duplicate data sets (n=2).

Sample	Skatole Sensor (ppm)	Skatole GC (ppm)
1	0.12	0.09
2	0.14	0.13
3	0.46	0.32
4	0.18	0.27
5	0.22	0.21
6	0.18	0.14
7	0.02	0.07
8	0.10	0.06
9	0.02	0.05
10	0.00	0.00
11	0.01	0.03
12	0.00	0.02
13	0.02	0.02
14	0.05	0.06

Table 17. Androstenone concentrations, measured in adipose tissue samples, for the preliminary comparison of the amperometric biosensor method and the corresponding GC-FID method (n=21). All concentrations are mean values calculated from duplicate data sets (n=2).

Sample	Androstenone Sensor (ppm)	Androstenone GC (ppm)
1	1.336	0.590
2	3.916	4.240
3	1.299	1.930
4	0.942	0.920
5	1.004	0.970
6	1.313	0.980
7	1.322	1.060
8	3.870	4.380
9	0.743	0.840
10	0.498	0.430
11	0.435	0.490
12	0.768	0.870
13	0.652	0.570
14	0.967	0.720
15	0.818	0.820
16	0.442	0.370
17	0.463	0.770
18	0.901	0.830
19	0.622	0.590
20	1.500	1.350
21	1.001	1.090

Table 18. Concentration of androstenone and skatole in the adipose tissue of pig carcasses. Quantification performed using gas chromatography and the dual electrochemical sensor-biosensor system. Electrochemical measurements made on the abattoir processing line.

Carcass	GC Androstenone (ppm)	Biosensor Androstenone (ppm)	GC Skatole (ppm)	Sensor Skatole (ppm)	Pig Type
1	NM	NM	0.016	0.005	Mature boar
2	NM	NM	0.024	0.010	Sow
3	NM	NM	0.344	0.594	Mature boar
4	1.195	2.332	0.020	0.039	Sow
5	0.800	1.582	0.004	0.013	Sow
6	1.678	4.110	0.004	0.023	Sow
7	1.824	4.456	0.084	0.046	Boar
8	1.295	3.421	0.019	0.023	Boar
9	0.657	0.972	0.026	0.012	Boar
10	0.789	0.893	0.032	0.019	Boar
11	0.675	0.781	0.031	0.000	Boar
12	0.805	2.282	0.021	0.000	Boar
13	0.890	2.000	0.016	0.038	Boar
14	0.868	1.552	0.015	0.016	Gilt
15	1.362	3.705	0.033	0.032	Boar
16	NM	NM	0.021	0.013	Gilt
17	0.677	1.147	0.011	0.027	Gilt
18	0.651	2.028	0.017	0.168	Gilt
19	1.065	1.524	0.077	0.156	Boar
20	0.561	2.109	0.091	0.151	Boar
21	0.648	1.922	0.094	0.096	Boar
22	0.830	2.008	0.015	0.024	Gilt
23	0.500	0.546	0.031	0.023	Gilt
24	0.668	2.145	0.095	0.040	Boar
25	0.455	0.378	0.078	0.016	Boar
26	0.523	1.495	0.028	0.061	Gilt
27	0.355	0.505	0.041	0.055	Boar
28	0.358	1.059	0.032	0.035	Gilt
29	0.730	1.954	0.020	0.025	Gilt
30	0.678	1.757	0.018	0.028	Gilt
31	NM	NM	0.007	0.000	Boar
32	1.125	1.742	0.005	0.007	Sow
33	0.709	2.327	0.008	0.000	Sow
34	0.823	2.115	0.020	0.013	Sow
35	0.807	2.085	0.024	0.016	Sow
36	0.904	2.126	0.006	0.035	Mature boar
37	0.965	2.309	0.016	0.000	Sow
38	0.916	2.355	0.004	0.002	Sow
39	1.085	2.162	0.000	0.094	Sow
40	0.829	2.241	0.010	0.017	Sow
41	1.097	2.220	0.002	0.004	Sow
42	0.979	2.212	0.003	0.027	Sow
43	1.156	2.455	0.003	0.024	Sow
44	1.200	2.163	0.002	0.016	Sow
45	0.678	2.330	0.001	0.010	Sow